Voorwoord

Alhoewel de omslag van het proefschrift meestal laat uitschijnen dat het werk vorm heeft gekregen door de inzet van slechts twee mensen (doctorandus en promotor), is ook dit werk slechts tot stand gekomen door de gezamenlijke inzet van een groot aantal personen.

Laat ik beginnen met mijn ouders en mijn zus die in de eerste plaats een dankjewel verdienen. Van hen heb ik gedurende al die jaren veel steun, aanmoediging en liefde gekregen. Papa en mama, herinneren jullie je nog die vele uren achter ons schoolbord in de keuken tijdens de lagere school? Het heeft jullie veel moeite gekost, want ik was dikwijls een moeilijke leerling, maar we zijn er samen geraakt! Ik hou van jullie!

Een speciaal woordje van dank richt ik vervolgens aan David. Hij heeft de evolutie van dit doctoraat van heel dichtbij meegemaakt. Ik mag hem dan ook heel dankbaar zijn voor de tijd die hij heeft vrijgemaakt voor het nalezen van elk woord in mijn thesis. Het was soms niet alles hé! Zonder zijn geduld, begrip, maar vooral zijn liefde was dit werk maar een half werk geworden.

Ook wil ik vrienden, familie en mensen uit de dagelijkse werkomgeving bedanken, die misschien op een zeer onopvallende wijze ook hebben meegewerkt aan het welslagen van dit project. Zij hebben mij, elk op hun manier, weten te plezieren met een leuke conversatie, wat humor, of simpelweg een vriendelijk bedoelde glimlach. De aangename ontspannings-momenten (labo-weekendjes in de ardennen, BPG congressen, uiteenlopende conversaties in de koffiekamer) die ik met elk van u de afgelopen vier jaren heb mogen beleven, heb ik zeer weten te appreciëren.

Bij de mensen met een concrete inbreng in dit werk dank ik op de eerste plaats mijn promotor, Prof. dr. Dirk Vanderzande, voor zijn motivatie en wetenschappelijk advies gedurende de voorbije jaren. Hij heeft mij tevens de mogelijkheid aangeboden om in Diepenbeek te doctoreren. Prof. dr. Jan Gelan, dank ik voor zijn vertrouwen in mijn onderzoek. Naast zijn interesse in de meest vreemde NMR resultaten, mag ik hem ook dankbaar zijn voor het maken en verwerken van de digitale foto's in dit proefschrift. Het is ook mede dankzij hun begeleiding dat ik me door de, toch wel zenuwslopende, IWT examens kon slaan.

Prof. dr. Ir. Bruno Van Mele en Steven Swier van de V.U.B. dank ik voor de samenwerking op MDSC gebied. Zij waren de drijvende kracht achter het MDSC onderzoek, hetgeen algauw een boeiend en divers domein bleek te zijn waarin vele mogelijkheden aangeboden werden. Bovendien wil ik ook thesisstudent Arvid Suls en de andere studenten van FYSC bedanken.

Ook Prof. dr. Peter Adriaensens wil ik bedanken voor de steun bij het ontrafelen van NMR-spectra.

Jan Czech ben ik als echte expert op het gebied van massa spectrometrie gaan beschouwen. Ik dank hem voor zijn enthousiaste hulp bij het analyseren van massa spectra. Guy Reggers dank ik voor de vele TGA analyses die hij voor mij heeft opgenomen.

Lieve en Veerle bedank ik voor het opnemen van de vele GPC staaltjes en het bespreken van de resultaten ervan.

Huguette Penxten was steeds bereid voor IR- en UV-metingen op te starten op de dagen dat ik aan de V.U.B. aan het werken was. Zij heeft ook de besturing van de oventjes zeer goed van mij overgenomen.

Koen was niet alleen handig met computers en software, maar bij hem kon ik steeds terecht als er weer eens een verwarmingselement kapot gesprongen was en een kortsluiting veroorzaakte!

Margreet de Kok zou ik ook nog willen bedanken voor haar hulp tijdens mijn proefschrift. Zij heeft mij in de eerste maanden wegwijs gemaakt doorheen mijn onderwerp: "De eliminatie reactie". Ik hoop dat mijn werk een toegevoegde waarde geleverd heeft aan jouw hoofdstuk zes van je thesis.

Ondertussen heb ik ook geleerd dat je zonder een technische en administrative ploeg nergens staat. Hiervoor dank aan het SBG-secretariaat, Christel Rappoort, Jos Kaelen en Sali Imic.

Tenslotte ben ik natuurlijk ook het IWT dankbaar, voor de vier jaar durende financiële steun.

Table of Contents

I

General Introduction

I.A Conjugated Polymers

Conjugated polymers are a novel class of semiconducting materials that combine the electronic and optical properties of semiconductors and the processability of conventional polymers [1]. The semiconducting properties of conjugated polymers originate from the delocalized π-orbitals formed in carbon-containing compounds. Figure I.1 shows the chemical structure of a small number of a few commonly used conjugated polymers.

Polyacetylene (PA) is the simplest example of a conjugated polymer, a polymer in which the "backbone" atoms are joined alternatively by single and double bonds. The conjugation in PA, however, is not sufficient to render the polymer conductive. For this reason it is necessary either to remove electrons (oxidation) or to insert electrons (reduction) into the material. These processes are known as *p*- and *n*-doping respectively, as the created holes or the extra electrons can move along the polymer backbone, the polymer becomes electrically conductive.

The electrical properties of a material are determined by its electronic band structure. The simple band theory can provide useful information on the doping-induced changes occurring in electronic band structure. Overlap of

adjacent atomic p_z-orbitals yields lower energy bonding (π) and higher energy anti-bonding (π^*) molecular orbitals. When many molecular orbitals are spaced together in a given range of energy, the π-orbitals generate an apparently continuous, occupied valence band (VB), while the π^*-orbitals produce the conduction band (CB). The energy spacing between the highest occupied molecular orbital (HOMO) and the lowest unoccupied molecular orbital (LUMO) is called the bandgap (E_g). The size of this bandgap, which in general lies between 1 and 4 eV for conjugated polymers, determines the electrical and optical properties of the material. Within the polymer material, charge-carrying species (solitons, polarons and bipolarons) can be created through doping or optical absorption [2].

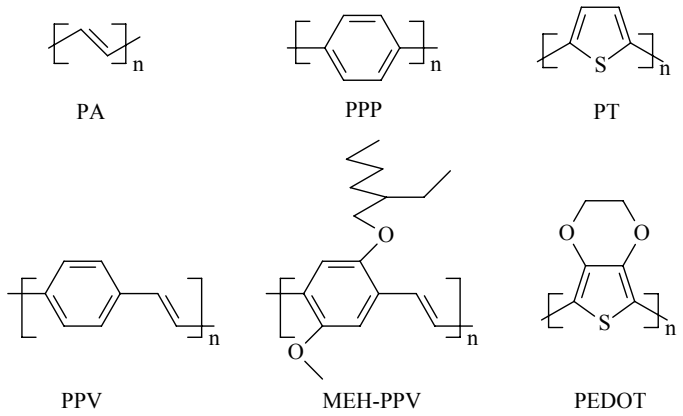

Figure I.1: *The chemical structure of frequently used conjugated polymers.*

Alan J. Heeger, Alan G. Mac Diarmid and Hideki Shirakawa were rewarded with the year 2000 Nobel Prize in Chemistry for "the discovery and development of electrically conductive polymers". This trio of scientists discovered in 1977 that *trans*-polyacetylene, the prototype conducting polymer (Figure I.1), could be chemically *p*-doped (oxidised) or *n*-doped (reduced) with a simultaneous increase of its electrically conductivity [3]. Since then, π-conjugated polymers have emerged as viable semiconducting electronic materials for numerous applications and opened up important new vistas for chemistry and physics, and for technology in general. At first, the poor processability and environmental stability of the first conductive polymers hampered commercial succes. But, during the 1980s, the material properties are

enhanced significantly due to improved synthesis methods and processing technology. This has led to improved purity and solubility of conjugated polymers, which enabled their exploitation as the active materials in field-effect transistors [4], photovoltaic solar cells [5], smart windows [4c,e], polymer batteries [4] and Polymer Light Emitting Diodes (PLEDs). Since 1990, when Burroughes *et al.* [6] reported that poly (*p*-phenylene vinylene), PPV can serve as the emissive layer in Light Emitting Diodes (LEDs), the property of electroluminescence became the subject of intense research and development world-wide. As a result, thin film devices and large-area polymer optoelectronic devices can be easily fabricated with relatively low cost.

I.B Electroluminescence

Electroluminescence (EL) is the emission of light generated from the radiative recombination of electrons and holes electrically injected into a luminescent semiconductor. Closely related is the phenomenon of photoluminescence (PL), which leads directly to the emitting species via absorption of light. These two processes are depicted in Figure I.2.

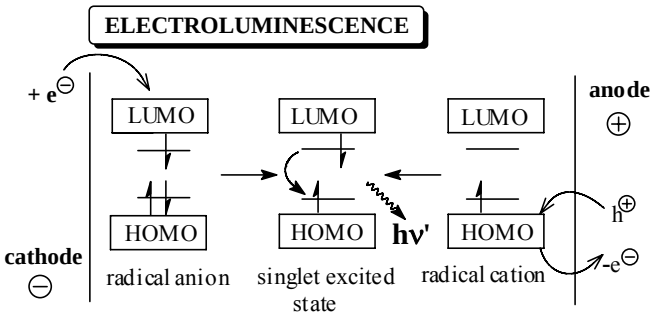

Electroluminescence: From the cathode electrons are injected in the LUMO to form radical anions (negative polarons). The anode extracts electrons from the HOMO, or in other words injects holes, to form radical cations (positive polarons). The resulting charges migrate within the polymer film under influence of the applied electric field. Somewhere in the bulk of the polymer electron and hole recombine, forming an exciton which can emit light by passing to the ground state.

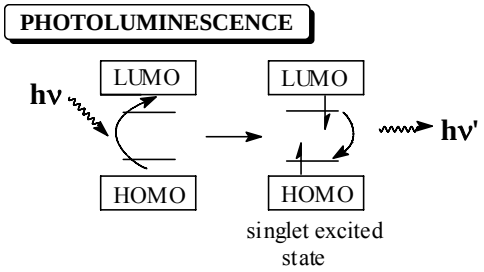

Photoluminescence: An electron is promoted from the HOMO to the LUMO of a fluorescent polymer by irradiation with light. In a typical conjugated polymer, two new energy states are generated upon relaxation within the bandgap and are each filled with one electron of opposite sign (singlet excited state). This exciton can decay to the ground state radiatively or non-radiatively. The radiative decay is called photoluminescence.

***Figure I.2**: Schematic representation of electroluminescence and photoluminescence in conjugated polymers.*

A major breakthrough was the observation of EL of the conjugated polymer PPV, sandwiched between two injecting electrodes [6]. A schematic representation of a polymer LED (PLED) is shown in Figure I.3. The single layer PLED depicted in Figure I.3 consists of four layers. A thin layer of Indium Tin Oxide (ITO) is used as a transparent hole-injecting anode, while a metal, for instance Ca or Al, is used as the electron injecting cathode. This pair of electrodes can be applied to glass or a flexible substrate like PET (*poly*(ethylene terephtalate)) [7]. A thin layer of the emissive polymer is sandwiched between the anode and cathode. Proper encapsulation prevents diffusion of water and oxygen into the active area of the device. By applying a bias, electrons and holes are injected in the emissive polymer. These entities migrate towards each other under the influence of the applied field. Charge carrier recombination may result in an exciton which can decay radiatively or non-radiatively. The wavelength of the emitted light is determined by the bandgap of the material [8]. For PPV the bandgap is 2.4 eV, emitting yellow-green light. The device operation of a PLED is thus determined by three processes: charge injection, charge transport and recombination. The following properties, among others, are of importance for commercial application of PLEDs: color and brightness, efficiency, lifetime, purity, stability and solubility of the emissive polymer.

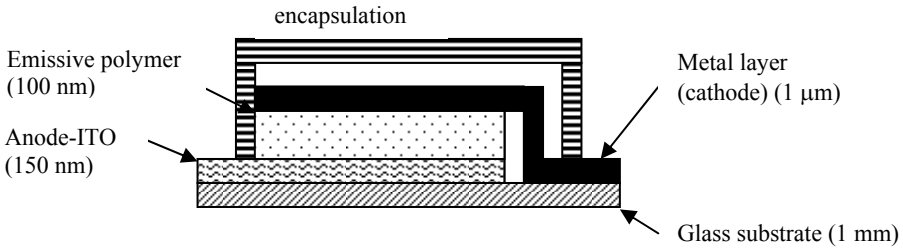

Figure I.3 *Schematic structure of a Polymer Light Emitting Diode (PLED).*

I.C Several precursor routes and their elimination behaviour towards PPV

PPV is a polymer with a very low solubility in commonly used organic solvents. As a result, it is a polymer very difficult to process. Since research in this domain has been extented to the synthesis and study of soluble conducting polymers, it has led to two important approaches in the preparation of conjugated polymer thin films: the precursor and the side-chain approach [9].

I.C.1 The side chain approach

The side-chain approach is the use of soluble PPV-derivatives like for example MEH-PPV and OC_1C_{10}-PPV. These alkoxy substituted PPV-derivatives are soluble because of the large side groups and thus can be processed in the conjugated form. A drawback of these soluble conjugated materials is that they will easily mix with different soluble layers. In addition, the T_g of these soluble materials is lower than the T_g of PPV (220°C) [10], deteriorating the mechanical properties of the conjugated polymer.

I.C.2 The precursor approach

The precursor approach relies on the design and synthesis of an intermediate, soluble precursor polymer that can be cast into thin films, before solid-state conversion to the final conjugated polymer. For well performing polymer electronic devices, the device parameters as well as the material

properties of the conjugated PPV polymer are very important. The microstructure and the morphology of the material have a decisive influence on the quality of the polymer layer. PPV is often put on a substrate starting from a PPV precursor polymer (non-conjugated polymer) that can then be transformed into the conjugated polymer via a thermal elimination process. Knowledge of this elimination step is very important, because the substrates, onto which precursor polymers are put while manufacturing polymer electronic devices, have to withstand the required elimination temperatures. Also, a lot of material properties such as crystallinity and defects (carbonyl functions) seem to put serious limits on the quantum efficiency (relation between the number of transported electrons and the amount of emitted light) of materials. The quantum efficiency is also influenced by the conjugation length and the film morphology of the conjugated polymer [11]. All the latter material properties, and hence also the properties of a LED, are dependent on the elimination step [12]. The use of precursor polymers will be necessary for multilayer systems (LED-devices fabricated with multiple polymer layers), as the polymers can be rendered insoluble after film deposition. Polymer replacements for ITO and design of polymer transistors also imply the use of precursor polymers. Although the conversion step is of crucial importance for the functionality of these polymers in their applications, only little systematic research is done on such conversion reactions. Several clever synthetic precursor routes have been developed in the past. The most important are discussed in the following paragraphs. A lot of attention is paid to the conversion process of the eliminable group in the different precursor routes.

I.C.2.a Sulphonium (polyelectrolyte) precursor route

The sulphonium precursor route was discovered more than 30 years ago by Wessling and Zimmerman [13]. The precursor sulphonium polyelectrolyte **III** is obtained in aqueous solution from a bis-sulphonium salt of *p*-xylene by a base-initiated polymerisation reaction (Figure I.4, **step 1**).

The reaction conditions of the polymer must be optimised in a way to minimise the amount of unsaturated segments on the polymer chains, through premature basic elimination. This involves the use of low temperatures ($T \ll 0°C$), low monomer concentrations (0.2 to 0.5 mmol l^{-1}), base to monomer ratios below 1 and also the exclusion of oxygen from the polymer reaction.

When these precautions are not taken, the precursor solutions generally show a weak blue/green fluorescence, which can be attributed to very short conjugated lengths, arising from a limited amount of preliminairy basic elimination. This elimination can also leads to gel formation and to insoluble precursor polymers. The polymerisation reaction is terminated by the addition of dilute HCl and the solution is then dialysed against water for a period of a week or longer in order to separate the high-molecular-weight fraction from monomer residues, Na^+ and Cl^- ions (Br^- ions) and oligomer material.

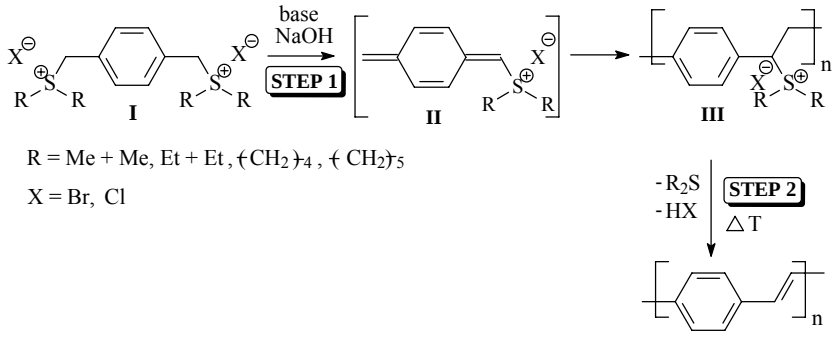

Figure I.4: *Sulphonium precursor route.*

The polymerisation mechanism has been studied by different groups [13b, 14]. It is accepted that the first steps involve proton abstraction and 1,6-elimination of a thioether to give the reactive *p*-xylylene derivative **II**. This *p*-xylylene derivative is the actual monomer, which polymerises spontaneously either by an anionic or a radical mechanism. Recently Cho *et al.* [14] showed that the sulphonium route proceeds via an elimination free radical polymerisation mechanism, although the exact nature of the free radical initiator could not be detected. In the polymerisation reactions carried out by Wessling and co-workers [15], the principal derivatives of moiety **I** in Figure I.4 have been dimethyl and diethyl sulphonium salts, with either chloride or bromide counterions. However, while high molecular weight polymers can be prepared from these monomers, the polymerisation yields obtained were generally quite low and in the range of 10-20 %. The low yields may be explained by undesirable side reactions during polymerisation and storage of the sulphonium precursor polymers, because they are not very stable at ambient temperature. The kind of defects that can occur are shown in Figure I.5. These side reactions are the result of the symmetrical character of the (pre)monomers. The

sulphonium group has to fulfil three important tasks: that of a so-called polariser, which enables proton abstraction at the benzylic position, that of a leaving group to afford the actual monomer, a *p*-xylylene derivative, and that of (thermally) eliminable group to afford the conjugated system. Since a sulphonium group is both a good polariser and a leaving group, even at ambient temperature, side reactions (nucleophilic substitutions) are almost unavoidable. The extreme sensitivity of the symmetric monomer to polymerisation conditions limits the possibilities of this precursor route for material manufacturing. Other sulphonium salt monomers were evaluated and the tetrahydrothiophene (THT) derivative is considered superior [16].

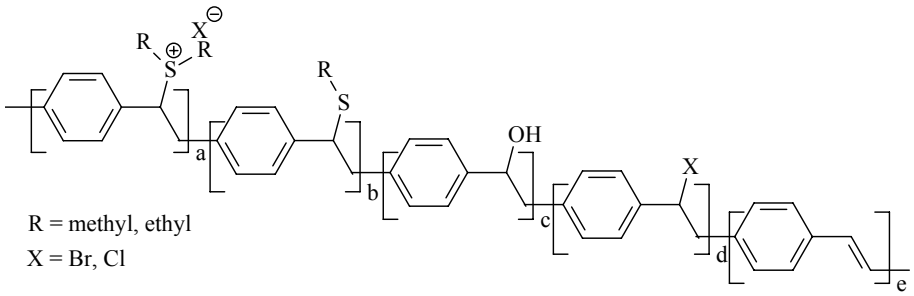

Figure I.5: *Defects (SR, OH, X, double bond) in the sulphonium precursor polymer.*

After precursor synthesis and purification, the precursor is to be converted into the conjugated polymer PPV. Normally, this is achieved by a thermal treatment under vacuum or in an inert gas atmosphere. The idealised reaction scheme (Figure I.4, **step 2**), involves the elimination of dialkylsulphide (R_2S) and hydrogen halide (HX) in case of a dialkyl sulphonium salt. Full conversion of precursor to PPV requires an elimination temperature of at least 300°C. Annealing at a temperature above 400°C, however, leads to polymer degradation and will finally lead to polymer decomposition at approximately 550°C. The use of an inert atmosphere or vacuum for the heat treatment is necessary in order to avoid the formation of carbonyl moieties through oxidation of the vinylene carbons during the elimination reaction. Heat treatment at temperatures below 300°C results in a copolymer containing saturated and unsaturated segments.

In the next paragraphs, step by step different proposals are discussed concerning the possible elimination mechanisms. According to the authors, different ideas for the elimination mechanism are given a chance. Interpretation of these results, however, must be performed with precaution, because in literature a lot of disagreement about the exact nature of processes occurring during the elimination process has surfaced the last few years. In a first part, the thermal elimination reactions have been studied in materials containing dialkyl sulphides by Gagnon *et al*. and Montaudo *et al.* [17]. In a second part, the elimination mechanism of cyclic sulphides is emphasized by Massardier *et al*., Gmeiner *et al*. and Shah and Arbuckle [18-23]. Explanations given in some of the articles are susceptible to serious criticism.

The thermal conversion of poly (*p*-xylene-α-dialkyl sulphonium halides) into poly (*p*-phenylene vinylene), PPV takes place via three related reactions [17] as shown in Figure I.6.

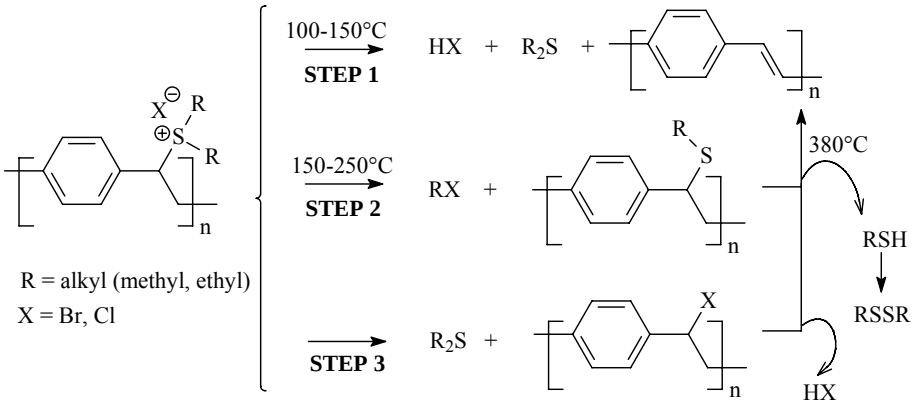

Figure I.6: *Elimination reactions of alkyl sulphonium ion precursor polymers into PPV.*

In the first reaction (Figure I.6, **step1**), HX and a dialkylsulphide are eliminated at a relatively low temperature (100-150°C). In the intermediate temperature range (150-250°C) (Figure I.6, **step 2**), the second mechanism takes place through a nucleophilic attack of the halide counterion on a sulphonium alkylgroup to form an alkylhalide and a thioether precursor polymer. Thus, at elimination temperatures between 150 and 250°C the partially eliminated copolymer can be best described as having the structure shown in Figure I.7. Finally a thermal elimination of this intermediate to the conjugated PPV polymer occurs at about 380°C.

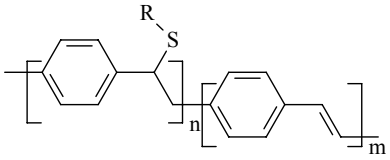

Figure I.7: *Copolymer obtained by elimination between 150-250°C.*

Sulphonium salts can also undergo a S_N2-reaction by displacement of the sulphonium group (Figure I.6, **step 3**) [17a]. This reaction is believed to be not a major elimination route. Since no residual chlorine was present after treatment above 150°C.

An important improvement in the poly (arylene vinylene) synthesis was achieved by replacing the dialkylsulphide group in the poly (*p*-phenylene vinylene) precursor by a cyclic sulphide such as tetrahydrothiophene [18]. Then, the two side reactions mentioned before, can be avoided, while thermal conversion occurs at lower temperatures and yields products with elimination of tetrahydrothiophene and acid [19].

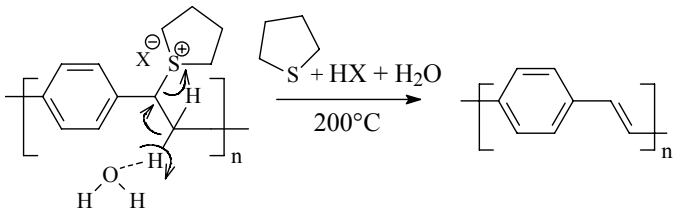

X = halide, acetate

Figure I.8: *Simple E_2 elimination reaction of a THT sulphonium precursor polymer into PPV.*

Elimination is essentially complete after 12 hours at 200°C instead of 380°C in the case of a dialkyl sulphonium ion precursor polymer and is depicted in Figure I.8. Whether these compounds are simultaneously released from the polymer matrix depends on the elimination conditions.

Massardier *et al.* [20] demonstrated that thermal conversion of the THT sulphonium ion precursor of PPV begins as soon as the heating process is started. First, the associated water is eliminated, followed by THT. Most of the

HX is evolved at higher temperatures, with transient formation of an intermediate benzylidene halide group. The origin of the C-X structure is not quite clear and can be due to nucleophilic substitution of the sulphonium group (S_N2 mechanism), or a two step S_N1 mechanism (E_2 and E_1 respectively according to reference 20), or even to readdition of HX onto vinylene bonds.

Shah and Arbuckle [21] clearly show that the elimination reaction is not a single-step process but involves at least two steps. Therefore, the bimolecular elimination mechanism, E_2, can be ruled out for this reason. They believe that the elimination predominantly follows an E_1 mechanism. Massardier *et al.* [20] have suggested an alternate route which involves the formation of an intermediate product with a C-X covalent bond. This is considered to be one of the undesirable side reactions in the dialkyl sulphide precursor. Hence the mechanism suggested by Massardier *et al.* is probably only valid for dialkyl sulphide type precursors [21].

Very recently, Gmeiner reported on a study of the thermal conversion of THT sulphonium ion precursor polymers to PPV [22]. A ThermoGravimetric Analysis (TGA) and *in-situ* UV-Vis spectroscopy of the freestanding precursor film indicated that as volatiles are related by the polymer due to the loss of THT and HCl by thermal elimination, the conjugation of the π-orbitals increases gradually. Clearly evident in the UV-Vis spectra of the precursor measured at constant temperature of 140°C was the simultaneous appearance of the three isobestic-points at 329, 282 and 244 nm. This is a clear evidence that the reaction proceeds without intermediate. The IR spectra measured during the reaction revealed that the IR absorption bands of water in the polymer at 675, 1636 and 3388 cm^{-1} decreased rapidly and could not be observed at temperatures higher than 100°C. This result is inconsistent with the E_2 (or $E1_{cb}$) mechanism, in which the water acts as the promoting base (Figure I.8). Also the C-S stretch band at 608 cm^{-1} vanished while the C-Cl stretch vibration at 630 cm^{-1} reached its maximum at 125°C, and then decreased at 150°C. This indicates that new C-Cl bonds must be formed as the THT is lost, which is again inconsistent with the simultaneous elimination of THT and HCl required for the E_2 or $E1_{cb}$ mechanism. Finally the gradual increase of the *trans* vinylene double bond at 962 cm^{-1} indicates a monotonous increase in the degree of conjugation. The sulphur and chlorine content is measured with Energy-Dispersive X-ray analysis (EDX) as a function of temperature. The sulphur

content in the polymer starts to decrease at about 75°C. This decrease is finished at 125°C, indicating that the THT is eliminated between 75 and 125°C. On the other hand, a higher temperature of 150°C is required to eliminate the chlorine from the polymer film. This clearly demonstrates that THT and HCl do not eliminate simultaneously. Other important results were obtained from ThermoGravimetric Analysis (TGA) measurements on the polymer film and simultaneous detection of the released products with mass spectroscopy. There are three steps present during the conversion of the precursor polymer to PPV, i.e. (1) 75°C: THT splits off, (2) 125°C: THT splits off, (3) 150°C: HCl splits off. This provides additional evidence that elimination of THT and HCl do not occur simultaneously.

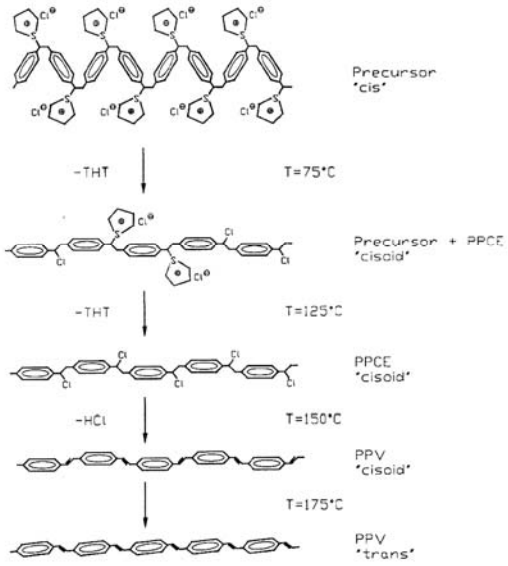

Figure I.9: *Gmeiner's mechanism for the elimination reaction of THT sulphonium precursor polymer.*

To propose a reasonable mechanism, Gmeiner considered the configurations of the polymer chain. There are three possible configurations, *cis*, *cisoid* and *trans* of the prepolymer. The *trans* configuration is sterically

hindered because the neighbouring side groups THT^+ and Cl^- are on the same side of the polymer chain, whereas *cis* and *cisoid* configurations are sterically less hindered as the neighbouring groups are now on the opposite sides. Therefore, it seems reasonable to assume that the prepolymer consists mainly of *cis* and *cisoid* configurations rather than the *trans* form. Gmeiner's mechanism is shown in Figure I.9.

When starting from *cis* prepolymer the THT groups split off first at about 75°C by the S_N2 (or S_N1) displacement reaction of the chloride. The driving force for this reaction appears to be the steric strain in the *cis* prepolymer, which is drastically reduced after this substitution. It is assumed that the polymer chain then undergoes an isomerisation from *cis* to *cisoid*. The nucleophilic substitution of the *cisoid* configuration by the chloride occurs at a temperature above 125°C. According to the authors, because of the smaller steric strain. Afterwards, the chlorine is eliminated as HCl at about 150°C. At temperatures ≥ 175°C a further isomerisation takes place, increasing the number of *trans*-segments in the polymer.

Later results obtained from Shah and Arbuckle [23] provide evidence that an E_2 mechanism takes place at low temperatures by simultaneous release of THT and HCl. At higher temperatures, the elimination seems to occur solely via an E_1 mechanism. In an E_1 mechanism, the elimination will occur via the formation of an intermediate carbocation, which in this case will be resonance stabilised and therefore can be quite long-lived. The final step in the elimination reaction, is the nucleophilic attack of a base (chlorine ion) on the aliphatic carbon and the release of HCl. This mechanism, as published in the paper of Shah *et al*., is shown in Figure I.10 A.

According to us, some criticism is necessary on the proposed elimination mechanism by Shah and Arbuckle. Their assumed E_1 elimination mechanism, excisting of two thermal distinguishable steps, is in contradiction with the fact that in an E_1 elimination the rate determining step is the formation of a carbocation. Therefore, it is more plausible that a S_N1 reaction occurs, which leads to a substitution of the THT functional group by the chloro (THT is a good leaving group in the absence of water) and that in a second step HCl is formed via an E_1 elimination. Our alternative mechanism is shown in Figure I.10 B.

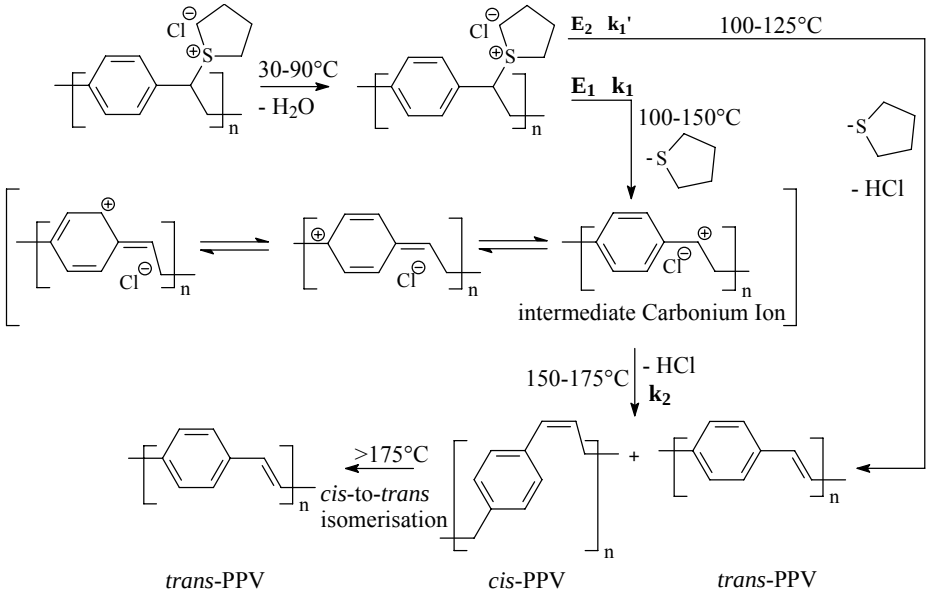

Figure I.10 A: *Proposed thermal elimination reaction sequence in the PPV precursor by Shah and Arbuckle.*

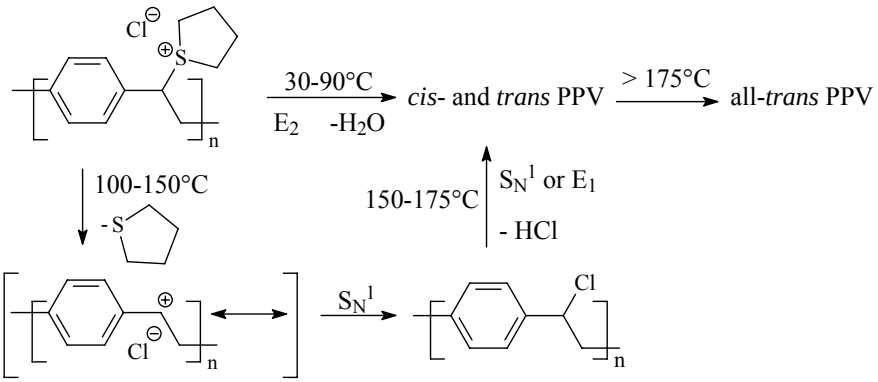

Figure I.10 B: *Alternative elimination mechanism according to us.*

Another discussion point to us is the temperature on which the E_2 elimination occurs. According to Shah and Arbuckle, the E_2 elimination takes place in a temperature range between 100 and 125°C, which is not quite different from the temperature on which the E_1 elimination occurs. A question to us is how do they separate these two processes? According to us, an E_2 elimination already occurs in a temperature range from 30 till 90°C, assuming water will act as the base [24].

The authors conclusion that both E_1 and E_2 mechanism may be operating with the shift from E_2 to E_1 being dependent on reaction temperature and stereochemistry of the polymer is to a limited extent in agreement with a study of Massardier *et al.* [20]. Schlenoff and Wang [19] have reported an E_2 mechanism and Halliday *et al.* [16b] have reported an E_1 mechanism. This is now comprehensible given that both mechanisms are operative.

It has been shown that full conversion of a dialkyl sulphonium ion precursor at high temperatures (≥ 350°C) is required to obtain PPV with good optical and electrical properties [16a]. However, high conversion temperatures are incompatible with most multilayer device fabrication processes. Therefore, a criterion for optimising the conversion process is the rapid elimination of the leaving group at the lowest possible temperature, by this guarantee both a high degree of conjugation and thermal stability necessary for device applications. Unfortunately, a route that combines low conversion temperatures and well-defined, stable polymer structures is still lacking. The conversion of the THT sulphonium precursor into PPV, which needs a rather long thermal treatment above 200°C, may be a drawback to production of PPV on an industrial scale. A novel method is developed by which PPV may be obtained rapidly and directly and with almost no side reactions. This method consists in treating the sulphonium precursor with strong acids at ambient temperature [25]. It is interesting to note that the choice of counterion (Br^- or Cl^-) has an effect on the elimination temperature. The bromide tetrahydrothiophenium undergoes complete elimination at about 100°C, while the elimination temperature observed for the chloride polyelectrolyte is about 250°C [21, 24, 26]. Very recently, a rapid conversion of poly(*p*-phenylene vinylene) films at low temperatures was investigated [27]. It is possible to fabricate stable PPV films with a high conjugation length at 115°C within only 3 minutes. This was accomplished by a controllable substitution of the chloride anion in the aqueous solution of the THT sulphonium precursor polymer with a long-chain dodecylbenzenesulphonate (DBS) anion. Such flexibility in film fabrication and efficient low-temperature conversion to PPV offer an advantageous alternative to the standard conversion procedures, which may have important implications in device applications. However, in the end the sulphonium precursor route has substantial disadvantages. The polyelectrolyte sulphonium precursors are only soluble in polar solvents such as water and methanol. These solvents are poor solvents for spinning high-quality films. Moreover, characterisation of

molecular weight by gel permeation chromatography (GPC) is troublesome. The sulphonium precursor route cannot be used with more lipophilic side group derivatives due to solvent incompatibility, but can only be used for the preparation of poly (*p*-phenylene vinylene), PPV. The sulphonium precursor route is liable to side reactions and the HCl released during elimination can react with the ITO electrolyte and the products, possibly indium chloride, can quench the PL [28].

I.C.2.b Gilch (chlorine) precursor route

This precursor route, first described by Gilch and Wheelwright in 1966 [28], employs the treatment of α, α'-dihalo-*p*-xylenes with an excess (10 eq.) of potassium-*tert*-butoxide (tBuOK) in organic solvents. Alkyl and alkoxy substituents on the aromatic ring are often used to impart solubility to the PPV (e.g. MEH-PPV, OC_1C_{10}-PPV) [28]. A disadvantage of the chlorine precursor route to soluble PPVs is the precipitation which occurs during the polymerisation. This precipitation is ascribed to high-molecular weight, semi-crystalline and crosslinked polymers [30]. To prevent premature precipitation Swatos *et al*. presented a modification of the Gilch route, the chlorine precursor route, that uses about 1 equivalent of tBuOK instead of an excess of base, to yield a soluble precursor polymer that can be converted to the conjugated form [30d]. The Gilch precursor route is depicted in Figure I.11.

The mechanism of the Gilch polymerisation is still under discussion. The first step is the base-induced elimination of HCl, leading to the "real" monomer, a quinodimethane derivative. The complexity of the chemistry involved in the whole polymer synthesis makes the nature of the polymerisation uncertain. For the second step, the polymerisation itself, there are two possibilities: (1) a free radical mechanism, which is claimed for precursor polymers e.g. by Vanderzande *et al.* [31], or (2) an anionic induced polymerisation, which is described by Hsieh *et al.* [32]. The third and last step is the conversion of chlorine PPV precursors to the conjugated material by heat treatment (300°C, 1 hour) [33], or in case of soluble PPV derivatives by basic elimination (tBuOK/THF) [27] or (NaH/DMF) [34].

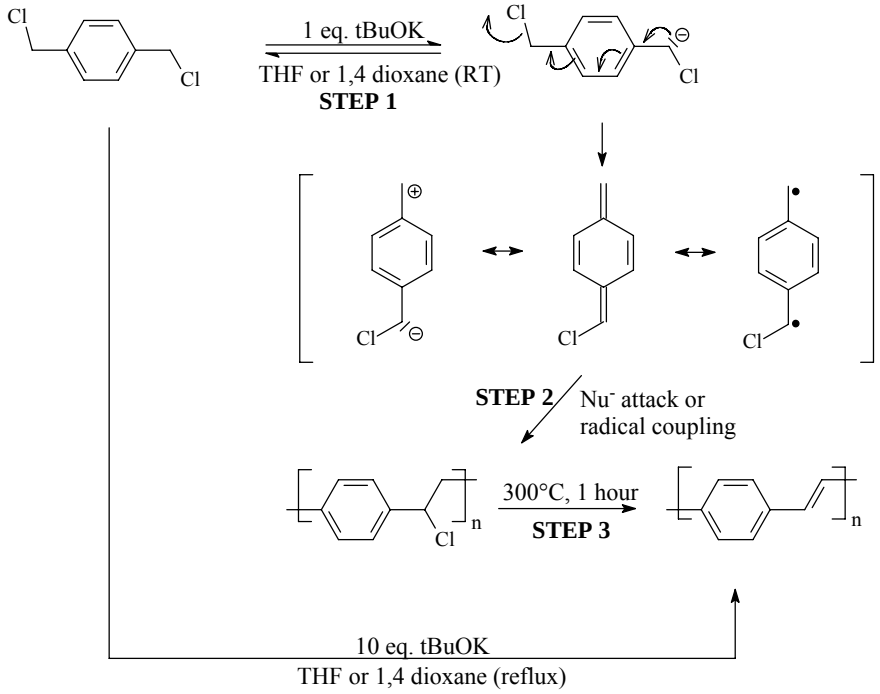

Figure I.11: *The Gilch precursor route.*

The chlorine PPV precursor is insoluble in most common organic solvents such as acetone, chloroform and THF. This relatively bad solubility and the high conversion temperature make this precursor route not attractive to PPV. For the soluble PPVs, however, the basic elimination is often used.

For the synthesis of PPV, the Gilch precursor route has no real advantages over the Wessling-Zimmerman route. Both of them involve the liberation of HCl gas, which may react with the ITO electrodes, leading to poor device performances. For PPVs prepared following the Gilch procedure, a defect structure into the polymer main chain was investigated [35]. This defect can easily be explained by a head-to-head and tail-to-tail instead of regular head-to-tail reaction. For OC_1C_{10}-PPV 1.5 to 2.2 % of these irregularities were proven via ^{13}C labeling experiments. This defect has large influence on various properties of PPVs. Nevertheless, at present, the Gilch route is in industry the most commonly used synthesis method, because in comparison with the Wessling method it allows easier access to a large range of substituted PPV derivatives, soluble in organic solvents.

I.C.2.c Xanthate precursor route

Another precursor route which shows interesting prospects is the xanthate precursor route. This route was preserved as a modification of the Wessling-Zimmerman route in an attempt to circumvent the problems inherent to the latter [36]. The use of a xanthate group is an adaption of the Chugaev reaction [37]. S. Son *et al.* have modified the reaction to lower the conversion temperature and to simplify monomer preparation.

In Figure I.12, monomer **I** was synthesised in one step and was found to be stable enough to store as a solid at ambient temperature without any sign of degradation or hydrolysis. The monomer was polymerised by dissolving it in tetrahydrofuran (THF) and then reacting it with potassium-*tert*-butoxide at 0°C.

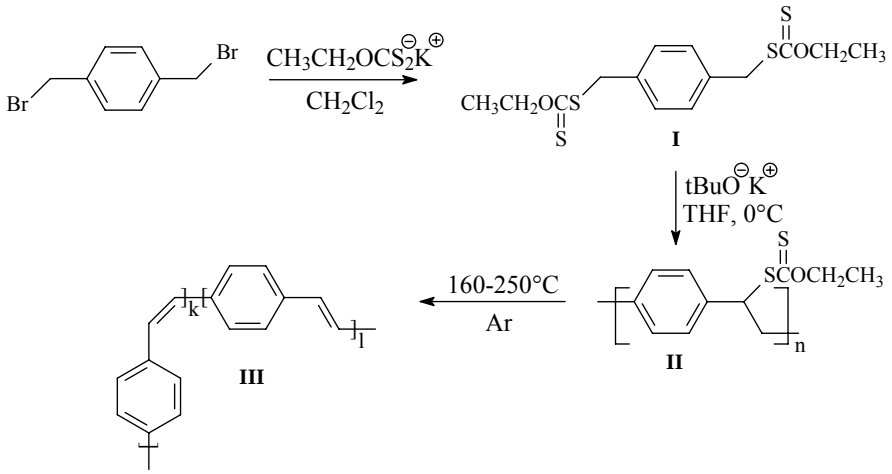

Figure I.12: *The xanthate precursor route.*

The reaction appears to proceed via a quinoid intermediate, because the solution becomes red almost immediately after addition of the base [36a]. Although this may be an indication that the formation of an anion cannot be excluded. The resulting precursor polymer **II** was completely soluble in common organic solvents such as THF, chloroform, 1,4 dioxane, toluene and cyclohexanone. Size exclusion chromatography against polystyrene standards results in a M_w of $6x10^5$ g/mol with a polydispersity of 3.4, yields were not mentioned. The conversion process of the xanthate functionalities takes place

between 160 and 250°C and is thought to follow an elimination mechanism similar to that of the Chugaev reaction which is known to produce a mixture of *cis* and *trans* double bonds **III** in solution through a six-membered ring formation [38]. The presence of *cis* double bonds are confirmed by an IR absorption around 860 cm^{-1} [39]. The thermal elimination reaction in the xanthate precursor occurs in two distinct steps [40] and the xanthate group breaks down into COS and CH_3CH_2SH [41]. The xanthate precursor route is shown in Figure I.12.

The transition state of most elimination reactions is planar: all assisting functionalities, sulphur groups and ethane bridges are within one plane as depicted in Figure I.13. This planar conformation can account in general for the selectivity to form *trans* double bonds: sterical hindrance between phenyl groups could obstruct a *cis* double bond from being formed. The mechanism of the elimination of xanthate groups is described as a cyclic, concerted *syn*-elimination [38]. Coplanarity is not required for the 6-membered transition state [42] as in the xanthate elimination. The formation of *cis* vinylene bonds out of xanthate precursors can therefore not be excluded on PPV formation.

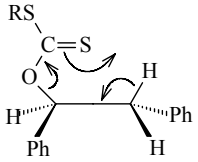

Figure I.13: *Transition state for syn-elimination.*

Different precursor routes leading to the same PPV polymer can give rise to conjugated polymers with different electronic properties. Son *et al.* reported that LEDs containing PPV, prepared via the *O*-ethyl xanthate precursor route, showed a higher quantum efficiency (0.22 %) than LEDs in which the PPV was produced via the more traditional sulphonium precursor route (0.01 %) [6]. The improvement in efficiency of LEDs produced via the *O*-ethyl xanthate precursor route was attributed to the amorphous nature of the "PPV". The amorphous nature in this case is due to the fact that the polymer contains some saturated links and some *cis* next to *trans* linkages. These cause shorter effective conjugation lengths, since the overlap of π-units is reduced. This efficiency decreased with increasing conversion temperature, that is, higher

xanthate elimination and higher *trans* content caused by a *cis-trans* isomerisation. However, a recent publication by Burn *et al.* questions this explanation. In this report the authors explain the higher efficiencies by two important alternative explanations. First, the PPV prepared via the *O*-ethyl xanthate precursor might be inherently more luminescent than PPV prepared via the sulphonium route. Secondly, the by-products (COS, CH_3CH_2SH) from the elimination reaction from the *O*-ethyl xanthate precursor, where a xanthate prepared PPV is used as active material, may be less damaging to the electrode material (ITO) [43]. Burn *et al*. also reported on the first use of xanthate precursor polymers for the preparation of low HOMO-LUMO energy gap poly(arylene vinylene)s, namely poly(2,5-dimethoxy-1,4-phenylene vinylene) (DMEOPPV) and poly(2,5-thienylene vinylene) (PTV) [44].

This clearly shows the potential the xanthate groups offer in the synthesis of PPV as well as the importance of a controlled elimination reaction in a device structure. Although this route offers certain advantages over the Wessling-Zimmerman route such as stability and solubility, the number of publications on this subject is rather limited, but has been increasing during the past few years. It is striking that in some publications no polymer yields are reported, while in other papers yields of 60-70 % are mentioned.

I.C.2.d Sulphinyl precursor route

All precursor routes described previously make use of symmetrical premonomers, in which the same functional group serves both as polariser and as leaving group. These premonomers polymerise via a *p*-xylylene derivative, which is the actual monomer. If the implemented functional group is a good leaving group, this will lead to unstable precursor polymers, because of easily occuring substitution and elimination reactions. The use of a weak leaving group will hamper the formation of the actual monomer, and thus hinder the polymerisation. It is known that, especially for the sulphonium route, this compromise leads to all kind of side reactions which in the end damage the conjugated material and thus the performance of the material in the devices. A new route was designed to overcome these problems. This route combines a smooth polymerisation with a controllable elimination of the obtained precursor polymer. To simultaneously control the polymerisation process and the stability of precursor polymers, there is a need for a chemical differentiation between both functionalities. For this reason the sulphinyl route was developed in our

laboratory. Differentiation and careful choice of the polariser and leaving group would lead to a better control over the whole process going from monomer to conjugated polymer incorporated in a device. Halides were chosen as leaving group, because of their high leaving group capacity, while they are bad polarisers. The leaving group undergoes a 1,6-elimination yielding the *p*-quinodimethane system. Sulphinyl groups with a solubilising side chain (R) introduce the opposite behaviour and fulfil the function of polariser, which is in fact threefold. Upon reaction with a base, these monomers are selectively deprotonated at the side of the polariser and a 1,6-elimination from a *p*-xylene derivative **I** leads to the *in-situ* formation of the actual monomer, the *p*-quinodimethane system **II**, as is shown in Figure I.14.

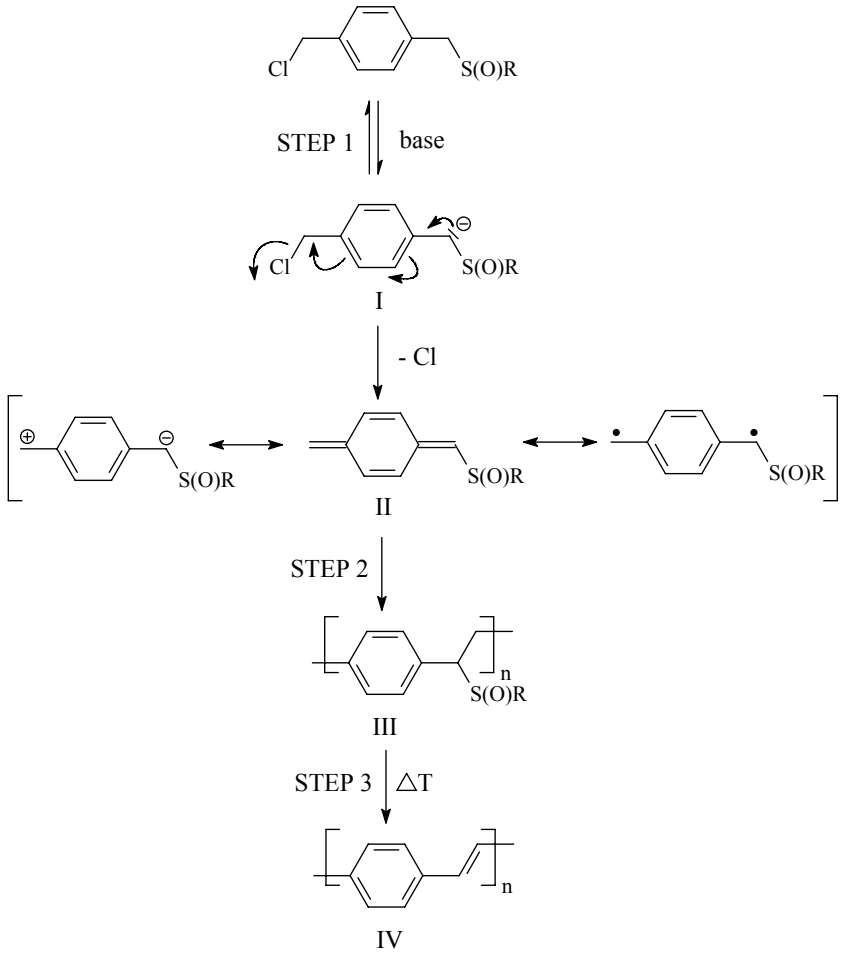

Figure I.14: *Sulphinyl precursor route from monomer to PPV.*

Secondly, this intermediate polymerises spontaneously with formation of high molecular weight precursor polymers **III**. Proton abstraction is considered to be the rate determining step. Initiation occurs most probably via a dimerisation of quinodimethane units with formation of a biradical [45]. Propagation occurs via a radical mechanism [46]. Besides enabling proton abstraction, the polariser has to fulfil two other requirements. First, it should introduce selectivity in the addition step of the polymerisation. Secondly, it should also be eliminable with formation of a double bond **IV** (Figure I.14). Our precursor route has the important advantage that the precursor is stable at ambient temperature. This allows us to isolate the polymer by precipitation. Sulphinyl groups have only a very limited leaving group capacity and are very well suited as a thermal eliminable group to yield a double bond, and thus these functionalities have been used frequently in organic synthesis [47]. By altering the R-group, the resulting precursor polymers are soluble in almost all organic solvents, so all types of characterisation techniques can be applied (e.g. spincoating) [48]. Due to the flexibility of the sulphinyl route, monomers with electron withdrawing and electron donating [49] substituents can be polymerised. Moreover, unlike the Wessling-Zimmerman route, also polymerisation of the monomers with extented aromatic systems, like the 2,6-naphtalene and the 4,4'-biphenyl derivatives is feasible [50]. Partial reduction or oxidation of the sulphinyl group in the precursor can lead to a conjugated polymer with restricted conjugation length. Due to the higher elimination temperatures of obtained sulphanyl (S) and sulphonyl ($S(O)_2$) functionalities respectively, careful tuning of the elimination conditions can lead to a selective removal of the sulphinyl groups [51]. The elimination mechanism is considered to take place via a *syn*-elimination (via a 5-ring) in which the intermediate has a planar structure. For this intermediate, two transition states, leading towards a *cis* and *trans* double bond, are possible. Because of the steric hindrance of the eclipsed polymer chains in intermediate **A**, such a transition state is of higher energy than intermediate **B**, resulting in a selectivity towards all-*trans* vinylene bonds (Figure I.15, **I**). This process leads to the expulsion of sulphenic acids as the vinylene bond is formed [52]. The sulphenic acids which are split off are unstable [53] and immediately dimerise to give thiosulphinates with concomitant loss of water. The thiosulphinates disproportionate with the formation of thiosulphonates and disulphides (Figure I.15, **II**) [54]. These sulphur compounds are called elimination products in this study and will be discussed in detail in Chapter IV.

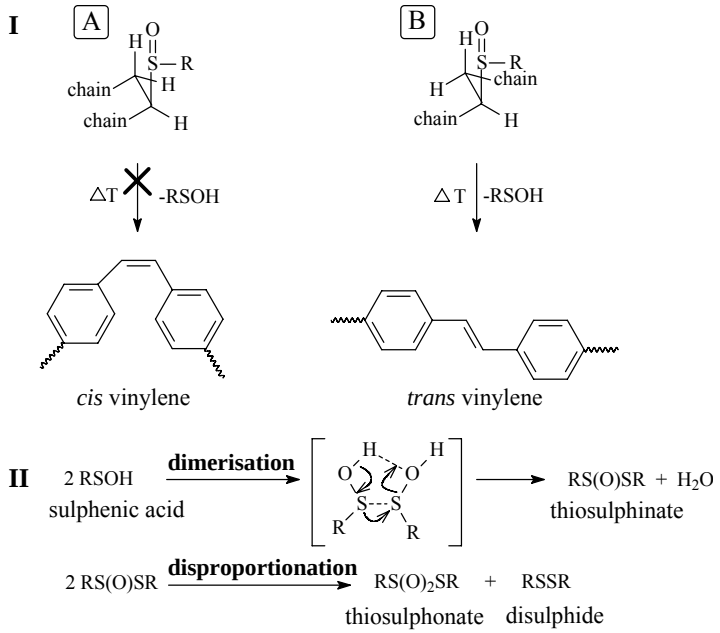

Figure I.15 *I: Mechanism of elimination. II: Dimerisation and disproportionation of sulphenic acids.*

I.D Aim of the thesis

The principal aim of this project is to get a deeper insight in the processes and phenomena that occur during the conversion step (Figure I.14, **step 3**) from a precursor polymer to the conjugated material. The synthesis of the conjugated material is performed via available precursor routes, in which the conjugated polymer is obtained by a thermal elimination step at the end of the process. Sulphur containing functional groups, for instance xanthate groups, sulphinyl groups [36,55] or sulphonyl groups, will be used in the thermal conversion step. It is to be expected that the quality and morphology of the final conjugated material will strongly depend on the elimination reaction. The importance of good control of this elimination step, providing the ultimate conjugated system, is confirmed by the numerous articles dealing with the effect of defects in the electroluminescent material [12]. Therefore, insight in the elimination process and in the occurrence of side reactions is of utmost importance. In order to monitor the elimination reaction of precursor polymers, several *in-situ* analytical techniques are combined (TGA, DIP-MS, *in-situ* FT-IR and UV-Vis spectroscopy, MTDSC,…).

I.E Questions concerning the elimination reaction

From previous experiments performed by de Kok *et al.* [56], it has become clear that the understanding of the last step in our precursor route, the thermal elimination step, is not straightforward. Results obtained thus far point in different directions, conclusions for the entire process are difficult to draw. Only structural information about the process can be obtained when the elimination can be evaluated in every stage. In the conversion of sulphinyl precursor polymers to PPV, different parts of chemical and physical reactions can be distinguished.

1) Evaporation of water.
2) Formation of vinylic bond and sulphenic acids: elimination.
3) Dimerisation and disproportionation of sulphenic acids.
4) Diffusion and evaporation of low molecular weight products out of the PPV matrix.

To unravel these 4 stages in the complex process of elimination, methods have to be developed which allow us to monitor the different aspects of the elimination process as a function of reaction conditions and time. With the knowledge gathered from these experiments, unwanted side-effects may be excluded, and suitable protocols can be designed to obtain thin layers of good quality, leading to better performing materials.

Several issues have been solved by de Kok *et al.*, although more experimental evidence, especially on the four parts of the elimination process, is necessary.

1) Evaporation of water

As is shown by TGA-IR measurements, water is present in the samples containing hygroscopic sulphinyl groups. In TGA, the samples show a weight loss around 100°C. Apart from the water already present on the precursor polymers, water is also formed during conversion.

2) Formation of vinylic bond and sulphenic acids: elimination

This is the actual conversion of the polymer into a conjugated system. This part of the process is influenced by several factors such as temperature, atmosphere and vacuum. Monitoring of this part of the process is complicated because also elimination products are present. Not only the IR analysis is disturbed by the elimination products, the plasticizing sulphur compounds will also have an influence on the elimination process itself. We also need to investigate the role of the elimination reaction, the matrix mobility and the other stages of the process, like diffusion of elimination products and evaporation of low molecular weight products on the formation of conjugated polymers.

3) Dimerisation and disproportionation of sulphenic acids

Sulphenic acids are unstable compounds which can undergo dimerisation and disproportionation to give other sulphur compounds. The rate of these reactions will also be influenced by temperature, time and conditions of atmosphere. The diffusion of the resulting sulphur compounds will be determined among others, by the matrix. Therefore the diffusion rate is varied as the reaction proceeds. Issues concerning the elimination products are: how is the conversion of sulphenic acids to other products affecting the elimination itself? What is the effect of the elimination products in a PPV matrix? At this stage, no indications can be found for the hypothesis that reaction of the sulphenic acid or radicals that are formed, affect the conjugated system. Can reactions of these elimination products with the conjugated system be excluded?

4) Diffusion and evaporation of low molecular weight products out of the PPV matrix

To obtain a purified PPV without the presence of elimination products, all low molecular weight products, including water, have to be removed. This removal involves diffusion of the elimination products to the surface and evaporation of products. Both of these physical processes are influenced by temperature and pressure. Moreover, the matrix of the reacting polymer is influenced by (the evaporation of) these plasticizers. A study with polymer films of standardised thickness could possibly give us a better insight in the processes that occur. The presence of low molecular weight products during elimination could jeopardise the stability of the material.

I.F Model compounds

In our study of the elimination behaviour from precursor polymers to conjugated materials, three different types of precursor polymers are used; PPV **(I)**, PTV **(II)** and OC_1C_{10}-PPV **(III)** with different kinds of eliminable groups **(P)** (Figure I.16).

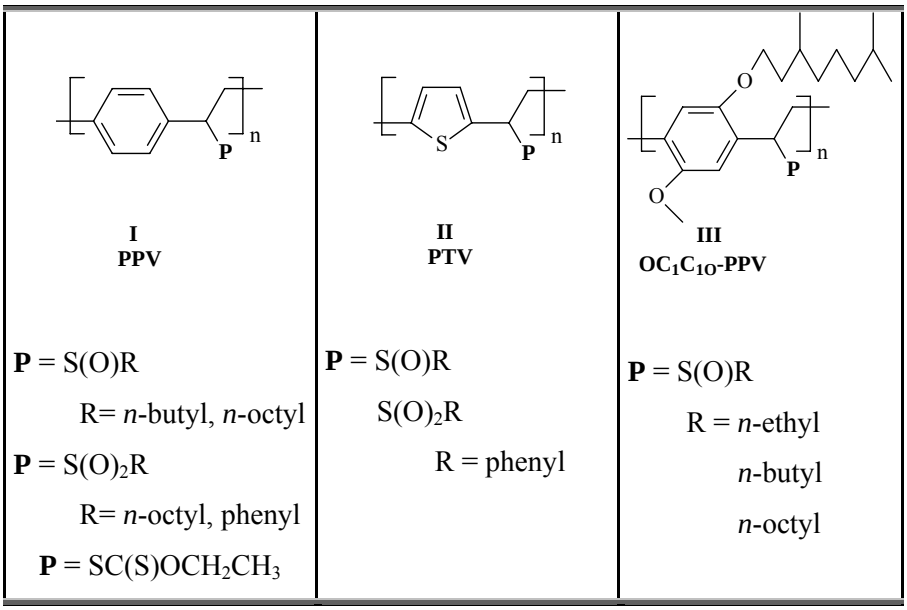

Figure I.16: *Different precursor polymers.*

In many cases, the conjugated polymer is insoluble. This insolubility gives conjugated polymers some attractive features for use in LEDs. For instance, many of the more efficient LEDs contain more than one layer. If the light emitting polymer layer is rendered insoluble, another layer such as an electron transport material can be easily deposited by solution processing (e.g. spincoating) without the polymer layer being removed. The fact that the conjugated polymer is insoluble implies a more easy patterning of a LED as the deposited material will be more stable to solvents that might be used in the patterning process. In addition, the conversion reaction has a second advantage in that it ensures that the processing solvent is adequately removed.

Poly (*p*-phenylene vinylene) (PPV) **(I)**, is an example of such an insoluble polymer and is therefore not easy to handle after the conversion has taken place. Nevertheless, this polymer is examined in our study because of its "crystalline morphology" and its principal structure as basis of all kinds of PPV derivatives (Chapter II, V).

Recently, increased attention is paid to poly (*p*-thienylene vinylene) (PTV) **(II)**, in view of the fact that this semiconducting material is well suitable for the application in plastic electronics. Since precursor approaches are also applicable in this case, study of the elimination behaviour of this PTV polymer is useful (Chapter II).

Much of the recent research of conjugated polymers for LEDs has concentrated on soluble conjugated polymers. This is in part due to the fact that soluble polymers are relatively easily processed. Soluble conjugated polymers also have disadvantages including removal of the processing solvent, so the more difficult preparation of multilayer devices is. The solubility of these PPV derivatives is imparted by the attachment of long lipophilic groups [57].

As an example of the soluble conjugated polymers, poly [2-(3',7'-dimethyloctyloxy)-5-methoxy-*p*-phenylene vinylene] (OC_1C_{10}-PPV) **(III)** is studied. This dialkoxy substituted PPV derivative is still soluble in lots of organic solvents, even after conversion to the conjugated polymer, in contrast to the pure PPV polymer. The alkoxychains are placed in a random position on the polymer backbone. Because this polymer is soluble during the whole process, it offers extra possibilities in this field of research. It is also a workhorse in all kinds of development of device application (Chapter III, IV).

I.G Outline of the thesis

Chapter II investigates the formation of PPV, as a model system, from a PPV precursor polymer with sulphinyl as well as sulphonyl eliminable groups. This chapter also discusses the *in-situ* analytical techniques we have used to study the conversion process with (ThermoGravimetric Analysis (TGA), Direct Insert Probe Mass Spectrometry (DIP-MS), *in-situ* Fourier Transform Infrared Spectroscopy (FT-IR) and *in-situ* Ultraviolet Visible Spectroscopy (UV-Vis)).

Also the elimination behaviour of PTV copolymers with sulphinyl and sulphonyl eliminable groups is discussed.

In Chapter III, the elimination behaviour of the OC_1C_{10}-PPV polymer, as working horse for the conversion, is fully examined with *in-situ* analytical techniques. Chapter IV presents a kinetic study of the conversion of the OC_1C_{10}-PPV precursor polymer with *in-situ* UV-Vis spectroscopy and *in-situ* FT-IR spectroscopy. Modulated Temperature Differential Scanning Calometry (MTDSC) is used to get a deeper insight in the mechanism of the elimination process of the OC_1C_{10}-PPV precursor polymer.

The final chapter, Chapter V, shows an evaluation of the possibilities the xanthate group offers in the synthesis of PPV. For this purpose, three different monomers, combining sulphinyl and xanthate functionalities were synthesised and polymerised by us. Once the precursor polymers were formed, the thermal conversion of a xanthate PPV precursor polymer and a sulphinyl PPV precursor oligomer, synthesised via a modified sulphinyl precursor route, was studied with *in-situ* analytical techniques.

I.H References

[1] J.W. Blatchford, A.J. Epstein, *Am. J. Phys.,* 64 **(1996)** 120.

[2] J.-L. Brédas, G.B. Street, *Acc. Chem. Rev*., 18 **(1985)** 309.

[3] a) H. Shirakawa, E.J. Louis, A.G. Macdiarmid, C.K. Chiang, A.J. Heeger, *J. Chem. Soc., Chem. Commun.,* **(1997)** 578; b) C.K. Chiang, C.R. Fincher, Y.W. Park, A.J. Heeger, H. Shirakawa, E.J. Louis, S.C. Gau, A.G. Macdiarmid, *Phys. Rev. Lett.,* 39 **(1997)** 1098.

[4] a) P. Nigrey, D. MacInnes, D. Nairns, A.G. Macdiarmid, A.J. Heeger, *J. Electrochem. Soc.,* 128(8) **(1981)** 1651; b) A. Wirsén, *"Electroactive Polymer Materials",* Technomic publishing AG, Switzerland, **(1987)**; c) M.G. Kanatzidis, *C&EN*, 3 **(1990)** 36; d) J. Miller, *Adv. Mater.,* 5(9) **(1993)** 671; e) S. Roth, *"One-Dimensional Metals",* Weinheim VCH, **(1995)** 209.

[5] a) J.J.M. Halls, C.A. Walsh, N.C. Greenham, E.A. Morsedlia, R.H. Friend, S.C. Moratti, A.B. Holmes, *Nature,* 376 **(1995)** 498; b) G. Yu, J. Gao, J.C. Hummelen, F. Wudl, A.J. Heeger, *Science*, 270 **(1995)** 1789; c) R.F. Service, *Science,* 269 **(1995)** 91; d) L. Dai, *J.M.S.-Rev. Macrom. Chem. Phys.,* C39(2) **(1999)** 273; e) G.G. Wallace, P.C. Pastoor, D.L. Offices, C.O. Too, *Chemical Innovation,* april **(2000)** 15; f) L. van der Ent, *Kunststof magazine,* april(3) **(2001)** 38.

[6] J.H. Burroughes, D.D.C. Bradley, A.R. Brown, R.N. Marks, K. Mackay, R.H. Friend, P.L. Burn, A.B. Holmes, *Nature,* 347 **(1990)** 539.

[7] a) M. Herold, J. Gmeiner, M. Schwoerer, *Acta. Polym.,* 45 **(1994)** 392**;** b) G. Gustafsson, Y. Cao, G.M. Treacy, F. Klavetter, A. Colaneri, A.J. Heeger, *Science,* 357 **(1992)** 477.

[8] a) J. Roncali, *J. Chem. Rev.,* 97 **(1997)** 173 ; b) J.-L. Brédas, J. Cornil, A.J. Heeger, *Adv. Mater.,* 8 **(1996)** 447.

[9] R. Friend, D. Bradley, A. Holmes, *Physics World,* november **(1992)** 42.

[10] O. Schafer, A. Gmeiner, J. Pommerehne, W. Guss, H. Vestueler, H.Y. Tak, H. Bassler, C. Schmidt, G. Lussem, B. Schartel, V. Stumpflen, J.H. Wendorff, S. Spiegel, C. Moller, H.W. Spies, *Synth. Met.,* 82 **(1996)** 1.

[11] a) D. Braun, A.J. Heeger, *Appl. Phys. Lett*., 58 (**1991)** 1982**;** b) N.C. Greenham, S.C. Morati, D.D.C. Bradley, R.H. Friend, O.L. Burn, A.B. Holmes, *Nature*, 365 (**1993)** 629**;** c) C. Zhang, H. von Seggern, K. Pakbaz, B. Krabel, H.W. Schmidt, A.J. Heeger, *Synth. Met*., 62 (**1994)** 35; d) I.N. Kang, D.H. Hwang, H.K. Shim, Y. Zyung, J.J. Kim, *Macromolecules*, 29 (**1996)** 165**;** e) D. Braun, E.G.J. Staring, R.C.J.E. Demandt, G.L.J. Rikken, Y.A.R.R.

Kessener, A.H.J. Venhuizen, *Synth. Met*., 66 (**1994)** 75; f) D.D.C. Bradley, *Adv. Mater.,* 4 (**1992)** 756; g) F. Wudl, S. Hoger, C. Zhang, K. Pakbaz, A.J. Heeger*, Polym. Prepr*., 34 **(1993)** 197; h) S. Soi, M. Kuwabara, T. Noguchi, T. Ohnishi, *Synth. Met*., 55 **(1993)** 4174.

[12] M. Herold, J. Gmeiner, W. Reiss, W. Schwoerer, *Synth. Met.,* 76 **(1996)** 109.

[13] a) R.A. Wessling, R.G. Zimmerman, *U.S. Patent,* **(1968)** 3401152; b) R.A. Wessling, *J. Polym. Sci., Polym. Symp.,* 72 **(1985)** 55.

[14] a) B.R. Cho, M.S. Han, Y.S. Suh, K.J. Oh, S.J. Jeon, *J. Chem. Soc., Chem. Commun.,* **(1993)** 564; b) B.R. Cho, Y.K. Kim, M.S. Han, *Macromolecules*, 31 **(1998)** 2089.

[15] a) I. Murase, T. Ohnishi, T. Noguchi, *U.S. Patent,* **(1985)** 4.528.118; b) I. Murase, T. Ohnishi, T. Noguchi, M. Hiroka, *Polym. Commun.,* 25 **(1984)** 327.

[16] a) R.W. Lenz, C.C. Han, J. Stenger-Smith, F. Karasz, *J. Pol. Sc. Part A: Pol. Chem.,* 26 **(1988)** 3241; b) D.A. Halliday, P.L. Burn, R.H. Friend, A.B. Holmes, *J. Chem. Soc., Chem. Commun.,* **(1992)** 1685.

[17] a) D.R. Gagnon, J.D. Capistran, F.E. Karasz, R.W. Lenz, S. Antoun, *Polymer,* 28 **(1987)** 567; b) G. Montaudo, D. Vitalini, R.W. Lenz, *Polymer*, 28 **(1987)** 837; c) 16a.

[18] a) 15a; b) M. Hirooka, I. Murase, T. Gnishiand, T. Noguchi, *Frontiers of Macromolecular Sciences* (T. Saegusa *et al.*, Eds.), Blackwell Scientific, **(1989)** 425.

[19] J.B. Schlenoff, L.-J. Wang, *Macromolecules,* 24 **(1991)** 6653.

[20] V. Massardier, T. van Hoang, A. Guyot, *Polym. For Adv. Technol.,* 5 **(1995)** 656.

[21] H.V. Shah, A.R. Mc. Ghie, G.A. Arbuckle, *Thermochimico Acta,* 287 **(1996)** 319.

[22] M. Herold, J. Gmeiner, M. Schwoerer, *Polym. Adv. Technol.,* 10 **(1999)** 251.

[23] a) 21; b) H.V. Shah, G.A. Arbuckle, *Macromolecules,* 32 **(1999)** 1413.

[24] A. Beerden, D. Vanderzande, J. Gelan, *Synth. Metals,* 52 **(1992)** 387.

[25] a) V. Massardier, A. Guyot, V.H. Tran, *Polymer,* 35(7) **(1994)** 1561; b) V. Masssardier, O. Sagnes, J.C. Dubois, V.H. Tran, A. Guyot, *French Patent,* **(1991)** 9104721.

[26] R.O. Garay, V. Baier, C. Bubeck, Müllen, *Adv. Mater.,* 5 **(1993)** 561.

[27] A. Marletta, D. Goncalves, N. Oliviera, R.M. Faria, F.E.G. Guimaraes, *Adv. Mater.,* 12(1) **(2000)** 163.

[28] a) M. Herold, J. Gmeiner, C. Drummer, M. Schwoerer, *J. Mater. Sci.,* 32 **(1997)** 5709; b) W. Brutting, M. Meier, M. Herold, S. Karg, M. Schwoerer, *Synth. Met.,* **(1997)** 163.

[29] H.G. Gilch, W.L. Wheelwright, *J. Polym. Sci. Part A: Polym. Chem.,* 4 **(1966)** 1337.

[30] a) B.R. Hsieh, H. Antoniadis, D.C. Bland, W.A. Feld, *Adv. Mater.,* 7(1) **(1995)** 36; b) P.L. Burn, A.W. Grice, A. Tajbakhsh, D.D.C. Bradley, A.C. Thomas, *Adv. Mater.,* 9(15) **(1997)** 1171; c) Y.Yu, A.C. Vanlaeken, H. Lee, B.R. Hsieh, *Pol. Prepr.,* 39(1) **(1998)** 161; d) W.J. Swatos, B. Gordon, *Pol. Prepr.,* 31(1) **(1990)** 505.

[31] L. Hontis, V. Vrindts, L. Lutsen, D. Vanderzande, J. Gelan, *Polymer,* 42 **(2001)** 5793.

[32] B.R. Hsieh, Y. Yu, A.W. Forsythe, G.M. Schaaf, W.A. Field, *J. Am. Chem. Soc.,* 120 **(1998)** 231.

[33] S. Iwatsuki, M. Kubo, T. Kumeuchi, *Chem. Lett.,* **(1991)** 1071.

[34] H.H. Horhold, J. Opferman, *Die Makromol. Chemie,* 131 **(1990)** 105.

[35] H. Becker, H. Spreitzer, K. Ibrom, W. Kreuder, *Macromolecules,* 32 **(1999)** 4925.

[36] a) S. Son, A. Dodabalapur, A.J. Lovinger, M.E. Galvin, *Science,* 269 **(1995)** 376; b) S. Son, A.J. Lovinger, M.E. Galvin, *Polym. Mater. Sci. and Engin.,* 72 **(1995)** 567.

[37] C.H. Depuy, R.W. King, *Chem. Rev.,* 60 **(1990)**.

[38] H.R. Nace, *Org. React.,* 12 **(1962)** 57.

[39] a) 36a; b) S.-C. Lo, A.K. Sheridan, I.D.W. Samuel, P.L. Burn, *J. Mater. Chem.,* 10 **(2000)** 275.

[40] G. Arbuckle-Keil, Y. Liszewski, J. Peng, B. Hsieh, *Pol. Prepr.,* 41(1) **(2000)** 826.

[41] G. Arbuckle-Keil, Y. Liszewski, J. Wilking, B. Hsieh, *Pol. Prepr.,* 42(1) **(2001)** 306.

[42] J. March, *Advanced Organic Chemistry J. Wiley & Sons* New York, 4th. Ed., **(1992)** 1007.

[43] S.-C. Lo, L.-O. Palsson, M. Kilitziraki, P.L. Burn, I.D.W. Samuel, *J. Mater. Chem.,* 11 **(2001)** 2228.

[44] W.J. Michell, C. Pena, P.L. Burn, *J. Mater. Chem.,* 12 **(2002)** 200.

[45] A. Issaris, D. Vanderzande, J. Gelan, *Polymer,* 38 **(1997)** 2571.

[46] A. Issaris, D. Vanderzande, J. Gelan, *Macromol. Symp.,* 125 **(1997)** 189.

[47] a) T. Durst, *Comprehensive Organic Chemistry,* Vol. 3, Permagon Press, Oxford, **(1997)** 121; b) B.M. Trost, T.N. Salzmann, K.J. Hiroi, *J. Am. Chem. Soc.,* 98 **(1976)** 4887; c) B.M. Trost, *Acc. Chem. Res.,* 11 **(1978)** 453.

[48] A.J.J.M van Breemen, *Ph. D. Dissertation,* **(1999)**, Limburgs Universitair Centrum, Diepenbeek, België.

[49] M. Van Der Borght, D. Vanderzande, J. Gelan, *J. Synth. Met.,* 84 **(1997)** 399.

[50] M. Van Der Borght, D. Vanderzande, J. Gelan, *Polymer,* 39 **(1998)** 4174.

[51] M. de Kok, *Ph. D. Dissertation,* **(1999)**, Limburgs Universitair Centrum, Diepenbeek, België.

[52] C.A. Kingsburry, D.J. Cram, *J. Am. Chem. Soc.,* 82 **(1960)** 1810; b) J.R. Shelton, K.E. Davis, *Int. J. Sulfur Chem.,* 8 **(1973)** 205; c) T. Yoshimura, E. Tsukurimichi, Y. Iizuka, H. Mizuno, H. Isaji, C. Shimasaki, *Bull. Chem. Soc. Jap.,* 62 **(1989)** 1891.

[53] a) 52; b) B.M. Trost, K.K. Leung, *Tetrahedron Lett.,* 48**(1975)** 4197.

[54] a) P. Koch, E. Ciuffarin, A. Fava, *J. Am. Chem. Soc.,* 92 **(1970)** 5971; b) J.L. Kice, J.P. Cleveland, *J. Am. Chem. Soc.,* 95 **(1973)** 109; c) F.A. Davis, J.A. Jenkins, R.L Billmers, *J. Org. Chem.,* 51 **(1986)** 1033.

[55] F. Louwet, D. Vanderzande, J. Gelan, J. Mullens, *Macromolecules,* 28 **(1995)** 1330.

[56] M.M. de Kok, A.J.J.M. van Breemen, R.A.A. Carleer, P.J. Adriaenssens, J.M. Gelan, D.J. Vanderzande, *Acta Polym.,* 50 **(1999)** 28.

[57] A. Kraft, A.C. Grimsdale, A.B. Holmes, *Angew. Chemie, Int. Ed.,* 37 **(1998)** 402.

II

Study of thermal elimination and degradation processes of PPV precursor polymers and modified PTV precursor copolymers

II.A Thermal elimination and degradation of sulphinyl PPV precursor polymers

II.A.1 Introduction

As was discussed in Chapter I, the microstructure of the conjugated polymers is of major importance for their performance in the final applications. Quality and morphology of the conjugated system strongly affects the performance of the material in LEDs. Both these properties are strongly influenced by the elimination reaction. A large number of published papers deal with the conversion of sulphonium PPV precursor polymers [1]. The broad range of elimination conditions that are defined in these reports, however, underline the difficulty of monitoring the conversion reaction. For the sulphinyl PPV precursor polymers the elimination was performed at 280°C based on TGA analysis [2], because other tools for studying the elimination reaction were not available at that time. A few years later, Margreet de Kok investigated the

elimination process in more detail by doing some *ex-situ* heating experiments [3]. A lot of questions, however, were not answered yet. This means that, in order to monitor the elimination reaction of sulphinyl PPV precursor polymers towards conjugated polymers, the use of several complementary *in-situ* analytical techniques is necessary.

With *in-situ* techniques, we are also able to study the degradation process of the conjugated PPV polymers. Poly(*para*-phenylene vinylene), PPV as the active layer in LEDs, is subjected to several physical and chemical phenomena, which could affect the stability of the material [4]. As an example, the polymeric material is subjected to an applied bias that it has to withstand, and that should help in the transport of electrons and holes. Also the excited states which are formed in the process of electroluminescence, show a special reactivity. For instance, the best documented excited state reaction is the oxidation of double bonds to carbonyl sites. These functionalities act as quenching sites and severely lower device performance [5]. Another observed phenomenon is the burning in of the metallic contact into the organic active material, which can lead to an instability of the material at the interface in LEDs [6]. The electrochemical reaction between the electrodes, leading to corrosion and microstructural changes in both electrode materials, is suspected to be one of the causes for this degradation [7]. Also, the conjugated material is exposed to the generated light. Together with Joule heating, this could affect the performance of the material. It is difficult to discriminate between all the contributions that may lead to a bad performing device in the operating LED, neither of these intrinsic properties can be determined separately. However, restricting ourselves to the thermal degradation of polymers, a simple set of experiments can lead to a reasonable explanation of the behaviour of PPV upon elevated temperatures. An experimental difficulty, however, is the exact determination of temperatures inside the material, because Joule heating will increase the temperature very locally. Temperatures up to 500ºC have been reported. At these temperatures chemical changes can occur, resulting in destruction of the conducting material, and leading to failure of the LED. In this chapter we will focus on the thermal elimination and degradation reaction of PPV under inert atmosphere. Two precursor polymers will be investigated: a *n*-butyl- and a *n*-octyl-sulphinyl PPV precursor polymer. These precursor polymers can be converted to the conjugated poly(*para*-phenylene vinylene) (PPV) by thermal elimination of the sulphur groups.

II.A.2 Thermal analysis: TGA and DIP-MS

Two techniques were used to study the thermal stability of the precursor polymers. The first technique is ThermoGravimetric Analysis (TGA), a second technique is Direct Insert Probe Mass Spectrometry (DIP-MS). In TGA, the weight loss is recorded as a function of temperature. The conversion from a sulphinyl PPV precursor polymer to a conjugated polymer, as shown in Figure II.1, can easily be monitored with TGA, because the conversion reaction is accompanied by weight loss due to evaporation of the elimination products.

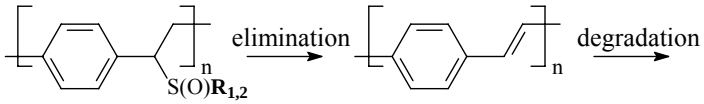

R_1 = *n*-butyl
R_2 = *n*-octyl

Figure II.1: *Elimination and degradation of PPV polymers.*

The TGA analysis is carried out on a TA INSTRUMENT 951 thermogravimetric analyser with a continuous flow of argon (80 ml/min) and a heating rate of 10°C/min. Samples (10 mg) of precursor polymers are inserted in the solid state. The weight of the sample is measured in real-time, while constantly increasing the temperature. To determine the temperature of maximum weight loss, also the derivative of weight loss to the temperature is calculated and depicted in Figure II.2. For each precursor polymer weight loss is observed in three temperature regions. Firstly, a relatively small loss of weight is observed just below 100°C, which is assigned to evaporation of water, present on the hygroscopic sulphinyl groups [8]. Above 100°C, two major steps of weight loss are visible, the first step (max. at 146°C for the *n*-butyl-S(O) **(1)**, max. at 256°C for the *n*-octyl-S(O) **(2)**) is related to the elimination of the S-groups itself and to the evaporation of the elimination products that are liberated during the elimination process. If we compare the *n*-butyl-sulphinyl precursor **(1)** with the *n*-octyl-sulphinyl precursor **(2)** (an increase in weight of the side groups), this will lead to an increase of the boiling points of the corresponding elimination products which are set free during the elimination process. The second major weight loss with a max. at 546°C (for **1**) and 549°C (for **2**) accounts for the degradation of the conjugated PPV polymer, which is in

agreement with the literature data for PPV [9]. In conclusion, the elimination and degradation behaviour of the polymers is the same. But, there are some differences between the elimination and degradation temperatures. The experimental residual weight percentage after elimination (48.8 % for the *n*-butyl **(1)** and 45 % for the *n*-octyl **(2)**) is approximately in accordance with the theoretical residual values of weight (49 % and 39 % respectively). The discrepancies between theoretical and experimental values for derivative **2** may be due to incomplete elimination or incomplete evaporation of the elimination products.

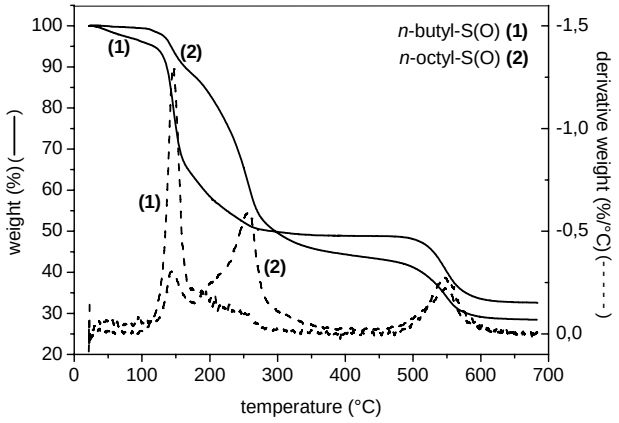

Figure II.2: *TGA spectra of poly[1,4 phenylene-(1-n-butyl-sulphinyl)-ethylene]* ***(1)*** *and poly[1,4 phenylene-(1-n-octyl-sulphinyl)-ethylene]* ***(2)*****.**

Note that we have to be careful with the interpretation of the results obtained. We do not monitor the elimination of the sulphinyl group or the degradation of the conjugated system itself, but only keep track of weight loss and thus the evaporation of the elimination or degradation products that are liberated during the elimination or degradation process respectively. If the reaction product has a boiling point higher than the temperature at which the elimination reaction occurs, the observed weight loss does not agree with the real reaction temperature.

A second important technique we use in the study of the thermal stability of *n*-alkyl-sulphinyl PPV polymers and to get information about the structure of the elimination products, is thermal analysis by Direct Insert Probe Mass Spectrometry (DIP-MS). The DIP-MS analysis is carried out on a FINNIGAN TSQ 70. In this technique, the precursor polymer is first dissolved in a volatile solvent ($CHCl_3$) and is then applied on the heating element of the probe. After evaporation, a thin film is formed. The probe is inserted in the mass spectrometer and heated at 10°C/min, to ensure a good comparison with TGA data. The fragments that are liberated from the polymer while heating are bombarded with electrons (Electron Impact) and detected. The electron energy of the electroionisation is 70 eV.

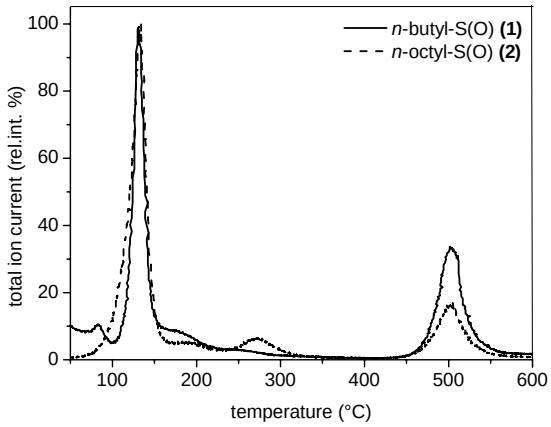

Figure II.3: *DIP-MS thermogram of poly[1,4 phenylene-(1-n-butyl-sulphinyl)-ethylene]* ***(1)*** *and poly[1,4 phenylene-(1-n-octyl-sulphinyl)-ethylene]* ***(2)*****.**

The total reconstructed ionchromatogram depicted in Figure II.3, in which the total ion current (TIC) is plotted versus increasing temperature, shows two signals. The first signal shows a maximum at a temperature of 131°C for the *n*-butyl-S(O) **(1)** and at 134°C for the *n*-octyl-S(O) **(2)**. The fragments observed in the mass spectrum of the first peak are consistent with dimerisation and disproportionation processes of sulphenic acids (Figure I.15), thus the elimination itself (Table II.1).

Table II.1: *Fragmentation (EI) of elimination products.*

n-butyl-sulphinyl **(1)**		*n*-octyl-sulphinyl **(2)**	
m/z	fragment (rel.int.)	*m/z*	fragment (rel.int.)
210	$C_4H_9S(O)_2SC_4H_9^+$ (0.3)	290	$C_8H_{17}SSC_8H_{17}^+$ (2)
194	$C_4H_9SS(O)C_4H_9^+$ (2)	194	$SS(O)C_8H_{17}^+$ (5)
178	$C_4H_9SSC_4H_9^+$ (3)	161	$S(O)C_8H_{17}^+$ (54)
138	$HSS(O)C_4H_9^+$ (13)	145	$SC_8H_{17}^+$ (68)
105	$S(O)C_4H_9^+$ (27)	71	$OC_4H_7^+$ (70)
89	$SC_4H_9^+$ (17)	63	CH_3SO^+ (27)
63	CH_3SO^+ (18)	57	$C_4H_9^+$ (100)
57	$C_4H_9^+$ (100)	43	$C_3H_7^+$ (71)

The second signal in the ionchromatogram is related to the degradation of the conjugated polymer. The total reconstructed ionchromatogram shows a second maximum at a temperature of 501°C for the *n*-butyl-S(O) **(1)** and at 502°C for the *n*-octyl-S(O) **(2)**. For all precursors, the mass spectra of the fragments in the second peak are consistent with the degradation of the conjugated PPV system [3a]. Thermogravimetric data show that after degradation a relatively high rest fraction is present at 650°C (*n*-butyl: 32.6 % and *n*-octyl: 28.6%). This rest fraction is probably formed via crosslinking and formation of polyaromatic hydrocarbons [10] through isomerisation and aromatisation processes (Figure II.13).

The difference between TGA and DIP-MS analysis is the atmosphere in which the experiment is carried out. TGA is performed in argon atmosphere, whereas DIP-MS experiments are executed in high vacuum conditions (10^{-6} mmHg). The high vacuum in the mass spectrometer causes a weight loss and a corresponding ion current at lower temperatures, because the evaporation is faster compared with a heating process in argon atmosphere (TGA). In DIP-MS, an apparent lower thermal stability can be derived for most functionalities. Comparison of the DIP-MS observations with the TGA data indicates that under argon flow the elimination reaction and evaporation of the elimination products

are kinetically separated, more so for the *n*-octyl than for the *n*-butyl derivative. Consequently, evaporation and elimination are no longer separated in the high vacuum conditions in DIP-MS [11]. As a result, a signal at the same temperature is observed in DIP-MS measurements, whereas in TGA, two signals are visible. Hence the elimination temperature retrieved from DIP-MS is more realistic than that obtained from TGA.

II.A.3 In-situ FT-IR spectroscopy

II.A.3.a Set-up of the apparatus

Four years ago, all measurements that have been performed to study the thermal elimination reaction of sulphinyl PPV precursor polymers were carried out *ex-situ* [2]. By doing so, a first attempt was made to monitor the elimination process by the change of IR absorbance during the elimination process. *n*-Octyl- and *n*-butyl-sulphinyl PPV precursor polymers were applied from $CHCl_3$ solutions to a KBr pellet. The polymer film was then inserted in an oven which was preheated at a certain temperature. After a period of time the sample was removed from the oven and analysed by FT-IR spectroscopy. Attention should be paid to the fact that the samples need a heating period before they reach the temperature of the oven. This experimental approach was therefore a study of qualitative elimination behaviour rather than a quantitative one. The main disadvantages of this method are the time-consuming experiments and the errors introduced by this discontinuous monitoring, e.g. the exact time evolution of the signals appearing and disappearing during the elimination reaction. Also, no direct information about phenomena occurring during the elimination reaction are available here.

Therefore, a set-up was assembled which allowed *in-situ* monitoring of the elimination process by FT-IR spectroscopy. In a small heatable cell (Harrick High Temperature cell from Safir) (HHT-cell), shown in Figure II.4, equiped with sodium chloride windows on both ends, a KBr pellet (diameter 25 mm) with a polymer film can be heated. The temperature of the sample can be measured in the cell by a thermocouple, connected with a Watlow temperature controller (serial number 999, dual channel), which is controlled by a computer. A computer program is available to put the desired heating program in a file and

to register the time-temperature data during the measurement. The volume of the HHT-cell is much smaller in comparison with the oven used for the *ex-situ* measurements. In the HHT-cell we also have the opportunity to do the elimination reactions under an inert atmosphere as well as under vacuum conditions. The achieved vacuum is better than in the *ex-situ* measurements: 2.10^{-2} mbar instead of 5 mbar. In this HHT-cell also a water cooling system is present. This is very important for the lifetime of the three heating elements (230 V-100 W) and to prevent that the temperature of the metal block, controlled by another thermocouple, would get too high (Figure II.4). There is a difference in temperature between the metal part of the HHT-cell and the sample itself, depending on the atmosphere used. We directly measure the temperature of the sample itself by one of the two available thermocouples.

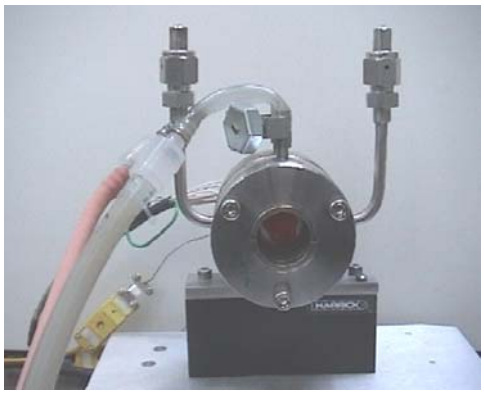

Figure II.4: *Infrared Harrick High Temperature cell (HHT-cell).*

This high temperature cell can be fastened on the bottom and put in the beam of a FT-IR spectrometer (Perkin Elmer Spectrum One Spectrometer) (Figure II.5). "Timebase Software", supplied by Perkin Elmer, is used to integrate the regions of interest. So, we are now able to do *in-situ* thermal elimination reactions with FT-IR spectroscopy.

The elimination process of sulphinyl PPV precursor polymers is considered to proceed via a *syn*-elimination (concerted 5-ring), resulting in a selectivity for all-*trans* vinylene double bonds, as shown in Figure II.6 [12]. In IR, we follow the decrease of the sulphinyl absorbance at 1038 cm^{-1}, because this absorbance has a large extinction coefficient and changes in direct relation

with the elimination. This sulphinyl eliminable group is disappearing during the elimination process. At the same time, we also follow the increase of the IR absorbance of the *trans* vinylene double bond at 965 cm^{-1}, which is formed during the elimination process.

Figure II.5: *Harrick High Temperature cell (HHT-cell) inserted in the beam of the FT-IR spectrometer.*

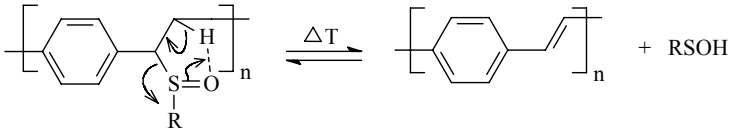

sulphinyl PPV precursor polymer conjugated PPV polymer

Figure II.6: *Syn-elimination of sulphinyl PPV precursor polymers to a conjugated PPV polymer.*

II.A.3.b The elimination and degradation reaction of PPV (precursor) polymers studied with in-situ FT-IR spectroscopy

All *in-situ* experiments using a FT-IR spectrometer were performed using the following procedure: A KBr pellet with a diameter of 25 mm is used. From this blanco KBr pellet, a background spectrum is taken at ambient temperature. 6 mg precursor polymer is dissolved in 1 ml $CHCl_3$. With this solution a polymer film is spincoated on the KBr pellet using a very small rotation speed (500 rpm). Afterwards the sample (KBr pellet with polymer film) can be inserted in the HHT-cell where the elimination reaction is carried out.

To obtain information about the temperature range in which the elimination and degradation reaction take place, an *in-situ* heating reaction under a continuous flow of nitrogen is performed on the *n*-butyl-sulphinyl PPV precursor polymer at 2°C/min starting from ambient temperature up to 450°C. The elimination from precursor to conjugated PPV polymer can be followed via the formation of the *trans* vinylene double bond (965 cm^{-1}) as well as by the vanishing of the IR absorbances of the sulphinyl group (1038 cm^{-1}) and the CH_2 asymmetrical stretch (2925 cm^{-1}). The degradation of the conjugated PPV polymer can be followed by the disappearance of the *trans* vinylene double bond at 965 cm^{-1}. During elimination, we monitor the IR absorbance at a certain wavelength versus time using "Timebase Software". With our "Watlow" computer program, which is connected with the temperature controller, we are able to transform these time values into a temperature scale. Following this procedure, Figure II.7 A is obtained. The same curves are also available when measuring the area (with 2 basepoints) under a peak at a certain wavelength (not shown here).

The increase and decrease of the *trans* vinylene double bond absorption at 965 cm^{-1}, respectively elimination and degradation of the conjugated PPV polymer, and the decrease of the sulphinyl absorption at 1038 cm^{-1} and the alkyl absorption at 2925 cm^{-1} (elimination) versus increasing temperature are displayed in Figure II.7 A. The elimination for the *n*-butyl-sulphinyl PPV precursor polymer starts already at 65°C and is complete at 120°C. The IR absorbances of the sulphinyl group at 1038 cm^{-1} and the alkyl group at 2925 cm^{-1} have no detectable absorption anymore after elimination at 120°C. In the region between 120 and 350°C, there is a slight decrease in the absorbance of the double bond. This is not due to decomposition of the PPV material, but it is related to a thermochromic effect as was demonstrated by successive heat-cool cycles (paragraph III.H). At temperatures around 350°C (fast decrease in the absorbance at 965 cm^{-1}), degradation of the conjugated system occurs.

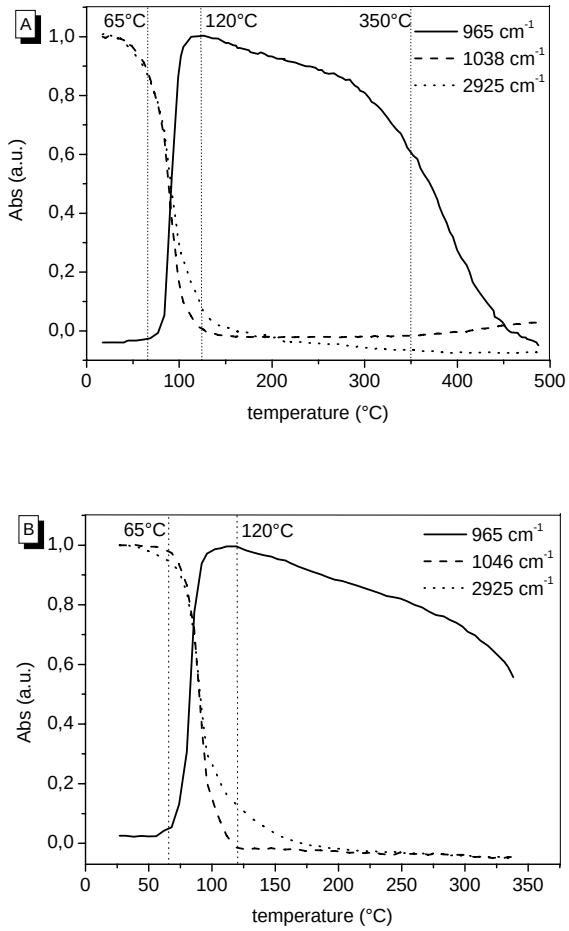

Figure II.7: *The absorbance at 965, 1038/1046 and 2925 cm^{-1} versus increasing temperature for the n-butyl-sulphinyl PPV precursor polymer (upper) and for the n-octyl-sulphinyl PPV precursor polymer (bottom).*

Identical results in elimination and degradation behaviour are obtained with the *n*-octyl-sulphinyl as eliminable group (Figure II.7 B), but as can be observed, the elimination and evaporation of the elimination products are kinetically separated for the *n*-octyl derivative, which is not the case for the *n*-butyl derivative. The absorbance at 2925 cm^{-1} decreases much slower compared to the absorbance at 1046 cm^{-1}, which means that it is more difficult for the

n-octyl elimination products to evaporate out of the polymer matrix, while the elimination reaction is complete at 120°C (the same temperature as for the *n*-butyl derivative). These results confirm the interpretation of the results obtained from TGA and DIP-MS.

Before heating, the sulphinyl PPV precursor polymer is a white solid product which turns into yellow during the elimination between 65 and 120°C. Due to the degradation of the conjugated polymer the fluorescent yellow color turns into dark brown at higher temperatures (> 350°C). Spectra of the *n*-butyl-sulphinyl PPV precursor polymer at ambient temperature and the conjugated PPV polymer at 120°C are shown in Figure II.8.

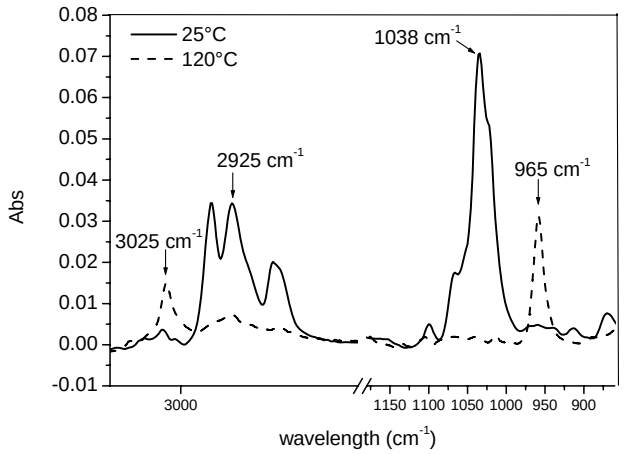

Figure II.8: *Enlarged part of the IR spectra before and after elimination of the n-butyl-sulphinyl PPV precursor polymer.*

The IR absorption peaks of the final product at 120°C are in agreement with similar PPV spectra, obtained via the sulphonium route [13]. No *cis* double bonds can be detected.

II.A.4 In-situ UV-Vis spectroscopy

Another analytical technique that gives insight in the elimination reaction is *in-situ* UV-Vis spectroscopy, by which the formation of the conjugated system itself can be evaluated. The UV absorption of the conjugated polymer is due to the π-π^* transition in the conjugated backbone and depends on the "effective" conjugation length [14].

II.A.4.a Set-up of the apparatus

The *in-situ* heating set-up is the same as in the FT-IR experiment (paragraph II.A.3.a), except for the fact that the HHT-cell is equiped with quartz windows instead of sodium chloride windows on both ends. In the middle of the cell a quartz disc (diameter 25 mm, thickness 3 mm), instead of a KBr pellet, can be heated and simultaneously measured.

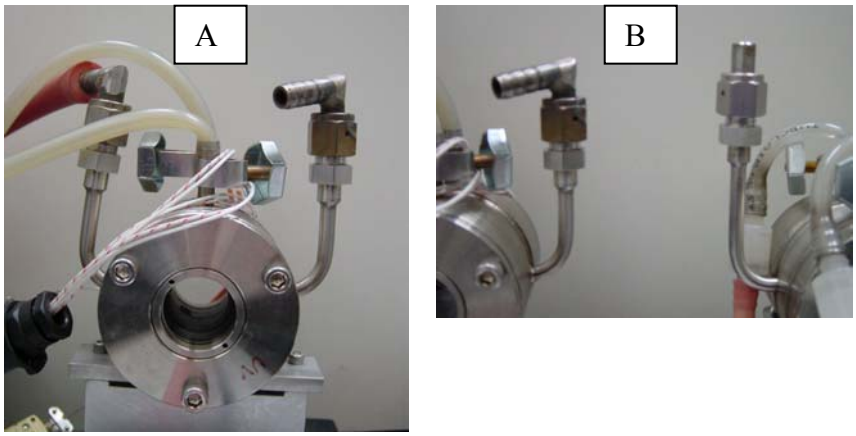

Figure II.9 A: A) *The specially adapted HHT-cell for doing elimination reactions in-situ with UV-Vis spectroscopy.* ***B)*** *The vacuum or nitrogen tube of the UV-HHT-cell (left) is shortened compared to that of the IR-HHT-cell (right).*

The HHT-cell is specially adapted so that it fits in the chamber of the CARY 500 UV-Vis-NIR spectrophotometer (interval 1 mm, scan rate 600 nm/min, continuous scan from 200 to 600 nm), which is also specially adapted by Varian to contain the HHT-cell. This equipment is shown in Figure II.9 A

and B. “Scanning Kinetics Software”, supplied by Varian, is used to measure the regions of interest. With this equipment we are able to study *in-situ* thermal elimination reactions by UV-Vis spectroscopy.

Figure II.9 B: *Harrick High Temperature cell (HHT-cell) positioned in the beam of the UV-Vis spectrophotometer.*

II.A.4.b The elimination and degradation reaction of PPV (precursor) polymers studied with in-situ UV-Vis spectroscopy

All UV-Vis experiments carried out *in-situ* are performed using the following procedure. First, a background spectrum is taken at ambient temperature from a blanco quartz disc. 6 mg precursor polymer is dissolved in 1 ml $CHCl_3$. The precursor polymer is then spincoated on a quartz disc at 1000 rpm. Subsequently, the spincoated quartz disc is put in the HHT-cell that can then be positioned in the beam of the UV-Vis spectrophotometer. Fully covering of the high temperature cell is necessary to start the measurement.

In the measurements a similar procedure is used as for FT-IR. The samples are heated at 2°C/min from ambient temperature up to 450°C. During the elimination step, a gradual red-shift is observed as oligomeric fragments start to form. In a further stadium, the absorption band becomes broad as the conjugation length increases (Figure II.10).

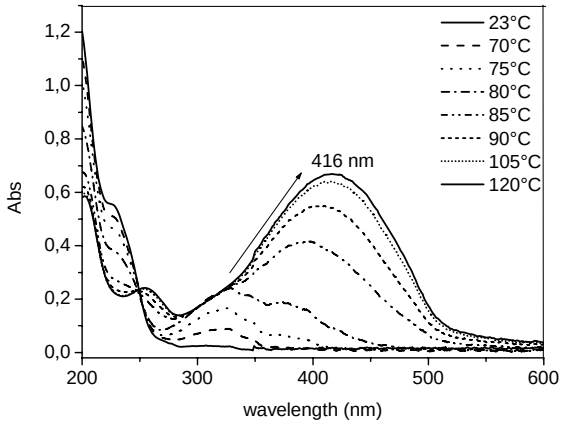

Figure II.10: *UV-absorption spectra of n-butyl-sulphinyl PPV precursor polymer (red-shift = elimination).*

The absorbance of the absorption maximum (λ_{max} = 416 nm) is measured as a function of temperature. Figure II.11 shows the formation of the conjugated system in a temperature range starting at 65 untill 120°C, as the absorbance at 416 nm increases.

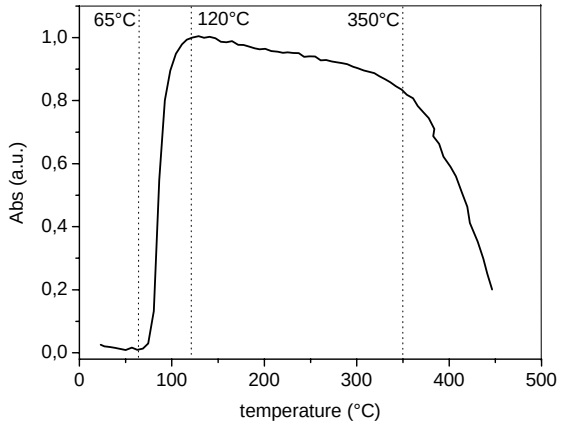

Figure II.11: *The absorbance of the absorption peak at 416 nm as a function of increasing temperature for the n-butyl-sulphinyl PPV precursor polymer.*

Between 120 and 350°C, the slight decrease in absorbance is related to a thermochromic effect as was demonstrated by successive heat-cool cycles. After 350°C, degradation of the conjugated PPV polymer occurs, leading to a steep decrease in the absorbance at the absorption maximum as a function of temperature. This interpretation is also confirmed by *in-situ* FT-IR for which a clear decrease of the absorption at 965 cm^{-1} is observed in the same temperature range. The striking similarity with the results obtained with FT-IR demonstrates clearly that both techniques are complementary. The strong hypsochromic shift (blue-shift) at temperatures around 350°C is interpreted as the degradation of the conjugated system which leads to a reduction of the "effective" conjugation length [15], shown in Figure II.12. The absorption peak around 250 nm is in agreement with the formation of phenantrene units as phenantrene has an absorption from 200 untill 300 nm [4] and causes some flattening of the signal at lower wavelengths upon degradation (Figure II.12, 450°C).

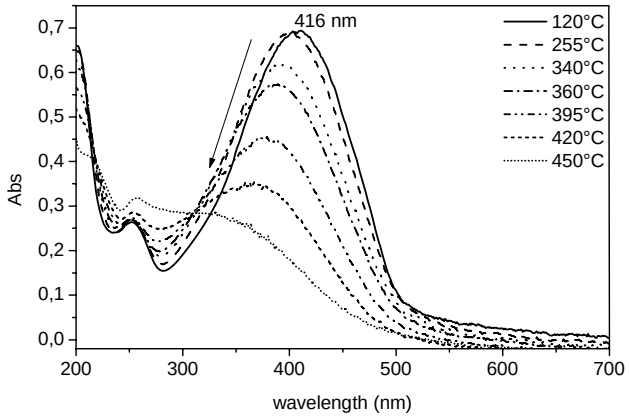

Figure II.12: *UV-absorption spectra of n-butyl-sulphinyl PPV precursor polymer (blue-shift = degradation).*

This interpretation is based on the phenantrene formation as key step in the degradation of PPV. In this proposed theory it is assumed that by the formation of phenantrene units and simultaneous reduction of the vinylene double bond the resulting saturated ethane bridge becomes the weakest spot and cleavage of this bond is the initial step in the degradation of the backbone (Figure II.13).

Evaporation of these degradation products occur at much higher temperatures as can be derived from TGA and DIP-MS measurements (550°C (normal pressure) and 500°C (vacuum) respectively) compared to the temperatures where the actual PPV chromophore is destroyed (T ≅ 350°C according to *in-situ* UV-Vis and *in-situ* FT-IR measurements).

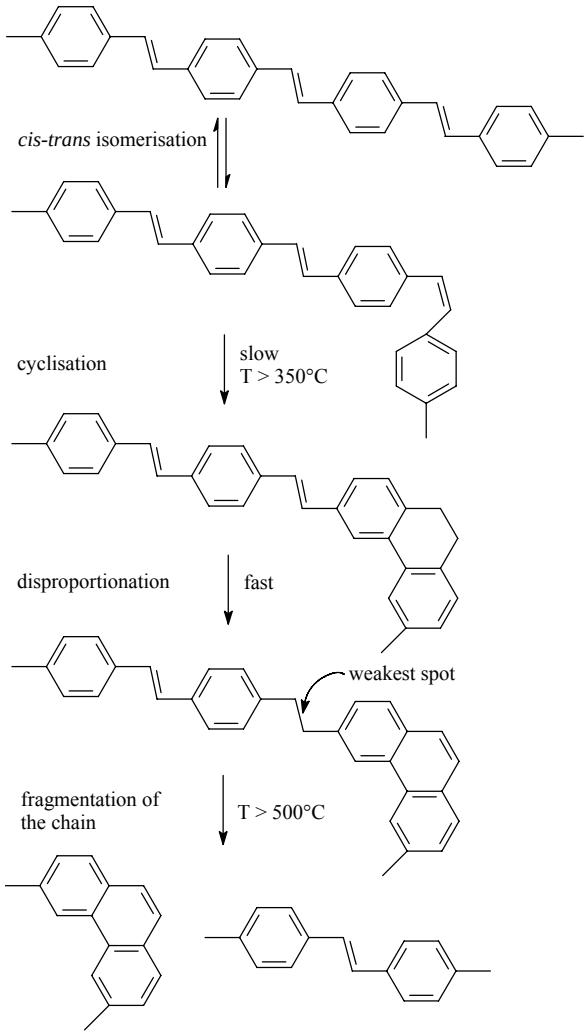

Figure II.13: *Degradation reactions of PPV by phenantrene-unit formation.*

In Figure II.14, the change in λ_{max} as a function of temperature is depicted. Between 85 and 95°C a transition from oligomeric fragments (330 nm) to longer conjugated segments (374 nm) is visible. At 120°C, the absorption maximum is observed at 416 nm. From 120 till 350°C this wavelength of maximum absorption gradually shifts from 416 till 395 nm, due to a thermochromic effect. Between 350 and 450°C the wavelength of maximum absorption shifts finally to shorter wavelengths (351 nm), which corresponds to the absorption maximum of an oligomer again [16]. This means that at temperatures ~ 350°C mainly degradation of the conjugated system occurs (blue-shift of 44 nm in a temperature range of 100°C). Data derived from UV-absorption of degraded PPV are summarised in Table II.2.

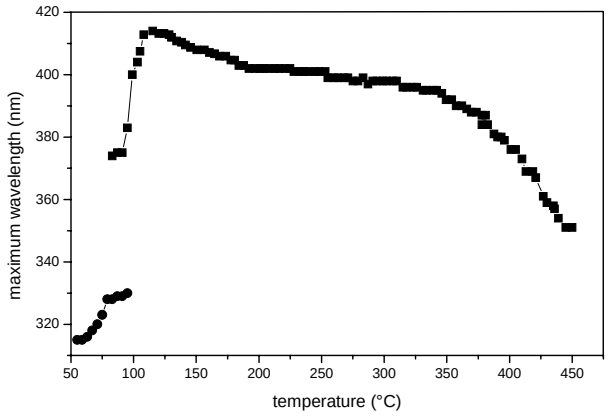

Figure II.14: *The wavelength at maximum absorption (nm) as a function of increasing temperature.*

To demonstrate further that degradation starts around 350°C an additional experiment is carried out on the *n*-butyl-sulphinyl PPV precursor polymer. In this experiment, the precursor polymer is heated at 10°C/min up to 250°C. The polymer is kept at a constant temperature of 250°C for 30 minutes, after which the sample is heated up to the next temperature plateau shown as a dotted line in Figure II.15. The absorbance of the absorption maximum of the PPV polymer (λ_{max} = 416 nm) is plotted versus time in the same figure.

Table II.2: *Data derived from UV-absorption of degraded PPV.*

temperature (ºC)	λ_{onset} (nm)	bandgap (eV)	λ_{max} (nm)
120	521.6	2.37	411
255	525.2	2.35	403
340	524.3	2.35	394
360	520.8	2.37	389
395	521.6	2.37	379
420	518.2	2.38	367
450	"518.2"	"2.38"	"351"

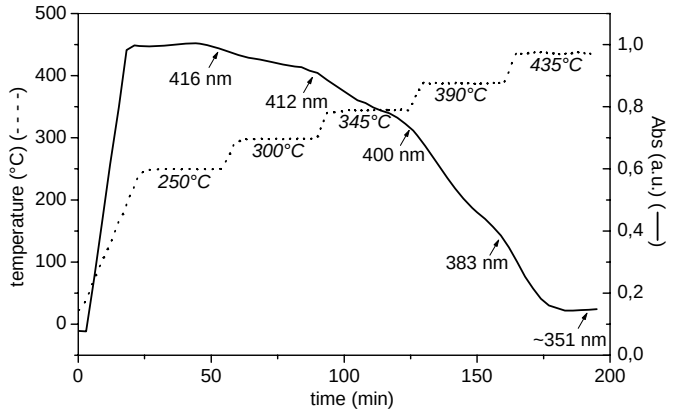

Figure II.15: *The absorbance of the absorption maximum at 416 nm versus time and temperature.*

From Figure II.15 it is again visible that degradation of the conjugated PPV polymer mainly starts at a temperature around 350°C. At temperatures higher than 350°C, there is a steeper decrease in the absorbance at 416 nm and a larger blue-shift of the wavelength because of accelerated degradation (see corresponding UV-absorption maximum at the end of each isothermal part shown in Figure II.15).

II.A.5 Conclusions

We were able to study the elimination and degradation reaction of *n*-alkyl-sulphinyl PPV (precursor) polymers with *in-situ* spectroscopic techniques. From *in-situ* FT-IR and UV-Vis experiments, we can conclude that the elimination reaction starts already at 65°C. In case of larger aliphatic chains of the eliminable group, a kinetic separation occurs between the elimination reaction and the evaporation of the elimination products. The PPV polymer remains stable up to 350°C. Above that temperature, degradation occurs, implying that the "effective" conjugation length irreversibly decreases.

II.B Thermal conversion reaction of sulphonyl PPV precursor polymers. Evidence for the formation of PPV structures?

II.B.1 Introduction

Because sulphonyl functional ($S(O)_2$) groups eliminate at much higher temperatures than the sulphinyl (S(O)) groups, we have synthesised sulphonyl functionalised PPV precursor polymers to evaluate the consequence of highly stable functionalities. Sulphinyl groups were chosen in early applications involving precursor polymers towards PPV [3b] (paragraph I.A), because they are well-known functional groups to form a double bond. For the sulphonyl homopolymers, TGA measurements revealed a degradation temperature of 472°C. In DIP-MS, the fragments that were observed were consistent with the formation of PPV. This implies that these sulphonyl functionalities, although thermally far more stable than other functional groups in precursors, still give rise to the formation of PPVs. Intrigued by this possibility, we decided to investigate the thermal stability of *n*-octyl- and phenyl-sulphonyl PPV precursor polymers in more detail with *in-situ* FT-IR spectroscopy and *in-situ* UV-Vis spectroscopy. After elimination the conjugated polymers obtained were analysed by photoluminescence spectroscopy and also photoluminescence efficiencies were determined in formal work.

II.B.2 Synthesis of sulphonyl PPV precursor polymers

Synthesis of the *n*-octyl-sulphonyl PPV precursor polymer by oxidation of the *n*-octyl-sulphinyl macromolecule is performed by use of *meta*-chloroperbenzoic acid (*m*-CPBA) in CH_2Cl_2. Because of the instability of the phenyl-sulphinyl PPV precursor polymer [17], the phenyl-sulphonyl PPV precursor polymer is synthesised by polymerisation of the phenyl-sulphonyl premonomer (Figure II.16).

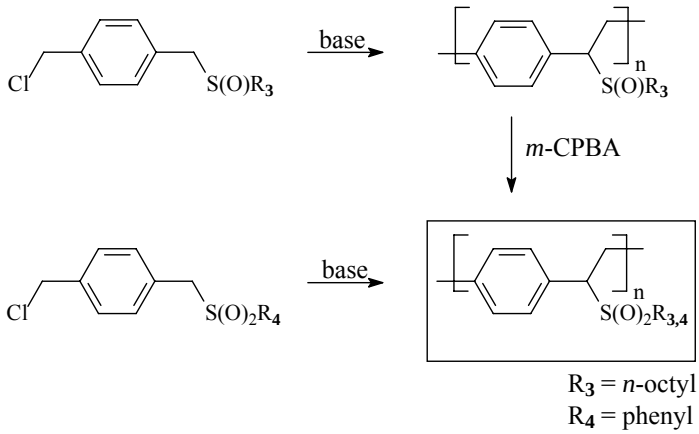

Figure II.16: *Synthesis of sulphonyl PPV precursor polymers by different methods.*

II.B.3 Thermal behaviour of sulphonyl PPV precursor polymers studied with TGA and DIP-MS

In TGA experiments, two distinct temperature ranges of weight loss are observed for the sulphonyl PPV precursor polymers (R_3= *n*-octyl and R_4= phenyl) as is shown in Table II.3. A first region (around 300°C) is related to the elimination of the sulphonyl functional group, while a second (around 450°C) indicates the degradation of the conjugated polymer.

Table II.3: *Elimination and degradation temperature derived from TGA and DIP-MS (heating rate 10°C/min).*

PPV precursor polymer	TGA (°C)[a]		DIP-MS (°C)[b]	
	elimination	degradation	elimination	degradation
n-octyl-sulphinyl **(2)**	284	573	168	502
n-octyl-sulphonyl **(3)**	329	472	285	335
phenyl-sulphonyl **(4)**	283	437	250	380

[a] ambient pressure (argon flow)

[b] under vacuum (10^{-6} mmHg)

To obtain more information about the structure of the elimination products, we have also used DIP-MS. In accordance with the TGA measurements, two signals were observed in a reconstructed ionchromatogram, which can be assigned to an elimination and degradation step on the basis of the fragments observed. The decrease in elimination and degradation temperature compared with TGA most probably is a consequence of the high vacuum in the probe which results in faster evaporation of the elimination products (Table II.3).

The fragments observed for the elimination step are presented in Table II.4 and are consistent with the formation of sulphinic acid as eliminating group and would imply the formation of a double bond and thus PPV. The sulphinic acid is known to dimerise and disproportionates like sulphenic acids do, yielding a thiosulphonate and a sulphonic acid (Figure II.17), which are clearly detected during the elimination step, shown in Table II.4 [18]. Whether the sulphinic acid is formed via a concerted or radical pathway is beyond the scope of this research.

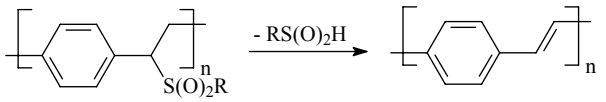

$$3\ RS(O)_2H \longrightarrow RS(O)_3H + RSS(O)_2R + H_2O$$

sulphinic acid — sulphonic acid — thiosulphonate

Figure II.17: *Thermolysis of sulphonyl PPV precursor polymers.*

Table II.4: *Comparison of the thermolysis of sulphonyl PPV precursor polymers.*

DIP-EI			
n-octyl-sulphonyl **(3)**		phenyl-sulphonyl **(4)**	
m/z	fragment	*m/z*	fragment
290	$C_8H_{17}SSC_8H_{17}^+$	250	$C_6H_5SO_2SC_6H_5^+$
161	$C_8H_{17}SO^+$	218	$C_6H_5SO_2C_6H_5^+$
145	$C_8H_{17}S^+$	158	$C_6H_5SO_3H^+$
114	$C_8H_{18}^+$	142	$C_6H_5SO_2H^+$
113	$C_8H_{17}^+$	141	$C_6H_5SO_2^+$
112	$C_8H_{16}^+$	125	$C_6H_5SO^+$
85	$C_6H_{13}^+$	109	$C_6H_5S^+$
71	$C_5H_{11}^+$	94	$C_6H_5OH^+$
64	SO_2^+	77	$C_6H_5^+$
57	$C_4H_9^+$	64	SO_2^+
48	SO^+		

II.B.4 Thermal behaviour of sulphonyl PPV precursor polymers studied with in-situ FT-IR and in-situ UV-Vis spectroscopy

To obtain more detailed information concerning the processes occuring upon increasing the temperature, we turned to *in-situ* UV-Vis and *in-situ* FT-IR spectroscopy. For all experiments we used the same high temperature cell as the one used in heating experiments on the sulphinyl PPV precursor polymers (paragraph II.A.3.a). Films of precursor polymer were spincoated on a quartz disc or a KBr pellet.

An *in-situ* thermal elimination reaction was performed with a temperature ramp speed of 2°C/min starting from ambient temperature up to 350°C under a continuous flow of nitrogen for as well the *n*-octyl- **(3)** as phenyl-sulphonyl PPV precursor polymer **(4)**. To be able to make adequate comparisons with the sulphonyl derivatives, corresponding data for the *n*-octyl-sulphinyl PPV precursor polymer **(2)** are also presented [3b]. During elimination from precursor to a conjugated polymer, the formation of the *trans* vinylene double bond is observed through increase of the absorbance at 965 cm^{-1}. Simultaneously, the sulphonyl absorption band at 1300 cm^{-1} disappears

(not shown) [15a]. Another absorption band is found at about 1130 cm^{-1} for the *n*-octyl-sulphonyl and 1146 cm^{-1} for the phenyl-sulphonyl. For the sulphinyl group an absorption band is visible at 1046 cm^{-1}. From Figure II.18, which shows the increase of the *trans* vinylene double bond absorbance at 965 cm^{-1} as a function of increasing temperature, it becomes clear that elimination of the *n*-octyl- and phenyl-sulphonyl PPV precursors leads to PPV in a similar way as it occurred for the *n*-octyl-sulphinyl PPV precursor.

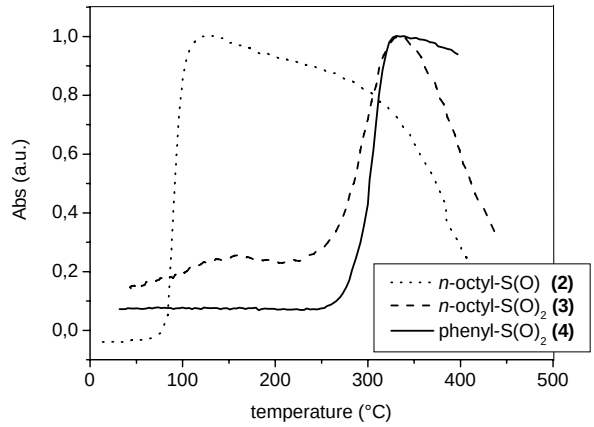

Figure II.18: *Absorbance of the trans vinylene double bond at 965 cm^{-1} as a function of temperature.*

In this case, the elimination process starts around 250°C and is completed at around 330°C. The *n*-octyl-sulphinyl PPV precursor polymer eliminates much faster (temperature range: 65-120°C). At higher temperatures, no sulphonyl or sulphinyl functionalities are visible anymore in IR. In addition, Figure II.18 also seems to indicate that the conjugated PPV polymer obtained from the *n*-octyl-sulphonyl PPV precursor polymer shows lower thermal stability compared to the PPV polymer obtained from the phenyl-sulphonyl PPV precursor polymer.

The elimination reaction was also studied further in an experiment in which the precursor polymer is heated at 10°C/min up to 250°C (= starting temperature of elimination). Then it is kept at a constant temperature of 250°C for two hours, shown in Figure II.19. Again, both sulphonyl PPV precursor

polymers start to eliminate at 250°C. The conjugated system is stable in both cases at 250°C. In this experiment the *n*-octyl-sulphonyl derivative seems to eliminate somewhat faster than the phenyl-sulphonyl derivative.

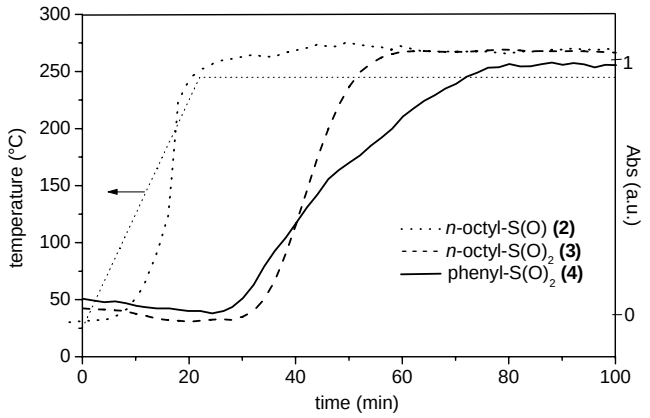

Figure II.19: *Absorbance of the trans vinylene double bond at 965 cm^{-1} as a function of time at 250°C.*

An additional experiment with isothermal heating at 330°C for two hours shows that the absorbance at 965 cm^{-1}, for the *trans* vinylene double bond, slightly decreases for the *n*-octyl-, and stays unchanged for the phenyl-sulphonyl substituent as shown in Figure II.20. These observations indicate a possible slight difference in structure of the PPV materials obtained, possibly related to a difference in number of defects. More specifically, the results obtained seem to indicate that the structure of the PPV polymer resulting from the conversion of the *n*-octyl-sulphonyl PPV precursor polymer is less well defined than that of the PPV material obtained from the phenyl-sulphonyl PPV precursor polymer. These results substantiate the relation assumed between thermal instability and the presence of structural defects or irregularities in the material.

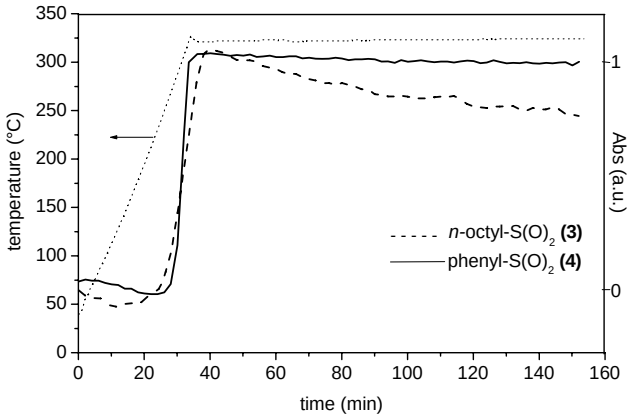

Figure II.20: *Absorbance of the trans vinylene double bond at 965 cm^{-1} as a function of time at 330°C.*

Since λ_{max} increases with the conjugation length, *in-situ* UV-Vis spectroscopy can be used to monitor the increase of the "effective" conjugation length with temperature as the elimination reaction proceeds. Each precursor polymer is heated at 2°C/min from ambient temperature up to ~ 400°C under a continuous flow of nitrogen. To monitor the elimination process, the absorbance at λ_{max} is plotted as a function of temperature as shown in Figure II.21.

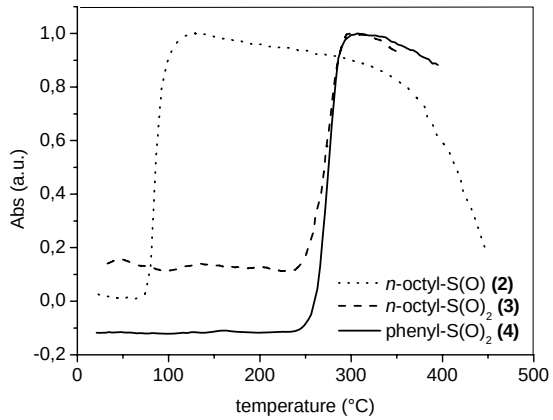

Figure II.21: *Absorbance of λ_{max} of the conjugated system as a function of temperature.*

The obtained UV-Vis spectroscopic results are summarised in Table II.5. Data of the elimination reaction of a *n*-octyl-sulphinyl PPV precursor polymer is shown as a reference, because it has been established before that after elimination, pristine PPV without any defects is obtained (λ_{max} = 416 nm) (paragraph II.A.4.b).

Table II.5: *UV-data results concerning the elimination process.*

	λ_{max} (nm)	elimination temperature (°C)	$\lambda_{max,em.}$ (nm)	PL-efficiency (%)
n-octyl-sulphinyl **(2)**	416	65-120	552	7
n-octyl-sulphonyl **(3)**	375	250-300	502	12
phenyl-sulphonyl **(4)**	402	250-307	554	11

Upon comparison of the UV absorption bands of the eliminated *n*-octyl-sulphinyl precursor (Figure II.10) and the eliminated phenyl-sulphonyl precursor (λ_{max} = 402 nm) depicted in Figure II.22, almost no differences can be observed, except for the value of λ_{max} which is slightly blue-shifted (14 nm) for the phenyl-sulphonyl precursor.

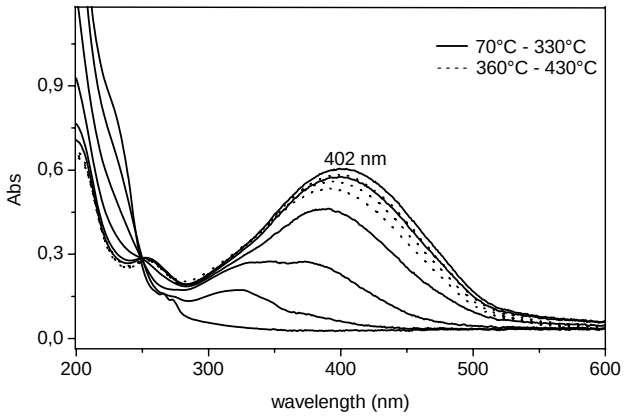

Figure II.22: *UV-absorption spectra obtained from the phenyl-sulphonyl PPV precursor polymer (solid line = red-shift = elimination; dotted line = blue-shift = degradation).*

The conjugated polymer obtained from the conversion of the *n*-octyl-sulphonyl precursor with a λ_{max} = 375 nm is strongly blue-shifted and is displayed in Figure II.23, suggesting a much smaller "effective" conjugation length. The finestructure that is due to the various vibrational levels visible for the absorption band of the eliminated *n*-octyl-sulphonyl polymer, confirms the presence of shorter conjugated units. This limited "effective" conjugation length indicates that a substantial amount of structural defects are present in this material.

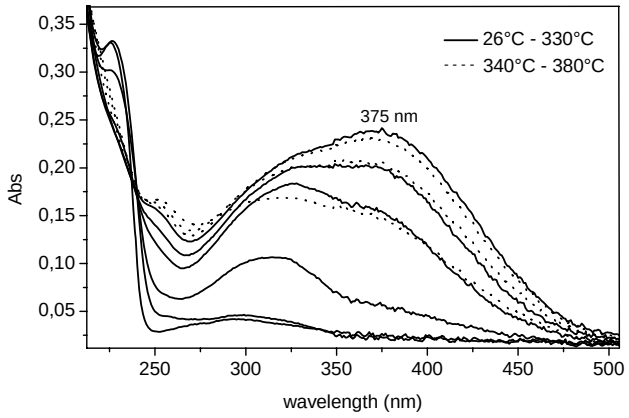

Figure II.23: *UV-absorption spectra obtained from n-octyl-sulphonyl PPV precursor polymer (solid line = red-shift = elimination; dotted line = blue-shift = degradation).*

An additional experiment with isothermal heating at 330°C for two hours shows that the absorbance at 375 nm for the *n*-octyl-sulphonyl derivative, slightly decreases and the absorbance at 402 nm for the phenyl-sulphonyl derivative stays unchanged, as is shown in Figure II.24. These observations are complementary with the FT-IR results and again indicates that the PPV polymer obtained from the *n*-octyl-sulphonyl derivative is less well defined and thus also less stable than the PPV polymer obtained from the phenyl-sulphonyl derivative.

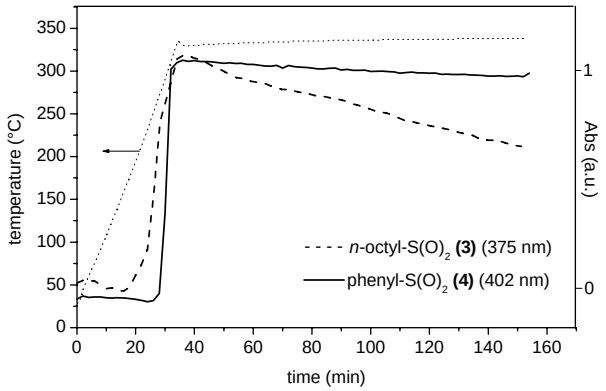

Figure II.24: *Absorbance at 375 nm and 402 nm for the n-octyl- and phenyl-sulphonyl derivative respectively as a function of time at 330°C.*

From the shape of the photoluminescence (PL) spectra and the emission maximum observed it is clear that the conjugated system of PPV obtained from a *n*-octyl-sulphonyl PPV precursor polymer consists of relatively small conjugated fragments as shown in Figure II.25 [19]. The fact that the *n*-octyl-sulphonyl PPV precursor polymer yields PPV, in which only one emission band is visible, indicates a restricted conjugation length.

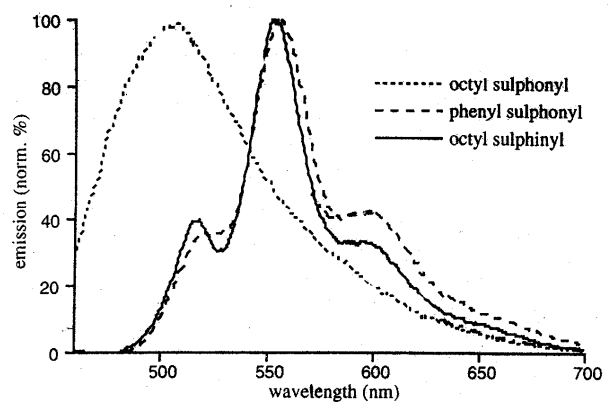

Figure II.25: *Normalised photoluminescence of eliminated sulphonyl PPV precursor polymers and a n-octyl-sulphinyl PPV precursor polymer (350°C, 30 min, 0,2 mbar), excitation wavelength: 430 nm.*

The spectrum of the eliminated phenyl-sulphonyl PPV precursor polymer, however, is almost identical to the PPV obtained from the *n*-octyl-sulphinyl PPV precursor. The phenyl-sulphonyl derivative produces a reasonable PPV polymer on base of the obtained λ_{max}, although a PPV polymer with a higher PL efficiency than the *n*-octyl-sulphinyl derivative is observed. These spectroscopic results are summarised in Table II.5. These higher efficiencies of PPV obtained from the *n*-octyl-sulphonyl PPV precursor and even from the phenyl-sulphonyl PPV precursor polymer, correspond to an interrupted conjugated system [20].

II.B.5 Conclusions

PPV can be formed out of the thermal conversion of sulphonyl PPV precursor polymers. However, the PPV that is prepared from an alkyl-sulphonyl PPV precursor polymer has optical properties which are quite different from the PPV derived from the phenyl-sulphonyl PPV precursor polymer. The alkyl derivative, yields a PPV with large amounts of structural defects which give rise to a restricted "effective" conjugation length. The phenyl derivative however, yields PPV which is almost identical to PPV obtained from sulphinyl precursors.

II.C Modification of sulphinyl PTV precursor polymers to sulphonyl PTV (co)polymers

II.C.1 Introduction

The discovery by Burroughes *et al.* in 1990 [21], that conjugated polymers can be used as active light emitting layers in light emitting devices, triggered extensive research on this class of polymers [22]. Conjugated polymers have been successfully used as active components in lasers [23], photovoltaic devices [24] and field-effect transistors [25]. Currently, one of the active research areas dealing with this class of conjugated polymers encompasses control of color and efficiency of light emission, which is important for applications in full-color displays [25b]. The efficiency of luminescence is not only dependent on the structure of the device and the electrodes used, but also depends strongly on the material properties of the

active layer consisting of the conjugated polymer. Segmented conjugated polymers, where conjugated segments of varying lengths are separated electronically by insulating spacers, is one approach to control both the color of the emitted light and the efficiency of the emission [26]. The efficiency was also shown to increase when polymers were blended in an inert matrix like poly(styrene) [27]. Several earlier attempts to control conjugation lengths, by changing elimination time [28] and temperature [29] resulted only in limited success. Other approaches to prepare PPV derivatives with controlled conjugation length include the following: controlled oxidation (dehydrogenation) of a precursor polymer [30] and the use of condensation approaches [31] to incorporate non-conjugated segments randomly along the polymer backbone and by controlling the fraction of non-conjugated units via quantitative post-functionalization, for e.g. the post-halogenation of poly(*p*-2,5-dihexyloxy-phenylene vinylene) (DHO-PPV) using *N*-bromo-succinimide (NBS) or *N*-chlorosuccinimide (NCS).

In this paragraph, we describe another method that allows us to control the conjugation length by selective elimination of a phenyl poly(*p*-thienylene vinylene) (PTV) precursor polymer containing two types of eliminable groups (sulphinyl and sulphonyl groups). Similar work is published by Padmanaban *et al.* [32]. Their method for control of conjugation length in poly(2,5-dimethoxy-1,4-phenylene vinylene) (DMOPPV) and poly[2-methoxy-5-((2'-ethylhexyl)oxy)-1,4-phenylene vinylene) (MEH-PPV) is based on the selective thermal elimination of acetate groups, without affecting the methoxy groups.

A similar approach was also demonstrated by de Kok *et al*. in our lab [20] using a sulphinyl-*co*-sulphonyl "PPV" precursor polymer. In the latter work, the elimination reactions were carried out *ex-situ*, which has a lot of disadvantages (paragraph II.A.1.a). Therefore, the selective elimination of a phenyl-sulphinyl-*co*-sulphonyl "PTV" precursor polymer is examined with *in-situ* analytical techniques that are available in our lab now (paragraph II.A.3.a and II.A.4.a).

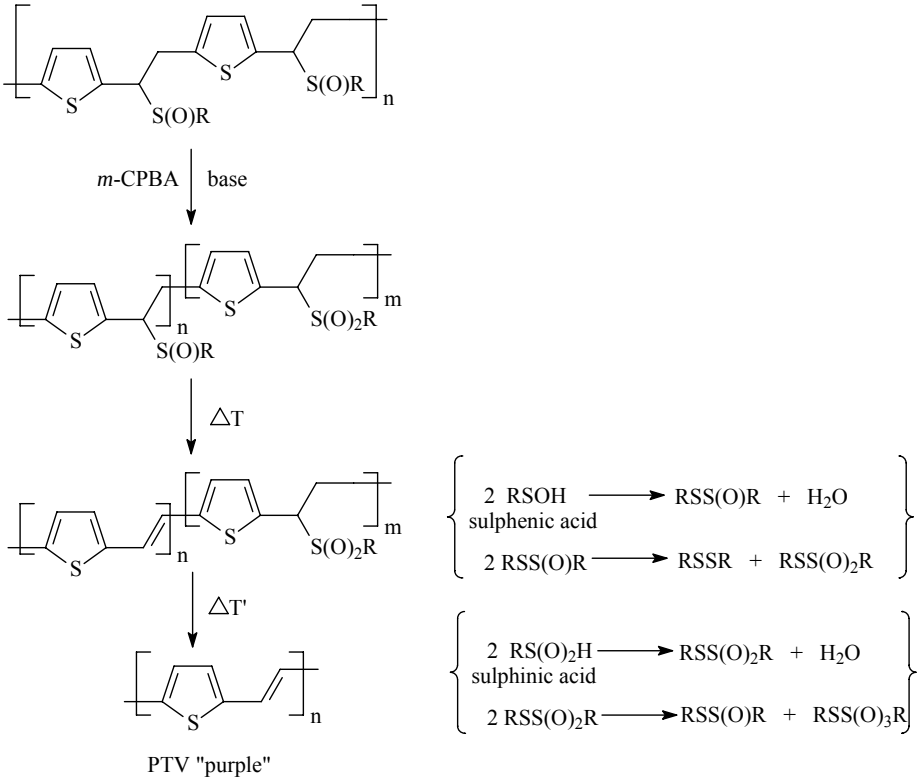

monomeric unit (R = phenyl)	weight (g/mol)
RS(O)	234
$RS(O)_2$	250
PTV	108

Figure II.26: *Copolymers by modification: controlled conjugation length by oxidation. Assumed processes upon heating of sulphinyl-co-sulphonyl PTV (co)polymers.*

The complete range of copolymers can be generated from the same batch of homo phenyl-sulphinyl PTV precursor polymers by oxidation of the sulphinyl groups. Treating a copolymer with sulphinyl and sulphonyl groups at a temperature at which only the sulphinyl groups eliminate, yields a copolymer with conjugated segments interrupted by sulphonyl groups (sp^3 defects). The sequence of the eliminable groups that are not eliminated from the backbone and the amount of these groups will determine the average and distribution of conjugation lengths in the final PTV polymer after conversion (Figure II.26).

II.C.2 Thermal behaviour of sulphinyl-co-sulphonyl PTV precursor (co)polymers studied with TGA and DIP-MS

By partial oxidation of a phenyl-sulphinyl PTV precursor polymer a series of PTV precursor copolymers was obtained and shown in Table II.6.

Table II.6: *Sulphinyl-co-sulphonyl PTV polymers by oxidation of homo sulphinyl PTV polymers with m-CPBA.*

	R = phenyl				
fraction S(O)	1	0.75	0.5	0.25	0
fraction $S(O)_2$	0	0.25	0.5	0.75	1
polymer abbreviation	100/0	75/25	50/50	25/75	0/100
	light yellow				*orange*

The thermal elimination and degradation behaviour of the copolymers can be studied by two different techniques (TGA and DIP-MS). In the first technique, ThermoGravimetric Analysis (TGA), the weight loss is recorded as a function of temperature. TGA analysis are performed at a heating rate of 10°C/min. For each precursor polymer two distinct periods of weight loss can be distinguished.

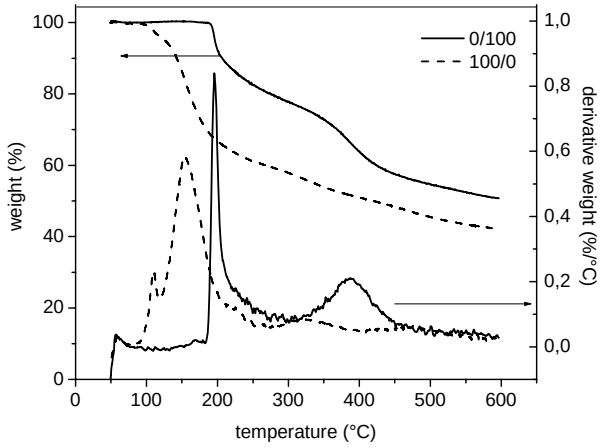

Figure II.27: *TGA thermogram of phenyl-sulphinyl and phenyl-sulphonyl PTV homopolymers*

The first period is assigned to elimination and evaporation of the sulphur groups, the second at higher temperatures to degradation of the converted precursor polymer. A small weight loss is recorded at temperatures below 100°C, which is assigned to the evaporation of water. The first large weight loss for the phenyl-sulphinyl (100/0) and phenyl-sulphonyl (0/100) PTV homopolymer takes place at a maximum of 154 and 196°C respectively, shown in Figure II.27. The first large weight loss of the sulphinyl-*co*-sulphonyl PTV copolymers lies somewhere in between those two temperatures, as can be seen in Table II.7.

Table II.7: *Elimination temperatures obtained with TGA and DIP-MS measurements.*

PTV (co)polymers (S(O)/S(O)$_2$)	elimination - evaporation max. at (°C) (TGA)[a]	elimination max. at (°C) (rel.int.) (DIP-MS)[b]
100/0	109-154	83 (100)
75/25	114-163	89 (100)-194 (15)-250 (11.5)
50/50	117-174	104 (100)-215 (59)-264 (48)
25/75	133-180	202 (100)-269 (55)
0/100	196	223 (100)-274 (33.7)

[a] Ambient pressure (argon flow)

[b] under vacuum (10^{-6} mmHg)

The final weight at 600°C (corrected for different starting weights) is different for each polymer. The highest residual weight is observed for the phenyl-sulphonyl PTV homopolymer, whereas a lowest residual weight for the phenyl-sulphinyl PTV homopolymer (Figure II.27, Table II.9).

Another important observation is that the polymers that are formed also show degradation. For the phenyl-sulphinyl PTV homopolymer, two steps of degradation are observed. The first is observed at 328°C, the second one at 474°C (low intensity), which is respectively lower and higher than the degradation temperature of the phenyl-sulphonyl PTV homopolymer which degrades at a temperature maximum at 387°C. The degradation of the PTV copolymers shows a maximum weight loss between the two homopolymers and their maximum of weight loss increases with increasing amount of sulphonyl present in the copolymer, shown in Table II.8.

Table II.8: *Degradation temperatures of the PTV (co)polymers obtained with TGA and DIP-MS.*

polymer	rest fraction at 600°C (%)	degradation (°C)	degradation (°C)
	TGA	TGA	DIP-MS
100/0	42.1	328-474	415
75/25	46.4	354	404
50/50	49.4	370	401
25/75	50.1	380	387
0/100	50.7	387	371

The second technique used is thermal analysis by Direct Insert Probe Mass Spectrometry (DIP-MS) (paragraph II.A.2). By plotting the total ion current against temperature, the stability of the precursor polymers can be visualised. Thermograms show that the two sulphur containing groups have different stabilities as can be seen in Figure II.28 and Table II.7. The fragments analysed in the first step of thermolysis for the two homopolymers are collected in Table II.9 and corresponds with the thermolysis of sulphenic and sulphenic acids respectively. These fragments, for both precursor polymers, are the reason that in both cases PTV is formed.

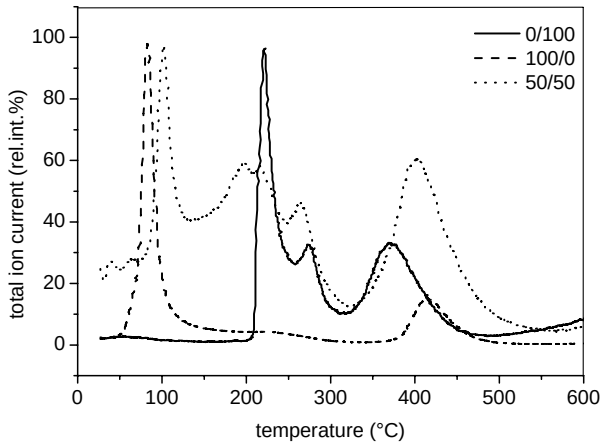

Figure II.28: *Reconstructed ionchromatogram (EI) of phenyl-sulphinyl-co-sulphonyl PTV (co)polymers, heating rate 10°C/min.*

Table II.9: *The mass fragments of the elimination products (R = C_6H_5).*

phenyl-sulphinyl (100/0)		phenyl-sulphonyl (0/100)	
m/z	fragments	*m/z*	fragments
234	$RSS(O)R^+$	250	$RSS(O)_2R^+$
218	$RSSR^+$	218	$RSSR^+$
125	RSO^+	158	$RS(O)_3H^+$
109	RS^+	142	$RS(O)_2H^+$
77	R^+	141	$RS(O)_2^+$
65	$S(O)_2H^+$	125	RSO^+
		109	RS^+
		94	ROH^+
		81	$S(O)_3H^+$
		77	R^+
		65	$S(O)_2H^+$

The phenyl-sulphonyl PTV homopolymer (0/100), having the lowest stability, degrades around 371°C. This could be expected, because more sulphonyl groups incorporated in the polymer leads to more sp^3-defects. The benzylic bond could easier break, degradation occurs faster and the rest fraction at 600°C is higher (Table II.8). The phenyl-sulphinyl PTV homopolymer has the highest stability (415°C). The degradation temperatures of the PTV copolymers are in between those of the two PTV homopolymers (Table II.8). The trends seen with DIP-MS show the opposite behaviour as the trends in the TGA experiments. This could be explained by the atmosphere in which the experiments are carried out. In TGA, argon flow is used by which the elimination products remain in the film and could influence the degradation. In DIP-MS, vacuum conditions (10^{-6} mmHg) are used by which the elimination products are removed from the polymer film. A conclusion is that the observed phenomena are dependent from the conditions in which the experiment is carried out. DIP-MS gives more realistic information since more "original" fragments are detected because delay by transport is not applicable to DIP-MS.

II.C.3 Study of the elimination reaction of phenyl-sulphinyl-co-sulphonyl PTV (co)polymers with in-situ FT-IR spectroscopy

First, *in-situ* non-isothermal heating experiments at 2°C/min from ambient temperature up to 275°C under a continuous flow of nitrogen were carried out with each PTV (co)polymer. To have an idea in which temperature range the elimination recation occurs, the absorbance of the *trans* vinylene double bond at 933 cm^{-1} is plotted versus increasing temperature and is displayed in Figure II.29. The elimination or formation of the *trans* vinylene double bond, for the phenyl-sulphinyl PTV homopolymer (100/0), takes place between 50 and 90°C. For the phenyl-sulphonyl PTV homopolymer (0/100), elimination occurs in a temperature range from 150 to 205°C. Around 135°C, all sulphinyl groups are eliminated out of the PTV copolymers, because the absorption peak from the sulphinyl groups at 1045 cm^{-1} is no longer present at 135°C, while the absorption due to sulphonyl groups at 1146 and 1307 cm^{-1} stays unchanged. All the sulphonyl groups are eliminated at 205°C. At this temperature a fully conjugated PTV polymer is formed.

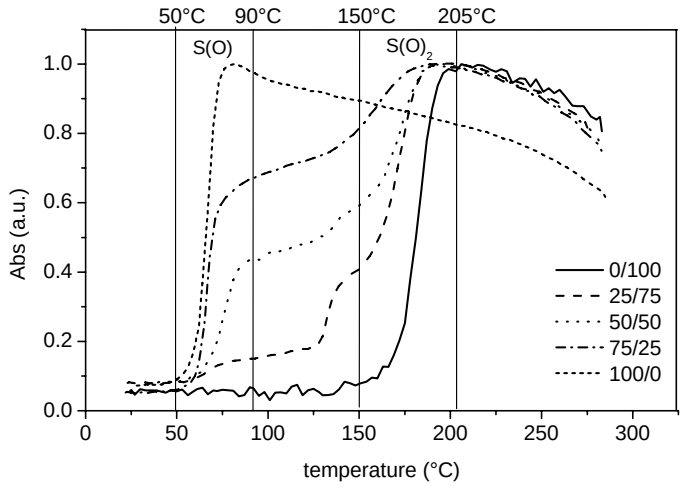

Figure II.29: *The absorbance at 933 cm^{-1} as a function of increasing temperature.*

We have also performed isothermal experiments on the PTV (co)polymers. A temperature of 120°C is chosen to see if the phenyl-sulphinyl groups eliminate selectively from the polymer backbone at a certain constant temperature. Each PTV precursor (co)polymer is heated at 10°C/min from ambient temperature up to 120°C and is kept isothermally at 120°C for 5 hours under a continuous flow of nitrogen. After the non-isothermal heat treatment at 10°C/min up to 120°C, all sulphinyl groups are removed from the polymer backbone and some part of the double bonds are formed. During the isothermal part at 120°C also the sulphonyl groups present in the PTV (co)polymers start to eliminate. The absorbance of the *trans* vinylene double bond at 933 cm^{-1} increases further and at the same time a decrease in the absorbance corresponding with the sulphonyl groups at 1146 cm^{-1} is observed and the absorbance at 1045 cm^{-1} for the sulphinyl groups stays constant (e.g. copolymer 75/25 in Figure II.30).

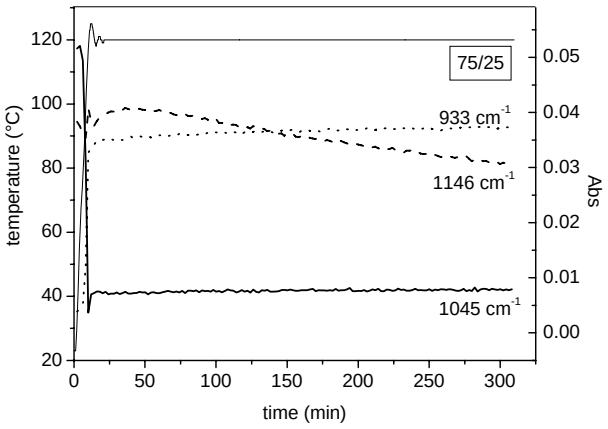

Figure II.30: *Absorbance at 933, 1146 and 1045 cm^{-1} as a function of time at 120°C for the copolymer 75/25.*

For the phenyl-sulphinyl PTV homopolymer (100/0), the fully conjugated PTV polymer is already formed during the non-isothermal part up to 120°C. Hence, no increase in the absorbance at 933 cm^{-1} is observed during the isothermal part at 120°C. The phenyl-sulphonyl PTV homopolymer (0/100) does not change upon heat treatment till 120°C, but after a certain time at 120°C the sulphonyl groups partially disappear and some double bonds are formed. To

keep all the sulphonyl groups in the polymer, it is recommended to do the elimination on an isothermal temperature lower than 120°C (for e.g. 90°C). At 90°C, the elimination of phenyl-sulphinyl groups is very selective towards elimination of the phenyl-sulphonyl groups, as shown in Figure II.31. The absorbance corresponding to the sulphinyl functionality at 1045 cm^{-1} disappears upon elimination at 90°C for 5 hours, while the absorbance of the sulphonyl groups at 1146 cm^{-1} stays constant. The absorbance of the *trans* vinylene double bond at 933 cm^{-1} remains unchanged during the isothermal part at 90°C for all PTV copolymers.

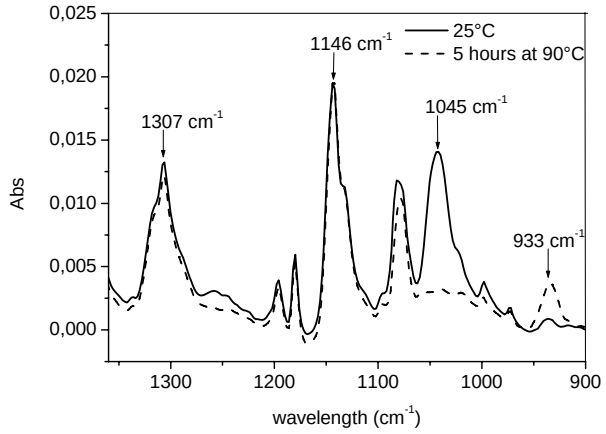

Figure II.33: *Enlarged part of the IR-spectra of PTV copolymer 50/50 at ambient temperature and after 5 hours at 90°C.*

II.C.4 Study of the elimination reaction of phenyl-sulphinyl-co-sulphonyl PTV (co)polymers with in-situ UV-Vis spectroscopy

The properties that are most important for the application of conjugated materials in LEDs, are their optical properties. The absorption of the conjugated materials in the UV-Vis region is due to the absorption of single benzene rings (σ-σ^*, around 250 nm) and the π-π^* transition of the extented conjugated system (300-700 nm). The energy corresponding to the π-π^* transition depends strongly on the delocalisation of the π-electrons, which is determined by the "effective conjugation length". The effective conjugation

length is also influenced by the amount of structural and conformational defects in the polymer backbone and by the interchain interactions between polymer backbones. Therefore, UV absorption measurements are important because information about conjugation length and disorder can be obtained from this technique. The more perfect a structure becomes or the less defects are present in a polymer, the longer the effective conjugation length will be, and the more the absorption maximum will be red-shifted.

Series of PTV (co)polymers (0/100, 25/75, 50/50, 75/25, 100/0) were spincoated on a quartz disc. First, non-isothermal experiments at 2°C/min starting from ambient temperature up to 270°C under a continuous flow of nitrogen were performed (the same as in FT-IR). The absorbance of the absorption maximum at 225°C for all PTV (co)polymers (λ_{max} = 544 nm) is plotted versus increasing temperature and is shown in Figure II.32. From these curves the development of the conjugated system could be followed. The absorption maximum at 225°C is chosen because at this temperature all sulphinyl and sulphonyl groups are removed from the polymer backbone and a pristine PTV is formed.

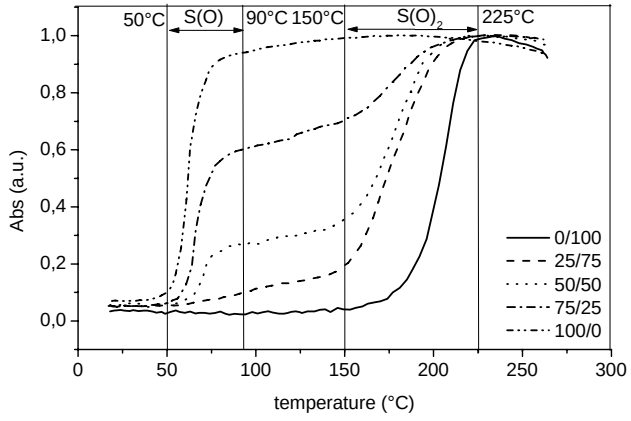

Figure II.32: *The absorbance of the absorption maximum at 225°C (λ_{max} = 544 nm) as a function of increasing temperature.*

The conjugated system is formed between 50 and 90°C for the phenyl-sulphinyl PTV homopolymer (100/0) and between 150 and 225°C for the phenyl-sulphonyl PTV homopolymer (0/100). Formation of the conjugated PTV system takes place in one step for the PTV homopolymers and in two steps for the PTV copolymers. There is a striking similarity with the results obtained with *in-situ* FT-IR spectroscopy.

After the *in-situ* non-isothermal UV-Vis experiments and the results obtained from the *in-situ* FT-IR measurements, each PTV (co)polymer is heated at 10°C/min up to 90°C and is kept at that temperature for 5 hours under a continuous flow of nitrogen. UV-absorption spectra for each PTV (co)polymer after 5 hours at 90°C are collected in Figure II.33.

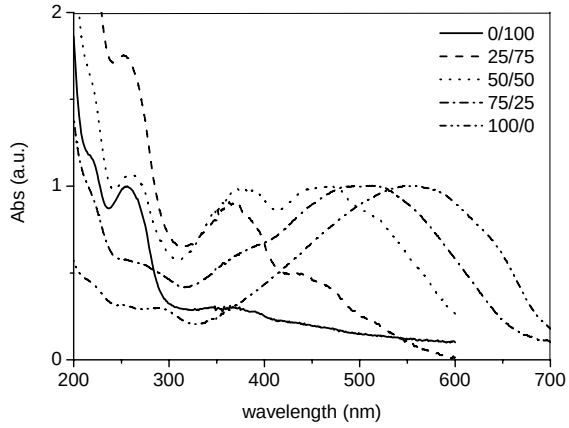

Figure II.33: *UV-absorption of the PTV (co)polymers after 5 hours at 90°C.*

The phenyl-sulphonyl PTV homopolymer (0/100) does not change in color upon elimination. The UV-absorption at 250 nm for the single PTV rings doesn't decrease and no other UV-absorption is formed under the applied conditions. The more sulphonyl groups incorporated in the PTV (co)polymer, the more sp^3-defects present, the shorter the effective conjugation length and the more the absorption maximum shifts to shorter wavelengths (blue-shift, hypsochromic shift) as the average conjugation length decreases. This hypsochromic shift is in agreement with a less extented π-system in which the

energy difference between π and π^* becomes higher and the absorption thus blue-shifted [33]. From the λ_{onset} a larger bandgap as a function of increasing content of sp^3-defects can be derived and is depicted in Table II.10. For PTV copolymer (50/50) with 50% of sulphonyl defects as compared to converted sulphinyl groups, the vibronic structure due to a restricted number of conjugation lengths becomes visible and is displayed in Figure II.34 A. PTV copolymer (25/75) shows a vibronic structure which is even more blue-shifted and from which can be derived that longer conjugation lengths are almost absent in this polymer, shown in Figure II.34 B.

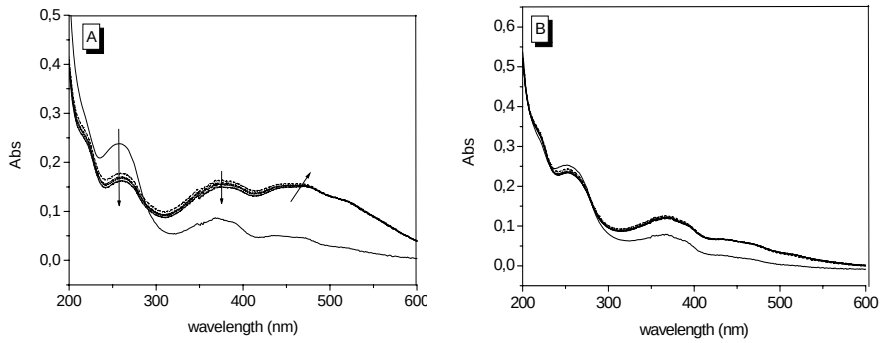

Figure II.34 A, B: *UV-absorption of the PTV copolymer 50/50 and 25/75 respectively at ambient temperature and after 20, 30, 80, 110, 200, 250 minutes and 5 hours at 90°C.*

Table II.10: *UV-data results of the PTV (co)polymers.*

polymer	fraction $S(O)_2$	λ_{max} (abs) (nm) 90°C	λ_{onset} (abs) (nm) 90°C	bandgap (eV) 90°C
0/100	1	254	/	/
25/75	0.75	367	586	2.11
50/50	0.5	470	638	1.93
75/25	0.25	514	682	1.81
100/0	0	544	716	1.72

II.C.5 Conclusions

The synthesis of PTV samples with varying extents of conjugation was achieved by selective elimination of the sulphinyl groups from a PTV precursor copolymer that contains a random distribution of sulphinyl and sulphonyl groups. These sulphonyl groups function as sp^3-defects in the conjugated material because of their higher thermal stability. Moreover sulphonyl groups will cause the inter-chain distance to increase. This method provides a new tool for tuning the material properties. With increase in the extent of elimination the absorption spectra exhibited the expected bathochromic shift: the color of absorption was thus tunable between 367 and 514 nm in the films (after 5 hours on 90°C).

II.D Experimental part

II.D.1 General remarks and instrumentation

^{1}H-NMR spectra were obtained in a deuterated solvent ($CDCl_3$ or D_2O) at 400 MHz on a Varian Inova spectrometer using a 5 mm probe. Chemical shifts (δ) in ppm were determined relative to the residual non deuterated solvent absorption (7.24 ppm for $CHCl_3$, 4.72 ppm for H_2O). The ^{13}C-NMR experiments were recorded at 100 MHz on the same spectrometer using a 5 mm broad-band probe. Chemical shifts were determined relative to the ^{13}C resonance shift of $CHCl_3$ (77.0 ppm). All spectra were obtained at ambient temperature. Column chromatography was carried out using Merck Kieselgel 60 using the eluents indicated. Thin layer chromatography (TLC) was carried out on Merck precoated silica gel 60 F254 plates using the eluents indicated. Melting points were determined on an Electrothermal 9100 and are uncorrected. Molecular weights and molecular weight distributions were determined relative to polystyrene standards (Polymer Labs) with a narrow polydispersity by Size Exclusion Chromatography (SEC). Separation to hydrodynamic volume was obtained using a Spectra series P100 (Spectra Physics) equipped with a pre-column (5 μm, 50 mm*7.5 mm, guard, Polymer Labs) and two mixed-B columns (10 μm, 2x300 mm*7.5 mm, Polymer Labs) and a Refractive Index (RI) detector (Shodex) at 40°C. SEC samples are filtered through a 0.45 μm filter. HPLC grade THF (p.a.) is used as the eluent at a constant flow rate of 1.0 ml/min. Toluene is used as flow rate marker. Instruments used to study the elimination reaction with are described in the text (TGA, DIP-MS, *in-situ* FT-IR and UV-Vis spectroscopy).

II.D.2 Materials

*II.D.2.a Synthesis of the n-alkyl-sulphinyl PPV precursor polymers **(5)*** [34]

1,4-Bis(Tetrahydrothiopheniomethyl)xylenedichloride (2) A solution of **1** (52.5 g, 0.3 mol) and tetrahydrothiophene (THT) (105 ml, 1.19 mol) in MeOH (105 ml) was stirred for 60 hours at ambient temperature. The reaction mixture was precipitated in acetone (420 ml) at –10°C. The precipitate was collected and washed with cold acetone (600 ml). Evaporation of the solvent gave a white hygroscopic solid (95.9 g, 91 %): ^{1}H-NMR (D_2O, 400 MHz) δ 2.12-2.30 (m, 8 H, $SCH_2C\underline{H}_2$), 3.31-3.50 (m, 8H, $SC\underline{H}_2$), 4.48 (s, 4H, $ArC\underline{H}_2S$), 7.53 (s, 4H, Ar<u>H</u>) ppm.

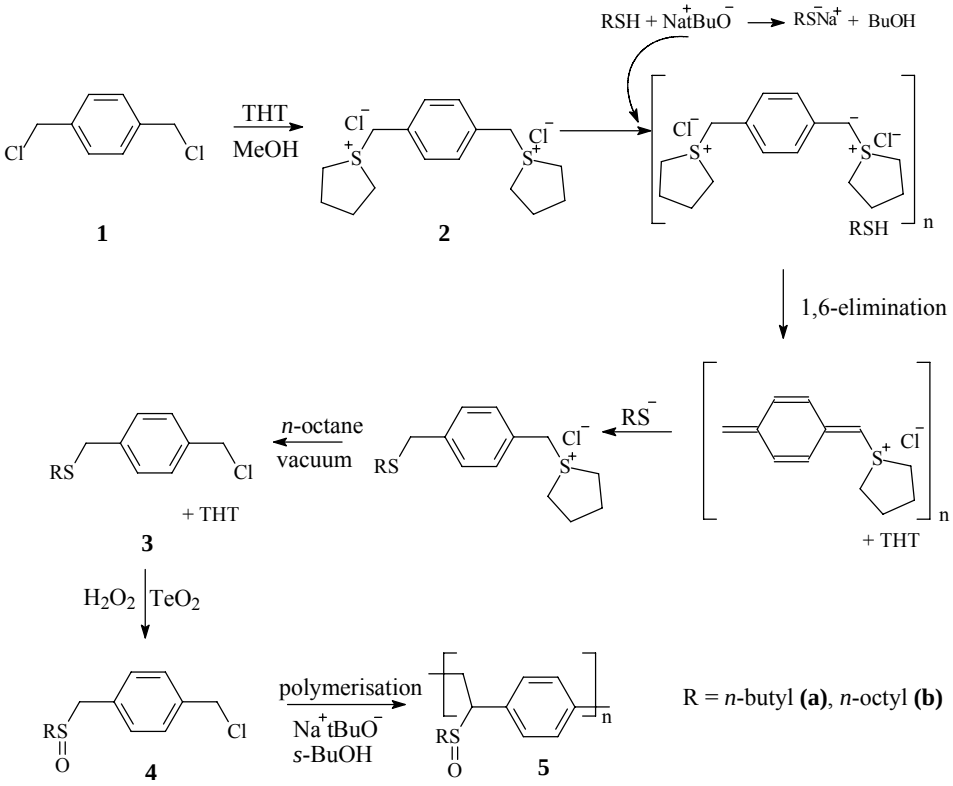

Figure II.38: *Synthetic pathway towards (OC_1C_{10}-)PPV precursor polymers.*

General procedure for 1-(Chloromethyl)-4-[(alkylsulphanyl)methyl] benzenes (3) A mixture of NatBuO (1.83 g, 19 mmol) and thiol (19 mmol) in MeOH (40 g) was stirred for 30 minutes at ambient temperature. The clear solution was added in one portion to a stirred solution of **2** (6.68 g, 19 mmol) in MeOH (100 g). After one hour the reaction mixture was neutralised with aqueous HCl (1 M), if necessary, and concentrated in vacuum. The crude product was diluted with $CHCl_3$ (200 ml) and the precipitate was filtered off. The filtrate was concentrated in vacuum. The oil thus obtained was diluted with *n*-octane or petroleum ether (boiling range 100-130°C, 75 ml) and concentrated to remove tetrahydrothiophene. This sequence was repeated three times.

1-(Chloromethyl)-4-[(*n*-butylsulphanyl)methyl]benzene (3a) This compound was synthesised according to the general procedure, starting from *n*-butanethiol (1.71 g, 19 mmol) to give a crude mixture of **1**, **3a** and α,α'-dibutylsulphanyl-*p*-xylene as a light yellow oil (yield 4.30 g).

1-(Chloromethyl)-4-[(*n*-octylsulphanyl)methyl]benzene (3b) This compound was synthesised according to the general procedure, starting from *n*-octanethiol (2.78 g, 19 mmol) to give a crude mixture of **1**, **3b** and α,α'-dioctylsulphanyl-*p*-xylene as a light yellow oil (yield 5.30 g).

General procedure for the oxidation of thioethers (4) An aqueous (35 wt.%) solution of H_2O_2 (3.4 g, 35 mmol) was added dropwise to a solution of crude thioether (~ 17 mmol) in MeOH (125 ml) and TeO_2 (5 mol%, 0.28 g). After 6 hours the reaction was quenched by adding a saturated aqueous NaCl solution (75 ml). The reaction mixture was extracted with $CHCl_3$ (3 x 50 ml) and the combined organic layers were dried over $MgSO_4$ and concentrated in vacuum. The reaction mixture was purified by column chromatography (SiO_2, eluent $CHCl_3$) and subsequent crystallisation from CH_2Cl_2/hexane. The yields given below are refered to starting compound **1**.

1-(Chloromethyl)-4-[*n*-butylsulphinyl)methyl]benzene (4a) This compound was synthesised according to the general procedure starting from the crude mixture to give **4a** as a white solid (3.46 g, 68 %): m.p. 111.5-112.5°C. ^{1}H-NMR ($CDCl_3$, 400 MHz): δ 0.90 (t, J = 7.2 Hz, 3H, C$\underline{H}_3$), 1.41 (m, 2H, $CH_2CH_2C\underline{H}_2CH_3$), 1.70 (m, 2H, $CH_2C\underline{H}_2CH_2CH_3$), 2.65 (t, J = 8.0 Hz, 2H,

S(O)C$\underline{H}_2$CH$_2$-), 3.93 (dd, J_{AB}=13.2 Hz, 2H, PhC$\underline{H}_2$S(O)), 4.55 (s, 2H, C$\underline{H}_2$Cl), 7.27 (d, J = 8.0 Hz, 2H, Ar$\underline{H}$), 7.38 (d, J = 8.0 Hz, 2H, Ar$\underline{H}$); ^{13}C-NMR ($CDCl_3$, 100 MHz):13.1 (CH_3), 21.3 ($\underline{C}$-CH$_3$), 23.8 (S(O)-C-$\underline{C}$), 45.1 ($\underline{C}$-Cl), 50.2 (Ph-$\underline{C}$-Cl), 56.9 (Ph-$\underline{C}$-S(O)), 128.4 ($\underline{C}$-C-C-Cl), 129.8 ($\underline{C}$-C-C-S(O)), 129.9 (C-C-S(O)), 136.8 (C-C-Cl) ppm; IR (KBr): 2965, 2902, 2870 ν (CH_2 asym.), 1025 ν (S(O)) cm^{-1}; MS (EI, *m/z,* rel.int. (%)): 244 ([M]$^+$, 9), 209 ([$C_{12}H_{17}OS$]$^+$, 5), 139 ([C_8H_8Cl]$^+$, 100), 104 ([C_8H_8]$^+$, 19), 77 ([C_6H_5]$^+$, 5).

1-(Chloromethyl)-4-[*n*-octylsulphinyl)methyl]benzene (4b) This compound was synthesised according to the general procedure starting from the crude mixture to give **4b** as a white solid (4.25 g, 68 %): m.p. 109.5-110.5°C. ^{1}H-NMR ($CDCl_3$, 400 MHz): δ 0.84 (t, J = 6.8 Hz, 3H, C$\underline{H}_3$), 1.23 (m, 8H, (C$\underline{H}_2$)$_4$-CH3), 1.36 (m, 2H, C$\underline{H}_2$CH$_3$), 1.70 (m, 2H, S(O)CH$_2$C$\underline{H}_2$), 2.53 (t, J = 7.8 Hz, 2H, S(O)C$\underline{H}_2$CH$_2$), 3.92 (dd, J_{AB}=13.0 Hz, 2H, PhC$\underline{H}_2$S(O)), 4.55 (s, 2H, C$\underline{H}_2$Cl), 7.26 (d, J = 8.0 Hz, 2H, Ar$\underline{H}$), 7.37 (d, J = 8.0 Hz, 2H, Ar$\underline{H}$); ^{13}C-NMR ($CDCl_3$, 100 MHz):14.0 (CH_3), 22.4, 22.5, 28.7, 28.9, 29.1, 31.6 (($\underline{C}H_2$)$_6$), 45.6 ($\underline{C}$-Cl), 51.0 (S(O)$\underline{C}H_2$), 57.6 ($\underline{C}$H-S(O)), 129.1 ($\underline{C}$-C-C-Cl), 130.2 ($\underline{C}$-C-C-S(O)), 137.5 ($\underline{C}$-C-Cl) ppm; IR (KBr): 3031 ν (C-H arom.), 2955, 2927, 2870 ν (CH_2 asym.), 1462 ν (C-H), 1036 ν (S(O)), 850 ν (1,4 subst.arom.) cm^{-1}; MS (EI, *m/z,* rel.int. (%)): 300 ([M]$^+$, 5), 265 ([$C_{16}H_{25}OS$]$^+$, 82), 139 ([C_8H_8Cl]$^+$, 100), 104 ([C_8H_8]$^+$, 45), 77 ([C_6H_5]$^+$, 5).

General procedure for the precursor polymers (5) A solution of monomer (2 mmol) in *s*-BuOH (14 ml) and a solution of sodium *t*-butoxide (0.25 g, 2.6 mmol) in *s*-BuOH (6 ml) was degassed for 1 hour at 30°C by passing through a continuous stream of nitrogen. The base solution was added in one portion to the stirred monomer solution. After one hour the reaction mixture was poured in a well stirred amount (200 ml) ice water. The mixture was neutralised with aqeous hydrogen chloride (1 M) and extracted with $CHCl_3$ (3 x 100 ml). The combined organic layers were concentrated in vacuum. The crude product was dissolved in $CHCl_3$ (12.5 g) and precipitated in a mixture of *n*-hexane:diethylether 1:1, w/w (125 g). The polymer was collected and dried in vacuum. The residual fraction was concentrated in vacuum.

Poly[*p*-phenylene(1-*n*-butylsulphinyl)ethylene] (5a) This compound was synthesised according to the general procedure starting from **4a** (0.49 g) to give **5a** as a white solid (0.34 g, 82 %): M_w = 540 000, M_w/M_n = 2.5, T_g = 68°C; ^{1}H-

NMR ($CDCl_3$, 400 MHz): δ 0.6-0.9 (3H, br), 1.1-1.4 (2H, br), 1.4-1.7 (2H, br), 1.8-2.1 + 2.1-2.5 (2H, br), 2.9-3.3 (1H), 3.3-3.9 (2H, br), 6.7-7.5 (4H, br); ^{13}C-NMR ($CDCl_3$, 100 MHz): δ 14.1, 22.4 + 22.6, 24.9 + 25.5, 36.6 + 36.9, 49.6 + 50.2, 65.8 + 70.6, 129.0, 129.3, 129.6, 130.0, 130.5, 131.9, 132.2, 133.1, 138.8 ppm; IR (KBr): ν 2958, 2929, 2871, 1031 cm^{-1}.

Poly[*p*-phenylene(1-*n*-octylsulphinyl)ethylene] (5b) This compound was synthesised according to the general procedure starting from **4b** (0.6 g) to give **5b** as a white solid (0.47 g, 88 %): M_w = 238 000, M_w/M_n = 2.0, T_g = 49°C; ^{1}H-NMR ($CDCl_3$, 400 MHz): δ 0.75-0.9 (3H, br), 1.05-1.4 (10H, br), 1.4-1.75 (2H, br), 1.8-2.1 + 2.1-2.4 (2H, br), 2.75-3.35 (1H), 3.35-3.85 (2H, br), 6.7-7.3 (4H, br); ^{13}C-NMR ($CDCl_3$, 100 MHz): δ 14.0, 22.3 + 22.5, 22.9, 28.6, 28.9, 29.0, 31.6, 35.9 + 36.3, 49.2 + 49.8, 65.1 + 69.9, 128.0, 128.5, 128.9, 129.3, 129.8, 131.3, 131.6, 132.3, 132.5, 133.1, 138.1 ppm; IR (KBr): ν 2955, 2926, 2855, 1046 cm^{-1}.

II.D.2.b Synthesis of the sulphonyl PPV precursor polymers

The *n*-octyl-sulphinyl monomer **(4b)** was synthesised and polymerised as described before and afterwards oxidised to the sulphonyl. The phenyl sulphonyl polymer was synthesised by polymerisation of the sulphonyl monomer.

Poly[*p*-phenylene(1-*n*-octylsulphonyl)ethylene] Prior to use the *m*-CPBA used was titrated with KI and starch as an indicator. An activity (content of peroxy acid) of 83 % was determined and used to calculate active equivalents of oxidising agent. *n*-Octyl sulphinyl polymer **(5b)** is dissolved in dichloromethane (100 ml) under anhydrous conditions and cooled down to 0°C before a solution of *m*-CPBA (4.88 mmol, 828 mg) was added dropwise. After one hour at 0°C the reaction mixture was stirred for another hour at ambient temperature. The organic phase was washed with water (3x) and washed with 0.1 M $NaHCO_3$-solution. The organic phase was concentrated in vacuum and the polymer was precipitated in a mixture of diethylether:hexane 1:1 from a solution of dichloromethane. Sulphonyl polymer was obtained in 94 % yield. ^{1}H-NMR ($CDCl_3$, 400 MHz): δ 0.78 (3H, $C\underline{H}_3$), 1.20 (8H, $S(O)_2CH_2CH_2CH_2(C\underline{H}_2)_4CH_3$), 1.54 (2H, $S(O)_2CH_2CH_2C\underline{H}_2$-), 1.66 (2H, $S(O)_2CH_2C\underline{H}_2$-), 2.54 (2H,

$S(O)_2C\underline{H}_2CH_2$-), 3.15 (1H, $PhCHS(O)_2CH\underline{H}Ph$), 3.66 (1H, $PhCH(S(O))C\underline{H}HPh$), 4.08 (1H, $PhC\underline{H}S(O)_2$), 6.75-7.10 H (4H, Ar$\underline{H}$); ^{13}C-NMR ($CDCl_3$, 100 MHz): δ 14.00 ($\underline{C}H_3$), 21.23 ($\underline{C}H_2CH_3$), 21.40 ($\underline{C}H_2CH_2CH_3$), 22.48 ($\underline{C}H_2(CH_2)_2CH_3$), 28.35 ($\underline{C}H_2(CH_2)_3CH_3$), 31.57 ($\underline{C}H_2(CH_2)_4CH_3$), 33.44 (-$S(O)_2CH_2\underline{C}H_2CH_2$-), 33.44 ($\underline{C}H_2CHS(O)$), 50.70 (S(O)-$\underline{C}H_2$), 69.06 ($\underline{C}H$-S(O)), 130.00 (qu.ar.C-$\underline{C}$-CH-), 129.59 (2C, prim. ar.), 138.09 (qu.ar. $\underline{C}$-CH_2); IR (KBr): 2955, 2925, 2870 ν (CH_2 asym.), 1457 ν (C-H deformation), 1298 ν (SO_2 asym.stretch), 1129 ν (SO_2 sym.stretch), 873 ν (quadrant in-plane bending benzene), 829 ν (1,4-disubstituted *p*-phenylene C-H out-of-plane bend), 612 ν (SO_2 scissors deformation), 570 ν (*p*-phenylene out-of-plane) cm^{-1}.

1-[(Chloromethyl)methyl-4-(phenylsulphonyl)benzene] Synthesis is similar to the monomers described in paragraph II.D.2.a. M.p.:170.3-170.9°C; ^{1}H-NMR ($CDCl_3$, 400 MHz): δ 4.52 (s, 2H, $PhC\underline{H}_2Cl$), 4.28 (s,2H, $PhC\underline{H}_2S(O)_2Ph$), 7.07 (d, 2H, $\underline{Ph}CH_2S(O)_2Ph$), 7.26 (d, 2H, $PhCH_2S(O)_2\underline{Ph}$), 7.44 (t, 2H, $S(O)_2Ph$), 7.62 (q, 2H, $S(O)_2\underline{Ph}$) ppm; MS (70eV, EI): 280 ($[M]^+$), 245 ($[M]$-$Cl)^+$, 139 ($[M]$-$S(O)_2Ph)^+$, 104 (CH_2-Ph-CH_2), 77 (C_6H_5); IR (KBr): 3053 ν (C-H benzene stretch in-plane), 2950 ν (CH_2 asymm. stretch), 1609, 1583 ν (both C-C benzene ring stretch), 1515, 1443, 1410 ν (all semi-circle stretching benzene), 1290 ν (sulphone asymm. stretch), 1150 ν (sulphone symm. stretch), 1084 ν (semi-circle ring stretch phenyl group), 1020 ν (benzene C-C vibration), 930 ν (out-of-plane wag benzene), 845 ν (1,4-disubstitution *p*-phenylene C-H out-of-plane wag), 750 ν (phenyl 5 adjacent H's), 722 ν (out-of-plane sextant ring bend vibration benzene), 688 ν (ring bend phenyl), 662 ν (benzylic chloride), 608 ν (sulphone sciccors deformation), 539 ν (out-of-plane quadrant ring bending phenyl group), 508 ν (sulphone wag) cm^{-1}.

Poly[*p*-phenylene(1-phenylsulphonyl)ethylene] The 1-[(chloromethyl) methyl -4-(phenylsulphonyl)benzene] was polymerised similar to the monomers described in paragraph II.D.2.a in 55 % yield in CH_2Cl_2. M_n = 3.400.000, M_w = 2.900.000; T_g = 117°C; ^{1}H-NMR ($CDCl_3$, 400 MHz): δ 3.15 (1H, PhCH-C$\underline{H}_2$), 3.6 (1H, PhCH-C$\underline{H}_2$), 4.15-3.9 (Ph-C$\underline{H}$-), 6.8-6.6 (4H, CH_2PhCH_2), 7.45-7.0 (5H, $S(O)_2Ph$) ppm; IR (KBr): 3060 ν (aromatic C-H stretch), 2955, 2927, 2870 ν (CH_2 asymm. stretch), 1558 ν (ring stretch phenyl group, opposite quadrants), 1515, 1446 ν (all semi-circle stretching phenyl), 1298 ν (sulphone asymm. stretch), 1145 ν (sulphone symm. stretch), 872 ν (quadrant in-plane-bending

benzene), 827 ν (1,4 disubstituted *p*-phenylene C-H out-of-plane bend), 758 ν (H-wag phenyl group 5 adjacent H's), 688 ν (out-of-plane sextant ring bending phenyl), 612, 590 ν (sulphone sciccors deformation), 570 ν (*p*-phenylene out-of-plane), 505 ν (sulphone wag) cm^{-1}.

II.D.2.c Synthesis of the phenyl-sulphinyl-co-sulphonyl PTV (co)polymers

Modification of the precursor polymer was achieved by changing the oxidation state of the sulphur functionality. By oxidation of the sulphinyl group this functionality can be converted to a sulphonyl group. For the oxidation of a sulphinyl into a sulphonyl group, *m*-CPBA is used, the oxidant was titrated prior to be useful. The activity of *m*-CPBA is not 100 %, but 70 %. Oxidation with an equimolar quantity converted the homo sulphinyl precursor into the homo sulphonyl precursor. If you want to oxidise x mol sulphinyl, you have to use x mol *m*-CPBA. E.g. Synthesis of sulphinyl-*co*-sulphonyl PTV copolymer 75/25: Phenyl-sulphinyl PTV precursor polymer (0.70 g, 3.0 mmol) was dissolved in dichloromethane (75 ml) and cooled down to –10°C before a solution of *m*-CPBA (0.12 mmol) in dichloromethane (25 ml) was added dropwise. After addition, the resulting clear mixture was stirred for another hour at –10°C. The mixture was washed with 0.5 M $NaHCO_3$-solution (2 x 250 ml) and demi-water (15 g) and precipitated in diethylether (175 g). The polymer was collected and dried in vacuum. Quantitative ^{13}C-NMR on these materials is very difficult, because they are thermal unstable. The quantity of sulphonyl groups incorporated in the PTV copolymer is based on the probability of PPV, in which the building in of the sulphonyl groups correspond well to the amount of *m*-CPBA used [20].

II.E References

[1] a) R.A. Wessling, R.G. Zimmerman, *U.S. Patent,* **(1968)** 3401152; b) R.A. Wessling, *J. Polym. Sci., Polym. Symp.,* 72 **(1985)** 55.

[2] Ph. D. Thesis F. Louwet, **(1993)**, Limburgs Universitair Centrum, Diepenbeek.

[3] a) Ph. D. Thesis M. de Kok, **(1999)**, Limburgs Universitair Centrum, Diepenbeek; b) M.M. de Kok, A.J.J.M. van Breemen, R.A.A. Carleer, P.J. Adriaenssens, J.M. Gelan, D.J. Vanderzande, *Acta Polym.,* 50 **(1999)** 28.

[4] a) L.J. Rothberg, A.J. Lovinger, *J. Mater. Res.,* 11(12) **(1996)** 3174; b) J.R. Sheates, D.B. Raitman, *Synt. Met.,* 95 **(1998)** 79; c) E. Ettedgui, G.T. Davis, B. Hu, F.E. Karasz, *Synt. Met.,* **(1997)** 73; d) M. Itaf Khan, M.L. Renak, G.C. Bazan, Z.J. Popovic, *J. Am. Chem. Soc.,* 119 **(1997)** 5344.

[5] a) B.H. Cumpston, I.D. Parke, K.F. Jensen, *J. Appl. Phys.*, 81(8) **(1997)** 3719; b) R.D. Scurlock, B.J. Wang, P.R. Ogilby, J.R. Sheats, R.L. Clough, *J. Am. Chem. Soc.*, 117(41) **(1995)** 10194; c) L.J. Rothberg, M. Yan, F. Papadimitrakopoulos, M.E. Galvin, E.W. Kwock, T.W. Miller, *Synth. Met.*, 80 **(1996)** 41; d) L.J. Rothberg, M. Yan, S. Son, M.E. Galvin, E.W. Kwock, T.M. Miller, H.E. Katz, R.C. Haddon, F. Papadimitrakopoulos, *Synth. Met.*, 78 **(1996)** 231; e) M. Yan, L.J. Rothberg, F. Papadimitrakopoulos, M.E. Galvin, T.M. Miller, *Mol. Cryst. Liq. Cryst.*, 256 **(1994)** 17; f) F. Papadimitrakopoulos, M. Yan, L.J. Rothberg, H.E. Katz, E.A. Chandross, M.E. Galvin, *Mol. Cryst. and Liq. Cryst.*, 25(6) **(1994)** 663; g) H. Antoniadis, L.J. Rothberg, F. Papadimitrakopoulos, M. Yan, M.E. Galvin, M.A. Abkowitz, *Phys. Rev. B*, 50 **(1994)** 14911; h) M. Yan, L.J. Rothberg, F. Papadimitrakopoulos, M.E. Galvin, T.M. Miller, *Phys. Rev. Let.,* 73 **(1994)** 744; i) B.H. Cumpston, K.F. Jensen, *Trends in Polymer Science,* 4 **(1996)** 151; j) J.C. Scott, J.H. Kaufman, P.J. Brock, R. DiPietro, J. Salem, J.A. Goitia, *J. Appl. Phys.*, 79 **(1996)** 2745.

[6] W. Bijnens, J. Manca, T.D. Wu, W. D'Olieslaeger, D. Vanderzande, J. Gelan, W. De Ceuninck, L. De Schepper, L.M. Stals, *Synth. Met.*, 83 **(1996)** 261.

[7] a) H. Aziz, G. Xu, *Synth. Met.,* 80 **(1996)** 7; b) H. Aziz, G. Xu, *J. Phys. Chem. B*, 101 **(1997)** 4009.

[8] M. Herold, J. Gmeiner, M. Schwoerer, *Acta Pol.,* 45 **(1994)** 392.

[9] G. Montaudo, D. Vitalini, R.W. Lenz, *Polymer,* 28 **(1987)** 837.

[10] G. Montaudo, C. Puglishi, J.W. de Leeuw, W. Hartgers, K. Kishore, K. Ganesh, *Macromolecules,* 29 **(1996)** 6466.

[11] E. Kesters, L. Lutsen, D. Vanderzande, J. Gelan, *Synth. Met.*, 119 **(2001)** 311.

[12] a) L.A. Kingsburry, D.J. Cram, *J. Am. Chem. Soc.,* 82 **(1960)** 1810; b) J.R. Shelton, K.E. Davis, *Int. J. Sulfur Chem.,* 8 **(1973)** 205; c) T. Yoshimura, E. Tsukurimichi, Y. Iizuka, H. Mizuno, H. Isaji, C. Shimasaki, *Bull. Chem. Soc. Jap.,* 62 **(1989)** 1891.

[13] a) D.D.C. Bradley, *J. Phys. D. Appl. Phys.,* 20 **(1987)** 1389; b) K.F. Voss, C.M. Foster, L. Smilowitz, D. Mihailovic, S. Askari, G. Srdanov, Z. Ni, S. Shi, A.J. Heeger, F. Wudl, *Phys Rev. B,* 43(6) **(1991)** 5109.

[14] P.L. Burn, A. Kraft, D.R. Baigent, D.D.C. Bradley, A.K. Brown, R.H. Friend, R.W. Gymer, A.B. Holmes, R.W. Jackson, *J. Am. Chem. Soc.,* 115 **(1993)** 10117.

[15] a) G. Zerbi, A. Galbiati, M.C. Gallazzi, C. Castiglioni, M. Del Zoppo, R. Schenk, K. Mullen, *J. Chem. Phys.,* 105(6) **(1996)** 2509; b) B. Tian, G. Zerbi, K. Mullen, *J. Chem. Phys.,* 95(5) **(1991)** 3198; c) B. Tian, G. Zerbi, R. Schenk, K. Mullen, *J. Chem. Phys.,* 95(5) **(1991)** 3191; d) D.A. Halliday, P.L. Burn, R.H. Friend, A.B. Holmes, *J.Chem. Soc. Chem. Commun.,* **(1992)** 1685; e) S. Webster, D.N. Batchelder, *Polymer,* 37(22) **(1996)** 4961; f) M. Woodruff, *Synth. Met.,* 80 **(1996)** 257; g) U. Stalmach, H. Kolshorn, I. Brehm, H. Meier, *Liebigs Ann.,* **(1996)** 1449; h) U. Stalmach, H. Detert, H. Meier, V. Gebhardt, D. Haarer, A. Backer, H.W. Schmidt, *Opt. Mater.,* 9 **(1998)** 77.

[16] K. Müllen, G. Wagner, Wiley-VCH, *Electronic Materials: The Oligomer Approach,* Weinheim Germany, **(1998)** p.58.

[17] F. Louwet, D. Vanderzande, J. Gelan, *Synth. Met.,* 52 **(1992)** 125.

[18] a) J.L. Kice, K.W. Bowers, *J. Org. Chem.,* 84 **(1962)** 605; b) W.G. Filby, K. Gunther, R.D. Penzhorn, *J. Org. Chem.,* 38(23) **(1973)** 4070.

[19] A.J.J.M. van Breemen, D.J.M. Vanderzande, P.J. Adriaenssens, J.M.J.V. Gelan, *J. Org. Chem.,* 64 **(1999)** 3106.

[20] M.M. de Kok, A.J.J.M. van Breemen, P.J. Adriaensens, A. van Dixhoorn, J.M. Gelan, D.J. Vanderzande, *Acta Polym.,* 49 **(1998)** 510.

[21] J.H. Burroughes, D.D.C. Bradley, A.R. Brown, H.N. Marks, K. Mackay, R.H. Friend, P.L. Burns, A.B. Holmes, *Nature,* 347 **(1990)** 539.

[22] a) D. Braun, A.J. Heeger, *Appl. Phys. Lett.,* 58 **(1991)** 1982; b) A. Kraft, A.C. Grinsdale, A.B. Holmes, *Angew. Chem., Int. Ed. Engl.,* 37 **(1998)** 402; c) R.H. Friend, R.W. Gymer, A.B. Holmes, J.H. Burroughes, R.N. Marks, C. Taliani, D.D.C. Bradley, D.A. dos Santos, J.L. Brédas, M. Lodglund, W.R. Salaneck, *Nature,* 397 **(1999)** 121.

[23] a) N. Tessler, G.J. Denton, R.H. Friend, *Nature,* 382 **(1995)** 695; b) F. Hide, Diaz-Garcia, B.J. Schwartz, P.Q. Andersson, A.J. Heeger, *Science,* 273 **(1996)** 1833; c) N. Tessler, *Adv. Mater.,* 11 **(1999)** 363.

[24] M. Granstrom, K. Petrisch, A.C. Arias, A. Lux, M.R. Andersson, R.H. Friend, *Nature,* 395 **(1998)** 257.

[25] H. Sirringhaus, N. Tessler, R.H. Friend, *Science,* 280 **(1998)** 1741.

[26] a) Y. Pang, J. Li, B. Hu, F.E. Karasz, *Macromolecules,* 32 **(1999)** 3946; b) B. Xu, J. Zhang, Y. Pan, Z. Peng, *Synth. Met.,* 107 **(1999)** 47; c) I.K. Spilipoulus, J.A.A. Mikroyannidis, *Macromolecules,* 34 **(2001)** 5711; d) A.M. Sarker, E.E. Gürel, M. Zheng, P.M. Lathi, F.E. Karasz, *Macromolecules,* 34 **(2001)** 5897; e) P.L. Burn, A.B. Holmes, A. Kraft, D.D.C. Bradley, A.R. Brown, R.H. Friend, *J. Chem. Soc., Chem. Commun.,* **(1992)** 32.

[27] M. Yan, L.J. Rothberg, E.W. Kwock, T.M. Miller, *Phys. Rev. Lett.,* 75 **(1995)** 1992.

[38] C. Zhang, D. Braun, A.J. Heeger, *J. Appl. Phys.,* 73 **(1993)** 5177.

[29] a) 28e; b) D. Braun, E.G.J. Staring, R.C.J.E. Demandt, G.L.J. Rikken, Y.A.R.R. Kessener, A.H.J. Venhuizen, *J. Synth. Met.,* 66 **(1994)** 75.

[30] Y. Yu, H. Lee, A. Van Laeken, B.R. Hsieh, *Macromolecules,* 31 **(1998)** 5553.

[31] a) M. Hay, F.L. Klavetter, *J. Am. Chem. Soc.,* 117 **(1995)** 7112; b) T. Ahn, M.S. Jang, H.-K. Shim, D.-H. Hwang, T. Zyung, *Macromolecules,* 32 **(1999)** 3279; c) 28a.

[32] a) A. Gowri, D. Mandal, B. Shivkumar, S. Ramakrishnan, *Macromolecules,* 31 **(1998)** 1819; b) G. Padmanaban, S. Ramakrishnan, *J. Am. Chem. Soc.,* 122 **(2000)** 2244.

[33] V. Gelhardt, A. Bacher, M. Thelakkat, U. Stalmach, H. Meier, H.W. Schmidt, D. Haarer, *Synth. Met.,* 90 **(1997)** 123.

[34] a) A.J.J.M. van Breemen, P.J. Adriaensens, A.C.J. Issaris, M.M. de Kok, D.J.M. Vanderzande, J.M.J.V. Gelan, *Magn. Reson. in Chem.,* 38 **(2000)** 129; b) A.J.J.M. van Breemen, M.M. de Kok, P.J. Adriaensens, D.J.M. Vanderzande, J.M.J.V. Gelan, *Macrom. Chem. Phys.,* 202 **(2001)** 343.

III

A detailed study of the elimination and degradation reaction of the *n*-alkyl-sulphinyl OC_1C_{10}-PPV precursor polymers with *in-situ* analytical techniques

III.A Introduction

The conjugated polymers that have been described thus far in this thesis, are insoluble polymers (PPV and PTV). This insolubility prevents direct application of the conjugated material on the electrode to construct a polymer LED. This problematic characteristic of PPV can be circumvented by use of a precursor route [1], or by using materials that are soluble in their conjugated form [2]. The last years, much of the research emphasis has done on the latter polymers, because of their relatively easy synthesis, their good processing capabilities into single-layer devices and their high luminescence yields [3]. An important disadvantage of such materials, however, is that in some cases it is difficult to develop the multilayer structures that are required for highly efficient LEDs, since co-solubility of the different materials is hard to avoid. Soluble poly[2-(2'-ethylhexyloxy)-5-methoxy-1,4-phenylene vinylene] (MEH-PPV), displayed in Figure I.1, has been widely investigated and successfully used in single-layer LEDs [2a,b].

The soluble PPV derivative that has been used in this study is poly[2-(3',7'-dimethyloctyloxy)-5-methoxy-1,4-phenylene vinylene], attributed as OC_1C_{10}-PPV and shown in Figure III.1. The reason for the use of OC_1C_{10}-PPV as a conjugated polymer is its excellent solubility in several organic solvents. On top of this, OC_1C_{10}-PPV exhibits very good properties, like luminescence efficiency, light brightness at low voltage, and therefore finds common use as an active layer in polymer LEDs [4]. Even more recently promising results are obtained for its use in photovoltaic cells (= solar cells) [5]. Therefore, OC_1C_{10}-PPV has become a standard electroluminescent material inside the PLED and plastic solar cell research.

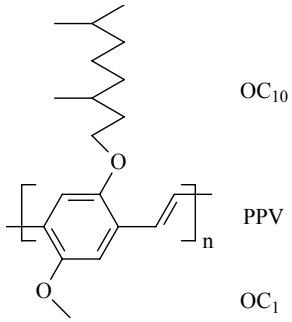

Figure III.1: *Structure of poly[2-(3',7'-dimethyloctyloxy)-5-methoxy-1,4-phenylene vinylene (OC_1C_{10}-PPV).*

The most useful synthetic route to prepare the OC_1C_{10}-PPV conjugated polymer is the direct "Gilch route", a one-step synthesis in basic environment (paragraph I.C.2.b) [6], shown as **(I)** in Figure III.2. Another synthetic route to prepare the conjugated OC_1C_{10}-PPV polymer is a non-ionic precursor route developed at the LUC, the "sulphinyl route" (paragraph I.C.2.d). A schematic representation of this synthetic route is depicted as **(II)** in Figure III.2. Through a chemical differentiation between the leaving group (Cl) and the polariser (S(O)R), the disadvantages of the Gilch route, which are summarised in paragraph I.C.2.b, are excluded [7]. Note that because the OC_1C_{10}-PPV conjugated polymer is a soluble PPV derivative, the thermal elimination from a precursor polymer **(A)** to the conjugated form **(B)** can also be carried out in solution. This implies that there are 3 different routes to obtain a conjugated OC_1C_{10}-PPV film, as is depicted in Figure III.3. The processing that is used can have a strong influence on the properties of the polymer film. Therefore it is possible to study the differences between a conjugated OC_1C_{10}-PPV film synthesised via a thermal treatment in solution **(III)** and in film **(IV)**.

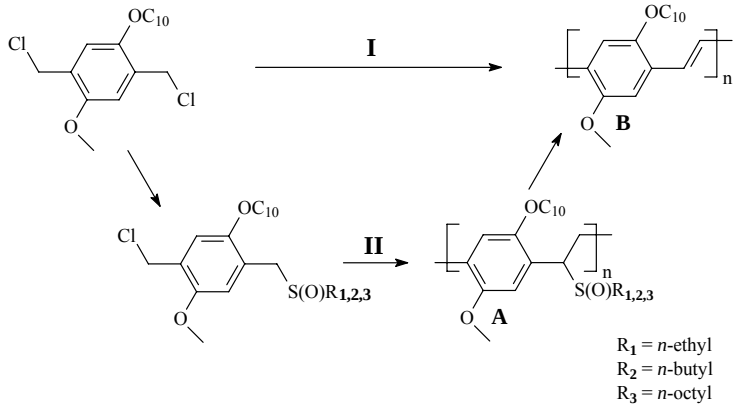

Figure III.2: *Schematic representation of the synthetic routes towards OC_1C_{10}-PPV: The "Gilch route"* ***(I)*** *and the "sulphinyl route"* ***(II)****.*

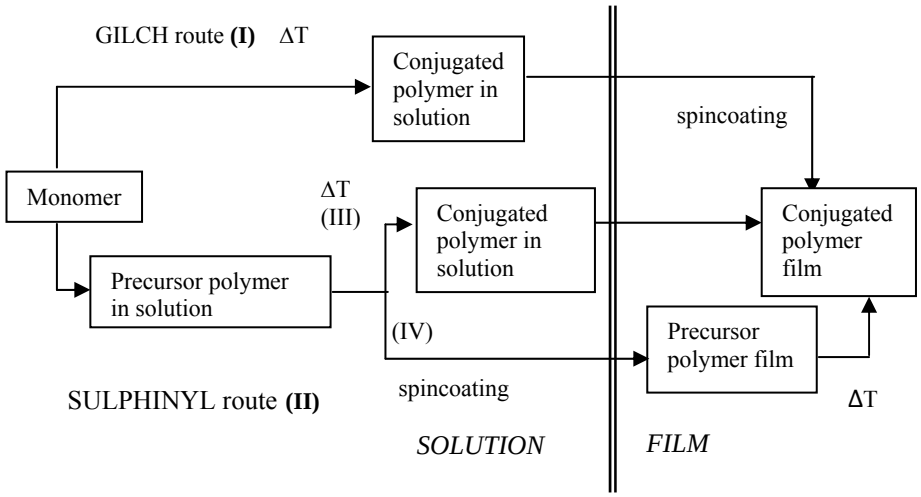

Figure III.3: *Schematic representation of 3 different possible routes to synthesis the soluble OC_1C_{10}-PPV precursor polymer to a conjugated OC_1C_{10}-PPV film.*

In this chapter, the elimination and degradation process of the OC_1C_{10}-PPV polymer is studied starting from an OC_1C_{10}-PPV precursor polymer thermally eliminated in film (**IV**, Figure III.3), like we have done in Chapter II.

III.B Thermal behaviour of the *n*-alkyl-sulphinyl OC_1C_{10}-PPV polymers: TGA and DIP-MS

III.B.1 ThermoGravimetric Analysis, TGA

The conversion from a precursor polymer to a conjugated polymer can be monitored with TGA. In TGA, the weight of the sample is measured as a function of temperature. The set-up of the TGA analysis is the same as in paragraph II.A.2. For the three *n*-alkyl-sulphinyl OC_1C_{10}-PPV precursor polymers, three temperature regions in which weight loss occurs are observed. These regions are clearly visible in Figure III.4.

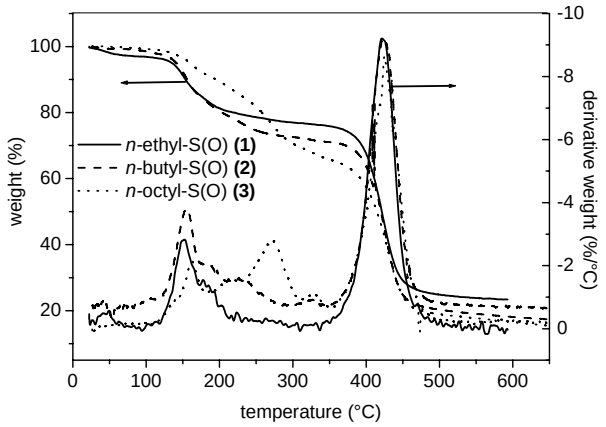

Figure III.4: *TGA thermogram of n-ethyl- **(1)**, n-butyl- **(2)** and n-octyl- **(3)** sulphinyl OC_1C_{10}-PPV precursor polymers. The heating rate is 10°C/min.*

The relatively small loss of weight just before 100°C is assigned to water evaporation. Above 100°C, two major steps of weight loss are visible, the first step (max. at 151°C for the *n*-ethyl-S(O) **(1)**, max. at 154.9°C for the *n*-butyl-S(O) **(2)** and a max. at 162.1°C for the *n*-octyl-S(O) **(3)**) is related to the elimination itself. The second major weight loss with a max. at 423°C for **1**, max. at 423.1°C for **2** and a max. at 425.6°C for **3**, accounts for the degradation of the conjugated OC_1C_{10}-PPV polymer. There is a large difference in weight

percentage measured directly after elimination at 175°C (80% for **1**, 85% for **2** and 91% for **3**) and the calculated residual values of weight (79% for **1**, 73% for **2** and 64% for **3**). The discrepancies between the calculated and experimental values for the *n*-octyl-sulphinyl derivative **(3)** may be due to incomplete evaporation of the elimination products, because of the higher boiling point of the *n*-octyl elimination products compared to the smaller *n*-ethyl elimination products. Around 350°C, the calculated and experimental weight percentages are comparable with each other (*n*-ethyl-S(O) **(1)**: calc. 79%, exp. 76%; *n*-butyl-S(O) **(2)**: calc. 73%, exp. 71%; *n*-octyl-S(O) **(3)**: calc. 64%, exp. 65.5%). At 350°C, all elimination products are evaporated from the polymer matrix. All the TGA results are summarised in Table III.1.

Table III.1: *TGA results of the n-alkyl-sulphinyl OC_1C_{10}-PPV precursor polymers.*

polymer	elim.temp.	elim. – evap.	weight after elimination		degrad. temp.	rest fraction
			calc.	exp.		600°C
n-ethyl **(1)**	151°C	115.6-230°C	79%	80%	423°C	23.5%
n-butyl **(2)**	154.9°C	120-348°C	73%	85%	423.2°C	18.25%
n-octyl **(3)**	162.1°C	110-353°C	64%	91%	425.6°C	16.77%

A TGA thermogram of the OC_1C_{10}-PPV polymer, eliminated in solution, is shown as **(A)** in Figure III.5. In this case, the *n*-butyl-sulphinyl OC_1C_{10}-PPV precursor polymer is heated in toluene at 110°C for 4 hours under a continuous flow of nitrogen. The resulting red solution was precipitated in a non-solvent (methanol). The conjugated OC_1C_{10}-PPV polymer was then collected and dried in vacuum. Following this procedure, elimination products are not present anymore in the conjugated material. This is proven by the fact that no signal appears in the temperature region from ambient temperature up to 300°C. Comparing the TGA thermogram of the OC_1C_{10}-PPV polymer, eliminated in solution and shown in Figure III.5 (sulphinyl route) with the TGA thermogram starting from the *n*-butyl-sulphinyl OC_1C_{10}-PPV precursor polymer **(2)** (Figure III.4), it was noticed that the degradation of the conjugated system for both polymers is maximal at 423°C. In TGA, no difference is observed in degradation temperature when starting the heating process with an OC_1C_{10}-PPV

precursor polymer (elimination products are liberated during the heating program) or with a conjugated OC_1C_{10}-PPV polymer (without elimination products). And thus in TGA, the elimination products have no influence on the degradation temperature of the conjugated OC_1C_{10}-PPV polymer.

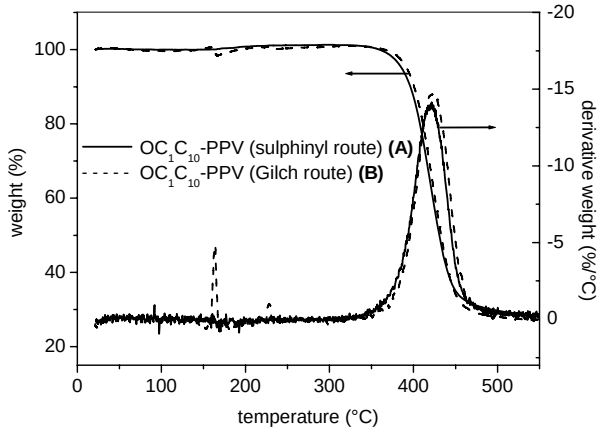

Figure III.5: *TGA thermogram of the conjugated OC_1C_{10}-PPV polymer synthesised via the sulphinyl **(A)** and Gilch **(B)** route. The heating rate is 10°C/min.*

In Figure III.5 **(B)**, also a TGA thermogram is shown of the conjugated OC_1C_{10}-PPV polymer synthesised via the Gilch route. Comparing this conjugated OC_1C_{10}-PPV polymer with the conjugated OC_1C_{10}-PPV polymer synthesised via the sulphinyl route **(A)** (in solution), almost no difference in degradation temperature is observed. Degradation of the OC_1C_{10}-PPV conjugated system is max. at 423 and 421°C for the OC_1C_{10}-PPV synthesised via the sulphinyl route and the Gilch route respectively. The remaining weight percentages at 550°C for the OC_1C_{10}-PPV (sulphinyl and Gilch) are respectively 26.7% and 25.5%, which are relatively high, probably because of the formation of crosslinked structures and polyaromatic hydrocarbons.

III.B.2 Direct Insert Probe Mass Spectrometry, DIP-MS

A second technique to study the thermal stability of the OC_1C_{10}-PPV precursor polymers is DIP-MS. The set-up of DIP-MS is the same as described in paragraph II.A.2. In Figure III.6, the total reconstructed ionchromatogram, in which the total ion current is plotted versus temperature, shows 2 signals. The first maximum in the total ion current appears at a temperature of 132°C for the *n*-ethyl-S(O) **(1)**, 135°C for the *n*-butyl-S(O) **(2)** and 145°C for the *n*-octyl-S(O) **(3)**. The fragments observed in the mass spectrum for the first peak are consistent with dimerisation and disproportionation processes of sulphenic acids, thus the elimination itself. These fragments are summarised in Table III.2.

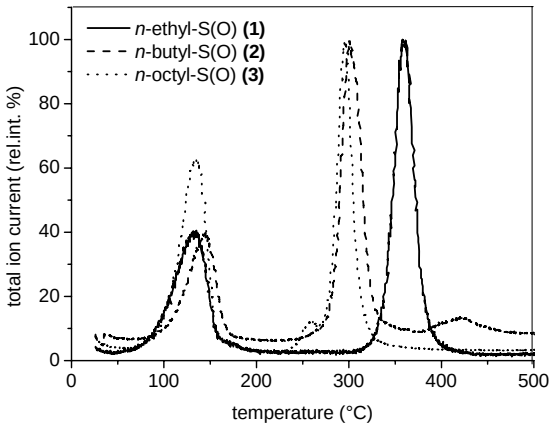

Figure III.6: *DIP-MS ionchromatogram of n-ethyl- **(1)**, n-butyl- **(2)** and n-octyl- **(3)** sulphinyl OC_1C_{10}-PPV precursor polymers. Heating rate 10°C/min.*

The total reconstructed ionchromatogram shows a second maximum in total ion current at 358°C for **1**, at 301°C for **2** and at 297°C for **3**. The mass spectra of the products of the second peak are for all precursor polymers consistent with the degradation of the conjugated system. These temperatures are lower compared to the degradation temperature of PPV (paragraph II.A.3).

Table III.2: *Fragmentation (EI) of n-alkyl-sulphinyl elimination products.*

n-ethyl-sulphinyl **(1)** ($R=C_2H_5$)		*n*-butyl-sulphinyl **(2)** ($R=C_4H_9$)		*n*-octyl-sulphinyl **(3)** ($R=C_8H_{17}$)	
m/z	fragment	*m/z*	fragment	*m/z*	fragment
137	$RSS(O)R^+$	194	$RSS(O)R^+$	307	$RSS(O)R^+$
122	$RSSR^+$	178	$RSSR^+$	289	$RSSR^+$
78	$RSOH^+$	122	$RS(O)_2H^+$	162	$RSOH^+$
		106	$RSOH^+$	161	RSO^+
		89	RS^+	145	RS^+
		64	SO_2^+	85	$C_6H_{13}^+$
		57	R^+	77	$C_6H_6^+$
		47	SO^+	71	$C_5H_{11}^+$
		41	$C_3H_5^+$	64	SO_2^+
		39	$C_3H_3^+$	57	$C_4H_9^+$
				48	SO^+
				43	$C_3H_7^+$
				39	$C_3H_3^+$

Comparing these observations with the TGA data indicates, that under argon flow (TGA) the elimination reaction and the evaporation of the elimination products are kinetically separated. In DIP-MS, the high vacuum will gradually shift the evaporation temperature downwards until evaporation and elimination are no longer separated.

III.C *In-situ* analytical techniques: FT-IR and UV-Vis spectroscopy

The *in-situ* experiments with Fourier Transform Infrared Spectroscopy (FT-IR) are performed in a Harrick high Temperature cell (HHT-cell), which is positioned in the beam of a Perkin Elmer Spectrum One FT-IR spectrometer (nominal resolution 4 cm^{-1}, summation of 16 scans). The temperature of the sample and the metal part is controlled by a Watlow (serial number 999, dual channel) temperature controller. A precursor polymer was spincoated from a chloroform solution (6mg/ml) on a KBr pellet at 500 rpm. The spincoated KBr pellet (diameter 25 mm, thickness 1 mm) is in contact with the metal part. A background spectrum is recorded before heating and spectra are scanned continuously. "Timebase Software" is used to follow the IR absorbance in the wavelength region of interest as a function of time (paragraph II.A.3.a).

The *in-situ* experiments with Ultraviolet Visible Spectroscopy (UV-Vis) are performed on a Cary 500 UV-VIS-NIR spectrophotometer (interval 1 nm, scan rate 600 nm/min, continuous run from 200-700 nm). A precursor polymer was spincoated from a chloroform solution (6mg/ml) on a quartz disc at 1000 rpm. The spincoated quartz disc (diameter 25 mm, thickness 3 mm) was heated in the HHT-cell. This HHT-cell is also positioned in the beam of the UV-VIS-NIR spectrophotometer. A background spectrum is recorded before heating. "Scanning Kinetics Software" is used to monitor the absorbance at a certain wavelength as a function of time (paragraph II.A.4.a).

There is a difference in heat transport between the metal block of the HHT-cell and the sample (KBr pellet or quartz disc). The applied atmosphere (nitrogen flow or vacuum) is important in this heat transport. In Figures III.7 and III.8 respectively, the temperature of the KBr pellet or the quartz disc and the metal block of the HHT-cell, each controlled with two different thermocouples, are plotted as a function of time. The difference in atmosphere (vacuum (10^{-2} mmHg) or nitrogen flow) used during the heating process (2°C/min) is also shown.

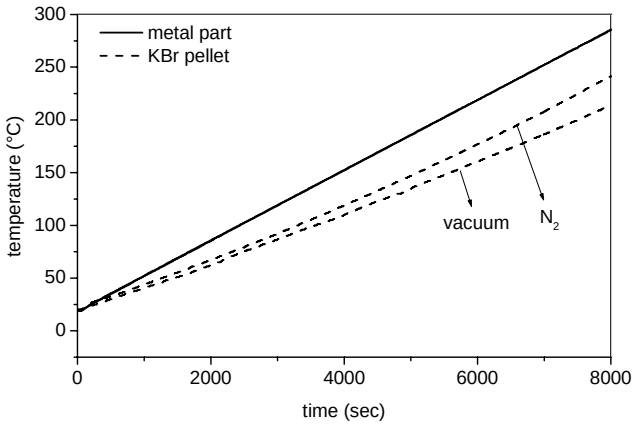

Figure III.7: *Temperature-time data of the KBr pellet (FT-IR spectroscopy) and the metal part of the HHT-cell, heated under vacuum and nitrogen flow.*

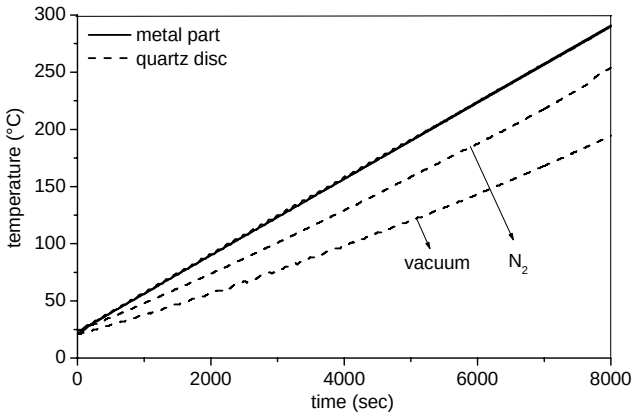

Figure III.8: *Temperature-time data of the quartz disc (UV-Vis spectroscopy) and the metal part of the HHT-cell, heated under vacuum and nitrogen flow.*

A conclusion is that the heat transport from the metal block of the HHT-cell to the KBr pellet or quartz disc is better in nitrogen flow compared to vacuum conditions. In the following experiments discussed in this chapter, the temperature of the thermocouple which is connected with the sample itself (KBr pellet or quartz disc) is always registered.

III.D Definitions of boundary conditions of thermal studies using *in-situ* spectroscopic techniques

This paragraph concerns the experimental studies on the preparation of OC_1C_{10}-PPV via the sulphinyl route in film, where special emphasis will be given to the conditions of the elimination reaction. First, we are going to check if *in-situ* FT-IR measurements are reproducible. Afterwards, the effect of thickness of the polymer film on the elimination reaction is studied. The effect of oxygen on the conjugated system is also investigated, which is the answer to the question: "Why should we use an inert atmosphere when performing the elimination reactions?". Finally, the effect of heating rate on the elimination reaction is also examined.

III.D.1 Reproducibility of the in-situ FT-IR analysis

FT-IR analysis that can be used to monitor the elimination reaction is only useful if the measurements show sufficient reproducibility. For this reason, 3 KBr pellets are prepared according to the procedure described in paragraph II.A.3.b. The precursor polymer examined is the *n*-butyl-sulphinyl OC_1C_{10}-PPV precursor polymer. The 3 samples are heated at 10°C/min up to 200°C under a continuous flow of nitrogen. To check if the IR measurements are reproducible, the IR absorbance of the sulphinyl group at 1038 cm^{-1} and the IR absorbance of the *trans* vinylene double bond at 965 cm^{-1} are plotted versus temperature, during the conversion from precursor polymer to the corresponding conjugated polymer, in Figure III.9. As soon as the eliminable group (a *n*-butyl-sulphinyl group) is eliminated (decrease in the absorbance at 1038 cm^{-1}) from the precursor polymer, a *trans* vinylene double bond with an IR-absorption at 965 cm^{-1} is formed (increase in the absorbance at 965 cm^{-1}).

The absorbance of the sulphinyl absorption is normalised to 100% at the start of the thermal treatment and the absorbance of the *trans* double bond absorption is normalised to 100% at the end of the thermal treatment (150°C), because the conjugated system is formed at this point. Results are summarised in Table III.3. From this Table III.3 and Figure III.9, the conclusion can be derived that the FT-IR analysis are surely sufficient "reproducible".

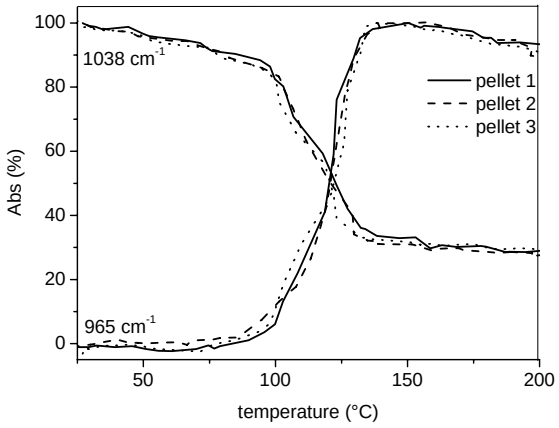

Figure III.9: *The reproducibility of the IR absorbance at 1038 cm^{-1} (sulphinyl group) and 965 cm^{-1} (trans vinylene double bond) as a function of temperature, for the 3 KBr pellets.*

Table III.3: *Percentages of the absorbance at 1038 and 965 cm^{-1}, at different temperatures, for the 3 pellets.*

		percentage (%)					
		25°C	75°C	90°C	120°C	150°C	200°C
1038 cm^{-1}	pellet 1	100	91.7	89.5	55.4	32.9	28.7
	pellet 2	100	91.9	89.3	52.7	31.7	27.6
	pellet 3	100	92.2	89.3	83.9	30.9	29.4
965 cm^{-1}	pellet 1	0	0	1	47.2	99.8	93.4
	pellet 2	0	0	4.5	45.1	99.8	89.6
	pellet 3	0	0	2.6	44.7	99	91

III.D.2 Effect of the polymer film thickness on the elimination reaction

It has already been reported that the thickness of the polymer film may have an influence on the elimination reaction itself and on the optical properties of the conjugated material. For instance, the elimination reaction of the

sulphonium precursor polymer is not only dependent on the temperature used, but also on the thickness of the polymer film [8]. Also in a polymer LED in which the emitter layer was a blend of an alternating block copolymer and poly(N-vinylcarbazole) (PVK) and an intermediate hole transporting layer of PPV, it was found that the photoluminescent and electroluminescent spectral properties of the system were dependent on the thickness of the PPV layer. In this case, the thickness of the PPV layer could be used to modulate the output color of the device [9].

We have also checked the influence of the polymer film thickness on the elimination reaction itself and on the evaporation of the elimination products. Polymer films of two different thickness are spincoated onto a KBr pellet: a thick film of 50 μm (spincoated at 200 rpm) and a thin film of 5 μm (spincoated at 1000 rpm).

With IR, the elimination and evaporation of the elimination products are followed. The experiment is performed on the *n*-butyl-sulphinyl OC_1C_{10}-PPV precursor polymer, which is heated in both cases at 10°C/min up to ~ 300°C under a continuous flow of nitrogen. In Figure III.10, the absorbance at 1038 cm^{-1} (sulphinyl), 2925 cm^{-1} (CH_2 asymmetrical stretch) and 965 cm^{-1} (C-H *trans* vinylene double bond) are plotted versus increasing temperature.

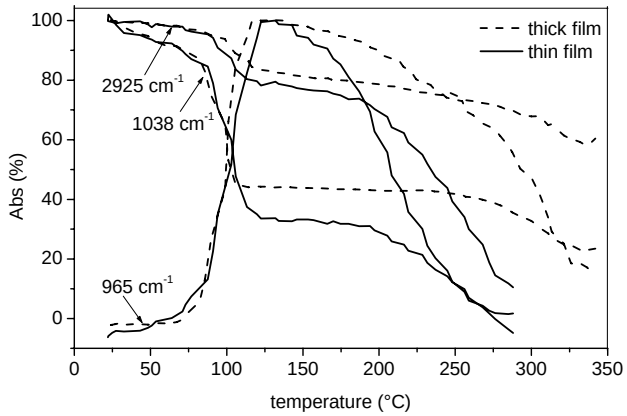

Figure III.10: *The absorbance at 1038, 2925 and 965 cm^{-1} versus increasing temperature for a thick and thin polymer film.*

These results indicate that for the absorbance at 1038, 2925 and 965 cm^{-1}, the thickness of the polymer film has no effect on the progress of the elimination reaction itself. The first decrease in the absorbance at 2925 cm^{-1} corresponds with the elimination of the *n*-butyl chain from the *n*-butyl-sulphinyl eliminable group. The difference in the absorbance here is negligible. In the increase of the absorbance at 965 cm^{-1}, which corresponds to the formation of the *trans* vinylene double bond during the elimination reaction, also no difference in elimination temperature is observed depending on the thickness of the polymer film. Depending on the thickness of the polymer film, there will be more or less sulphinyl groups left in the polymer matrix after elimination (~ 125°C) and even after evaporation of the elimination products (~ 250°C) as can be seen in the absorbance at 1038 cm^{-1}. For the absorbance at 2925 cm^{-1} the thickness of the polymer film does have an effect on the disappearance at higher temperatures (> 200°C), which is corresponding with the evaporation of the elimination products. In a thicker film it is probably much more difficult for the elimination products to evaporate or to diffuse out of the polymer matrix compared with thinner films (Figure III.10). The results are summarised in Table III.4.

Table III.4: *Percentages of the absorbance at 1038, 2925 and 965 cm^{-1} at different temperatures for a thick and thin polymer film.*

		percentages (%)							
	(°C)	25	85	100	125	170	210	250	285
1038 cm^{-1}	***thin***	100	84.6	59.9	33.6	32.6	25.3	10.9	~0
	thick	100	82.2	52.9	44.0	43.4	42.7	41.9	35.5
2925 cm^{-1}	***thin***	100	95.4	87.4	78.2	75.5	63.7	37.2	11.8
	thick	100	96.0	91.6	83.1	80.2	77.6	74.6	69.9
965 cm^{-1}	***thin***	0	13.1	51.6	99.4	87.2	48.1	10.5	1.5
	thick	0	13.5	52.9	100	95.7	86.4	72.9	57.6

In conclusion, the kinetics of the evaporation of the elimination products containing the alkyl groups is dependent on the thickness of the polymer film, whereas the progress of the elimination reaction itself is only affected by temperature, time and atmosphere (see later).

III.D.3 The effect of oxidation during the elimination process (oxidative degradation)

III.D.3.a Introduction

Electroluminescent polymers show interesting potential to replace inorganic light-emitting materials, particularly in novel applications, including large-area flexible displays. Considerable advances have been made to produce polymers that emit visible light and to fabricate devices that operate with greater quantum efficiencies. The greatest challenge, however, remains to improve the stability of these devices; a tenfold improvement of lifetime is required to compete commercially with inorganic materials. A great disadvantage for the application of conjugated polymers in devices (LEDs) and photovoltaic cells is the oxidation reaction of conjugated materials [10], because the formed carbonyl groups acts as exciton quenchers [11]. Currently, there is a great commercial interest in developing encapsulation materials to protect polymer LEDs from oxygen and moisture. But these encapsulation materials could fail. Therefore it is preferable to design polymers that have inherent environmental stability. It is important to determine which precautions should be taken in order to exclude oxidation of the material.

III.D.3.b Results and discussion

A *n*-butyl-sulphinyl OC_1C_{10}-PPV precursor polymer is heated at 2°C/min from ambient temperature up to 275°C in air. The absorbance of the *trans* vinylene double bond at 965 cm^{-1} is followed as a function of increasing temperature and is shown as a solid line in Figure III.11. The elimination or the formation of the double bond starts around 70°C and ends around 110°C. The absorbance at 965 cm^{-1} starts to decrease immediately after the formation of the double bond.

In Figure III.12, an enlarged part of some IR-spectra of the *n*-butyl-sulphinyl OC_1C_{10}-PPV (precursor) polymer at different temperatures is shown. The *trans* vinylene C-H out-of-plane bending band intensity at 965 cm^{-1} is decreased, reflecting the breaking of the backbone double bond. At the same time there is a substantial increase in carbonyl content (aromatic aldehyde C=O

stretch) at 1684 cm^{-1}. At the late stages of oxidation, an IR-absorption at 1746 cm^{-1} becomes quite prominent. The origin of this shoulder is still unclear. Higher oxidated products of aldehydes, such as carboxylic acid derivatives, could explain this higher IR-absorption.

From Figure III.11, it becomes clear that, as soon as the double bond absorbance begins to decrease (almost immediately after elimination), an increase in the absorbance of the aromatic aldehyde groups at 1684 cm^{-1} is visible. Around 200°C, the absorbance of the aromatic aldehydes starts to decrease. Instead of these aromatic aldehydes, higher oxidated products such as carboxylic acids (esters) are formed. At 175°C, an increase in the absorbance at 1746 cm^{-1} is observed and an acceleration in the decrease of the absorbance of the *trans* double bond takes place.

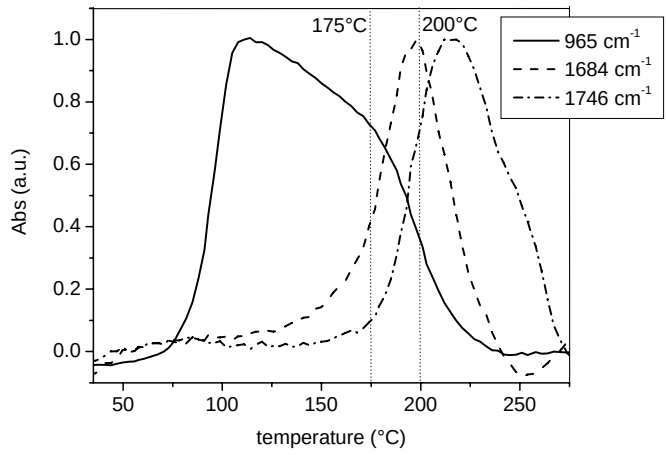

Figure III.11: *The absorbance at 965, 1684 and 1746 cm^{-1} as a function of increasing temperature for the n-butyl-sulphinyl OC_1C_{10}-PPV precursor polymer in air.*

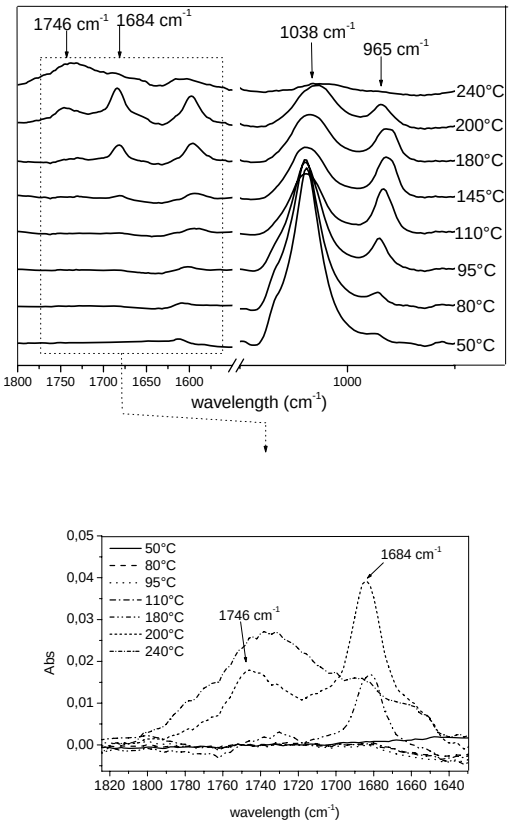

Figure III.12: *Enlarged part of the IR-spectra of the n-butyl-sulphinyl OC_1C_{10}-PPV polymer at different temperatures.*

The oxidation of double bonds to aldehyde groups [11] is a well known photooxygeneration reaction and is shown in Figure III.13 A, B. Oxygen forms weakly bond complexes with double bonds. It is very likely that the reaction proceeds via a 1,2-cycloaddition of the polarised oxygen to the double bond [12], resulting in the formation of dioxetane species **(1)**. These dioxetanes often decompose to form two terminal aldehydes **(2)**. Oxidation of an alkoxy-substituted PPV results in the formation of aromatic aldehyde groups (A), but also ester products are observed, shown in Figure III.13 B.

The result of this type of elimination, performed in air, is that a conjugated polymer with a certain amount of defects is formed. These defects

lower the stability of the conjugated polymer. This conclusion was also confirmed by the color of the conjugated polymer. A dark yellow-brown color is obtained at 125°C. Normally, a conjugated OC_1C_{10}-PPV polymer has a red color at that temperature.

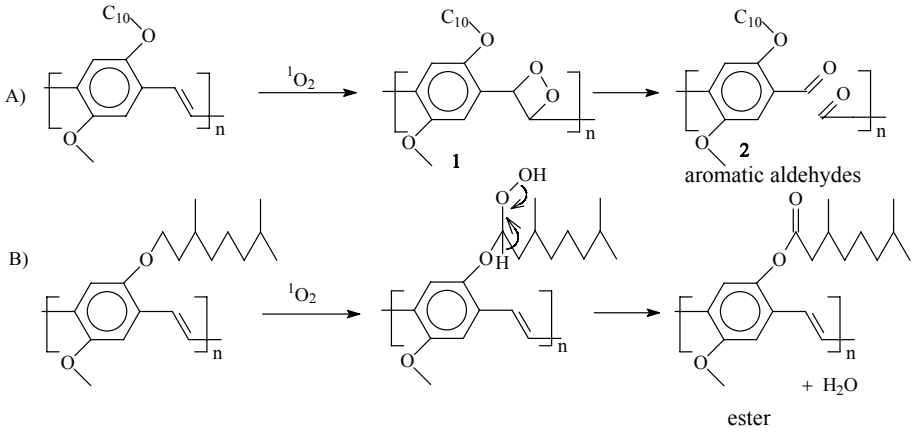

Figure III.13: *Oxidation mechanism for alkoxy-substituted PPV derivatives (OC_1C_{10}-PPV).*

From reports in literature, it is known that decreasing carbonyl concentrations, by converting PPV under a reducing atmosphere, increased PL decay lifetime by a factor of four [13]. To avoid oxidation of double bonds (oxidative degradation), the thermal elimination reactions in the further discussion are all carried out in an oxygen free environment. Therefore, the HHT-cell is always continuous purged with nitrogen flow.

III.D.4 The effect of heating rate: Kinetic analysis of derivative curves in thermal analysis

Knowledge of kinetic parameters, such as the reaction rate and activation energy, offers the opportunity to determine the reaction mechanism in solid phases. For non-isothermal heating experiments these kinetic parameters could be obtained by the method of Ozawa. When changes in the mechanism are observed, this can lead to a unique characteristic and hence a better knowledge of the materials. Besides this, there are also more practical reasons to know the reaction rates and their temperature dependence. The industry needs measurements of those parameters for treatment conditions, because augmentation of temperature or elongation of reaction time implies more costs.

III.D.4.a Method of Ozawa

In this method, the conversion process is followed experimentally with *in-situ* FT-IR spectroscopy. By increasing the temperaure, a precursor polymer in the solid state **(A)** is converted into a conjugated polymer **(B),** while a gas **(C)** is released (eq.III.1).

$$A(v) \longrightarrow B(v) + C(g) \qquad \text{(III.1)}$$

For the method of Ozawa, the absorbance of the sulphinyl group at 1038 cm^{-1} and the absorbance of the *trans* vinylene double bond at 965 cm^{-1} are followed during the conversion process at different heating rates. The "method of Ozawa" [14] is a non-isothermal isoconventional kinetic method and is independent of the reaction model (= model-free methodology). This model-free methodology allows us to determine the dependence of the activation energy on the extent of conversion. When the heating rate is increased, the absorbance at 1038 cm^{-1} (sulphinyl) and at 965 cm^{-1} (*trans* double bond) shift to higher temperatures. The method of Ozawa uses this shift to calculate the activation energy of the conversion reaction. The first derivative of these curves to the temperature, shows a maximum or minimum at a certain temperature T_m, which is dependent on the heating rate β. The heating rate β and the temperature T_m, for at least three measurements, permit to determine the activation energy of the conversion reaction (eq.III.2) [14]. When ln (β/T_m^2) is plotted as a function of T_m^{-1}, a straight line with as slope $-E_A/R$ is obtained. From this, the activation energy can then be calculated (E_A = -R * slope).

$$\ln\left(\frac{\beta}{T_m^2}\right) = -\frac{E_A}{RT_m} + \ln\left(\frac{AR}{E_A}\right) - \ln(g(\alpha)) \qquad \text{(III.2)}$$

With β = heating rate

T_m = temperature (in Kelvin) of the maximum or minimum in the first derivative of the absorbance of the *trans* double bond at 965 cm^{-1} and the sulphinyl group at 1038 cm^{-1} respectively.

R= gas constant (= 8.314 $J\,K^{-1}mol^{-1}$)

A = pre-exponential factor

g(α) = function of "degree of conversion"

III.D.4.b Results and discussion

The *n*-butyl-sulphinyl OC_1C_{10}-PPV precursor polymer is used in the non-isothermal heating experiments. The polymer is heated from ambient temperature up to 150°C, at different heating rates (1, 2, 4, 5 and 10°C/min) and under a continuous flow of nitrogen. To determine the temperature range in which the elimination takes place, the absorbance of the sulphinyl group at 1038 cm^{-1} and the absorbance of the *trans* vinylene double bond at 965 cm^{-1} are plotted versus increasing temperature in Figures III.14 and III.15 respectively. The sulphinyl absorbance is vanishing during the conversion process, while the absorbance of the *trans* double bond is increasing at the same time.

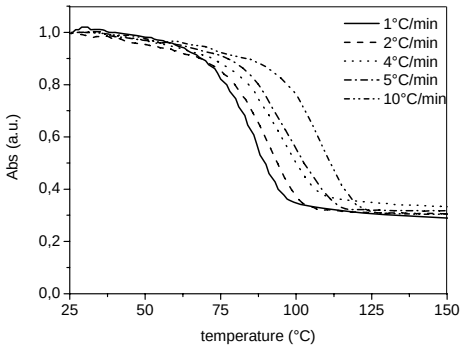

Figure III.14: *The absorbance of the sulphinyl group at* ***1038 cm^{-1}*** *as a function of temperature at different heating rates for the n-butyl-sulphinyl OC_1C_{10}-PPV (precursor) polymer.*

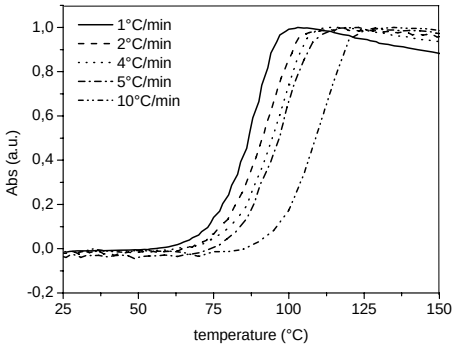

Figure III.15: *The absorbance of the trans double bond at* ***965 cm^{-1}*** *as a function of temperature at different heating rates for the n-butyl-sulphinyl OC_1C_{10}-PPV (precursor) polymer.*

From Figures III.14 and III.15 it is clear that by increasing the heating rate, the IR absorbance shifts to higher temperatures. The temperature of the sample itself is measured. If the sample is heated at a higher heating rate, a relatively larger temperature gradient exists in the sample and this broadens the curve. It seems more reasonable to perform the thermal analysis at a relatively slow heating rate in order to diminish the effect of temperature gradient. We have chosen to do all further conversion reactions at a heating rate of 2°C/min. To calculate the activation energy, we have determined the temperature T_m, which is the minimum or maximum temperature of the first derivative to the temperature of the sulphinyl absorbance and *trans* double bond absorbance at different heating rates (β), depicted in Figures III.16 and III.17 respectively.

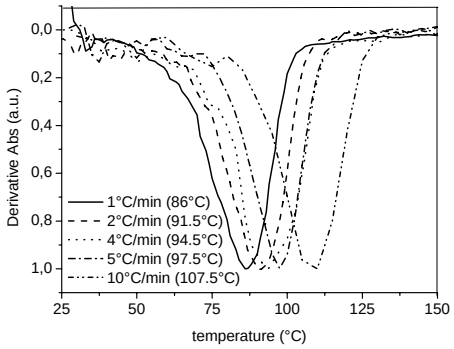

Figure III.16: *The first derivative of the absorbance of the sulphinyl group at* ***1038 cm^{-1}*** *at different heating rates.*

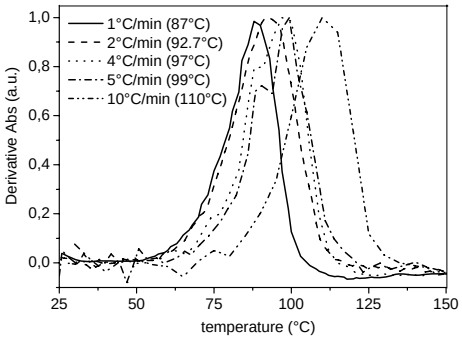

Figure III.17: *The first derivative of the absorbance of the trans double bond at* ***965 cm^{-1}*** *at different heating rates.*

To determine the activation energy, we make use of the non-isothermal isoconversional method of Ozawa, based on eq. III.2. For the experimental realisation, the different heating rates, ln (β/T_m^2) are plotted as a function of T_m^{-1} for the sulphinyl and *trans* double bond absorbance shown in Figure III.18.

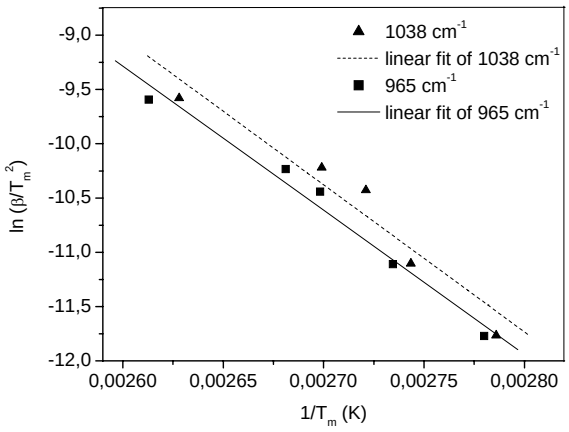

Figure III.18: *Ozawa plots for the sulphinyl and trans double bond absorbance.*

The activation energy (E_A) for the conversion process, calculated from the experimental data of the *trans* vinylene double bond absorbance at 965 cm^{-1} is 110,3 kJ/mol (26.4 kcal/mol). The activation energy for the conversion process derived from the experimental data of the sulphinyl absorbance at 1038 cm^{-1} at different heating rates is 115.7 kJ/mol (27.6 kcal/mol).

These apparent activation energies give us an idea about the activation energy of the conversion reaction. Further kinetic studies on the elimination reaction of *n*-alkyl-sulphinyl OC_1C_{10}-PPV precursor polymers are discussed in Chapter IV.

III.E A detailed study of the elimination and degradation reaction of *n*-alkyl-sulphinyl OC_1C_{10}-PPV (precursor) polymers with *in-situ* FT-IR spectroscopy

To obtain information about the elimination and degradation reaction, an *in-situ* heating experiment was performed with the *n*-butyl-sulphinyl OC_1C_{10}-PPV precursor polymer at 2°C/min from ambient temperature up to 350°C under a continuous flow of nitrogen. Before heating, at 25°C, the *n*-butyl-sulphinyl OC_1C_{10}-PPV precursor polymer is a yellow sticky solid product which turns into red after the elimination reaction. At much higher temperatures, the red color changes into black due to degradation of the conjugated polymer. Spectra of the *n*-butyl-sulphinyl OC_1C_{10}-PPV precursor polymer at ambient temperature and the conjugated OC_1C_{10}-PPV polymer at 110°C are shown in Figure III.19. The main differences between the two IR spectra are the disappearance of the stretching band of the sulphinyl group at 1038 cm^{-1}, the appearance of the olephenic C-H stretching at 3056 cm^{-1} and the increasing intensity of the *trans* vinylene double bond at 965 cm^{-1}. The absorbance of the CH_2 asymmetric stretch at 2925 cm^{-1} decreases partly. The IR absorption data of the *n*-alkyl-sulphinyl OC_1C_{10}-PPV (precursor) polymer are described in Table III.5.

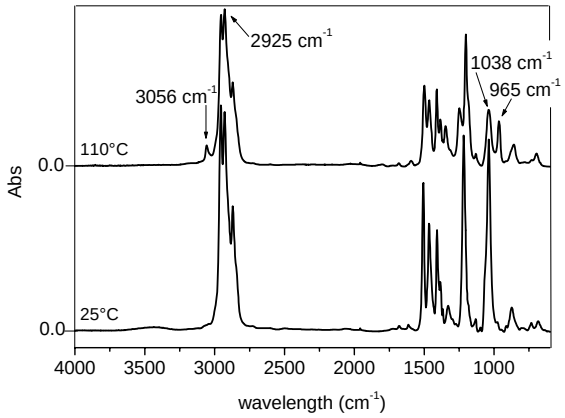

Figure III.19: *The IR spectra of the n-butyl-sulphinyl OC_1C_{10}-PPV precursor polymer at 25°C and the OC_1C_{10}-PPV conjugated polymer at 110°C.*

Table III.5: *IR absorption peaks of the n-alkyl-sulphinyl OC_1C_{10}-PPV (precursor) polymer.*

Figure III.19 (25°C): ***n*-butyl-sulphinyl OC_1C_{10}-PPV precursor polymer**	
absorption (cm^{-1})	attribution
682	*p*-phenylene out-of-phase ring bend
875	*p*-phenylene C-H out-of-plane bend
1038	S(O) stretching
1130	*p*-phenylene C-H in-plane bend
1218	*p*-phenylene C-H in-plane bend
1330	ring stretch
1410	*p*-phenylene semi-circular ring stretch
1464	(CH_3) asymmetrical bending
1508	*p*-phenylene semi-circular stretch
2870	CH_2 symmetrical stretch
2925	CH_2 asymmetrical stretch
2954	CH_2 asymmetrical stretch

Figure III.19 (110°C): **OC_1C_{10}-poly(*p*-phenylene vinylene)**	
absorption (cm^{-1})	attribution
860	*p*-phenylene C-H out-of-plane bend
965	C-H double bond wag vibration, in-phase out-of-plane
1202	ν (aryl-oxygen)
1248	vinyl C-H in-plane rock
1346	δ_s (CH_3) symmetrical bending
1384	ring stretch
1498	*p*-phenylene semi-circle ring stretch
1595	phenyl quadrant ring stretching asymmetrical
2870	CH_2 symmetrical stretch
2925	CH_2 asymmetrical stretch
2954	CH_2 asymmetrical stretch
3056	*trans* vinylene olephenic C-H stretch

For each *n*-alkyl-sulphinyl OC_1C_{10}-PPV precursor polymer, another shape of the sulphinyl absorption is obtained, as shown in Figure III.20.

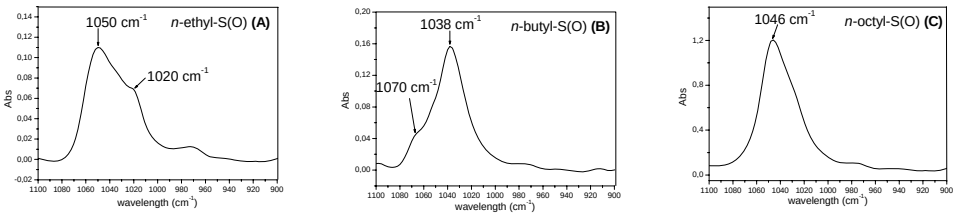

Figure III.20: *The sulphinyl absorption for the n-ethyl-**(A)**, n-butyl-**(B)** and n-octyl-**(C)** sulphinyl OC_1C_{10}-PPV precursor polymer.*

The *n*-ethyl-sulphinyl derivative **(A)** shows 2 shoulders, at 1050 cm^{-1} and 1020 cm^{-1}. The *n*-butyl-sulphinyl derivative **(B)** also has 2 shoulders, at 1070 cm^{-1} and 1038 cm^{-1} and the *n*-octyl-sulphinyl derivative **(C)** has only one shoulder at 1046 cm^{-1}.

The thermal elimination and degradation reactions have been studied extensively. The elimination reaction from precursor to conjugated polymer can be easily followed via the formation of the *trans* vinylene double bond (at 965 cm^{-1}), the vanishing of the sulphinyl group (at 1038 cm^{-1} for the *n*-butyl-sulphinyl eliminable group) and also by the partly disappearance of the absorbance of the CH_2 asymmetrical stretch (at 2925 cm^{-1}). The degradation of the conjugated OC_1C_{10}-PPV polymer can be examined by monitoring the decrease in the IR absorbance of the *trans* vinylene double bond at 965 cm^{-1} and of the CH_2 asymmetrical stretch absorbance at 2925 cm^{-1}. With "Timebase Software", there are three possibilities to demonstrate the elimination and degradation reaction of OC_1C_{10}-PPV (precursor) polymers. In Figure III.21 A, the wavenumber (cm^{-1}) is plotted as a function of time (min). The change in color at certain wavenumbers (1038 and 965 cm^{-1} are displayed here) shows the time frame in which the elimination and degradation reactions occur.

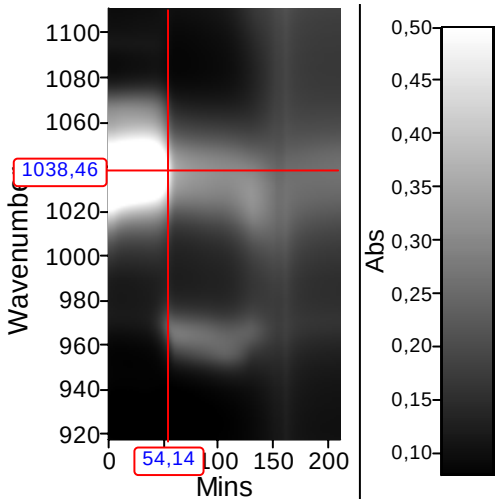

Figure III.21 A: *A color-plot of the wavelength (cm^{-1}) as a function of time (sec).*

In Figure III.21 B, a three-dimensional plot (absorbance-wavenumber (cm^{-1}) - time (sec)) of the IR spectra is shown, in which the absorbance at the most important wavelengths that are useful to study the elimination and degradation reaction, are shown. It is visible that during the non-isothermal heating process, the absorbance at 1038 cm^{-1} due to the S=O stretch of the sulphinyl group, decreases. A single band at 965 cm^{-1}, characteristic of long sequences of conjugated *trans* double bonds, is formed during the first part of the heating process (=elimination), but at higher temperatures, the absorbance at 965 cm^{-1} decreases again (=degradation).

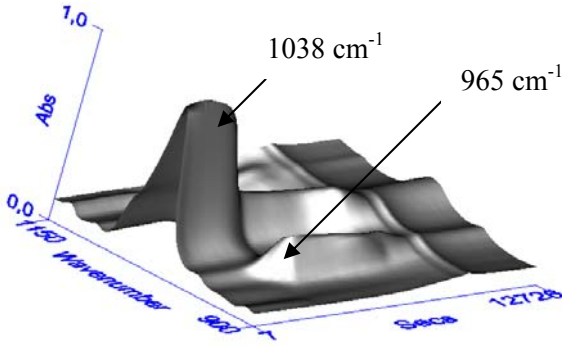

Figure III.21 B: *3D-plot (Abs-wavenumber (cm^{-1})-time (sec)) of the evolution of the absorptions at 1038 and 965 cm^{-1}.*

A third possibility to clarify the elimination and degradation reaction is shown in Figure III.22, in which the increase of the absorbance of the *trans* vinylene double bond (at 965 cm^{-1}) and the decrease of the absorbance of the sulphinyl group (at 1038 cm^{-1}) and alkyl group (at 2925 cm^{-1}) respectively are plotted as a function of increasing temperature. The elimination for the *n*-butyl-sulphinyl OC_1C_{10}-PPV precursor polymer starts at approximately 70°C and is completed at approximately 110°C at a ramp of 2°C/min.

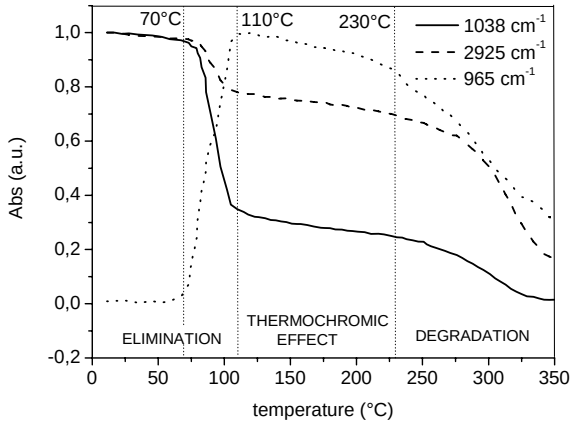

Figure III.22: *The absorbance at 1038, 2925 and 965 cm^{-1} as a function of increasing temperature for the n-butyl-sulphinyl OC_1C_{10}-PPV precursor polymer.*

The increase in absorbance, between 70 and 110°C, for the *trans* vinylene double bond at 965 cm^{-1}, is corresponding with the formation of the *trans* double bond during the elimination reaction. The decrease in absorbance of the sulphinyl group corresponds with the disappearance of the sulphinyl functionality present in the eliminable group (= S(O)-*n*-butyl). The decrease in the absorbance of the CH_2 asymmetric stretch, in the temperature range from 70 up to 110°C, corresponds with the disappearing of the *n*-butyl chain of the eliminable group. The elimination reaction for the *n*-alkyl-sulphinyl OC_1C_{10}-PPV precursor polymers occurs almost in the same temperature region as that for the *n*-alkyl-sulphinyl PPV precursor polymers, without alkoxy chains on the polymer backbone (Figure II.7).

After the temperature range in which elimination takes place (70-110°C), there is a slight decrease in the absorbance of the double bond between 110 and 230°C. This is not due to decomposition of the OC_1C_{10}-PPV polymer, but it is related to a thermochromic effect as was demonstrated by successive heat-cool cycles and will be explained in paragraph III.H. At temperatures around 230°C (fast decrease in the absorbance at 965 cm^{-1}), degradation of the conjugated system occurs. As soon as the conjugated polymer backbone begins to degrade, the absorbance of the CH_2 asymmetrical stretch at 2925 cm^{-1} decreases further. This means that once the degradation of the conjugated system occurs, also the alkoxy chain (OC_{10}) or part of the alkoxy chain is split off from the polymer backbone. By comparing the results of this experiment that is performed under nitrogen flow with the results of the heating experiment that was performed in air (presence of oxygen) (Figure III.11), it becomes clear that by doing the conversion reaction in an inert atmosphere, the stability of the conjugated OC_1C_{10}-PPV polymer up to 230°C is greatly enhanced. The absorbances of the aromatic aldehyde groups at 1684 cm^{-1} and higher oxidated products, such as carboxylic acid derivatives, at 1746 cm^{-1} are negligible, compared with the experiment in air. The nitrogen we have used in our lab contains 3 ppm O_2, 5 ppm H_2O, 1 ppm H_2 and is pure for 99.999%.

The start of the degradation process can also be visualised by an additional experiment which is performed on the *n*-butyl-sulphinyl OC_1C_{10}-PPV precursor polymer. In this experiment, the temperature is stepwise increased at a heating rate of 10°C/min up to the temperature levels shown in Figure III.23.

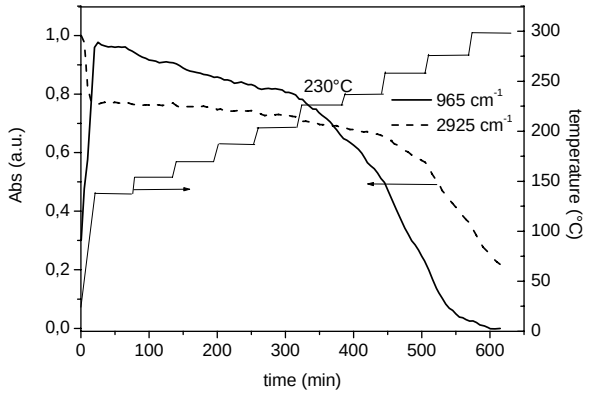

Figure III.23: *The absorbance at 965 and 2925 cm^{-1} plotted as a function of time and temperature (stepwise experiment).*

At each temperature level, the polymer remains isothermal for 60 minutes. In Figure III.23, the absorbance at 965 and 2925 cm^{-1} are plotted as a function of time and temperature. The observed phenomena are the same as the ones observed in the non-isothermal heating experiment (Figure III.22). Degradation of the conjugated OC_1C_{10}-PPV polymer starts at a temperature around 230°C. The decrease in the absorbance at 2925 cm^{-1} (CH_2 asymmetrical stretch) starts somewhat later, which was also visible in Figure III.22.

Looking back to Figure III.22, it becomes clear that ~ 30% of the sulphinyl absorbance is still present in the polymer film after elimination at 110°C. This was not the case after the thermal elimination from *n*-alkyl-sulphinyl PPV precursor polymers, without alkoxy chains on the polymer backbone, towards a conjugated PPV polymer (Figure II.7). After a non-isothermal elimination reaction at 120°C, followed with FT-IR spectroscopy, this conjugated PPV contains 0% of the sulphinyl absorbance in the polymer matrix. In Figure III.24 an enlarged part of the IR spectra (from 1100 to 990 cm^{-1}) of *n*-butyl-sulphinyl OC_1C_{10}-PPV precursor polymer is shown at different temperatures.

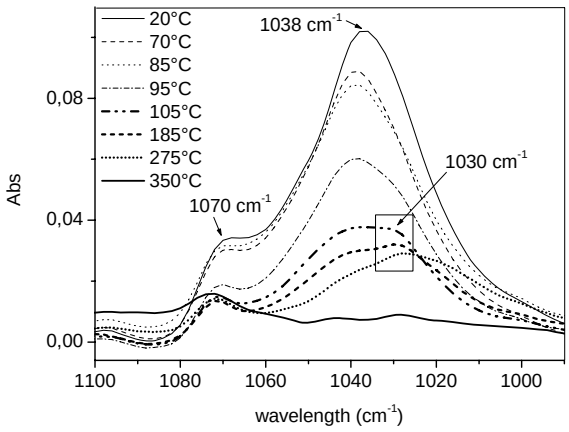

Figure III.24: *Enlarged part of the IR spectra (from 1100 to 990 cm^{-1}) of n-butyl-sulphinyl OC_1C_{10}-PPV precursor polymer at different temperatures.*

At ambient temperature, an absorbance at 1038 cm^{-1} with a small shoulder at 1070 cm^{-1} (typically for the *n*-butyl-sulphinyl group) is present. As soon as the elimination reaction takes place, the absorbance at 1038 cm^{-1}, due to the S=O stretch of the sulphinyl group, decreases and almost disappears. Around 105°C a small absorption band around 1030 cm^{-1} appears and becomes more dominant at higher temperatures (square in Figure III.24). This could be an effect of residing elimination products. The source of this interference are the thiosulphinates and thiosulphonates which contain a S(O) and $S(O)_2$ group respectively and are formed during the elimination reaction [15]. This is confirmed by IR analysis of synthesised *n*-butyl-thiosulphinate and *n*-butyl-thiosulphonate. It is clear that both elimination products cause disturbance of the 1100-990 cm^{-1} region.

A possible reason for the 30% of the absorbance of the *n*-butyl-sulphinyl group that is present in the OC_1C_{10}-PPV polymer matrix after elimination are the elimination products that are set free during the elimination process. These products are soluble in the OC_1C_{10}-PPV polymer matrix. The decane chain (from OC_{10}) which is covalently bonded with the polymer backbone acts as solvent. As a result, the elimination products are homogeneously distributed within the OC_1C_{10}-PPV polymer matrix. In the case of pure PPV, without alkoxy chains on the polymer backbone, the elimination products and the polymer matrix are incompatible leading to phase separation. In pure PPV, the elimination products are ejected more extremely from the polymer matrix.

To solve the problem of 30% elimination products left in the polymer matrix after elimination for the *n*-butyl-sulphinyl OC_1C_{10}-PPV polymer, we have performed a thermal elimination reaction on the *n*-ethyl-sulphinyl derivative, which has a smaller alkyl chain compared to the *n*-butyl-sulphinyl derivative. We also have used the *n*-octyl-sulphinyl derivative, which has a longer alkyl chain, to compare. Normally, the smaller the alkyl chain, the more volatile the elimination products are. The *n*-ethyl- and *n*-octyl-sulphinyl OC_1C_{10}-PPV precursor polymers are heated at 2°C/min from ambient temperature up to 250°C under nitrogen flow and under vacuum conditions (10^{-2} mmHg). In Figure III.25 A and B, the absorbance of the sulphinyl group at 1050 and 1046 cm^{-1} for the *n*-ethyl- **(A)** and the *n*-octyl- **(C)** sulphinyl derivative respectively, are plotted versus temperature. Also the absorbance of

the *trans* vinylene double bond at 965 cm^{-1} is plotted versus increasing temperature. A differentiation is made between doing the heating process in nitrogen flow and under vacuum conditions.

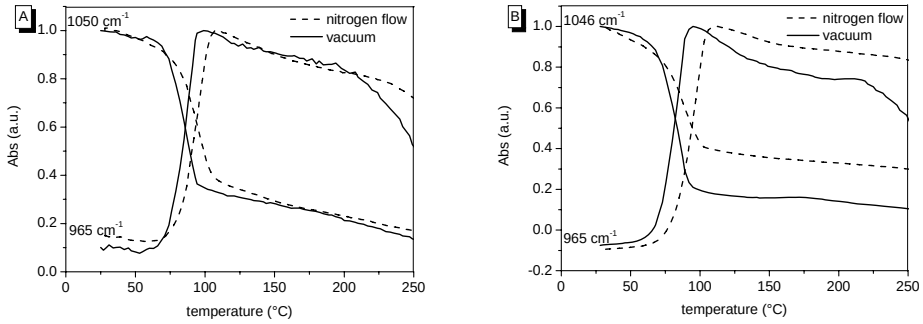

Figure III.25 A, B: *The absorbance for the sulphinyl group and the trans vinylene double bond for the n-ethyl-* ***(A)*** *and the n-octyl-****(B)*** *sulphinyl OC_1C_{10}-PPV precursor polymer versus temperature, under nitrogen flow and under vacuum conditions.*

First, the absorbance of the sulphinyl group for each *n*-alkyl-sulphinyl derivative under nitrogen flow is compared. The rest fraction of the sulphinyl group at temperatures higher than 110°C (after elimination) are due to the elimination products present in the polymer matrix. For the *n*-ethyl derivative **(A)**, the absorbance of the sulphinyl group constantly decreases at temperatures higher than 110°C. For the *n*-octyl **(B)** derivative the rest fraction of the absorbance of the sulphinyl group at temperatures higher than 110°C stays constant at ~ 36%. A conclusion is that the larger the alkyl chain, the higher the boiling point of the elimination products, the more difficult for the elimination products to evaporate or to diffuse out of the polymer matrix under nitrogen flow. These elimination products could attack the conjugated polymer (see Chapter IV). Therefore it is better to remove the elimination products out of the polymer matrix as fast and as much as possible. A solution for this is to do the same thermal elimination reaction, but now under vacuum conditions instead of nitrogen flow. The highest vacuum we could reach in our HHT-cell is 10^{-2} mmHg. When we compare the absorbance of the sulphinyl group for each *n*-alkyl derivative under vacuum conditions with these under nitrogen flow, we noticed that the rest fraction of the absorbance of the sulphinyl group and thus

also the rest fraction of the elimination products is less than under nitrogen flow, with the same thickness of polymer film in both atmospheres. The difference between the rest fraction of the elimination products in nitrogen flow and vacuum is greater when the alkyl chain is larger. 10^{-2} mmHg is not enough to remove all the elimination products out of the polymer matrix, therefore a higher vacuum is necessary. To obtain a good conjugated polymer film without elimination products in the polymer matrix, thus useful for practical applications, three topics are important. First, the alkyl chain has to be as small as possible. Secondly, the precursor film has to be as thin as possible and finally, the elimination reaction is best performed in high vacuum, to remove all the elimination products out of the polymer matrix.

The temperature range in which the elimination reaction occurs is also depending from the atmosphere used to do the elimination reaction with. To follow the elimination reaction, the absorbance of the *trans* vinylene double bond at 965 cm^{-1} for each *n*-alkyl derivative is plotted as a function of increasing temperature in Figure III.25 A and B. In nitrogen flow, the increase of the double bond (=elimination) occurs between 70 and 110°C for each *n*-alkyl derivative. Under vacuum conditions, the elimination reaction occurs between 53 and 95°C, which is earlier compared with the elimination reaction in nitrogen flow.

III.F A detailed study of the elimination and degradation reaction of *n*-alkyl-sulphinyl OC_1C_{10}-PPV (precursor) polymers with *in-situ* UV-Vis spectroscopy

There is the implied understanding that the infrared spectrum is only one source of information, and additional information is most likely required for a satisfactory analysis of the spectrum. Therefore, *in-situ* UV-Vis spectroscopy is used to make an extension of the study of the elimination and degradation reaction of the *n*-alkyl-sulphinyl OC_1C_{10}-PPV (precursor) polymers. More results concerning the conjugated sequences formed during the thermal conversion from *n*-alkyl-sulphinyl OC_1C_{10}-PPV precursor polymers towards conjugated OC_1C_{10}-PPV polymer can be derived from the UV-Vis spectra. It is well-known that the absorption maximum in the visible region of a conjugated

polymer is displaced to higher wavelengths when the number of conjugated double bonds increases [16]. The UV-absorption is due to π-π^* transition in the conjugated backbone and depends on the "effective conjugation length" [17].

To be sure that no changes occur at certain wavelengths due to the quartz disc itself, an *in-situ* UV-Vis non-isothermal heating experiment from ambient temperature up to 250°C is performed on a blanco quartz disc. The UV-absorption spectrum of a blanco quartz disc at ambient temperature is displayed in Figure III.26 A.

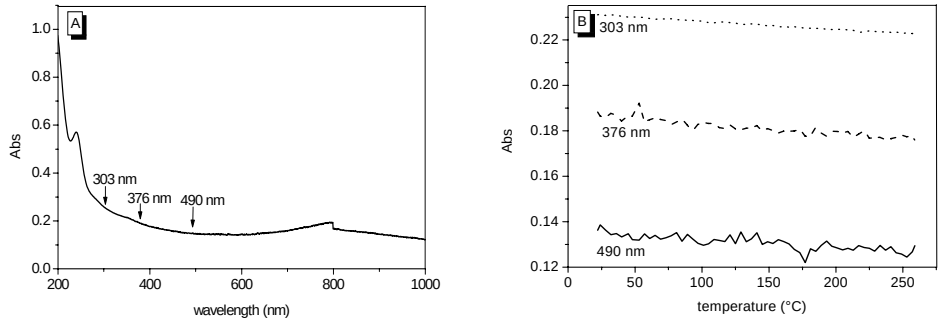

Figure III.26: A)*UV-absorption spectrum of a blanco (uncoated) quartz disc.* ***B)*** *The absorbance of the absorption maxima at 490, 376 and 303 nm as a function of temperature, for a blanco quartz disc.*

The absorbance of the most common wavelengths studied during the elimination and degradation process of OC_1C_{10}-PPV polymers, is plotted in Figure III.26 B for the uncoated quartz disc. The absorbance at 490, 376 and 303 nm remains unchanged during the experiment. This means that the quartz disc itself has no influence on the absorbance at these wavelengths during the elimination process from precursor polymer towards conjugated polymer.

To complete the study concerning the elimination and degradation reaction of OC_1C_{10}-PPV, obtained from the *in-situ* FT-IR spectroscopy, a similar procedure as that for FT-IR is used in UV-Vis. A non-isothermal heating experiment with a ramp of 2°C/min starting from ambient temperature up to 300°C under a continuous flow of nitrogen is performed. Figure III.27 displays

the UV-absorption spectra of an OC_1C_{10}-PPV in film (on quartz disc) at different temperatures, during the thermal elimination process. The presence of an isobestic point at 315 nm indicates that the elimination reaction is a simple transformation of one species to another (from precursor polymer to a conjugated material and sulphenic acid). At $\lambda > \lambda_{isob}$, the broad absorption band of the conjugated π-electron system between 350 and 600 nm increases in intensity and shows a bathochromic shift with increasing temperatures and the corresponding increase in the extent of conjugation. At lower extents of elimination, the variation in the intensity of the fine structure (Figure III.27, 85°C) reflects a gradual increase in the population of longer conjugated segments, the absorbance at longer wavelengths increase at the cost of the absorbance at shorter wavelengths.

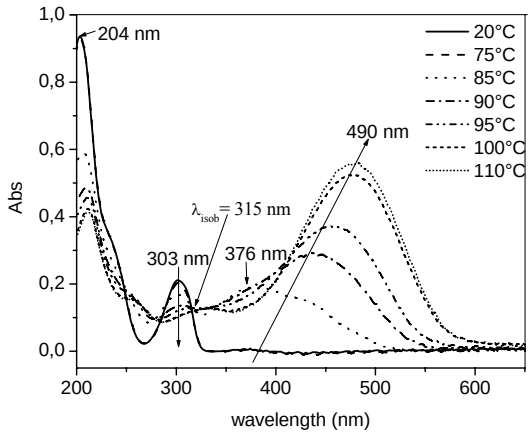

Figure III.27: *UV-absorption spectra of the n-butyl-sulphinyl OC_1C_{10}-PPV precursor polymer at different temperatures.*

At higher extents of elimination, however, the absorption band becomes broad and envelops the various oligomer bands within it. Absorptions at wavelengths below λ_{isob} (204 and 303 nm), which are corresponding to the π-π^* transition of the dialkoxy-substituted phenyl-ring, diminish progressively as the temperature increases. The broad low energy absorption is completed at 110°C as the absorption edge shows no further red-shifts (=saturation). The spectrum of the final red film, at 110°C, shows a strong broad band with a maximum at 490 nm ($=\lambda_{max}$). Elimination with an intermediate elimination

temperature (between 70 and 110°C) results in absorbance maxima between 303 and 490 nm at their specific temperatures. A few of the obtained spectra are shown in Figure III.27.

In Figure III.28, we have plotted the absorbance of three different absorption maxima (303, 376 and 490 nm) as a function of increasing temperature. The absorbance of the absorption maximum at 376 nm corresponds with the oligomeric fragments. The increase in the absorbance at 376 nm therefore indicates that the oligomeric fragments are formed between 50 and 75°C. As the elimination proceeds, between 75 and 110°C, the absorbance at 376 nm decreases. In the same time and temperature interval, the absorbance at 490 nm (λ_{max} of the conjugated OC_1C_{10}-PPV polymer) increases and the absorbance at 303 nm (λ_{max} of the OC_1C_{10}-PPV precursor polymer) decreases. This means that in a temperature range from 75 up to 110°C elimination takes place and a conjugated polymer is formed.

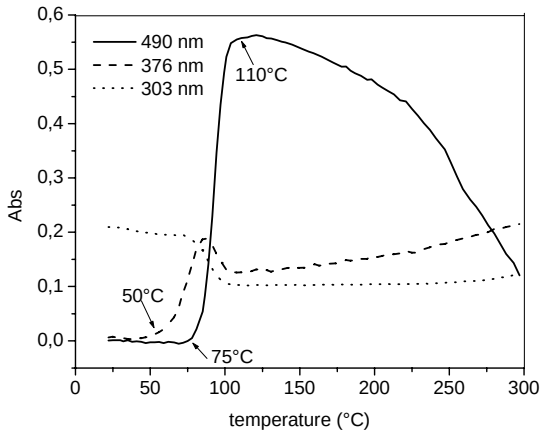

Figure III.28: *The absorbance of different absorption maxima (303, 376 and 490 nm) as a function of increasing temperature for the n-butyl-sulphinyl OC_1C_{10}-PPV precursor polymer.*

At temperatures higher than 110°C, the absorbance at 376 nm increases while the absorbance at 490 nm decreases again. This means that shorter conjugation lengths are formed at the cost of the higher conjugation lengths. Two phenomena can explain this observation. Between 110 and

~230°C, the slight decrease in the absorbance at 490 nm is related to a thermochromic effect (see paragraph III.H). The strong decrease in the absorbance at 490 nm at a temperature higher than ~230°C is related to the degradation of the conjugated OC_1C_{10}-PPV polymer. Both phenomena lead to a reduction of the effective conjugation length, visible as an increase in the absorbance at 376 nm.

It should also be noted that UV-visible light spectroscopy becomes insensitive to increasing conjugation when the conjugation lengths exceed 8 repeat units [18]. As a result, this method cannot be used as a quantitative technique for conjugated polymers with high degrees of elimination.

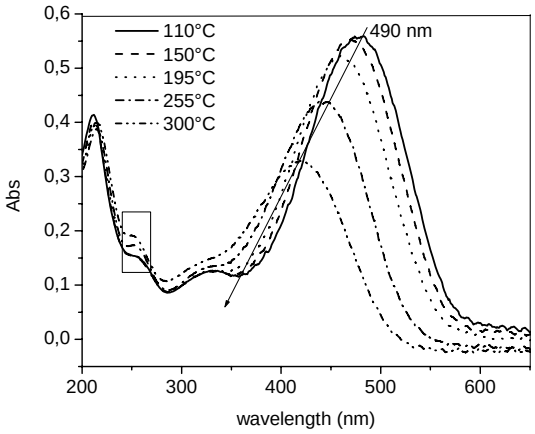

Figure III.29: *UV-absorption spectra of the OC_1C_{10}-PPV conjugated polymer at higher temperatures (= degradation process).*

In Figure III.29, UV-absorption spectra are shown at different temperatures (>110°C) to show the degradation process. At 110°C, the conjugated OC_1C_{10}-PPV system is formed with a λ_{max} at 490 nm. At higher temperatures, the degradation of the conjugated polymer causes a hypsochromic shift, a shift to shorter conjugation lengths, due to the loss of conjugation upon degradation. An additional effect of degradation is the appearance of an absorption band at 250 nm (at 255 and 300°C), which increases at higher temperatures. This absorption band corresponds with phenantrene units, which have an absorption between 200 and 300 nm [19].

To check the extend to which the conjugated OC_1C_{10}-PPV polymer is stable at temperatures higher than 110°C for longer periods of time, we have performed some isothermal experiments at 140, 155, 165, 190, 210, 240 and 270°C for a period of 300 minutes. All measurements were done under a continuous flow of nitrogen. In Figure III.30, the absorbance of λ_{max} at 490 nm is plotted versus time at different isothermal temperatures. The absorbance at 490 nm remains unaltered after 300 minutes heating at temperatures from 140 up to 210°C. At these temperatures, no degradation of the conjugated OC_1C_{10}-PPV polymer is taking place. At temperatures of 240 and 270°C, however, the absorbance at 490 nm decreases rapidly. Shorter conjugation lengths are formed and degradation occurs at these temperatures. From these isothermal experiments, it can be derived that degradation of the conjugated OC_1C_{10}-PPV polymer starts between 210°C and 240°C, which corresponds well with the onset temperature of degradation (~ 230C) obtained from the non-isothermal experiment.

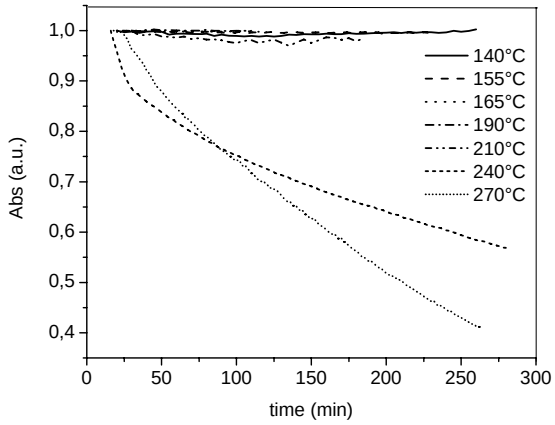

Figure III.30: *The absorbance of λ_{max} at 490 nm as a function of time at different isothermal temperatures.*

III.G UV-Vis and FT-IR results are complementary

An *in-situ* non-isothermal heating experiment on the *n*-butyl-sulphinyl OC_1C_{10}-PPV precursor polymer at 2°C/min from ambient temperature up to 300°C under a continuous flow of nitrogen was performed with FT-IR (paragraph III.E) and UV-Vis (paragraph III.F) spectroscopy. For the *in-situ* FT-IR and UV-Vis measurement respectively, the absorbance of the *trans* vinylene double bond at 965 cm^{-1} and the absorbance of λ_{max} at 490 nm are plotted versus increasing temperature in Figure III.31.

The evolution of the absorbance at both wavelengths corresponds with the development of the conjugated system. The decrease of both signals corresponds with the degradation of the conjugated polymer. Hence, we can conclude that both techniques are complementary, because the shape of the absorbance at 490 nm and 965 cm^{-1} coincides nicely.

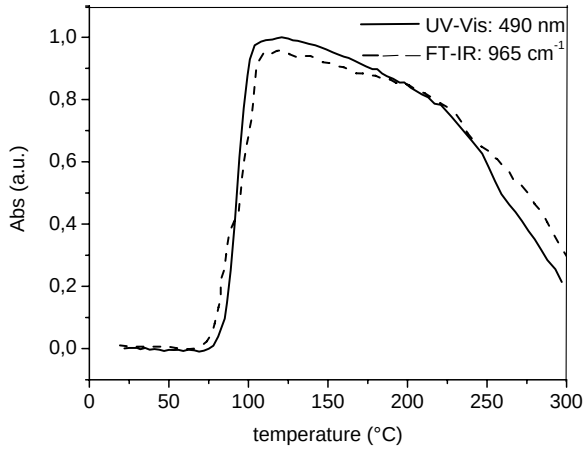

Figure III.31: *The absorbance at 965 cm^{-1} (FT-IR) and at 490 nm (UV-Vis) versus increasing temperature for the n-butyl-sulphinyl OC_1C_{10}-PPV precursor polymer.*

III.H Thermochromic effect

During the non-isothermal experiment (paragraph II.E and III.F), we have noticed that between 110 and 230°C, the absorbance at 490 nm and at 965 cm^{-1} is slightly decreasing. These observations may be caused by a "thermochromic effect" which is explained below. By heating the conjugated polymer, the mobility of the polymer chains increases, which implies an increase of the average torsion angle and thus the binding energy becomes smaller. The effective conjugation length decreases, which reflects in a blue-shift. This process is reversible. This means that by cooling down the polymer again, the mobility of the polymer chains decreases and again the effective conjugation length increases and a red-shift is observed.

III.H.1 Heating-cooling experiment

To prove that degradation of the conjugated OC_1C_{10}-PPV polymer starts only around 230°C, and that a "thermochromic effect" is responsible for the decrease in the absorbance at 490 nm in the non-isothermal heating experiment between 110 and 230°C, a heating-cooling experiment is performed on the already conjugated OC_1C_{10}-PPV polymer.

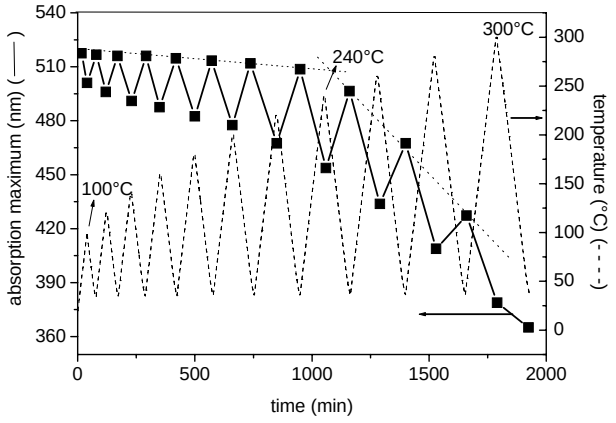

Figure III.32: *Temperature-time profile and the absorption maximum as a function of time and temperature for the conjugated OC_1C_{10}-PPV polymer.*

This red OC_1C_{10}-PPV polymer is eliminated in solution (toluene, 110°C for 4 hours) and precipitated in methanol. The conjugated OC_1C_{10}-PPV polymer was then collected and dried in vacuum. A solution (6mg/ml) of this conjugated OC_1C_{10}-PPV polymer in $CHCl_3$ is spincoated at 1000 rpm on a quartz disc. This quartz disc is then heated at 2°C/min up to different temperatures, and is cooled down again to 35°C each time, under a continuous flow of nitrogen. In Figure III.32, this time-temperature profile is depicted. Also, the absorption maximum (λ_{max}) at each maximum temperature (100°C,…, 240°C,…, 300°C) and minimum (35°C) in the temperature profile are displayed. The UV-data results are summarised in Table III.6.

Table III.6: *λ_{max} at each maximum and minimum in the temperature profile. The λ_{max} of OC_1C_{10}-PPV at ambient temperature is 517 nm.*

temperature (°C)	λ_{max} (nm) at maximum temperature	λ_{max} (nm) at 35°C after cooling
100	501	517
120	496	516
140	491	516
160	487.5	515
180	482.5	513
200	477.5	512
220	467.5	509
240	453.7	496.5
260	433.7	467.5
280	408.7	427.2
300	378.5	365

The absorption maximum (λ_{max}) of the conjugated OC_1C_{10}-PPV polymer eliminated in solution and measured in film at ambient temperature is 517 nm. By heating the conjugated OC_1C_{10}-PPV polymer, the effective conjugation length decreases. For instance, when the conjugated OC_1C_{10}-PPV polymer is heated up to 100°C, the λ_{max} is shifted from 517 nm to 501 nm. After cooling the conjugated OC_1C_{10}-PPV polymer again, the conjugated system is

fully recovered and a λ_{max} of 517 nm is observed again. This "thermochromic effect" can be repeated for higher temperatures. Up to ~ 220°C, the original λ_{max} is recovered after cooling. From 240°C on, however, and after cooling back to ambient temperature, a clear blue-shift (λ_{max} = 496.5 nm) is visible compared with the λ_{max} of the conjugated OC_1C_{10}-PPV polymer at ambient temperature (λ_{max} = 517 nm). This blue-shift becomes larger at temperatures > 240°C. The process now is not reversible anymore, meaning that degradation is taking place. The results discussed here are comparable with the results obtained from Figure III.28. The small decrease in the absorbance at 490 nm between 110 and 230°C is due to a thermochromic effect, while the fast decrease in the absorbance at 490 nm, at temperatures > 230°C, is due to degradation of the conjugated OC_1C_{10}-PPV polymer.

III.I Conclusions

The OC_1C_{10}-PPV polymer, soluble before and after elimination, can be synthesised via the Gilch and sulphinyl route. We have demonstrated that the *in-situ* FT-IR experiments are reproducible. We also have observed that the thickness of the polymer film does not have an influence on the elimination reaction itself, whereas the evaporation of the elimination products is dependent on the thickness of the polymer film. The elimination reaction of the *n*-alkyl-sulphinyl OC_1C_{10}-PPV precursor polymers starts at 70°C and ends around 110°C in nitrogen flow. At 110°C (after elimination) an absorption maximum at 490 nm is obtained for the conjugated OC_1C_{10}-PPV polymer. This effective conjugation length decreases again, by degradation of the conjugated system at 230°C. After elimination, a certain amount of elimination products, which are set free during the elimination reaction, remain in the polymer matrix, while in pure PPV (without alkoxy chains), the elimination products are ejected more effectively from the polymer matrix. When the elimination reaction is performed in vacuum conditions (10^{-2} mmHg), the elimination reaction shifts to a lower temperature (53-95°C). In these vacuum conditions also the elimination products diffuse and evaporate better out of the polymer matrix. The smaller the alkyl chain, the lower the boiling point of the elimination products, the more easy for the elimination products to evaporate or to diffuse out of the polymer matrix.

III.J Experimental part

III.J.1 General remarks and instrumentation

The same instruments are used to characterise the monomers and corresponding *n*-alkyl-OC_1C_{10}-PPV precursor polymers as described in paragraph II.D.1. The use of the Harrick High Temperature cell in the FT-IR spectrometer and UV-Vis spectrophotometer, to study the elimination and degradation reaction with, is explained in paragraph II.A.3.a and II.A.4.a respectively. Thermal analysis of the *n*-alkyl-OC_1C_{10}-PPV precursor polymers with TGA and DIP-MS is described in paragraph II.A.2.

III.J.2 Materials

Unless stated otherwise, all reagents and solvents were of analytical grade and used without further purification. All reactions were carried out under an inert atmosphere of nitrogen.

Bis-tetrahydrothiopheniumsalt of 1-[2,5-di(chloromethyl)-1,4-methoxy phenoxy]-3,7-dimethyloctane A solution of 1-[2,5-di(chloromethyl)-4-methoxyphenoxy]-3,7-dimethyloctane (70.5 g, 0.195 mol) and tetrahydro-thiophene (70 ml, 0.79 mol) in MeOH (150 ml) was stirred for 80 hours at ambient temperature. The reaction mixture was precipitated in diethylether (1750 ml). The precipitate was collected and washed with *n*-hexane (300 ml). Evaporation of the solvent gave a white hygroscopic solid (96.5 g, 85 %). ^{1}H-NMR (D_2O, 400 MHz) δ 0.82 (d, J = 3.0 Hz), 2.20 (m, 8H, $SCH_2C\underline{H}_2$), 3.40 (m, 8H, $SC\underline{H}_2$), 3.80 (s, 3H, $OC\underline{H}_3$), 4.07 (m, 2H, $OC\underline{H}_2$), 4.41 (s, 4H, $ArC\underline{H}_2S$), 7.12 (s, 2H, Ar<u>H</u>) ppm.

1-[2-[(Ethylsulphanyl)methyl]-5-(chloromethyl)-4-methoxyphenoxy]-3,7-di methyloctane A mixture of NatBuO (3.8 g, 0.011 mol) and *n*-ethanethiol (2.43 g, 26.9 mmol) in MeOH (75 ml) was stirred for 30 minutes at ambient temperature. The clear solution was added in one portion to a stirred solution of the bissulphoniumsalt (21.66 g, 37.3 mmol) in MeOH (120 ml). After one hour the reaction mixture was neutralized with aqeous HCl (1 M), if necessary, and

concentrated in vacuum. The crude product was diluted with $CHCl_3$ (175 ml) and the precipitate was filtered off. The filtrate was concentrated in vacuum. The oil thus obtained was diluted with *n*-octane or petroleum ether (boiling range 100-130°C) and concentrated to remove tetrahydrothiophene. This sequence was repeated three times to afford a light yellow viscous oil.

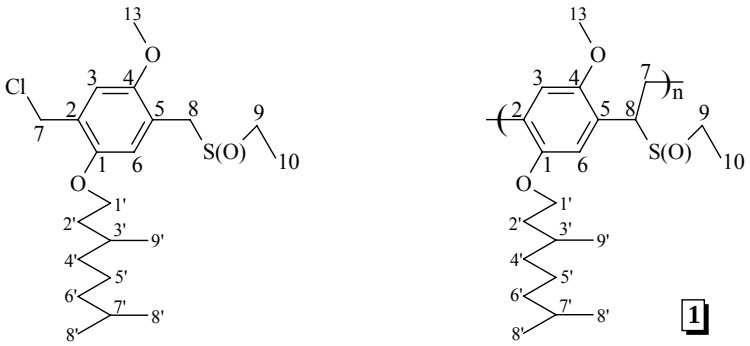

Figure III.34: *Atomic numbering scheme of n-ethyl-sulphinyl OC_1C_{10}-PPV monomer(left) and precursor polymer (right).*

1-[2-[(Ethylsulphinyl)methyl]-5-(chloromethyl)-4-methoxyphenoxy]-3,7-dimethyloctane (Figure III.34, left) An aqueous (35 wt.%) solution of H_2O_2 (4.78 g, 0.049 mol) was added dropwise to a solution of crude thioether (9.91 g, 2.95 mmol) in 1,4-dioxane (100 ml), TeO_2 (0.47 g, 2.97 mmol) and three drops of concentrated HCl. After three hours the reaction was quenched by adding a saturated aqueous NaCl solution (100 ml). The reaction mixture was extracted with $CHCl_3$ (3 x 100 ml), the combined organic layers were dried over $MgSO_4$ and concentrated in vacuum. The reaction mixture was purified by column chromatography (SiO_2, $CHCl_3$ 100 %) and a light yellow viscous oil is obtained (3 g, 28.8 %). ^{1}H-NMR ($C_2D_2Cl_4$, 400 MHz) δ 0.79 (d, 6H, H8'), 0.89 (d, 3H, H9'), 0.93 (t, 3H, H10), 1.15 (m, 2H, H6'), 1.15 + 1.24 (m, 2H, H4'), 1.31 (m, 2H, H5'), 1.51 (m, 1H, H7'), 1.59 + 1.81 (m, 2H, H2'), 1.62 (m, 1H, H3'), 2.63 (m, 2H, H9), 3.80 (s, 3H, H13), 3.97 (m, 2H, H1'), 3.85 + 4.06 (dd, 2H, H8), 4.64 + 4.66 (dd, 2H, H7), 6.80 (s, 1H, H6), 6.93 (s, 1H, H3) ppm; ^{13}C-NMR ($C_2D_2Cl_4$, 105°C, 100 MHz): δ 19.5 (C9'), 22.38 + 22.5 (C8'), 24.31 (C10), 24.41 (C5'), 27.67 (C7'), 29.52 (C3'), 35.97 (C2'), 36.93 (C4'), 38.88 (C6'), 41.30 (C7), 51.05 (C9), 52.39 (C8), 55.77 (C13), 67.09 (C1'), 112.60 (C3), 115.47 (C6), 119.69 (C5), 126.28 (C2), 150.18 (C1), 150.91 (C4) ppm.

***n*-Ethyl-sulphinyl OC_1C_{10}-PPV precursor polymer (1)** (Figure III.34, right) This compound was synthesized according to the general procedure described in paragraph II.D.2.a starting from 1-[2-[(ethylsulphinyl)methyl]-5-(chloro methyl)-4-methoxyphenoxy]-3,7-dimethyloctane (2 g) to give 1 as a yellow sticky solid (0.82 g). M_w = 225.376, M_w/M_n = 2.58; ^{1}H-NMR ($CDCl_3$, 400 MHz) δ 0.6-2.0 (br, 19H, H2'-H9'), 3.7-4.1 (br, 3H, H9), 4.1-4.4 (br, 2H, H1'), 7.1-7.3 (br, 2H, H7 + H8), 7.4-7.6 (br, 2H, H3 + H6) ppm; ^{13}C-NMR ($C_2D_2Cl_4$, 100MHz): δ 19.1 (C9'), 22.4 (C8'), 24.5 (C5' + C10), 27.7 (C7'), 28.2 + 29.0 (C8), 29.7 (C3'), 36.3 (C2'), 37.2 + 37.4 (C4'), 39.1 (C6'), 49.1 (C9), 54.0-59.0 (C7), 55.6 (C13), 66.9 (C1'), 110.7 (C3 + C6), 114.6 (C3 + C6), 122.0 (C5 + C2), 126.5 + 127.0 (C2 + C5), 150.1 (C1), 151.1 (C4) ppm; IR (KBr): ν 2959, 2931, 2865, 1504, 1465, 1410, 1215, 1050, 870 cm^{-1}.

***n*-Butyl- and *n*-octyl-sulphinyl OC_1C_{10}-PPV precursor polymers (2 and 3)** The synthesis of these precursor polymers is the same as for the *n*-ethyl-sulphinyl OC_1C_{10}-PPV precursor polymer and are synthesized before by A. van Breemen. Synthesis and characterization of the monomers and corresponding precursor polymers are described in the following articles [20].

Conjugated OC_1C_{10}-PPV polymer A solution of precursor polymer (1.5 mmol) in toluene (50 ml) was degassed for 1 hour by passing through a continuous stream of nitrogen. The solution was heated at 110°C under exclusion of light. After conversion the polymer was already partially precipitated. Toluene was removed in vacuum and the resulting solid was dissolved in hot (160°C) *o*-dichlorobenzene (30 ml). The resulting red clear solution was precipitated in MeOH (300 ml). The polymer was collected, washed with MeOH (3 x 50 ml) and dried in vacuum. A red solid was obtained.

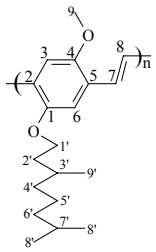

Figure III.35: *Atomic numbering of the conjugated OC_1C_{10}-PPV polymer.*

^{1}H-NMR ($C_2D_2Cl_4$, 105°C, 400 MHz):δ 0.6-2.0 (br, 19H, H2'-H9'), 3.7-4.1 (br, 3H, H9), 4.1-4.4 (br, 3H, H1'), 7.1-7.3 (br, 2H, H7+H8), 7.4-7.6 (br, 2H, H3+H6) ppm; ^{13}C-NMR($C_2D_2Cl_4$, 105°C, 100 MHz): δ 19.6 (C9'), 22.3 (C8'), 24.4(C5'), 27.6 (C7'), 30.2 (C3'), 36.6 (C2'), 37.3 (C4'), 39.1 (C6'), 56.7 (C9), 68.3 (C1'), 110.3 (C3), 111.5 (C6), 123.8+124.0 (C7+C8), 127.7 (C2+C5), 151.4 (C1), 151.9 (C4) ppm; IR(KBr): ν 3056, 2954, 2925, 2868, 1508, 1464, 1413, 1383, 1355, 1258, 1207, 1038, 966, 853, 691 cm^{-1}.

III.K References

[1] a) P.L. Burn, D.D.C. Bradley, R.H. Friend, D.A. Halliday, A.B. Holmes, R.W. Jackson, A. Kraft, *J. Chem. Soc. Perkin Trans,* 1 **(1992)** 3225; b) B.R. Hsieh, H. Antoniadis, D.C. Bland, W.A. Feld, *Adv. Mater.,* 7 **(1995)** 36.

[2] a) D. Braun, A.J. Heeger, *Appl. Phys. Lett.,* 58 **(1991)** 1982; b) E.G.J. Staring, R.C.J.E. Demandt, D. Braun, G.L.J. Rikken, Y.A.R.R. Kessener, T.H.J. Venhuizen, H. Wynberg, W. ten Hoeve, K.J. spoelstra, *Adv. Mater.,* 6 **(1994)** 934; c) J.-K. Lee, R.R. Schrock, D.R. Baigent, R.H. Friend, *Macromolecules,* 28 **(1995)** 1966; d) A. Hilberer, H.-J. Brouwer, B.-J. van der Scheer, J. Wildeman, G. Hadziioannou, *Macromolecules,* 28 **(1995)** 4525; e) D.U. Kim, T. Tsutsui, S. Saito, *Chem. Lett.,* **(1995)** 587.

[3] a) 2b-e; b) S.T. Kim, D.-H. Hwang, X.C. Li, J. Grüner, R.H. Friend, A.B. Holmes, H.K. Shim, *Adv. Mater.,* **(1996)** 979.

[4] H. Becker, H. Spreitzer, W. Kreuder, E. Kluge, H. Schenk, I. Parker, Yong Cao, *Adv. Mater.,* 12(1) **(2000)** 42.

[5] a) G.H. Gerlinck, J.M. Warman, E.G.J. Staring, *J. Phys. Chem.,* 100 **(1996)** 5485; b) C.J. Brabec, N.S. Sariciftci, J.C. Hummelen, *Adv. Funct. Mater.,* 11(1) **(2001)** 15; c) J. Manca, *LUC-nieuws*, oktober **(2001)** p.28; d) L. van der Ent, *Kunststof magazine,* april 3 **(2001)** p.38; e) T. Munters, T. Martens, L. Goris, V. Vrindts, J. Manca, L. Lutsen, W. De Ceuninck, D. Vanderzande, L. De Schepper, J. Gelan, N.S. Saricifci, C.J. Brabec, *Thin Solid Films,* 403 **(2002)** 247.

[6] H.G. Gilch, W.L.Wheelwright, *J. Polym. Sci. Part A: Polym. Chem.,* 4 **(1966)** 1337.

[7] a) F. Louwet, D. Vanderzande, J. Gelan, *Synth. Met.,* 52 **(1992)** 125; b) F. Louwet, D. Vanderzande, J. Gelan, J. Mullens, *Macromolecules,* 28 **(1995)** 1330; c) F. Louwet, D. Vanderzande, J. Gelan, *Synth. Met.,* 69 **(1995)** 509; d) A. Issaris, D. Vanderzande, J. Gelan, *Polymer,* 38(10) **(1995)** 2571.

[8] J. Gmeiner, S. Karg, M. Meier, M. Rieβ, P. Strohriegl, M. Schwoerer, *Acta Polym.,* 44 **(1993)** 201.

[9] B. Hu, F.E. Karasz, *Chem. Phys.,* 227 **(1998)** 263.

[10] I. Murase, T. Ohnishi, T. Nogushi, M. Hirooka, *Polymer Commun.,* 25 **(1984)** 327; b) D.D.C. Bradley, *J. Phys. D,* 20 **(1987)**1389.

[11] Ph. D. Thesis J. Hagting, **(1999)**, Rijksuniversiteit Groningen.

[12] B. Ranby, J.F. Rabek, *Photodegradation, Photo-oxidation, and Photo stabilization of Polymers,* John Wiley & Sons, **(1975)**.

[13] M. Yan, J.L. Rothberg, F. Papadimitrakopoulos, M.E. Galvin, T.M. Miller, *Phys. Rev. Lett.,* 73 **(1994)** 744.

[14] a) T. Ozawa, *J. Thermal Anal.,* 2 **(1970)** 301; b) K. Celis, I. Van Driessche, R. Mouton, G. Vanhoyland, S. Hoste, *Key Engineering Materials,* 206(2) **(2002)** 807.

[15] J. Cymerman, J.B. Willis, *J. Chem. Soc. London,* **(1951)** 1332.

[16] a) F. Sondheimer, D.A. Efraim, R. Wolousky, *J. Am. Chem. Soc.,* 83 **(1961)** 1675; b) V. Daniels, N.H. Rees, *J. Polym. Sci., Polym. Chem. Ed.,* 12 **(1974)** 2115.

[17] P.L. Burn, A. Kraft, D.R. Baigent, D.D.C. Bradley, A.K. Brown, R.H. Friend, R.W. Gymer, A.B. Holmes, R.W. Jackson, *J. Am. Chem. Soc.,* 115 **(1993)** 10117.

[18] G. Drefahl, R. Kuhmstedt, H. Oswald, H.H. Hoerhold, *Die Makromol. Chemie,* 131 **(1970)** 89.

[19] J.B. Schlenoff, L. J. Wang, *Macromolecules,* 24 **(1991)** 6653.

[20] a) Ph. D Thesis A. van Breemen, **(1999)**, Limburgs Universitair centrum, Diepenbeek; b) L. Lutsen, A.J. van Breemen, W. Kreuder, D.J.M. Vanderzande, J.M.J.V. Gelan, *Helvetica Chimica Acta,* 83 **(2000)** 3113.

IV

Kinetics and mechanism of the elimination process of *n*-alkyl-sulphinyl OC_1C_{10}-PPV precursor polymers

IV.A Chemical kinetics of the elimination reaction of *n*-alkyl-sulphinyl OC_1C_{10}-PPV precursor polymers

IV.A.1 Theoretical background

One reason for studying the reaction rates is the practical importance of being able to predict how fast a reaction mixture approaches equilibrium. In chemistry, we are concerned with how quickly a reactant is consumed or a product is formed. The rates of most chemical reactions are very sensitive to temperature, which means that the temperature must be held constant throughout the course of the reaction. Before starting the study of chemical kinetics, we need to define the reaction rate in terms of the concentration of a reactant or products. The conversion reaction studied in this chapter (Figure IV.1) is an unimolecular reaction, which means that a single reactant molecule splits up in two or more product molecules.

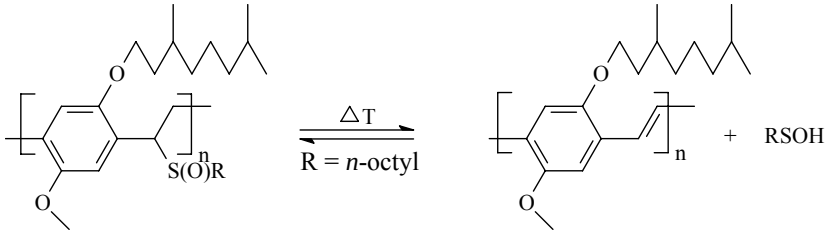

Figure IV.1: *Elimination reaction of the n-octyl-sulphinyl OC_1C_{10}-PPV precursor polymer.*

In this first order reaction, the concentration of reactant decays exponentially with time. The rate is proportional to the concentration (eq.IV.1):

$$v = k\,[A]^a \quad (a=1) \tag{IV.1}$$

The integrated rate law for a first order reaction predicts the concentration of reactant remaining after a given time. If the molar concentration of a reactant A at time t is written as $[A]_t$ and the initial concentration is denoted as $[A]_0$, the following equation IV.2 is obtained.

$$[A]_t = [A]_0 * e^{-kt} \tag{IV.2}$$

k = rate constant (s^{-1})

t = elapsed time

The integrated rate law is also used to determine whether a reaction is first order and, if it is, to measure its rate constant. If we take logarithms of both sides, we obtain eq. IV.3:

$$\ln[A]_t = \ln[A]_0 - kt \tag{IV.3}$$

which has the form of a linear equation (y = intercept + slope * x)

The rate constant k is independent of the concentrations, but strongly depends on the temperature. Common sense and chemical intuition suggest that,

the higher the temperature, the faster a given chemical reaction will proceed. Quantitatively, this relationship between the rate a reaction proceeds and its temperature is determined by the Arrhenius equation (eq. IV.4).

$$\ln k = \ln A - E_A/RT \qquad \text{(IV.4)}$$

A = pre-exponentional factor

E_A = activation energy

R = gas constant (= $8.314*10^{-3}$ J mol^{-1} K^{-1})

The activation energy (E_A) of a reaction can be determined by plotting ln k as a function of 1/T in degrees Kelvin. The intercept with the axis at 1/T = 0 is equal to ln A and the slope of the line is equal to - E_A/R. The greater the activation energy E_A, the stronger the temperature dependence of the reaction rate. Reactions with a small E_A ($\approx$ 10 kJ mol^{-1}) have rates that increase only slightly with the temperature.

IV.A.2 Results and discussion

To obtain kinetic data of the conversion reaction of the *n*-octyl-sulphinyl OC_1C_{10}-PPV precursor polymer, two spectroscopic techniques are used: *in-situ* FT-IR spectroscopy and *in-situ* UV-Vis spectroscopy. The isothermal temperatures at which conversion reactions are performed are chosen from the non-isothermal heating experiments in which the *n*-octyl-sulphinyl OC_1C_{10}-PPV precursor polymer is heated at 2°C/min from ambient temperature up to 300°C under a continuous flow of nitrogen (paragraph III.E, III.F).

In-situ UV-Vis and *in-situ* FT-IR spectroscopy are used to determine in which temperature range the elimination reaction takes place. From Figure III.22 and III.33, it is clear that the elimination reaction starts at a temperature around 70°C. Starting from this result, the kinetic experiments are done at isothermal temperatures above 60°C.

IV.A.2.a In-situ FT-IR spectroscopy

A series of *n*-octyl-sulphinyl OC_1C_{10}-PPV precursor polymers were prepared. Therefore a solution of the precursor polymer (6 mg/ml $CHCl_3$) is spincoated at 500 rpm on a KBr pellet. First, the Harrick High Temperature cell (HHT-cell) is pre-heated up to the desired isothermal temperature. Afterwards, the spincoated KBr pellet is brought into the HHT-cell, which is continuously flushed with nitrogen, and then positioned in the beam of the FT-IR spectrometer. At that moment, we start to measure the absorbance of the sulphinyl group at 1046 cm^{-1} and the absorbance of the *trans* vinylene double bond at 965 cm^{-1}, which are disappeared and formed respectively during the elimination reaction to the conjugated OC_1C_{10}-PPV polymer. We have chosen the absorption peak at 1410 cm^{-1}, from the *p*-phenylene semi-circular stretch, as reference peak, because this absorption peak may not change during the elimination reaction. Plotting the IR spectra before and after each isothermal experiment, we can conclude that the absorption peak at 1410 cm^{-1} stays constant throughout the elimination reaction, which means that it is not necessary to do an extra normalisation to measure the absorbance at 1046 and 965 cm^{-1} as a function of time. The absorbance of the sulphinyl group at 1046 cm^{-1} and the *trans* double bond at 965 cm^{-1} versus time at several isothermal temperatures are plotted in Figure IV.2 A and B respectively.

From Figure IV.2, we can conclude that the higher the isothermal temperature, the easier/faster the elimination reaction occurs (see also Table IV.1). All curves in Figure IV.2 A and B follow an exponentional decay and growth of first order respectively. This confirms that the conversion to the conjugated OC_1C_{10}-PPV polymer follows first-order kinetics. The exponentional fit used to determine the rate constant of the conversion reaction at each isothermal temperature is described in eq. IV.5:

$$y = m_1 * \exp(-m_2 * m_0) \qquad \text{(IV.5)}$$

With $y = [A]_t$, $m_1 = [A]_0$, $m_2 = k$ and $m_0 = t$.

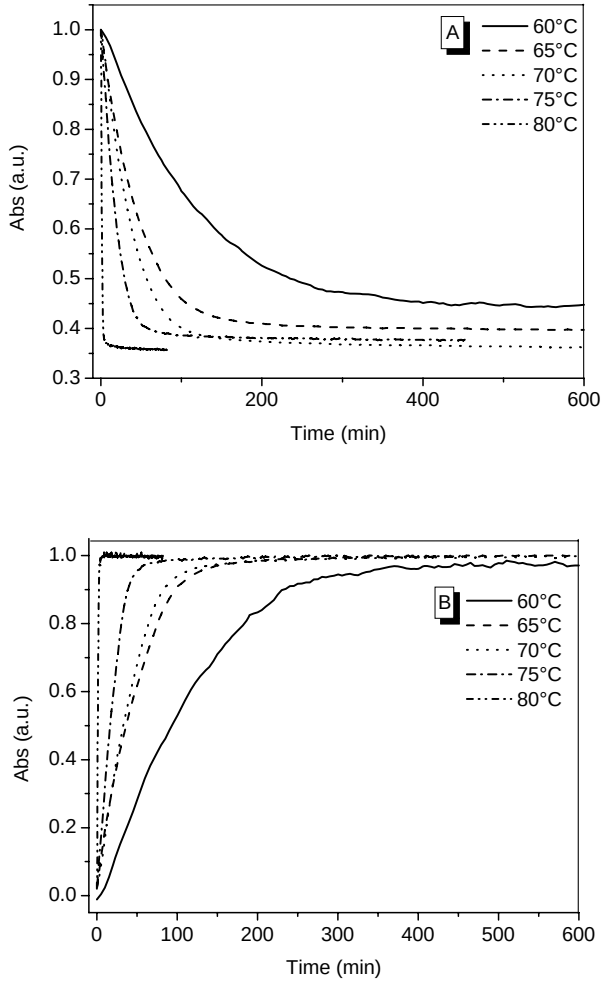

Figure IV.2: *The absorbance of the sulphinyl group at 1046 cm^{-1} (A) and the absorbance of the trans vinylene double bond at 965 cm^{-1}(B) versus time at 60, 65, 70, 75 and 80°C.*

From the variation of the rate constant with the temperature (Table IV.1), the activation energy (E_A) of the conversion reaction can be determined using the Arrhenius equation (eq.IV.4). If we plot ln k as a function of 1/T in degrees Kelvin, for the absorbance at 965 cm^{-1} and at 1046 cm^{-1}, the slope of the straight line is equal to $-E_A/R$, which is demonstrated in Figure IV.3.

Table IV.1: *The rate constants at different temperatures, obtained with in-situ FT-IR spectroscopy in solid state.*

$m_2 = k$	1046 cm^{-1} k (10^{-4} s^{-1})	965 cm^{-1} k (10^{-4} s^{-1})
60°C	1.5428	1.5525
65°C	3.6432	3.4956
70°C	4.5296	4.0368
75°C	9.2389	9.0835
80°C	12.6480	12.3530

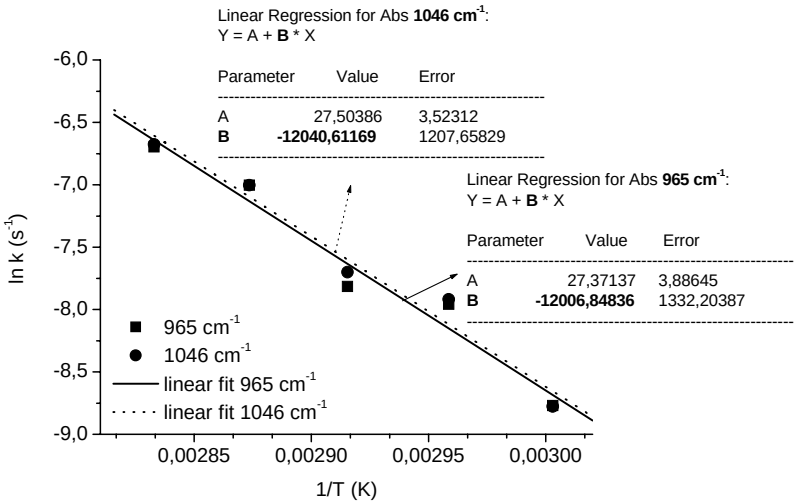

Figure IV.3: *Ln k as a function of 1/T in degrees Kelvin to calculate the E_A from in-situ FT-IR spectroscopy in solid state.*

The activation energy (E_A) calculated from the disappearance of the reactant, the *n*-butyl-sulphinyl OC_1C_{10}-PPV precursor polymer, which is monitored by the disappearance of the absorbance of the sulphinyl group at 1046 cm^{-1} as a function of time at different isothermal temperatures, is 100.1 kJ/mol (23.9 kcal/mol) (1 kcal = 4.184 kJ). On the other hand, the E_A of the formation of the product, the conjugated OC_1C_{10}-PPV polymer, followed by the absorbance of the *trans* vinylene double bond at 965 cm^{-1} as a function of time at several isothermal temperatures, is 99.8 kJ/mol (23.8 kcal/mol).

IV.A.2.b In-situ UV-Vis spectroscopy

UV-Vis absorbance measurements could be carried out at a constant temperature, in solution and in solid films. The main differences between the two sets of samples were attributed to the diffusion of the elimination products out of the bulk sample and the difference in concentration. As will be indicated, to obtain the activation energy of the conversion reaction with *in-situ* UV-Vis spectroscopy is much more complex than with FT-IR spectroscopy.

IV.A.2.b[1] *In-situ* UV-Vis spectroscopy in solid state form

A series of the *n*-octyl-sulphinyl OC_1C_{10}-PPV precursor polymer were prepared. Therefore, a solution of the precursor polymer (6 mg / ml $CHCl_3$) is spincoated at 1000 rpm on a quartz disc. The experiments can be performed in the same manner as the FT-IR measurements (paragraph IV.A.2.a). To determine the activation energy of the elimination reaction, the absorbance of the λ_{max} of the conjugated OC_1C_{10}-PPV polymer, which is 490 nm, is measured as a function of time at several isothermal temperatures (60, 65, 70 and 75°C), shown in Figure IV.4.

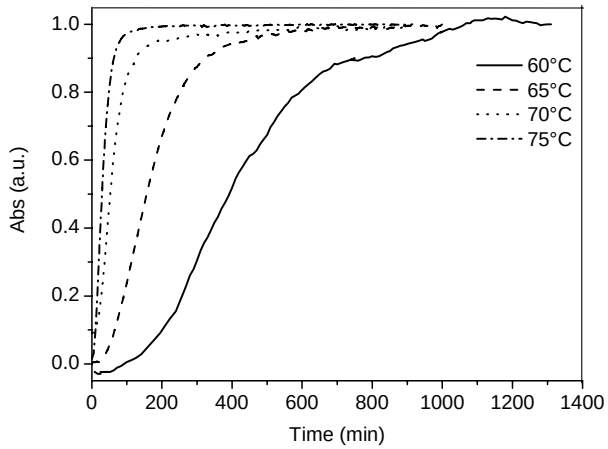

Figure IV.4: *The absorbance of the λ_{max} at 490 nm versus time at different isothermal temperatures.*

This method yields an "apparent" activation energy and gives not the real activation energy, because by plotting the absorption maximum as a function of time, the formation of the larger conjugated segments is observed, which are not directly formed upon elimination. The curves obtained in Figure IV.4 do not follow an exponential fit. An apparent activation energy of 111.7 kJ/mol (26.7 kcal/mol) is obtained by leaving the first points of each curve out of consideration. However, from this representation useful information concerning the construction of the conjugated polymer can be derived and it is an attempt to follow the "saturated" elimination reaction.

To determine the real activation energy, it is better to follow the formation of the smaller conjugated segments (oligomers), because as soon as the elimination reaction starts, a dimer is formed. Therefore the λ_{max} at 376 nm is plotted as a function of time at different isothermal temperatures, shown in Figure IV.5. At the start of the elimination there is an increase in the absorbance at 376 nm, but as soon as the elimination reaction progresses, longer conjugated segments are formed at the expense of the shorter ones, corresponding to a decrease in the absorbance at 376 nm.

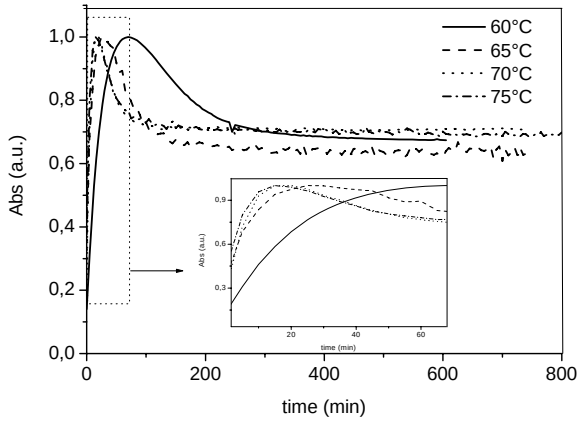

Figure IV.5: *The absorbance of λ_{max} at 376 nm as a function of time at different isothermal temperatures.*

To determine the activation energy we are only considering in the formation of the smaller conjugated segments. The increase in the absorbance at

376 nm represents an exponential fit of first order (insertion of Figure IV.5). Using eq. IV.5, the real rate constants of the conversion reaction are obtained and depicted in Table IV.2.

Table IV.2: *Rate constants at different isothermal temperatures, obtained with in-situ UV-Vis spectroscopy in solid state.*

temperature (°C)	k (10^{-4} s^{-1})
60	7.88
65	17.74
70	29.95
75	31.34

The E_A is calculated again by using the Arrhenius equation (eq. IV.4) and a value of ~ 92 kJ/mol (22 kcal/mol) is obtained. This E_A is consistent with the E_A received from the *in-situ* FT-IR measurements (100.4 kJ/mol = 24 kcal/mol). However, this procedure to determine the activation energy is expected to yield a less reliable value than the procedure used in FT-IR spectroscopy. There are less data points available in the beginning of the elimination reaction, because the shorter segments transform rapid into longer conjugated segments upon elimination.

IV.A.2.b[2] *In-situ* UV-Vis spectroscopy in solution

Some *in-situ* UV-Vis measurements in toluene are carried out in isothermal circumstances to compare the data obtained with the *in-situ* UV-Vis measurements in solid state. The isothermal temperatures were chosen at 70, 75, 80, 85, 90 and 100°C. To do the elimination of the *n*-octyl-sulphinyl OC_1C_{10}-PPV precursor polymer in toluene, a solution with a concentration of 8.33 10^{-5} g/ml is used in all the experiments. This solution is brought in a quartz cuvette and is then positioned in a small heating element purchased from Perkin Elmer, which could be placed in the beam of the UV-Vis spectrophotometer (a Perkin Elmer Lambda 45 UV-Vis spectrophotometer). The small heating element is in contact with a heating circulator (VWR international, Julabo Labortechnik GmbH) via rubber tubes, to control the temperature of the heating element. In

Figure IV.6, the absorbance of the λ_{max} of the conjugated OC_1C_{10}-PPV polymer at 490 nm, is plotted versus time for the different isothermal temperatures, to demonstrate how fast the elimination reaction reaches its maximum at a certain isothermal temperature.

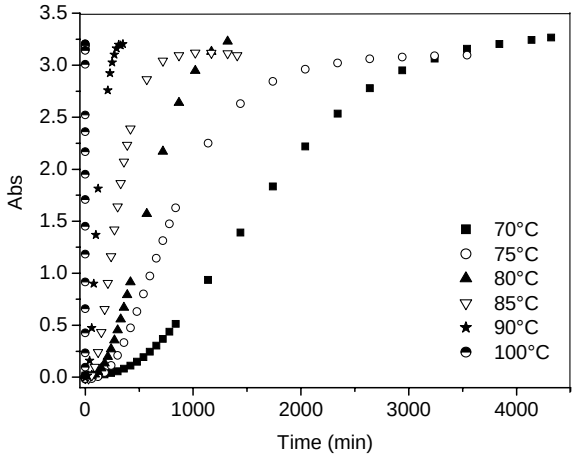

Figure IV.6: *The absorbance at 490 nm versus time at different isothermal temperatures.*

The time depicted in Table IV.3 is the time necessary to reach a constant plateau on which the elimination is complete and a conjugated polymer is formed with a λ_{max} of 490 nm.

Table IV.3: *The time necessary to reach a λ_{max} of 490 nm and the rate constants for each isothermal temperature, studied with in-situ UV-Vis spectroscopy in solution.*

isothermal temp. (°C)	time (min)	k (10^{-4} s^{-1})
70	4020	0.56
75	2700	1.26
80	1330	1.33
85	1025	2.73
90	370	3.86
100	45	5.52

From Table IV.3 and Figure IV.6, it is clear that the elimination reaction in solution (toluene) proceeds much slower than in the solid state (Figure IV.4), because of concentration effects. To determine the activation energy for the conversion reaction in solution, we have also plotted the absorbance at 376 nm as a function of time for each isothermal temperature (Figure IV.7) in the same manner as we have done it in the solid state (paragraph IV.A.2.b[1]). The rate constants for each isothermal temperature are summarised in Table IV.3. The activation energy is again determined with the Arrhenius equation (eq. IV.4), plotting ln k as a function of 1/T in degrees Kelvin. A value of 80.86 kJ/mol (19.3 kcal/mol) for the activation energy is obtained, which is lower compared to the activation energy retrieved from solid state UV-Vis spectroscopy (92 kcal/mol). The difference in E_A can be due to an effect of the solvent on the kinetic mechanism of the elimination reaction. Another possibility is a diffusion effect due to viscosity reasons and a third possibility is probably due to an interference of phase-separation with the UV-Vis signal. This effect could cause an additional acceleration in the UV-Vis signal.

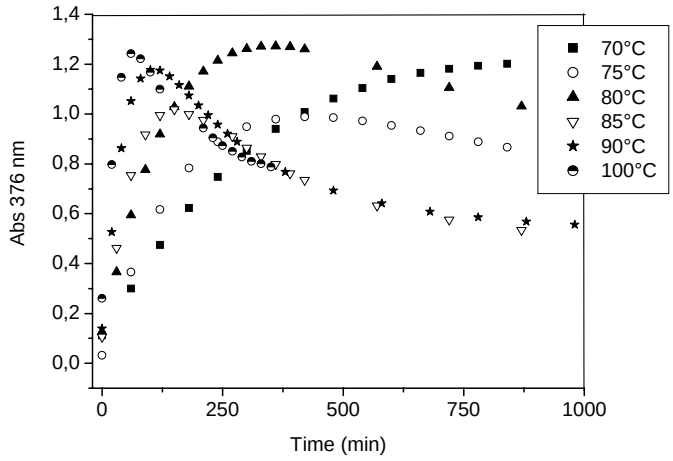

Figure IV.7: *The absorbance at 376 nm versus time at different isothermal temperatures.*

IV.A.3 Conclusions

The activation energy of the conversion reaction from a *n*-octyl-sulphinyl OC_1C_{10}-PPV precursor polymer to the conjugated OC_1C_{10}-PPV polymer is determined with several spectroscopic techniques. All data are summarised in Table IV.4.

Table IV.4: *Results obtained concerning the E_A of the conversion reaction with different spectroscopic techniques in solid state and in solution.*

	experiment	solid state E_A (kJ/mol)				solution E_A (kJ/mol)
in-situ FT-IR	isothermal	965	99.8	1038	100.1	/////
	non-isothermal	cm^{-1}	110.5	cm^{-1}	115.5	
in-situ UV-Vis	isothermal	92				80.9

From theoretical calculations, an E_A of 104.6 kJ/mol (25 kcal/mol) is obtained for the conversion reaction to *trans*-stilbene [1]. This is in good agreement with our experimental results. Non-isothermal measurements yield an estimate for the activation energy of the conversion reaction, but isothermal experiments are essential to realise a reliable measurement of the activation energy. The activation energy for the conversion reaction determined with UV-Vis spectroscopy in solution is much lower (~ 11 kJ/mol) than the activation energy obtained in solid state UV-Vis spectroscopy.

IV.B Study of the elimination process of *n*-alkyl-sulphinyl OC_1C_{10}-PPV precursor polymers by MTDSC and TGA

IV.B.1 Introduction

The aim of this work is to obtain information of all processes and phenomena that occur during the conversion from precursor polymer to the conjugated polymer. We have to investigate if elimination products, after being liberated during the elimination reaction, undergo reactions that are a possible source of unwanted defects. Side reactions could cause damage to the polymer microstructure, leading to a decreasing performance of the conjugated material in polymer electronic devices [2].

Different analytical techniques are applied to evaluate the elimination at each stage of the conversion process. Mainly, Modulated Temperature Differential Scanning Calorimetry (MTDSC) is used, it is an extension of DSC that adds a new dimension to the conventional approach. The usually linear rise in temperature is modulated by a small perturbation, in this case a sinusoidal wave. Next to the heat flow signal (non-reversing heat flow, NR), it is also possible to measure simultaneously the heat capacity (C_p), as well in isothermal as in non-isothermal conditions. These *in-situ* isothermal and non-isothermal measurements are carried out in solid state and in solution (toluene and chlorobenzene) to monitor the elimination reaction in both media. Changes in the thermodynamical heat capacity during the elimination and evaporation of the elimination products, are visible in the C_p-signal. We are mainly interested in the C_p-signals for the quasi-isothermal conditions. Heat-effects associated with these reaction steps occur exclusively in the NR-signal. TGA will provide complementary data. With TGA, the evaporation of the elimination products and degradation of the conjugated polymer, can be studied thoroughly.

IV.B.2 Theoretical background

IV.B.2.a Modulated Temperature DSC (MTDSC)

The technique and the extraction of the signals is introduced below, a more complete description can be found, for instance, in literature [3]. In MTDSC a sample is subjected to a modulated temperature programme obtained by superimposing a sine wave on the conventional isothermal or linearly changing temperature programme:

$$T = T_o + \frac{\beta}{60}.t + A_T.sin(\omega t) \qquad \text{(IV.6)}$$

where T is the temperature in K, T_o is the initial temperature in K, β is the (linear) heating rate in K.min^{-1}, A_T is the temperature modulation amplitude in K, ω is the modulation frequency in s^{-1}, and t is the time in s.

The modulated heating rate is (Figure IV.8):

$$dT/dt = \beta/60 + A_T\varpi\cos(\varpi t) = \beta/60 + A_{HR}\cos(\varpi t) \qquad \text{(IV.7)}$$

with: A_{HR} is the amplitude of the modulated heating rate in K/s

This modulated temperature input gives rise to a modulated heat flow response which consists of an underlying and a cyclic heat flow signal. Assuming that the temperature modulation is small so that over the temperature interval of one modulation the response of the rate of the kinetic processes to the temperature can be approximated as linear, the heat flow response can be written as [3]:

$$\frac{dQ}{dt} = C_p.\left(\frac{\beta}{60} + A_T.\omega.\cos(\omega t)\right) + f(t,T) + A_K.\sin(\omega t) \qquad \text{(IV.8)}$$

where Q in J is the amount of heat transferred to the sample, $f(t,T)$ in W is the average response of a kinetic phenomenon to the underlying temperature programme, and A_K in W is the amplitude of the kinetic response to the temperature modulation.

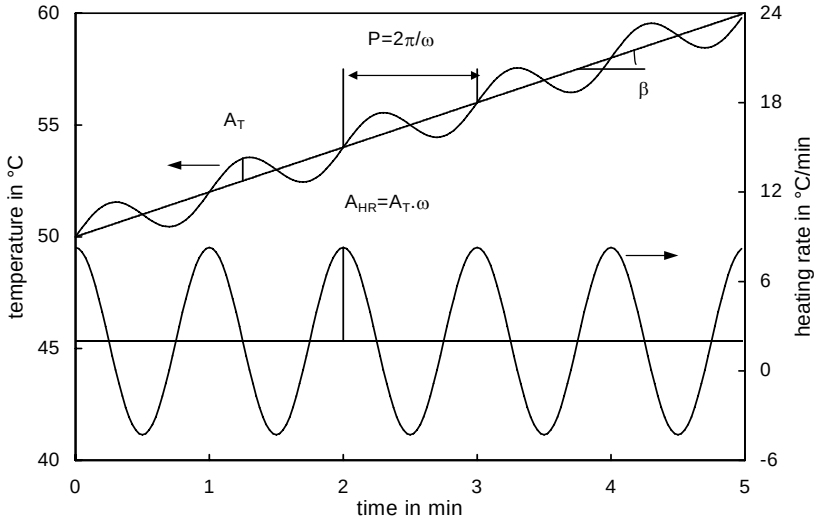

Figure IV.8: *MTDSC heating profile with modulated temperature and heating rate. A modulated amplitude of 1°C and a modulated period of 60s which are positioned on a heating rate of 2°C/min.*

The underlying signals for both temperature and heat flow are calculated by an averaging process that subtracts the effects of the perturbation. The resulting underlying or 'total' heat flow, ϕ_{tot} in W, and underlying temperature reconstitute quantitatively the thermoanalytical curve measured by conventional DSC. Using a discrete Fourier transform algorithm the cyclic component of both temperature input and heat flow response is extracted. Comparison of the amplitude of the cyclic heat flow, A_{HF}, with the amplitude of the heating rate, $A_T.\omega$, results in an additional signal: the 'cyclic' heat capacity C_p in $J.K^{-1}$:

$$C_p = \left(\frac{A_{HF}}{A_T.\omega} \right) \qquad \text{(IV.9)}$$

Multiplying the heat capacity by minus the (measured) underlying heating rate gives the 'reversing' heat flow, ϕ_R in W ; the 'nonreversing' heat flow, ϕ_{NR} in W, is the difference between the total heat flow and the reversing heat flow (eq. IV.10):

$$\phi_R = -C_p.\beta$$
$$\phi_{NR} = \phi_{tot} - \phi_R \qquad \text{(IV.10)}$$

Note that the extraction of the signals is done by a continuous integration, averaging and smoothing over more than one modulation period. For quantitative MTDSC measurements it is necessary to calibrate temperature and heat flow as in a conventional DSC ; the heat capacity signal is calibrated using a reference material with a known heat capacity. For isothermal experiments, the reversing heat flow equals zero because of a zero underlying heating rate and consequently the nonreversing heat flow equals the total heat flow.

MTDSC offers several advantages over conventional DSC. Events are separated into phenomena considered as reversible (R) and nonreversible (NR) material behaviour within the time scale of the perturbation, thus enabling a disentanglement of a number of overlapping thermal events, e.g., glass transition (R) and enthalpy relaxation (NR), and detection of metastable behaviour [2a]. Using MTDSC the heat capacity and its evolution with time and temperature can be measured accurately for non-isothermal as well as for isothermal underlying temperature programmes. Other benefits are an improved resolution and an increased sensitivity for changes in heat capacity [4].

IV.B.2.b The elimination process

The whole elimination process contains five different reaction steps (see Figure IV.9). The thermal decomposition of sulphinyl groups bearing a β-hydrogen atom provides a convenient route for the synthesis of olefins [5]. In this reversible reaction [6], that proceeds by the syn-intramolecular mechanism shown in Figure IV.9 **I**, sulphenic acids are produced. These sulphenic acids have a very high reactivity [7], due to the fact that in absence of trapping agents, they readily undergo intermolecular deshydratation to give thiosulphinates and water [8]. This deshydratation reaction is called a dimerisation and is shown in Figure IV.9 **II**. The sulphenic acids, associated by hydrogen bonds, may behave both as S nucleophiles and S electrophiles [9]. The thiosulphinate itself is not thermally stable [10] and reacts further in a disproportionation reaction yielding a thiosulphonate and a disulphide. This reaction occurs via a radical mechanism

with a homolytical splitting of the S(O)-S bond (bond-strength = 35 kcal) [10] and is shown in Figure IV.9 **III** [11]. The formed thienyl radicals dimerise to give the disulphide **(III^1)** and the sulphinyl radicals dimerise to give thiosulphonates **(III^2)**. The latter products are called elimination products in this study. These elimination products could interact with the conjugated system (network formation) (Figure IV.9 **IV**). Ones the elimination products are formed, these products have to diffuse and evaporate out of the polymer matrix (Figure IV.9 **V**).

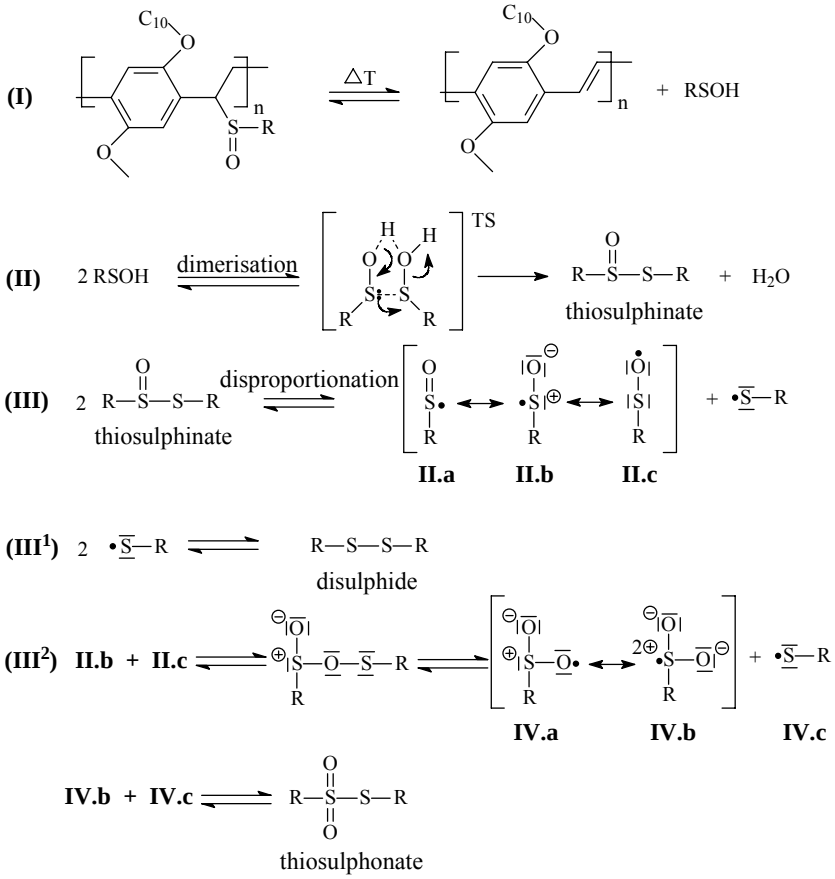

(IV) Network formation

(V) Diffusion and evaporation of the elimination products

Figure IV.9: *Five different reaction steps of the elimination process.*

IV.B.3 Results and discussion

IV.B.3.a Elimination of a n-alkyl-sulphinyl OC_1C_{10}-PPV precursor polymer in solid state

The motivation to study the conversion process in solid state thoroughly arises from the fact that the use of precursors is necessary in multilayer systems, transistors,…. [12]. In these circumstances, a layer of precursor polymer is coated on a substrate. Afterwards, this precursor film is thermally eliminated in solid state to the conjugated polymer. Therefore, the different reaction steps in the conversion process (elimination, dimerisation, disproportionation, network formation and diffusion/evaporation of the elimination products) from precursor polymer to the conjugated polymer and their possible interactions are investigated. Reactions of the elimination products (dimerisation and disproportionation) could possibly interfere with the conjugated polymer and could also influence the quality of the material. In addition, the elimination products could also act as plasticizers. Moreover, the presence of the elimination products could cause deceleration of the elimination reaction itself as well as cross-linking or network formation in the conjugated polymer.

As is mentioned before, MTDSC is applied to examine the elimination process. With this technique, we hope to investigate the three reactions (elimination, dimerisation and disproportionation) independently. In this way only, the influence of the different reactions on the conjugated polymer can be examined.

TGA measurements are performed to demonstrate the volatility of the elimination products during the elimination process and to investigate at which temperature degradation occurs.

IV.B.3.a [1] Non-isothermal elimination in solid state

In the MTDSC scan experiments (Figure IV.10), the non reversing heat flow (NR) and the heat capacity (C_p) allow us to monitor the elimination process and the subsequent reactions of the elimination products, because they

are associated with these reaction steps. Figure IV.10 shows that in the first heating run **(1)** an increase in the C_p-signal is observed in a temperature range around 36°C. This increase in C_p corresponds with the glass transition temperature (T_g) of the *n*-butyl-sulphinyl OC_1C_{10}-PPV precursor polymer. At higher temperatures in the same heating run **(1),** a second increase in C_p is observed around 126°C, that corresponds with an increase in heat capacity due to reactions of the elimination products, which are set free during the elimination process. It will turn out that this second increase in C_p is due to the disproportionation reaction of *n*-butyl-thiosulphinate (see further).

Upon cooling after the first heating run **(2)**, the water formed during the elimination process crystallizes. The absence of a glass transition in the cooling **(2)** and the second heating run **(3)** is probably due to elimination products present in the HPS pan, which act as a plasticizer in the conjugated OC_1C_{10}-PPV polymer, significantly lowering the T_g.

In the first heating run **(1)** of the NR-heat flow, a large exothermal heat-effect of 81 J/g is observed in a temperature range from 85 up to 170°C (threshold values). The assignment of the different reactions that occur during the elimination process to the different shoulders in the exothermal heat-effect, will be considered in the next paragraph.

From *in-situ* non-isothermal heating experiments on a *n*-alkyl-sulphinyl OC_1C_{10}-PPV precursor polymer with FT-IR and UV-Vis spectroscopy, it has become clear that the elimination reaction occurs between 70 and 110°C (paragraph III.E and III.F). Theoretical calculations of the elimination process [13], demonstrate that the elimination reaction itself is an endothermal reaction (ΔU = 11.17 kcal), while the dimerisation and disproportionation reaction are both exothermal reactions, ΔU = -16.8 kcal/mol and –13.71 kcal/mol respectively. From Figure IV.10, it is clear that in the temperature range between 70 and 110°C no heat-effect is visible. Probably, this means that the dimerisation reaction occurs almost simultaneously with the elimination reaction, cancelling out the heat-effect of the elimination process.

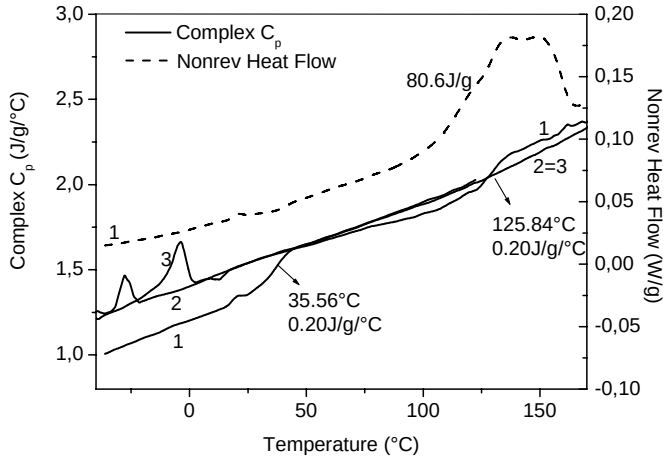

Figure IV.10: *MTDSC scan of a n-butyl-sulphinyl OC_1C_{10}-PPV precursor from –45°C up to 160°C at 2.5°C/min (1), followed by a cooling program (2) and a second heating at the same heating rate (3). This measurement is carried out in the solid state in a HPS pan.*

To prove that the second increase in C_p is probably due to the disproportionation reaction of thiosulphinate, a non-isothermal measurement is carried out on pure *n*-butyl-thiosulphinate, to examine the behaviour of this product in the same circumstances as for the *n*-butyl-sulphinyl OC_1C_{10}-PPV precursor polymer.

In Figure IV.11 and IV.12, non-isothermal experiments on *n*-butyl-sulphinyl OC_1C_{10}-PPV precursor polymer and *n*-butyl-thiosulphinate are compared to each other. In Figure IV.11, the C_p-signal for *n*-butyl-sulphinyl OC_1C_{10}-PPV precursor polymer and *n*-butyl-thiosulphinate are plotted versus temperature. It is demonstrated that the second increase in C_p at 126°C, in the first heating run of the *n*-butyl-sulphinyl OC_1C_{10}-PPV precursor polymer, is impute to the disproportionation reaction of the *n*-butyl-thiosulphinate, because the increase in C_p for the pure *n*-butyl-thiosulphinate occurs at almost the same temperature (~ 126°C).

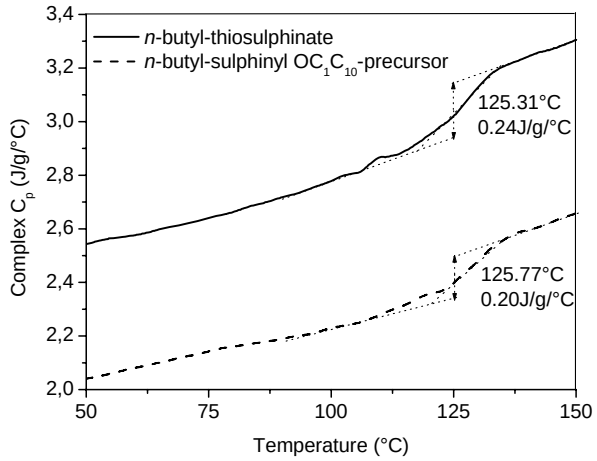

Figure IV.11: *The heat capacity as a function of temperature (non-isothermal: from –45°C up to 200°C at 2.5°C/min) for n-butyl-sulphinyl OC_1C_{10}-PPV precursor polymer and n-butyl-thiosulphinate.*

In the non-isothermal experiment with pure *n*-butyl-thiosulphinate, a change in heat capacity of 0.24 J/g/°C is obtained, while for the *n*-butyl-sulphinyl OC_1C_{10}-PPV precursor polymer a change in heat capacity of 0.20 J/g/°C is measured. The maximum quantity of *n*-butyl-thiosulphinate that could be released during the elimination process is equal to 24.7% (Table IV.9). In other words, the pure *n*-butyl-thiosulphinate could cause an increase in heat capacity around 0.06 J/g/°C ((0.24 J/g/°C * 24.7)/100). This is too small to explain the increase in C_p in the measurement of the *n*-butyl-sulphinyl OC_1C_{10}-PPV precursor polymer. Probably, the increase in heat capacity around 126°C is attributed to different reactions (dimerisation and/or disproportionation) in which the temperature intervals overlap each other. Because we are not able to completely distinguish between the different reactions using non-isothermal conditions, we have tried to decouple the reactions using isothermal conditions (paragraph IV.B.3.a [3]).

In Figure IV.12, the exothermal peaks in the NR-heat flow signal for the *n*-butyl- and *n*-octyl-sulphinyl OC_1C_{10}-PPV precursor polymers and for pure *n*-butyl-thiosulphinate are compared to each other. For both precursor polymers, this exothermal peak is normalised to the maximum percentage of

thiosulphinate that can be formed during the elimination process of the precursor polymer (Table IV.9). The *n*-butyl-sulphinyl OC_1C_{10}-PPV precursor polymer shows 3 shoulders in the exothermal heat-effect. The maximum of the 3 shoulders appears around 125°C **(1)**, 135°C **(2)** and 150°C **(3)** respectively. On the other hand, the pure *n*-butyl-thiosulphinate shows only 2 shoulders in the exothermal heat-effect of which the maxima are situated at 105°C **(1)** and 125°C **(2)** respectively. The first 2 shoulders of the precursor polymer are probably in accordance with those of the pure thiosulphinate, but they are shifted to a higher temperature, because in a polymer matrix it is more difficult for the thiosulphinate molecules to encouter each other to disproportionate. The third shoulder **(3)** in the precursor polymer around 150°C is absent in the exothermal peak of thiosulphinate.

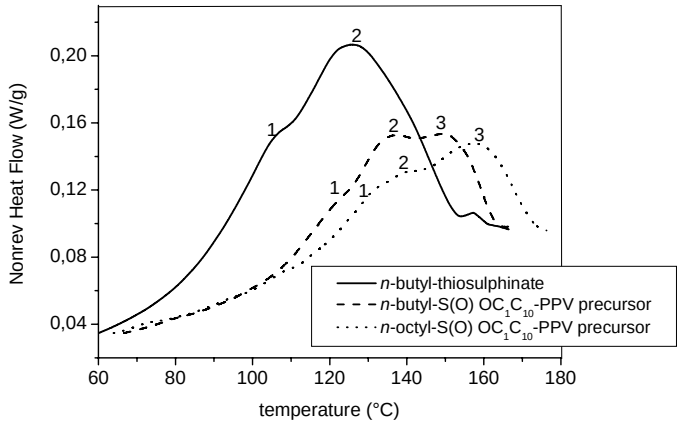

Figure IV.12: *The NR heat flow of n-alkyl-sulphinyl OC_1C_{10}-PPV precursor polymer and n-butyl-thiosulphinate versus temperature (non-isothermal: from –45°C up to 200°C at 2.5°C/min). The exothermal peaks of the precursor polymers are normalised to the quantity n-butyl-thiosulphinate maximal formed during the elimination process.*

When we compare the *n*-butyl- with the *n*-octyl-sulphinyl OC_1C_{10}-PPV precursor polymer (Figure IV.12), a shift in the exothermal peak between both polymers is observed. This shift to a higher temperature for the *n*-octyl is probably due to the fact that the diffusion of the elimination products in the

polymer matrix is more difficult for a larger R-group (see also comparison between pure *n*-butyl-thiosulphinate and *n*-butyl-sulphinyl OC_1C_{10}-PPV precursor polymer). Although the heat-effects differ in size, the same tendency in the NR-heat flow signal is observed for both polymers (3 shoulders).

Looking at Figure IV.11 it is clear that the increase in heat capacity, originating from the disproportionation reaction, ends around 135°C. This means that, the exothermal phenomena that appear above 135°C can be attributed to reactions other than the disproportionation reaction, visible in Figure IV.12. Probably, the appearance of the third shoulder above 135°C, in the exothermal peaks for the precursor polymers, is due to an interaction of the elimination products with the conjugated polymer, which causes network formation (crosslinks).

To find an evidence for this hypothesis of network formation, we have tried to solve the conjugated OC_1C_{10}-PPV polymer, obtained after the non-isothermal measurement up to 200°C, in $CHCl_3$. The polymer swells in the solvent, but is not soluble anymore. A non-isothermal heating experiment up to 140°C (before shoulder 3) however, yields a conjugated polymer that is still soluble in $CHCl_3$. This points out that the third shoulder is probably caused by the appearance of network formation.

A heating experiment at 2.5°C/min from – 45°C up to 140°C and 200°C is also performed on the already conjugated OC_1C_{10}-PPV polymer. To obtain this conjugated polymer, a precursor polymer is heated in toluene for 4 hours at 110°C. Afterwards, the polymer is precipitated in a non-solvent, in which the elimination products, that are liberated during the elimination reaction, are soluble. The conjugated polymer is isolated and dried in vacuum. In this case, a conjugated OC_1C_{10}-PPV polymer is obtained with almost no elimination products present in the polymer matrix. In both heating experiments (up to 140 and 200°C), no exothermal signal is present in the NR-signal between 85 and 170°C and after the experiment, both polymers are still soluble in $CHCl_3$. This is an extra evidence for the fact that the elimination products are the cause of network formation (Figure IV.13 **A**).

We have also heated a mixture of the already conjugated OC_1C_{10}-PPV polymer in the present of an excess (> 24.7%) of *n*-butyl-thiosulphinate at 2.5°C/min from –45°C up to 200°C. Again, a large exothermal signal with 3 shoulders is visible in the NR-signal between 85 and 170°C, shown in Figure IV.13 **B**. After this experiment, the polymer is not soluble anymore. The third exothermal peak at 155°C is corresponding to network formation. When a mixture of an already conjugated OC_1C_{10}-PPV polymer with an excess of *n*-butyl-disulphide and *n*-butyl-thiosulphonate, the end products of the disproportionation reaction, is heated at 2.5°C/min from – 45°C up to 200°C, an exothermal signal in the NR-signal is present with only one exothermal peak at 158°C, shown in Figure IV.13 **C**. These data confirm that the first two shoulders in the exothermal signal correlate with the disproportionation reaction. As the third shoulder in the exothermal signal corresponding to network formation is clearly visible in these experiments, it may be assumed that the elimination products are really responsible for network formation.

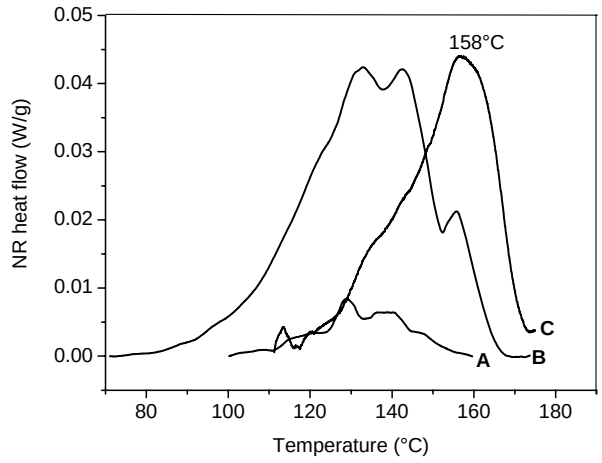

Figure IV.13: *A non-isothermal MTDSC experiment from – 45 up to 200°C in which the NR-heat flow is plotted as a function of increasing temperature for* ***A)*** *pure OC_1C_{10}-PPV,* ***B)*** *OC_1C_{10}-PPV with an excess of n-butyl thiosulphinate and* ***C)*** *OC_1C_{10}-PPV with an excess of n-butyl-disulphide and -thiosulphonate.*

We have also conducted a non-isothermal experiment up to 200°C on a *n*-butyl-sulphinyl OC_1C_{10}-PPV precursor polymer, that is kept under argon flow to create an oxygen free environment in the HPS pan. In this manner, the effect of atmosphere on network formation could be followed. From this experiment, we can conclude that the argon atmosphere has no influence on the elimination process itself, because the same heat-effects in the NR-heat flow signal are obtained. Both samples (the one prepared in air, the other one under argon flow) are not soluble anymore. This proves that oxygen is not the cause of network formation.

From the results obtained and from a practical viewpoint we can conclude that MTDSC is a useful technique to observe the disproportionation reaction. We could say that the disproportionation reaction occurs in a temperature range between ~ 85 up to 135°C. The elimination products that are formed, could further decompose and interact with the conjugated system to form crosslinks (network formation) in a temperature range around 140 – 160°C. Since network formation could occur, it is better to do the elimination reaction at relative low temperatures (T < 120°C) and in solution, because the elimination products are soluble in organic solvents and the chance to interact with the conjugated polymer is therefore much smaller.

IV.B.3.a [2] Evolution of the glass transition temperature during the elimination process

In this paragraph, a comparison is made between the conjugated OC_1C_{10}-PPV polymer eliminated in the MTDSC and the conjugated OC_1C_{10}-PPV polymer eliminated in toluene at 110°C for 4 hours. A T_g around 25°C and 35°C is obtained in the first heating for the *n*-octyl- and *n*-butyl-sulphinyl OC_1C_{10}-PPV precursor polymer respectively. This T_g decrease for the *n*-octyl derivative is due to the larger R-group, which enlarges the free volume between the polymer chains and so promote the free rotation around the single bonds. When using a refrigerated cooling system (RCS), no T_g is measured for the conjugated OC_1C_{10}-PPV polymer. The elimination products that act as plasticizers in the polymer matrix cause a T_g decrease. To measure the T_g of the conjugated OC_1C_{10}-PPV polymer, after doing the elimination in the MTDSC, a liquid nitrogen cooling accessory (LNCA) is used, that reaches temperatures up to –150°C. In such a non-isothermal measurement with LNCA from –100 up to 150°C, a T_g around –62°C is obtained for the conjugated OC_1C_{10}-PPV polymer.

A conjugated OC_1C_{10}-PPV polymer eliminated in toluene, contains no elimination products and has a very broad T_g between 25 and 75°C (around 50°C). This broad T_g is due to the fact that the alkoxy chains act as internal plasticizers and occur in a random position on the polymer backbone (as mentioned before), which probably causes also the broad, relatively low T_g.

To demonstrate the shift in T_g to lower temperatures, some quasi-isothermal experiments are performed on the *n*-octyl-sulphinyl OC_1C_{1O}-PPV precursor polymer at 2.5°C/min up to 70, 85 and 95°C. The polymer stays isothermal on these temperatures for 60, 120 and 30 minutes respectively. After the isothermal part we have cooled down the polymer again till – 45°C. This procedure is repeated several times. In the cooling, after each isothermal part, we have determined the endset of the T_g. For each temperature, the endset of T_g is shown in Figure IV.14.

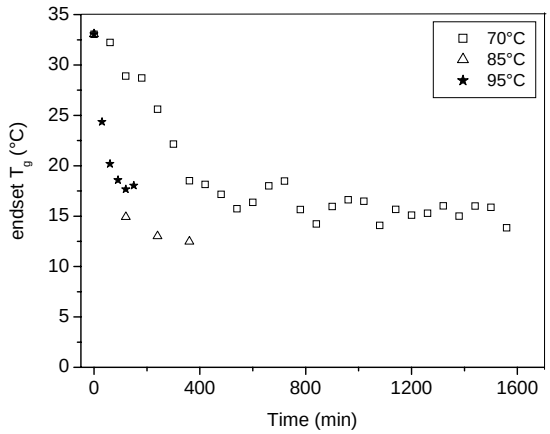

Figure IV.14: *The endset of the glass transition temperature plotted as a function of time for the quasi-isothermal experiments (70,85 and 95°C) on the n-octyl-sulphinyl OC_1C_{10}-PPV precursor polymer.*

Normally, longer periods of time at a certain temperature, but also an increase in isothermal temperature, mean a higher degree of elimination / conjugation, resulting in a T_g increase. From Figure IV.14, the opposite result is obtained. It is clear that there is a shift in the endset of the T_g to lower temperatures, because of water and elimination products that are released during

the elimination reaction. They act as plasticizers. The plasticizing effect (T_g-lowering during the elimination process) is only visible after longer periods of time at a certain isothermal temperature compared to the elimination reaction itself (Figure IV.2). This means that the formation of double bonds with liberation of sulphenic acids (the elimination reaction) is the initiation process for the plasticizing effect. From Figure IV.14 it is clear that at 85 and 95°C no T_g is visible anymore after 360 and 120 minutes respectively. The melting peak of water interferes with the T_g-determination, but it is also possible that the T_g is out of range. At 70°C, the endset of the T_g stabilizes at a value of 15°C only after 500 minutes at 70°C. This is probably due to the fact that a lower concentration of water is formed at 70°C compared to the amount of water formed at higher temperatures. The fact that the elimination process at 70°C stops after a certain elimination time (~ 500 min.) is probably again diffusion related.

IV.B.3.a [3] Isothermal elimination in solid state studied with MTDSC

As was mentioned before, one of the important goals of this research is to separate the different reactions of the elimination process, by doing isothermal experiments. Normally reaction heats are visible in the NR-heat flow, while studying the elimination process in isothermal conditions, no clear heat effect is visible in the NR-heat flow. Therefore the change in heat capacity (ΔC_p) is used to follow reactions of the elimination process. In this paragraph, the effect of temperature, atmosphere and R-group on the elimination process of the precursor polymer to the conjugated polymer in isothermal MTDSC experiments is discussed. The temperatures at which the isothermal experiments were performed, are chosen from non-isothermal experiments with *in-situ* FT-IR and UV-Vis spectroscopy and also from non-isothermal MTDSC measurements. From FT-IR and UV-Vis spectroscopy, we have determined that the elimination reaction occurs between 70 and 110°C, while from the non-isothermal MTDSC experiment on the *n*-octyl-sulphinyl OC_1C_{10}-PPV precursor polymer, it has become clear that the disproportionation reaction already starts around 85°C. To separate the elimination reaction and the disproportionation reaction as good as possible, it was decided to first do isothermal experiments at 70, 80 and 85°C. Later, also higher temperatures (90 and 95°C) are used, but the chance that the disproportionation reaction already starts is large at these higher temperatures.

Figure IV.15 shows that the experiments are nicely reproducible. This figure also shows the result of MTDSC measurements carried out on a *n*-octyl-sulphinyl OC_1C_{10}-PPV precursor polymer at 80°C in a PE pan created in an oxygen free (argon flow) environment. On this figure, it is visible that there is no significant difference between the samples made in air and under argon. Both in isothermal as in non-isothermal MTDSC measurements, the preparation procedure of the samples has no great influence on the elimination process of precursor polymers.

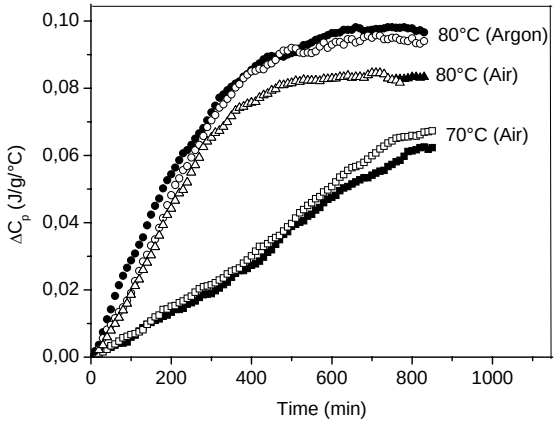

Figure IV.15: *The heat capacity change as a function of time. Isothermal MTDSC experiments at 70 and 80°C in which the PE pans are made in air and under argon flow. The figure also shows reproducible results.*

The influence of the R-group of the precursor polymer on the elimination reaction is also investigated in isothermal experiments. In Figure IV.16, a comparison is made between *n*-butyl- and *n*-octyl-sulphinyl OC_1C_{10}-PPV precursor polymer at 70, 80 and 85°C. From this figure it is clear that at these isothermal temperatures, there is no significant difference in the elimination behaviour between the two R-groups. Generally, we could state that the conversion at 70, 80 and 85°C from a *n*-alkyl-sulphinyl OC_1C_{10}-PPV precursor polymer to a conjugated OC_1C_{10}-PPV polymer does not depend on the R-group that is used.

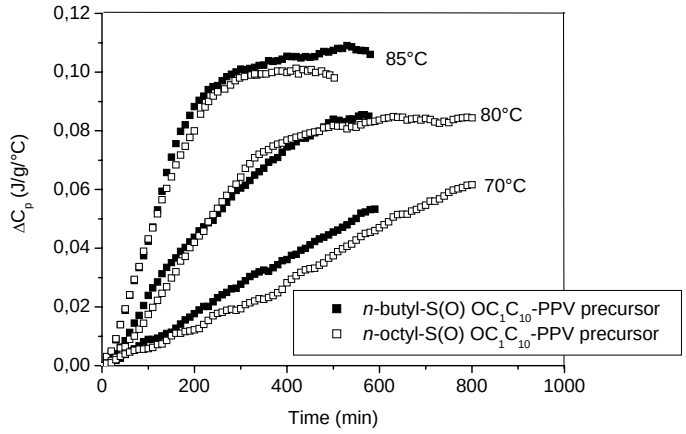

Figure IV.16: *Isothermal MTDSC experiments carried out on n-butyl- and n-octyl-sulphinyl OC_1C_{10}-PPV precursor polymers in a PE 10µl-0.15mm pan at 70, 80 and 85°C.*

After doing these first isothermal experiments, we have decided to do the isothermal elimination reactions on the *n*-octyl-sulphinyl OC_1C_{10}-PPV precursor polymer from which the pans are prepared in air. In Figure IV.17, the heat capacity change is plotted versus time for the isothermal part of the experiment on the *n*-octyl-sulphinyl OC_1C_{10}-PPV precursor polymer at 70, 80, 85, 90 and 95°C. The increase in the C_p-signal is due to the release of the elimination products, especially the release of water. Water contains a very high heat capacity (± 4.19 J/g/°C).

For the *n*-octyl-sulphinyl OC_1C_{10}-PPV precursor polymer at 70°C, a constant increase in the change of heat capacity is visible, that reaches a plateau level after 1400 minutes. At 80°C a stronger increase is clear in the C_p-signal till a plateau level is reached after about 600 minutes. At 85°C, the elimination gets even faster and the C_p-signal reaches a plateau after 300 minutes. At 90 and 95°C, the increase in the C_p-signal reaches a maximum after 200 and 120 minutes respectively, but decreases again to stabilize at the plateau level reached at 70°C after 1400 minutes. The percentages elimination products that are released can be deduced from the change in heat capacity during the isothermal experiment. These percentages are the subject of the research in paragraph IV.B.3.a [5].

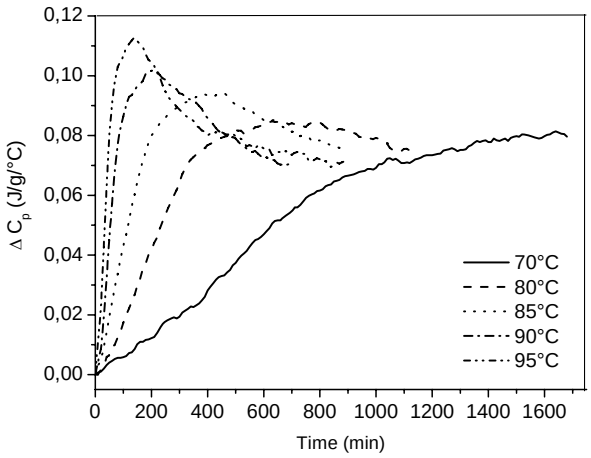

Figure IV.17: *Isothermal MTDSC experiments carried out on n-octyl-sulphinyl OC_1C_{10}-PPV precursor polymer at 70, 80, 85, 90 and 95°C in a PE 10µl-0.15mm pan. The heat capacity change is plotted versus time.*

From Figure IV.17, it is clear that the curves do not follow an exponential fit, but a sigmoidal fit. A hypothesis which can explain this observation is that the dimerisation reaction (liberation of water) and the disproportionation reaction (liberation of elimination products) are superimposed to each other. The dimerisation and disproportionation reaction are expected to be consecutive reactions. In the future, there is the intention to calculate kinetic data from these results with modelling processes.

After the isothermal MTDSC experiments in solid state, a GPC measurement in tetrahydrofuran (THF) is performed on each sample. The molecular weights (M_w) and polydispersities (PD) of each sample after the isothermal experiments in solid state, shown in Figure IV.17, are summarised in Table IV.6. The molecular weight and polydispersity of a pure conjugated OC_1C_{10}-PPV polymer is ~ 390.000 g/mol and 2.7 respectively.

Table IV.6: *Molecular weight (M_w) and polydispersity (PD) of each sample after the isothermal experiments in solid state, shown in Figure IV.17.*

experiment	M_w (g/mol)	PD
iso70°C-1700'	408.000	3.5
iso80°C-1100'	573.000	4.1
iso85°C-1200'	662.000	4.7
iso90°C-900'	965.000	5.9
iso95°C-600' (after max.)	841.000*	7.1
iso95°C-120' (at max)	744.000	2.9
iso95°C-50' (before max.)	325.000	2.5

*: Highest molecular fraction does not get through the filter.

From these GPC results, it is clear that the molecular weight and polydispersity increases with increasing isothermal temperature. We have also repeated the isothermal experiment at 95°C for 600 minutes with an isothermal period of only 50 minutes (just before reaching the maximum in the change of C_p) and 120 minutes (at the maximum in the change of C_p). From these samples, also a GPC measurement is performed in THF. At 95°C, the molecular weight and polydispersity increase with longer isothermal periods on 95°C. A FT-IR spectrum of the sample, which was isothermally heated at 80°C for 1100 minutes, indicates that the disproportionation reaction already occurs, because an absorption peak is present at 1130 cm^{-1}, which corresponds to the formation of *n*-butyl-thiosulphonate. It can be concluded that it is very difficult to separate the elimination reaction from the disproportionation reaction. Both GPC and FT-IR results indicate that crosslinking of the conjugated polymer (network formation) (GPC), caused by the elimination products that are liberated during the isothermal elimination reactions (FT-IR), is occurring at 80°C and especially at 90 and 95°C. Thus, at 90 and 95°C, the decrease after the initial increase in the change of C_p (Figure IV.17) is probably related to network formation (GPC) and not due to the disproportionation reaction. This is confirmed by isothermal MTDSC measurements on pure *n*-butyl thiosulphinate which show an increase in C_p, while no maximum is observed here (Figure IV.19).

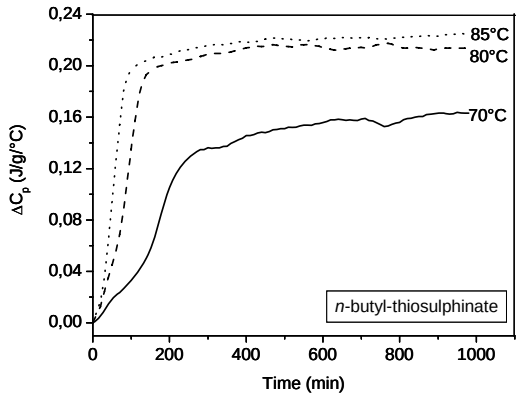

Figure IV.19: *Change in heat capacity as a function of time at isothermal temperatures 70, 80 and 85°C on the pure n-butyl-thiosulphinate.*

To check if the exothermal heat-effect obtained in the NR-heat flow signal of the non-isothermal MTDSC experiment (Figure IV.10) is fully decoupled from the elimination reaction, an experiment is carried out on a *n*-octyl-sulphinyl OC_1C_{10}-PPV precursor polymer that is eliminated isothermally at 80°C for 1100 minutes and afterwards heated up to 200°C. The two exothermal heat-effects are shown in Figure IV.20.

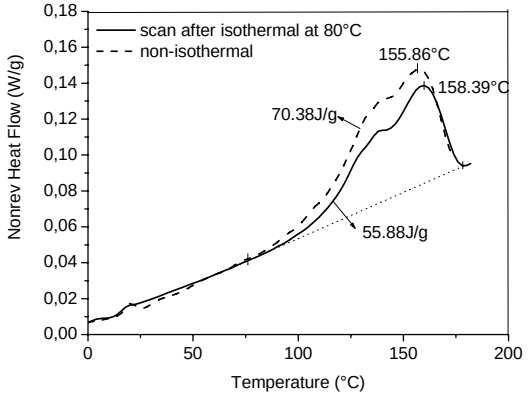

Figure IV.20: *Comparison of the exothermal heat-effect in the NR-heat flow signal reached in a non-isothermal MTDSC experiment and in a scan after an isothermal measurement at 80°C, both carried out on the n-octyl-sulphinyl OC_1C_{10}-PPV precursor polymer.*

In this figure, it is clear that after the isothermal elimination at 80°C, the exothermal heat-effect is a little bit smaller than the exothermal heat-effect obtained in the non-isothermal scan, which means that the disproportionation reaction partially has occurred at 80°C. A conclusion is that the different reaction steps in the elimination process are consecutive but not completely kinetic separated.

This is also evident from another experiment. In Figure IV.18 A, B and C, we have plotted the change in heat capacity (ΔC_p) and the change in enthalpy ($\Delta H_{water,m}$) as a function of elimination time at isothermal temperatures of 70, 85 and 95°C. The $\Delta H_{water,m}$ is calculated from the melting peak, after each isothermal part in the quasi-isothermal experiments at 70, 85 and 95°C, described in paragraph IV.B.3.a[2]. The ΔC_p at different time intervals is obtained from Figure IV.17. The $\Delta H_{water,m}$ indicates only the amount of water that is liberated during the elimination process, while ΔC_p not only increases due to the water that is formed, but the disproportionation reaction also causes an increase in heat capacity.

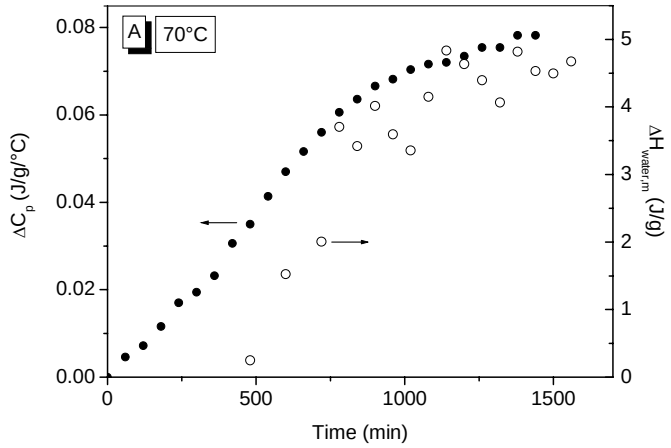

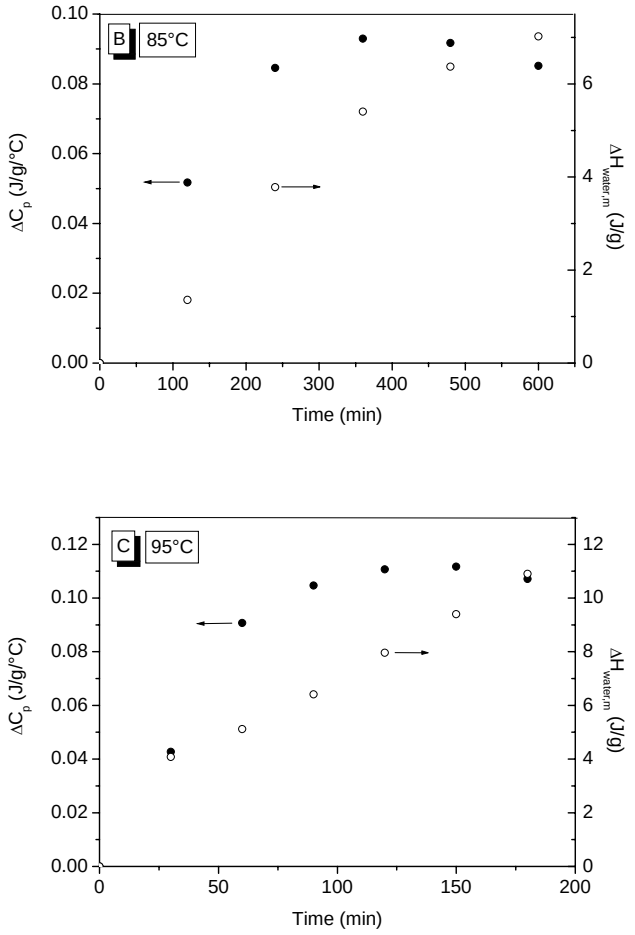

Figure IV.18: *ΔC_p and $\Delta H_{water,m}$ as a function of time at 70°C (A), 85°C (B) and 95°C (C).*

At an isothermal temperature of 70°C, no melting peak is visible ($\Delta H = 0$) at the beginning of the elimination process. Probably this means that the water, which is first liberated during the elimination process, interacts with the main chain via the alkoxy chains (H-bonding). This water could not melt and so no melting peak is visible in this region (0 up to 400 minutes at 70°C). From 400 minutes on, the melting peak of water is visible and taking into account the amount of H-bonded water, both curves (ΔC_p and $\Delta H_{water,m}$) have almost the same slope, which means that the disproportionation reaction does not yet occur

at 70°C. There is no additional effect present in ΔC_p which is due to the elimination products released during the disproportionation reaction. At higher temperatures (85 and 95°C), water is visible from the beginning of the elimination process. The change in heat capacity is not only due to the formation of water, also the disproportionation reaction occurs at these temperatures (from the beginning), as the change in heat capacity is much faster than the formation of water.

As was demonstrated before, we can obtain different kinds of information concerning the elimination process with several techniques used. It is a challenge to combine these data to one global picture. We have compared the isothermal MTDSC measurements with the isothermal FT-IR experiments in solid state (paragraph IV.A.2.a). However, MTDSC measurements are performed in a closed environment, while the FT-IR experiments are carried out in an open system. Therefore, we have repeated the FT-IR experiments in a closed system, by doing the elimination reaction between two KBr pellets, sticked together with a two component glue. No difference with the FT-IR measurements in an open system were obtained. Also no weight loss was observed. In the isothermal MTDSC measurements, the formation of water and elimination products is measured during the elimination process (= dimerisation and disproportionation reaction), which results in an increase in C_p, while in the isothermal FT-IR experiments, the formation of the *trans* vinylene double bonds is measured (elimination reaction), leading to an increase in the absorbance at 965 cm^{-1}. From Figures IV.17 and IV.2 we can conclude that the dimerisation reaction is much slower than the elimination reaction itself. For instance at an isothermal temperature of 70°C, the change in heat capacity reaches a maximum level after 1400 minutes in the MTDSC experiment (Figure IV.17), while in the FT-IR experiment, the conjugated polymer reaches its maximum absorption already after ~ 200 minutes (Figure IV.2).

IV.B.3.a [4] Diffusion and evaporation of the elimination products

The diffusion and evaporation can not be studied with MTDSC experiments, but ThermoGravimetric Analysis (TGA) is very useful for this study, as it offers the opportunity to obtain information about the diffusion and evaporation of the elimination products and the degradation of the conjugated OC_1C_{10}-PPV polymer simultaneously. In TGA, the diffusion and evaporation of

the elimination products after the elimination reaction will be crucial for mass loss. The effect of temperature, different R-groups and film thickness on the mass loss of the elimination products during the elimination process, will be evaluated in this paragraph.

To investigate the effect of temperature on the evaporation of the elimination products during the elimination reaction, measurements are performed on the *n*-octyl-sulphinyl OC_1C_{10}-PPV precursor polymer at 85°C and 100°C. The difference in sample weight (film thickness) for the two experiments was minimized. In Figure IV.21, the TGA thermograms for the *n*-octyl-sulphinyl OC_1C_{10}-PPV precursor polymer at 85°C and 100°C are shown. As can be anticipated, we observe a faster evaporation of the elimination products at higher temperatures. At 100°C, already 27% of weight loss is reached after 1000 minutes, while at 85°C a weight loss around 18% is obtained after 2500 minutes (max. = 36 %).

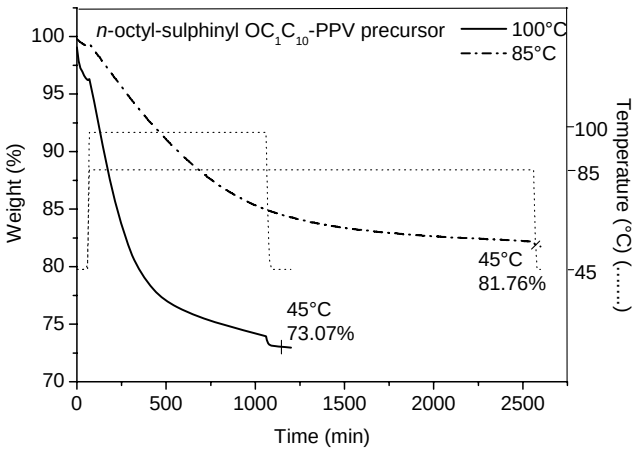

Figure IV.21: *TGA experiments are carried out on the n-octyl-sulphinyl OC_1C_{10}-PPV precursor polymer at temperatures of 85 and 100°C to check the effect of elimination temperature on the evaporation of the elimination products. The temperature profiles are shown in the dotted lines.*

Remark: In the TGA-experiments discussed in this paragraph, the sample weight is determined at 45°C, before and after each new isothermal segment of the measurement. This temperature (45°C) is used as reference temperature to calculate the weight loss (Figure IV.21).

To investigate if the evaporation or the diffusion of the elimination products is a slow process, we have performed isothermal TGA experiments on the pure *n*-butyl-thiosulphinate. From Figure IV.22 A, that displays this TGA result, it can be concluded that the evaporation of the elimination products is on this example a fast process, for instance after ~ 100 minutes at 85°C, all elimination products are evaporated. The evaporation of the elimination products out of the polymer matrix is decelerated by diffusion processes, because there is almost only 5 % mass loss visible after 100 minutes at 85°C for the *n*-butyl-sulphinyl OC_1C_{10}-PPV precursor polymer (Figure IV.22 B).

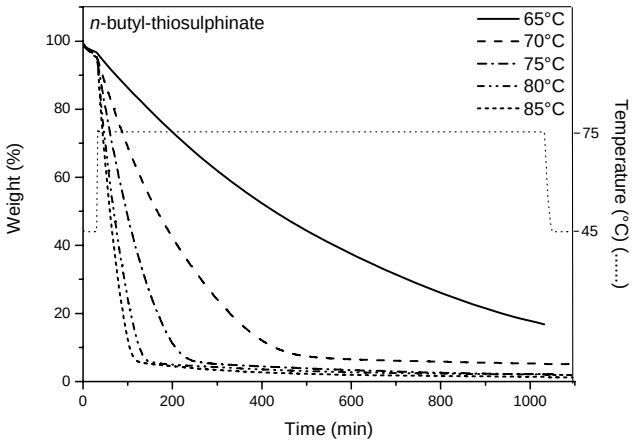

Figure IV.22 A: *Isothermal TGA experiments on pure n-butyl-thiosulphinate at 65, 70, 75, 80 and 85°C. Temperature profile of the experiment at 75°C is shown.*

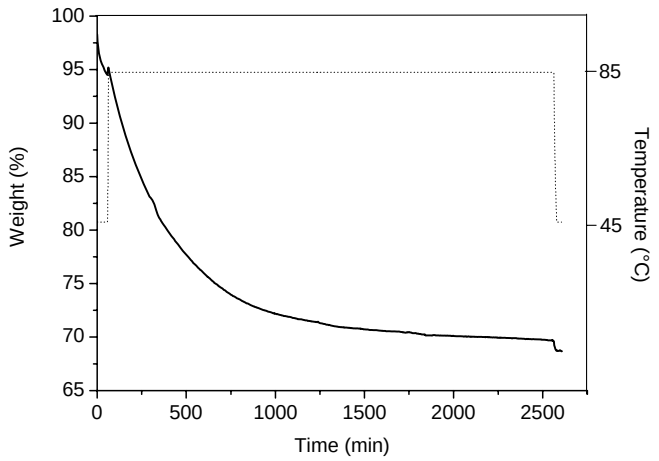

Figure IV.22 B: *Isothermal TGA experiment on n-butyl-sulphinyl OC_1C_{10}-PPV precursor polymer at 85°C.*

The film thickness may be important for the global kinetics of the elimination process. To ensure a good quality of the conjugated polymer in a film, it is important that all the elimination products can be evaporated from the polymer matrix. If elimination products would still be present, they could act as plasticizers, hence lowering the T_g, and reactions between the elimination products and the conjugated polymer could possibly occur.

To assess the influence of film thickness, isothermal TGA experiments are carried out on the *n*-octyl-sulphinyl OC_1C_{10}-PPV precursor polymer with different film thickness. In Figure IV.23, isothermal TGA experiments from a polymer film with different weights (0.55 mg, 0.73 mg and 2.64 mg) at 100°C are shown. From this figure it is clear that the film thickness is very crucial for the evaporation of the elimination products. The thinner the film, the faster the elimination products can diffuse out of the polymer matrix.

To relate these results with the practical use of precursor polymers, in which a film thickness of 0.01 μm is used, it is important to measure the thickness of the film applied in this TGA experiments. The bottom of the pan

has a surface of 67.2 mm^2. The polymer density is ~1 g/cm^3 [14]. For the three different weights, a film thickness can be calculated. For a film with a weight of 0.55 mg, 0.73 mg and 2.64 mg thickness of 5.6 μm, 7.2 μm and 24.8 μm are calculated respectively. Comparing these thickness with the film thickness used for practical applications, the time necessary for all the elimination products to diffuse out of the polymer matrix will be much shorter.

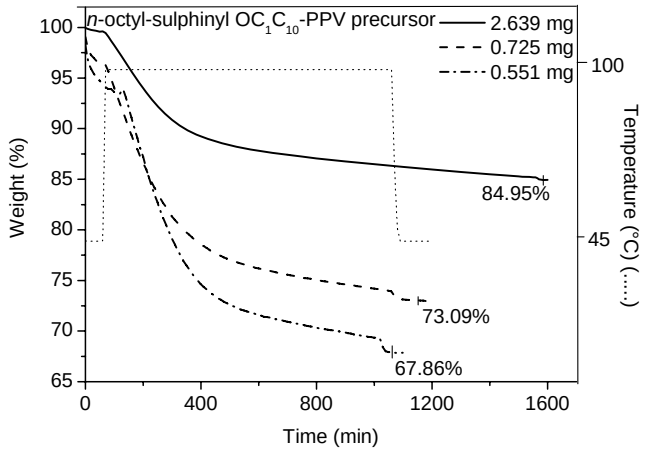

Figure IV.23: *TGA measurements performed on the n-octyl-sulphinyl OC_1C_{10}-PPV precursor polymer at an isothermal temperature of 100°C, to check the effect of film thickness on the evaporation of the elimination products.*

Since diffusion limitations probably occur in the polymer matrix, elimination products with a smaller R-group will probably diffuse faster out of the matrix than elimination products containing a larger R-group. The diffusion is dependent on the molecular weight of the species that will diffuse out of the polymer matrix [15]. To demonstrate this, TGA measurements are carried out on the *n*-ethyl-, *n*-butyl- and *n*-octyl-sulphinyl OC_1C_{10}-PPV precursor polymer. These curves are compared to each other in Figure IV.24.

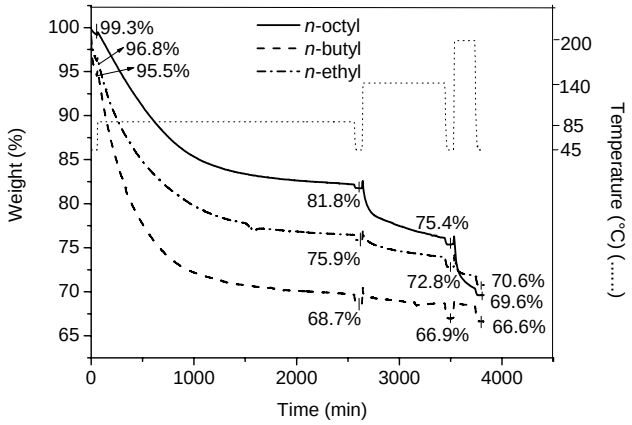

Figure IV.24 : *TGA measurements carried out on a n-alkyl-sulphinyl OC_1C_{10}-PPV precursor polymer with 3 different R-groups to check if degradation occurs at 85, 140 and 200°C.*

Table IV.7: *Mass percentages of the elimination products (sulphenic acids) calculated with the reaction equation of the elimination reaction (100%) for the three different R-groups.*

	precursor polymer	conjugated polymer	sulphenic acid	weight loss after 85°C
n-ethyl	366 g/mol	288 g/mol	78 g/mol	20.9 %
	100 %	79 %	21 %	
		(=100*288/366)	(=100*78/366)	
n-butyl	394 g/mol	288 g/mol	106 g/mol	26.8 %
	100 %	73 %	27 %	
n-octyl	450 g/mol	288 g/mol	162 g/mol	17.5 %
	100 %	64 %	36 %	

The weight losses obtained in TGA experiments will be compared to the mass percentages calculated from the reaction equation (Table IV.7). We have to remark that these are the hypothetical values, calculated for 100 % of elimination. These calculated values (Table IV.7) can be compared to the weight losses observed in TGA measurements at a reference temperature of

45°C (Figure IV.24). For the *n*-alkyl-sulphinyl OC_1C_{10}-PPV precursor polymers with a *n*-octyl, *n*-butyl and *n*-ethyl as R-group, a weight loss of 17.5 % (99.3 % - 81.8 %), 26.8 % (95.5 %- 68.7 %) and 20.9 % (96.8 % - 75.9 %) respectively is experimentally calculated from the isothermal experiment at 85°C after 2500 minutes. The experimental weight losses for the *n*-ethyl- and *n*-butyl precursor polymers, 20.9 % and 26.8 % respectively, are in good agreement with the calculated values (21 % and 27 %). The fact that the kinetics for the evaporation of the *n*-ethyl and *n*-butyl elimination products are almost the same is probably due to the difference in film thickness, as the factor of film thickness is very important for the diffusion of the elimination products out of the polymer matrix, as is shown before. The sample weight of the *n*-butyl and *n*-ethyl precursor polymer was equal to 0.56 mg (5.6 μm) and 0.77 mg (7.2 μm) respectively. Whereas we could have expected, the elimination products with a *n*-ethyl as R-group to diffuse faster out of the matrix. The 17.5 % experimental weight loss for the *n*-octyl precursor polymer is half of the calculated weight loss. A conclusion is, that the limited diffusion for the *n*-octyl precursor polymer leads to a slower evaporation of the elimination products. The sample was kept at 85°C for 2500 minutes, then at 140°C for 800 minutes and finally at 200°C for 200 minutes. At 140°C, the experimental weight loss for the *n*-butyl- and *n*-ethyl-sulphinyl OC_1C_{10}-PPV precursor polymer, 29 % and 24 % respectively, is larger than the calculated one, but these values are still within the measurement-error of the experiment. At 200°C, a slight increase in weight loss is visible. The weight loss for the *n*-ethyl-sulphinyl OC_1C_{10}-PPV precursor polymer at 200°C (26 %) can not be attributed to the evaporation of the elimination products only (too large), probably degradation already occurs. For the *n*-octyl-sulphinyl OC_1C_{10}-PPV precursor polymer a weight loss of 30 % is determined, which is still lower than the calculated value, even at 200°C.

In practice, much thinner polymer films are used, which means that the evaporation of elimination products occurs much faster. Nevertheless, it is efficient to use vacuum for an easier and better evaporation of the elimination products.

IV.B.3.a [5] Percentages of elimination products split off during the elimination process, calculated from (non)-isothermal MTDSC experiments

In this paragraph, the percentage of water that is released during the elimination process in isothermal and non-isothermal MTDSC experiments, is calculated and used as a measure for the rate of the dimerisation reaction. In the non-isothermal MTDSC experiments, this percentage is calculated from the melting peak of water, that appears in the total heat flow signal at around 0°C in the second heating run from –45°C up to 200°C (Figure IV.25)

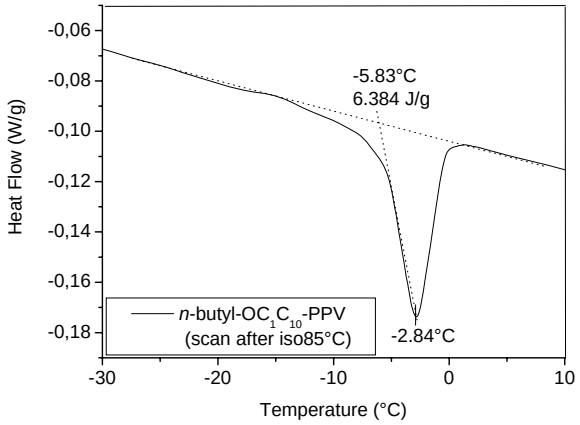

Figure IV.25: *Melting peak of water, calculated from the heat flow signal at around 0°C, in a MTDSC experiment carried out on a n-butyl-sulphinyl OC_1C_{10}-PPV precursor polymer. The heat flow in this figure is 6.384 J/g.*

In the isothermal MTDSC experiments, there are two possibilities to calculate the percentage water. The percentages can be calculated from the change in heat capacity during the elimination, but we have to mention that this change in heat capacity is not only due to water, but also due to a reaction of elimination products. To make a more reliable calculation of the percentage of liberated water, the sample is cooled down again to – 45°C after the isothermal part and then heated back up to 70°C. A melting peak of water is then obtained around 0°C. In Figure IV.25, a melting peak of water is presented. From the

melting heat, the percentage of water can be calculated using the melting enthalpy of water (at 0°C) from literature data, which is equal to 6.01 kJ/mol or 333.9 J/g [16]. The melting heat, obtained from the MTDSC experiment at 0°C, divided by 334 J/g delivers the percentage water liberated during elimination. In Figure IV.25, the percentage of water obtained in this way would be: (6.384 J/g)/(333.9 J/g) * 100% = 1.9 %.

To calculate the "percentage of water", that is liberated during the elimination reaction, from the change in heat capacity, this change in heat capacity has to be divided by the specific heat capacity of water from literature data [16]. The specific heat capacity of water for 70, 80 and 85°C at a pressure of 1 bar is equal to 4.19 J/g/°C, 4.20 J/g/°C and 4.20 J/g/°C respectively. It should be mentioned, however, that this calculation assumes that the change in heat capacity is mainly due to water.

Table IV.8: *Percentages of liberated water in the elimination process, calculated from the melting peak of water at around 0°C in the heat flow signal and from the change in heat capacity.*

R-group	experiment	melting heat (J/g)	% water calc. from melting heat	temp (°C)	C_p increase (J/g/°C)	% water calc.from C_p increase
n-butyl	non-isothermal	3.217	0.96	-4.28	////	////
	70°C-600'	0.487	0.15	-22/-7.1	0.056	1.33
	80°C-600'	4.253	1.27	-22/-7.1	0.095	2.26
	85°C-600'	6.384	1.92	-2.84	0.110	2.62
n-octyl	non-isothermal	6.148	1.84	-3.82	////	////
	70°C-600'	1.074	0.32	-3.14	0.051	1.22
	70°C-1700'	4.743	1.42	-3.13	0.083	1.98
	80°C-600'	5.351	1.6	-2.26	0.087	2.07
	80°C-1100'	6.035	1.81	-1.9	0.103	2.45
	85°C-600'	6.718	2.01	-3.14	0.090	2.14
	85°C-900'	7.376	2.21	-1.81	0.100	2.40
	90°C-900'	7.935	2.38	-2.69	/	/
	95°C-600'	7.725	2.31	-3.66	/	/

All the calculated percentages are included in Table IV.8. The theoretical percentage of water, that could maximally be set free during the elimination, could be calculated with the reaction equation of the dimerisation reaction that is shown in Table IV.9.

Table IV.9: *The theoretical percentage of water that can be formed during the elimination reaction.*

	sulphenic acid	thiosulphinate	water
n-butyl	312 g/mol	194 g/mol	18 g/mol
	27%*	24.7%	2.3%
n-octyl	162 g/mol	306 g/mol	18 g/mol
	36%*	34%	2%

* :For these percentages see Table IV.7.

When the calculated percentages are compared to the experimental percentages, it can be noticed that for the *n*-octyl-sulphinyl OC_1C_{10}-PPV precursor polymer after 600 minutes at 85°C, about the maximal percentage of water (out of the melting heat) is obtained, while at 80°C after more than 1100 minutes, the maximum percentage of water is "almost" reached. After 1700 minutes at 70°C, just 1.42 % of water is obtained, this means that at 70°C, the dimerisation reaction is not complete, even after 1700 minutes. The percentages, experimentally determined by the change in heat capacity, are greater and even exceed the calculated percentages. This is logical, because the change in heat capacity is not only due to the water that is formed, but also due to the formation of the conjugated polymer, thiosulphinate and the disproportionation reaction which already starts.

IV.B.3.b Elimination of a n-alkyl-sulphinyl OC_1C_{10}-PPV precursor polymer in solution

In solid state, the elimination process was studied extensively, but the conversion to the conjugated polymer is also be performed in solution. It was relevant to extend the study in liquid state, however, because of time limits this part must be viewed as preliminairy and needs further follow up.

With OC_1C_{10}-PPV, it is possible to do the elimination in solution, because the conjugated OC_1C_{10}-PPV is still soluble after elimination, due to the alkoxy chains (OC_{10} and OC_1) substituted on the polymer backbone. This is very important for practical applications, where an already conjugated polymer can be deposited on the substrate, instead of a precursor polymer film that has to be eliminated on the substrate itself (e.g. PPV).

A *n*-alkyl-sulphinyl OC_1C_{10}-PPV precursor polymer is eliminated in toluene at 110°C for 4 hours. Then, the conjugated OC_1C_{10}-PPV polymer is precipitated in a non-solvent (methanol), while the elimination products remain dissolved in methanol. A huge advantage of this elimination in solution with respect to the elimination in solid state, is that the subsequent reactions of the elimination products, such as the disproportionation reaction of thiosulphinate, do not occur anymore because these elimination products are removed and hence do not affect the conjugated polymer anymore in the application.

MTDSC will show us if there is an interaction between the conjugated polymer and the solvent. MTDSC is very useful in studying phase transitions in polymeric systems, so it can accurately detect the liquid-liquid demixing transition. Recently MTDSC measurements show that phase-separation between polymer-polymer and polymer-solvent systems could be measured in the heat capacity signal [17, 18]. Liquid-liquid demixing of polymer solutions is extensively studied since the last half of the twentiest century.

Experiments are done with two different solvents: chlorobenzene and toluene. Both solvents are used because they have high boiling points, 130 and 111°C respectively. Chlorobenzene is used in our laboratory because it is a good solvent to spincoat with, but it is less suitable on large scale because of healthy risks. Toluene is more used in industry.

IV.B.3.b [1] Non-isothermal elimination in solution

In Figure IV.26, a non-isothermal MTDSC experiment is shown which is carried out on a 43% (m/m) mixture of *n*-octyl-sulphinyl OC_1C_{10}-PPV precursor polymer in toluene. In the C_p-signal, a small baseline shift in heat capacity is visible at high temperatures. This is an indication for phase-separation (demixing/remixing) between the polymer and the solvent during which the composition of the co-excisting phases changes continuously as a function of increasing temperature [18, 19]. The onset of this baseline shift in heat capacity upon cooling is defined as the cloud point and is 110°C. The heating curves **(3)** have the same slope as the cooling curves **(2)**. Performing such MTDSC heating-cooling experiments over a large concentration range allows in principle the construction of the phase diagram of the polymer–solvent system. We suppose an Upper Critical Solution Temperature behaviour (UCST) for our polymer-solvent system [19].

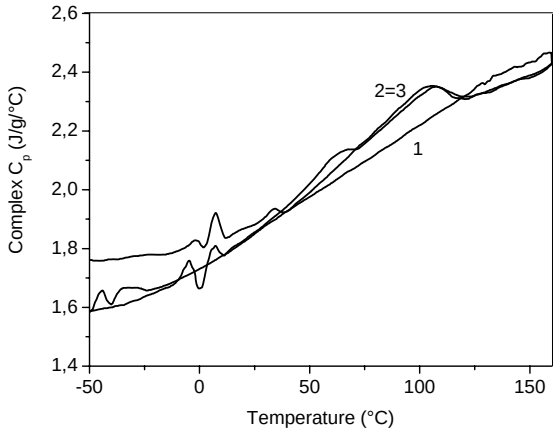

Figure IV.26: *MTDSC experiment on the n-octyl-sulphinyl OC_1C_{10}-PPV precursor polymer in toluene (43% (m/m)). The sample is heated from -50°C up to 200°C at 2.5°C/min (1), followed by a cooling process (2) and again a second heating (3) on the same heating rate.*

The changes in heat capacity with toluene are a little bit larger than with chlorobenzene (see paragraph IV.B.3.b[2]). This indicates that the increase in heat capacity is not only due to the elimination process. To demonstrate that phase-separation really occurs between the conjugated OC_1C_{10}-PPV polymer and toluene, a mixture (50% (m/m)) of conjugated polymer and toluene is prepared and heated. After heating the solution, the polymer is dissolved and a transparent red solution is obtained. After cooling down this solution again at ambient temperature for 15 minutes, phase-separation between the polymer and the solvent is visible. A dim red solution with some red polymer particles is obtained. By repeating this heating-cooling process, the same phenomena of mixing and demixing occur.

IV.B.3.b [2] Isothermal elimination in solution

In Figure IV.27 and IV.28, isothermal MTDSC experiments are plotted from 50/50% (m/m) mixtures of *n*-octyl-sulphinyl OC_1C_{10}-PPV precursor polymer in toluene and chlorobenzene respectively, at different temperatures (70, 80 and 85°C). In Figure IV.27, also the reproducibility of the

measurements at 70 and 80°C is displayed. In these figures, the observed tendencies are the same as was observed for the isothermal MTDSC measurements on a *n*-octyl-sulphinyl OC_1C_{10}-PPV precursor polymer in solid state (Figure IV.17), namely that the elimination occurs faster at higher temperatures. This phenomenon is again visible from the change in heat capacity at 70, 80 and 85°C (see Table IV.10). Hereby, it is important to note that the increase in heat capacity is larger for the elimination in solution compared to the elimination in solid state. This increase in heat capacity is not only due to the formation of water and elimination products, but also due to the phase-separation that occurs. This makes the study of the elimination in solution more difficult as two processes happen almost simultaneously, the elimination and phase-separation.

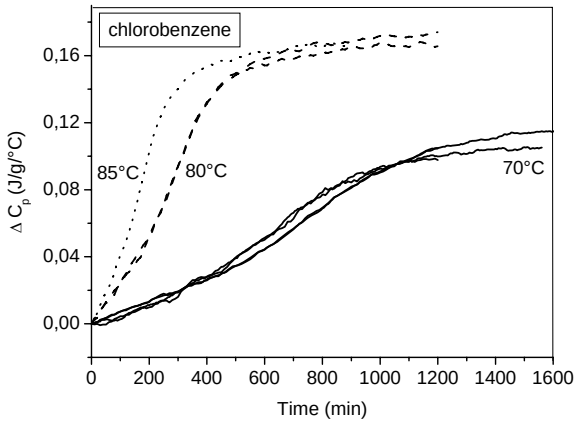

Figure IV.27: *Isothermal MTDSC experiments at 70, 80 and 85°C on a 50% (m/m) mixture of n-octyl-sulphinyl OC_1C_{10}-PPV precursor polymer in* ***chlorobenzene*** *in a PE 40μl-0.15mm pan.*

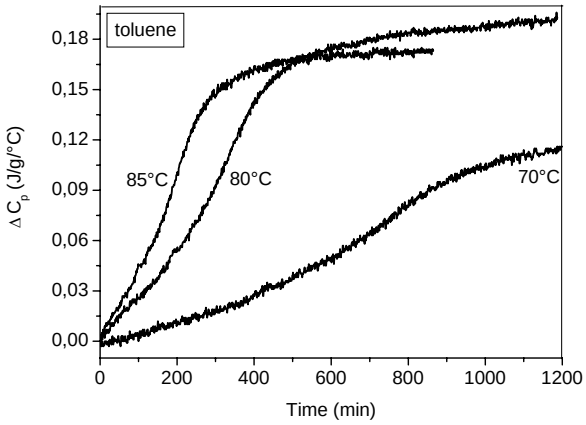

Figure IV.28: *Isothermal MTDSC experiments at 70, 80 and 85°C on a 50% (m/m) mixture of n-octyl-sulphinyl OC_1C_{10}-PPV precursor polymer in* ***toluene*** *in a PE 40µl-0.15mm pan.*

Phase-separation in isothermal conditions is also demonstrated with *in-situ* UV-Vis spectroscopy (light-scattering). A saturated mixture of *n*-octyl-sulphinyl OC_1C_{10}-PPV precursor polymer is dissolved in toluene and heated at 80°C for 300 minutes *in-situ* the UV-Vis spectrophotometer.

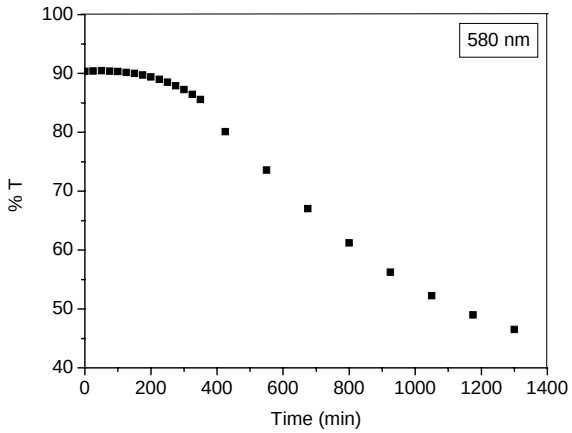

Figure IV.29: *Percentage transmission at 580 nm as a function of time at 80°C.*

The endset of the absorption peak of the conjugated OC_1C_{10}-PPV polymer is around 550 nm. After longer periods at 80°C, the endset of each UV-Vis spectra shifts to higher wavelengths, due to light-scattering from the particles that are formed. To demonstrate phase-separation independently from the elimination reaction, the absorbance at 580 nm (> 550 nm) is plotted as a function of time, shown in Figure IV.29. From this figure it is clear that phase-separation starts to occur around 230 minutes at 80°C.

IV.B.3.b [3] Percentages of water released during the elimination in solution

The percentage of water released during the elimination processin solution, can be calculated from the melting peak around 0°C in the total heat flow, using the same procedure as for the solid state case (paragraph IV.B.3.a[5]). By the fact that the increase in heat capacity is not only due to the formation of water, but also to the formation of elimination products and "phase-separation" which occurs, it is again not a correct way to calculate the percentage of water out of the heat capacity. In Table IV.10, the mass percentages of liberated water for the isothermal MTDSC experiments in solution, for both solvents, are summarised at different isothermal temperatures.

***Table IV.10**: Mass percentages of water set free, calculated from isothermal MTDSC measurements on the n-octyl-sulphinyl OC_1C_{10}-PPV precursor polymer in solution (50% (m/m)) in a PE 40µl- 0.15.*

solvent	experiment	melting heat (J/g)	% water (%) calc. from melting heat	C_p increase (J/g/°C)
chlorobenzene	70°C-1700'	1.52/1.22	0.46/0.37	0.107/0.114
	80°C-1100'	1.80/2.02	0.54/0.60	0.137/0.173
	85°C-900'	2.37/2.45	0.71/0.73	0.173/0.178
toluene	70°C-1700'	1.438	0.43	0.12
	80°C-1100'	////	////	0.19
	85°C-900'	2.201	0.66	0.19

The percentage of liberated water obtained in solution must be doubled in order to make a comparison with the values from the solid state elimination, because in solution a 50% (m/m) mixture is used. By applying this normalisation for 70, 80 and 85°C respectively, we obtained about 0.86%, 1.14% and 1.4% liberated water out of the melting heats. The percentage of water as obtained from the melting peaks is smaller in solution for the 3 temperatures with the same isothermal time as in the solid state.

IV.B.4 Conclusions

From a combination of isothermal and non-isothermal MTDSC experiments in solid state, we can say that the elimination process is a combination of consecutive reaction steps. The reaction steps happen so close after each other, that no real kinetic separation is possible. Unfortunately, no criterion in MTDSC is obtained which is directly related to the elimination reaction.

We also have studied the elimination process in solution (toluene/ chlorobenzene) with MTDSC. In (non)-isothermal MTDSC measurements, an indication for phase-separation is obtained. The phase-separation between polymer and solvent is also demonstrated with *in-situ* UV-Vis spectroscopy (light-scattering).

From isothermal TGA experiments, the diffusion and evaporation of the elimination products out of the polymer matrix is studied. A smaller R-group, a higher isothermal temperature and a thinner film promote the diffusion and evaporation of the elimination products. We could avoid the negative aspects of crosslinking by use of vacuum conditions.

IV.B.5 Experimental part

IV.B.5.a Thermal analytical techniques and sample preparation

Modulated Differential Scanning Calorimetry (MDSC)

The MTDSC measurements were performed on a TA Instruments Modulated 2920 DSC with MTDSC option and a RCS cooling system (Refrigerated Cooling System). Helium was used as a purge gas (25 ml min^{-1}) to ensure a uniform heat capacity. To calibrate the MTDSC, a baseline is taken by doing a measurement in an empty oven without pans. This baseline is subtracted from the real measurements to charge the asymmetry of the cell. Indium and cyclohexane were used for temperature calibration, the former was also used for enthalpy calibration. Heat capacity calibration was performed with a poly(methylmethacrylate) standard (PMMA), supplied by Acros [20]. We have to use the heat capacity difference between the two temperatures, one above (150°C) and one below (80°C) the glass transition temperature (T_g) of PMMA, to make sure that heat capacity changes were adequately measured. In this experiment, the same temperature modulation (= the same amplitude and period of the sinusoidal temperature program) is used as in the one used in the experiments that are performed. The calculated difference in heat capacity before and after the T_g of PMMA (ΔC_p, calculated) is compared with the corresponding literature value (ΔC_p, literature) and from these data, the calibration factor KC_p could be calculated (eq. IV.11). It is necessary to calibrate the instrument every time a new type of pan or a new heating rate is used.

$$KCp = \frac{\Delta Cp\,,lit}{\Delta Cp\,,calc} \qquad \text{(IV.11)}$$

The experiments in solid state are performed in Perkin-Elmer (PE) 10µl (volume)-0.15mm (thickness) pans and High Pressure Steel pans (HPS), while the experiments in solution are carried out in PE 40µl-0.15mm pans and also HPS pans. The HPS pans are used in experiments when temperatures above 100°C are applied (non-isothermal experiments), while PE pans are mostly used in isothermal experiments beneath 100°C. The superimposed sinusoidal temperature program (= temperature modulation) depends on the type of pan

used. For each type of PE pan, a temperature modulation of ± 0.5°C/60sec is used, while for HPS pans the temperature modulation is ± 0.5°C/100sec (HPS pans are heavier than the PE pans). The bottom and top of the PE pan are pressed on each other through a press, while the bottom and top of a HPS pan are screwed together with in between a seal.

The sample weight of PE pans is between 5 and 10mg and between 10 and 15mg for HPS pans. For the solid state MTDSC experiments, films of precursor polymer and conjugated polymer with a thickness of 500µm are pressed at 35°C between an aluminium foil. Reproducible MTDSC measurements were obtained using this method of sample preparation. For the experiments in solution, a mixture of 50% (m/m) is prepared in the pan itself. Each pan is closed very well, to ensure that no loss of weight can occur and also no elimination products could evaporate out of the pan. Each pan is weighed before and after an MTDSC experiment to check for weight losses.

Some measurements are carried out with another cooling system: LNCA (Liquid Nitrogen Cooling Accessory). This cooling system reaches temperatures up to –150°C, with assistance of liquid nitrogen. This cooling system is necessary to measure the T_g of the conjugated polymer, which is obtained by eliminating the precursor polymer in a MTDSC.

ThermoGravimetric Analysis (TGA)

The weight loss is measured in experiments in which the temperature is first kept isothermal at 85 and 100°C, afterwards isothermal at 140°C and finally isothermal at 200°C. To perform these measurements, a HI-Res Modulated TGA 2950 ThermoGravimetric Analyser from TA Instruments (TAI) is used. All measurements are carried out under a constant flow of helium to create an inert atmosphere and to ensure a uniform heat transport in the cell.

The TGA pan is first tarred and afterwards a mixture of 5% (m/m) polymer/$CHCl_3$ is sprayed on the bottom of the TGA pan. After the $CHCl_3$ is evaporated from that mixture, a polymer film is obtained. A second layer can be put on top of the first layer using the same method. Then, the pan is placed in a Heraeus Vacutherm vacuum oven from Kendro Laboratory Products, during 2 to 3 hours at 10^{-2}mmHg and 25°C to make sure that all $CHCl_3$ is evaporated. Using this method, uniform films with different thickness can be obtained.

IV.B.5.b Materials

***n*-alkyl-sulphinyl OC_1C_{10}-PPV precursor polymers and the OC_1C_{10}-PPV conjugated polymer** The synthesis and characterisation of these polymers are described in paragraph III.J.2.

Synthesis of the elimination products

***n*-butyldisulphide** This product is commercial available (ACROS). ^{1}H-NMR ($CDCl_3$, 400 MHz): δ 0.89 (t, 6H, C$\underline{H}_3$), 1.37 (qui, 4H, $CH_3(C\underline{H}_2)_3$), 1.63 (qui, 4H, C$\underline{H}_2CH_2S$), 2.65 (t, 4H, C$\underline{H}_2S$) ppm; IR (KBr): 2871 ν (CH_2 symm.), 1463 ν (CH_2-S deformation), 1268 ν (CH_2-S wag), 1216 ν (CH_2 twist) cm^{-1}; DIP-MS (EI, m/z, rel. int.): 178 ($[M]^+$, 40), 121 ($[M\text{-}C_4H_9]^+$, 30), 87 ($[M\text{-}SC_4H_9]^+$, 5), 57 ($C_4H_9^+$, 100).

***n*-butylthiosulphinate** [21] To a solution of *n*-butyldisulphide (1.00 g, 5.61 mmol) in dichloromethane (100 ml) cooled in ice-water bath was added a solution of *m*-CPBA (5.61 mmol, 1.17 g) in dichloromethane (10 ml). After stirring for 1 hour at 0°C and 2 hours at ambient temperature water (200 ml) was added. The organic layer was extracted with water (3 x 200 ml) and aqueous % $NaHCO_3$ (2 x 150 ml), dried with anhydrous magnesium sulphate and concentrated in vacuum. After purification by column chromatography on silica using chloroform as eluent *n*-butylthiosulphinate was collected as a colorless oil (0.76 g, 70 %). ^{1}H-NMR ($CDCl_3$, 400 MHz): δ 0.86 (t, 6H, C$\underline{H}_3$), 1.78 (m, 4H, C$\underline{H}_2CH_2S(O)SCH_2C\underline{H}_2$), 3.1 (m, 4H, C$\underline{H}_2S(O)SC\underline{H}_2$) ppm; ^{13}C-NMR ($CDCl_3$, 100 MHz): δ 13.9 (C$\underline{H}_3$), 30.7 ($\underline{C}H_2CH_2SS(O)$), 31.59 ($\underline{C}H_2CH_2S(O)S$), 32.62 ($\underline{C}H_2SS(O)$), 55.98 ($\underline{C}H_2$-S(O)S); IR (KBr): 2956, 2925 ν (CH_2 asymm.) 2871 ν (CH_2 symm.), 1462 ν (CH_2-S deformation), 1082 ν (S(O)) cm^{-1}.

***n*-butylthiosulphonate** To a solution of *n*-butanesulphonyl chloride (0.87 g, 5.55 mmol) in tetrahydrofuran (THF, 10 ml) was added a solution of *n*-butanethiol (0.6 g, 5.55 mmol) and NatBuO (0.53 g, 5.55 mmol) in THF (25 ml). The last solution was stirred in advance for 1 hour at ambient temperature. After stirring the mixture 12 hours at ambient temperature, the organic layer

was extracted with chloroform and concentrated in vacuum. After purification by column chromatography on silica using hexane as eluent, *n*-butylthiosulphonate was collected as a light yellow oil. ^{1}H-NMR ($CDCl_3$, 400 MHz): δ 0.89 (t, 6H, $C\underline{H}_3$), 1.36 (m, 4H, $CH_3C\underline{H}_2$), 1.65 (2H, m, $C\underline{H}_2CH_2S$), 1.82 (m, 2H, $C\underline{H}_2CH_2S(O)_2$), 3.09 (t, 2H, $C\underline{H}_2S$), 3.25 (t, 2H, $C\underline{H}_2S(O)_2$) ppm; IR (KBr): 2960, 2931 ν (CH_2 asymm.), 2873 ν (CH_2 symm.), 1463 ν (CH_2-S deformation), 1324, 1128 ν ($S(O)_2$) cm^{-1}.

IV.C References

[1] L. Claes, J.-P. Francois, M.S. Deleuze, *submitted for publication*

[2] M.M. de Kok, A.J.J.M. van Breemen, R.A.A. Carleer, P.J. Adriaensens, J.M. Gelan, D.J. Vanderzande, *Acta Polym.,* 50 **(1999)** 28.

[3] a) M. Reading, A. Luget, and R. Wilson, *Thermochim. Acta*, 238 **(1994)** 295; b) B. Wunderlich, Y. Jin and A. Boller, *Thermochim. Acta*, 238 **(1994)** 277; c) M. Reading, *Trends in Polymer Sci*., 1 **(1993)** 248.

[4] a) 3; b) P.S. Gill, S.R. Sauerbrunn and M. Reading, *J. Thermal Anal*., 40 **(1993)** 931; b) M. Reading, D. Elliot, and V.L. Hill, *J. Thermal Anal*., 40 **(1993)** 949.

[5] C.A. Kingsburry, D.J. Cram, *J. Am. Chem. Soc.,* 82 **(1960)** 1810.

[6] a) J.R. Shelton, K.E. Davis, *Internat. J. Sulphur Chem.,* 8 **(1973)** 205; b) R.D.G. Cooper, *J. Am. Chem. Soc.,* 92 **(1970)** 5010.

[7] a) 22; b) B.M. Trost, K.K. Leung, *Tetrahedron Lett.,* 48 **(1975)** 4197.

[8] D.N. Jones, D.R. Hill, D.A. Lewton, C. Sheppard, *J.C.S. Perkin I,* **(1976)** 1574.

[9] E. Block, J. O'Connor, *J. Am. Chem Soc.,* 96 **(1974)** 3929.

[10] P. Koch, E. Ciuffarin, A. Fava, *J. Am. Chem. Soc*., 92 **(1970)** 5971.

[11] D. Barnard, *J. Am. Chem. Soc.,* **(1957)** 4675.

[12] G. Horowitz, *Adv. Mater.*, 10(5) **(1998)** 365.

[13] L. Claes, J.P. Francois, M.S. Deleuze, *J. Am. Chem. Soc*., 124 **(2002)** 7563.

[14] J. Brandrup, E.H. Immergut, E.A. Grulke (J. Wiley & Sons, *Polymer Handbook,* 4th ed., p.IV-159.

[15] H.-G. Ehas, *An introduction to Polymer Science,* 1st ed., Weinheim, **(1997)** p.247.

[16] D.R. Lide: Handbook of Chemistry and Physics, CRC press **(1998)** p.6.3-6.119.

[17] a) G. Dreezen, G. Groeninckx, S. Swier, B. Van Mele, *Polymer,* 42 **(2001)** 1449 ; b) S. Swier, R. Pieters, B. Van Mele, *Polymer*, 43 **(2002)** 3611.

[18] P.L. Van der Heijden, M.H.V. Mulder, M. Wessling, *Thermochimica Acta*, 27 **(2001)** 378.

[19] J. Arnauts, R. De Cooman, P. Vandeweerdt, R. Koningsveld, H. Berghmans, *Thermochim. Acta,* 1 **(1994)** 238.

[20] U. Gaur, B. Wunderlich, *J. Phys. Chem. Ref. Data,* 11 **(1982)** 313.

[21] a) K. Kondo, A. Negishi, I. Ojima, *J. Am. Chem. Soc.*, 94 **(1972)** 5786; b) J. Buter, R.M. Kellogg, *J. Org. Chem.,* 42 **(1977)** 973.

V

Polymerisation behaviour of xanthate containing monomers towards PPV precursor polymers: Study of the elimination behaviour of precursor polymers with *in-situ* FT-IR and UV-Vis analytical techniques.

V.A Introduction

Over the last decades conjugated polymers evolved from a lab curiosity to commercial applications. Ever since Burroughes *et al.* discovered luminescence in PPV, the research to this polymer and its derivatives became increasingly important [1]. PPV can be synthesised in many different ways, usually from a precursor polymer which can be converted to the conjugated structure *in-situ* or in an additional conversion step. The Wessling route, the Gilch route and the sulphinyl route are known examples of such precursor routes [2,3,4]. The precursor route to which the least attention was devoted to till now is the xanthate precursor route [5,6]. Nevertheless, the xanthate precursor route shows interesting prospects. In this precursor route a xanthate group is used as thermally eliminable group to yield the double bound. We have already reported on the synthesis of PPV and some of its derivatives via the

sulphinyl precursor route [4,7,8]. Of further interest to us was an evaluation of the possibilities the xanthate group offers in the synthesis of PPV. To serve this purpose, three different monomers, combining sulphinyl and xanthate functionalities (Figure V.1) were synthesised and polymerised. Once the precursor polymers were formed, the thermal conversion to the conjugated structure was studied with *in-situ* FT-IR spectroscopy, *in-situ* UV-Vis spectroscopy, TGA and DIP-MS.

V.B Monomer synthesis and polymerisation reactions

In literature, monomers used in the xanthate precursor route are synthesised from a dihalogenide in a single step reaction [5] (paragraph I.C.2.c). Usually the *O*-ethyl xanthatic group is used. A drawback of the xanthate precursor route is the rather strict way in which the polymerisation has to be carried out. Dry THF is needed as a solvent and the polymerisation temperature must be sufficiently low to get good polymerisation yields and high molecular weight polymers. In the sulphinyl precursor route, the polymerisation conditions are less strict and polymerisations can proceed in a wide range of solvents at different temperatures [7]. Another advantage of the sulphinyl precursor route is the broad scope of PPV derivatives that can be synthesised whereas for the xanthate precursor route, so far, only a few PPV derivatives have been reported [5,6,9,10]. Another point worth mentioning is the fact that a sulphinyl group generally eliminates at lower temperatures compared to the xanthate group.

However, we have an interest in exploring both xanthate and sulphinyl precursor routes towards the synthesis of PPV in order to get a better understanding of the influence of the eliminable group on the properties of the final conjugated polymer. For this purpose, three different monomers (**3**, **4** and **5**) were synthesised. The different synthetic pathways towards PPV are shown in Figure V.1. All monomers consist of a 1,4-xylene unit to which different groups (xanthate, chlorine or sulphinyl) are attached. In the traditional symmetrical bisxanthate monomer **3** there is no chemical differentiation between polariser and leaving group. In monomer **4** one xanthate group is replaced by a chlorine atom and in monomer **5** a sulphinyl group is introduced. These chemical modifications also allow to evaluate the outcome of the polymerisation in relation to the chemical structure of the monomer.

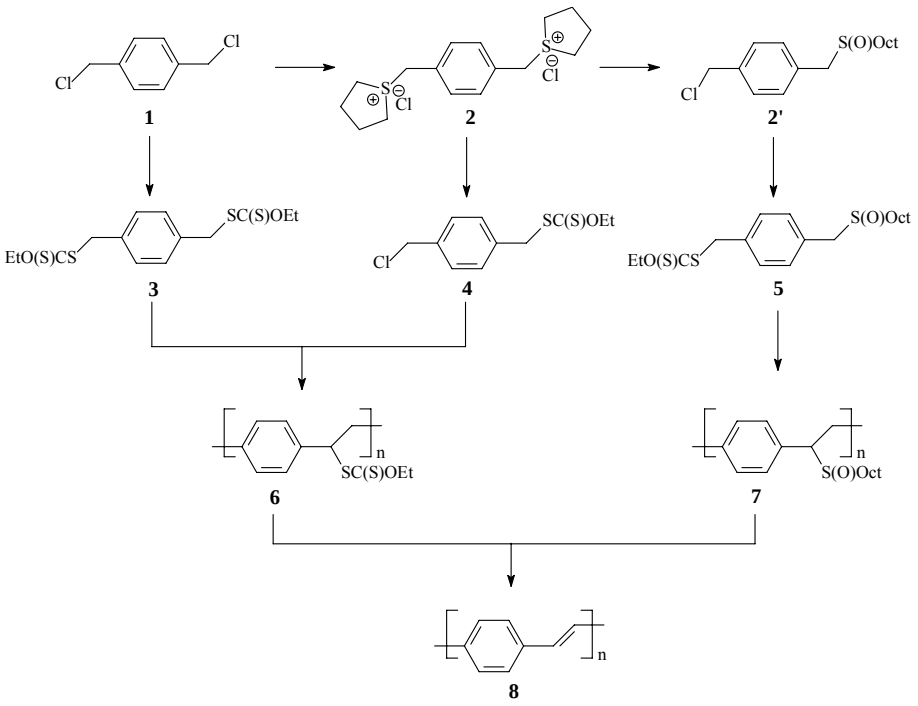

Figure V.1: *Different synthetic pathways towards PPV.*

The bisxanthate monomer **3** was synthesised from its dichloro analogue whereas the monoxanthate monomer **4** was synthesised departing from a bissulfonium salt **2**. This approach is similar to the one used in the synthesis of compound **2'**, and proved necessary to obtain monoxanthate **4** in a highly selective way [11]. Attempts to make compound **4** directly from the dichloride were less selective and a difficult chromatographic separation had to be carried out to separate the different products formed in this reaction. The sulphinyl-xanthate monomer **5** was synthesised by reacting compound **2'** with potassium *O*-ethyl xanthatic acid salt. These three monomers (**3**, **4** and **5**) were all polymerised in the same "standard" conditions (see Experimental part, paragraph V.E.2). Each monomer was polymerised at three different temperatures and dry THF was used as a solvent in all polymerisation reactions. Potassium *tert*-butoxide was used as a base and was added in solution in a slight excess of 1.05 equivalents. Polymerisation time was 1 hour, after which the reaction mixture was poured into ice water. The polymer was extracted with chloroform, concentrated and precipitated in diethylether/hexanes. The precursor polymers were soluble in organic solvents such as chloroform and THF.

Table V.1: *Polymerisation results for the different monomers. M_w and PD were determined by GPC versus PS standards using THF as eluent.*

	Temp (°C)	Yield (%)	M_w (g/mol)	PD
	-20	35	313.000	3.5
6 from **3**	0	34	300.000	2.6
	30	15	25.000	2.0
	-20	55	472.000	5.1
6 from **4**	0	26	272.000	5.5
	30	35	202.000	5.6
	0	23	1.600	1.3
7 from **5**	30	35	1.600	1.2
	50	65	1.600	1.3

Molecular weights and polydispersities were determined by gel permeation chromatography (GPC) versus polystyrene standards (eluent THF). Monomers **3** and **4** were polymerised to the xanthate precursor polymer **6** at –20, 0 and 30°C. The spectral data for these polymers are consistent with those in literature [5,9]. Monomer **3** could only be polymerised to high molecular weight polymer at temperatures equal or lower than 0°C whereas in the case of monomer **4** high molecular weight polymers were obtained at all temperatures tested (Table V.1). Polymerisation yields vary from rather low to good, but no clear trend could be observed. Note that the polydispersities of the precursor polymers obtained from monomer **4** are significantly higher than those obtained for the polymerisation of monomer **3**. From Table V.1 we observe an inverse relationship between the molecular weight and the temperature at which the polymerisation is performed. Decreasing the temperature in both cases leads to higher molecular weights. This observation is in accordance with our experience in the polymerisation of monomer **2'** in the sulphinyl precursor route. On the other hand, within a certain temperature domain (0-60°C), the polymerisation yield for monomer **2'** proved almost independent of temperature [12]. This is in contrast with the data obtained for the polymerisation of the bisxanthate monomer.

Monomer **5** was polymerised at 0, 30 and 50°C. For this monomer higher polymerisation temperatures were needed to keep the reagents soluble. To our surprise all polymerisations of monomer **5** only yielded oligomers of precursor **7**. GPC showed these oligomers all had very similar molecular weights. ^{1}H and ^{13}C NMR spectroscopy clearly showed different signals for the sulphinyl groups in the main chain compared to those situated at the end of the oligomer chain. Moreover, the similar integration of both signals suggests both sulphinyl groups exist for approximately an equal amount. Increasing the polymerisation temperature, left the molecular weight unchanged, but the polymerisation yield increased significantly (Table V.1). Combination of a xanthate group and a sulphinyl group in the same monomer apparently limits the polymerisation capabilities. Probably, the quinoid structure is not formed rapidly enough in concentrations that are necessary to obtain high molecular weight polymer.

V.C Results and discussion

V.C.1 Thermal conversion of the xanthate precursor polymer (6) to the conjugated structure

The final step in both the sulphinyl and xanthate precursor route is a thermal elimination reaction to form the double bond. In the latter the xanthate group is eliminated by a modified Chugaev reaction to yield the double bond. The xanthate group is attached to the polymer backbone via the sulphur atom instead of the oxygen atom in a normal Chugaev reaction. This effectively lowers the elimination temperature and also simplifies the monomer synthesis [5]. The elimination products that are liberated during elimination are unstable and further react to form ethanol and carbondisulphide on the one hand and ethanethiol and carbonoxysulphide on the other hand [13,14].

For comparison, in the sulphinyl precursor route the elimination process is an expulsion of sulphenic acid and the formation of a double bond on the polymer backbone. The double bond formed is mainly *trans* due to increased steric hindrance in the transition state which leads to the *cis* configuration [15]. The sulphenic acids which are split off are unstable and dimerise immediately to give water and thiosulphinates, which finally

disproportionate to yield thiosulphonates and disulphides [15]. In general, the conversion to the conjugated structure, as well as its thermal stability, can be studied by different techniques. The ones used here are *in-situ* FT-IR spectroscopy, *in-situ* UV-Vis spectroscopy, TGA and DIP-MS.

The thermal elimination and stability of the xanthate precursor polymers (**6**) was examined and proved to be similar for all xanthate precursor polymers independent of the monomer (**3** or **4**) and polymerisation temperature used. For simplicity reasons, only the graphs of the thermal behaviour of precursor polymer **6**, prepared from monomer **3** at 0°C are shown.

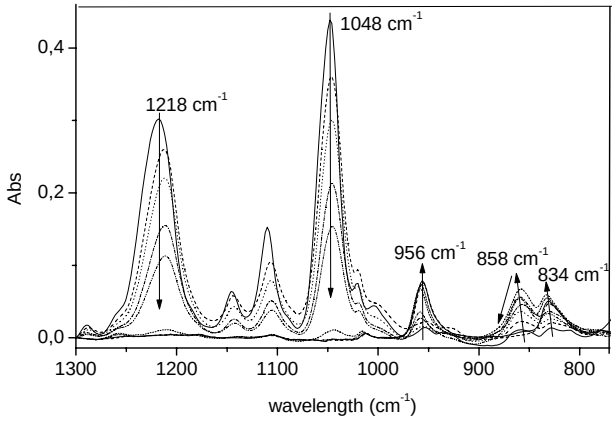

Figure V.2: *Enlarged part of the IR spectrum at different temperatures (24, 145, 160, 170, 190, 205, 235, 295 and 340°C).*

In-situ FT-IR spectroscopy measurements were carried out on film, spincoated on KBr pellets. An experimental set-up was used (see experimental part, paragraph V.E.1) which allowed *in-situ* monitoring of the elimination process. A non-isothermal heating program of 2°C/min from ambient temperature up to 340°C under a continuous flow of nitrogen was used. Figure V.2 shows an enlarged part of the IR spectrum at a few selected temperatures.

The xanthate precursor polymer **6** shows strong absorption peaks at 1218 and 1048 cm^{-1}, both arise from the *O*-ethyl xanthate leaving group. When the elimination progresses, a new absorption peak appears at 956 cm^{-1} that

originates from the *trans* vinylene double bond. The absorption peaks from the xanthate group gradually disappear with increasing temperature. The absorption at 858 cm^{-1} is assigned to the formation of some *cis* linkages in the conjugated structure [5,10]. No *cis* double bonds can be detected after conversion of a sulphinyl precursor polymer [15]. In Figure V.3, the evolution of the absorbance of the most important absorption peaks is visualised as a function of temperature. In this way the relative trends in elimination behaviour become clear.

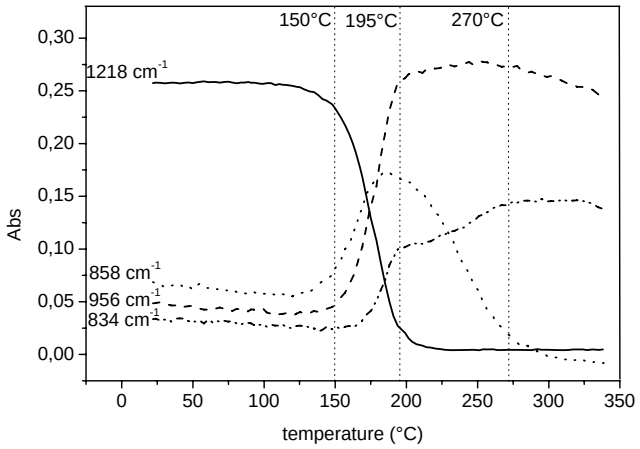

Figure V.3: *The absorbance at 834, 956, 858 and 1218 cm^{-1} versus temperature.*

Both elimination of the xanthate group and formation of the *cis* and *trans* double bond start around 150°C. Between approximately 195 and 270°C the absorbance of the *cis* vinylene double bond at 858 cm^{-1} decreases again while the absorbance of the *trans* vinylene double bond (956 cm^{-1}) slightly increases in this temperature domain. This phenomenon is interpreted as an isomerisation process of the *cis* double bonds into the thermodynamically more favourable *trans* double bonds. The absorbance of the *p*-phenylene C-H out-of-plane deformation at 834 cm^{-1} also increases during the elimination process [13]. After this *in-situ* non-isothermal experiment, we have proven the phenomenon of *cis-trans* isomerisation with some isothermal experiments at 150 and 200°C for 5 hours with *in-situ* FT-IR spectroscopy. In Figure V.4 A

and B, the absorbance of the *cis* and *trans* vinylene double bond at 858 and 956 cm^{-1} respectively and the absorbance of the xanthate group at 1218 cm^{-1} are plotted versus time at each isothermal temperature.

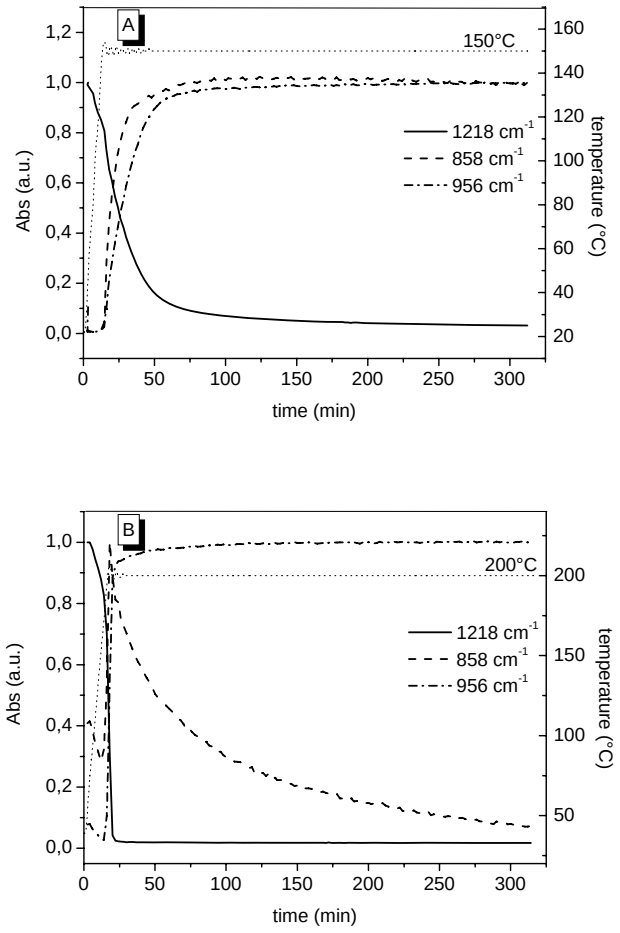

Figure V.4 A,B: *The absorbance at 1218, 858 and 956 cm^{-1} versus time at an isothermal temperature of 150* ***(A)*** *and 200°C* ***(B)****.*

From the non-isothermal experiment, we have noticed that 150°C is the starting temperature for the formation for as well *cis* as *trans* double bonds. At this temperature, no *cis-trans* isomerisation occurs, which is also visible in Figure V.4.A. At 150°C, there is an increase in the absorbance at 858 and 956 cm^{-1}, which means that at this temperature both *cis* and *trans* double bonds are

formed. From the non-isothermal experiment, we have also noticed that 200°C is the starting temperature for the *cis-trans* isomerisation. Figure V.4.B confirms that, because at an isothermal temperature of 200°C, the absorbance of the *cis* double bond decreases and after 5 hours at 200°C almost no *cis* double bonds are present in the conjugated polymer anymore. It became clear that an all-*trans* PPV polymer is obtained after 5 hours at 200°C instead of 15 hours or more at 250°C like often mentioned in literature [6].

In-situ UV-Vis spectroscopy measurements were carried out on film, spincoated on quartz. The heating set-up was identical as for the FT-IR measurements and a non-isothermal heating program of 2°C/min from ambient temperature up to 380°C under a continuous flow of nitrogen was used. Before heating, an absorption band from the xanthate precursor polymer (**6)** is present (λ_{max} at 287 nm). As the heating program progressed, a new absorption band appeared that red-shifts with increasing temperature (Figure V.5).

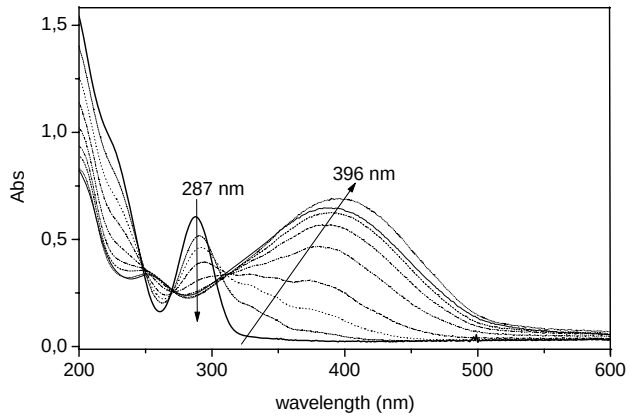

Figure V.5: *UV-Vis spectra of the gradual formation of the conjugated structure at a few selected temperatures (35, 160, 170, 180, 185, 195, 230 and 270°C).*

At higher temperatures, the fine structure disappears and the absorption band broadens to cover the various oligomer bands. At 270°C, the absorption reaches its maximum and a conjugated PPV polymer with a λ_{max} around 396 nm is obtained. This peak maximum is blue-shifted compared to a

PPV polymer prepared via the sulphinyl precursor route [4] (Figure II.10). This result may point to the fact that the PPV prepared via the xanthate precursor route has more chemical defects present in the structure compared to the sulphinyl prepared PPV.

When the absorbance at 396 nm is plotted versus increasing temperature shown in Figure V.6, it is clear that the absorption spectrum develops in two steps, a first step between 150 and 195°C (fast) leading to a λ_{max} value of 386 nm and a second step between 195 and 270°C (slower) which yields a final value of λ_{max} equal to 396 nm. The first step coincides with the decrease in IR absorbance of the xanthate group (λ_{max} at 287 nm), and this indicates that upon elimination of the xanthate group the "effective conjugation length" is limited by the simultaneous formation of *cis* and *trans* double bonds in the backbone of the conjugated system. The second step leads to an increase of "effective conjugation length" demonstrated by the red shift of λ_{max} and coincides with the decrease in IR absorbance of the *cis* double bonds. This is consistent with the interpretation from the IR data that a *cis-trans* isomerisation is responsible for the decrease of the *cis* double bond absorbance in IR in the temperature range from 195 up to 270°C.

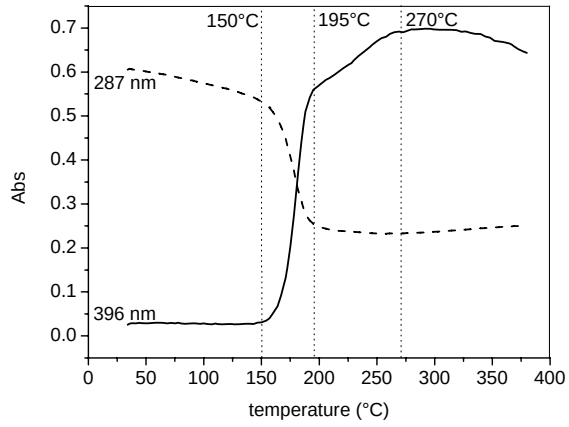

Figure V.6: *Absorbance at 287 and 396 nm versus temperature.*

ThermoGravimetric Analysis (TGA) was carried out at a heating rate of 10°C/min in argon atmosphere. The sample was heated from ambient temperature up to 600°C. The TGA thermogram of the xanthate precursor polymer (**6**) is shown in Figure V.7. Two major steps of weight loss are visible, the first (180-330°C) is due to the elimination of the xanthate group and evaporation of the elimination products. The second period of weight loss (520-600°C) accounts for the degradation of the polymer backbone.

The elimination was also studied by DIP-MS, with an identical heating rate of 10°C/min (as used in TGA experiments) under vacuum conditions (10^{-6} mmHg), to analyse the elimination products. For this technique, the precursor polymer is placed directly on the heating element of the probe. By plotting the total ion current versus temperature, the thermal stability of both precursor and conjugated polymer becomes visible (Figure V.7).

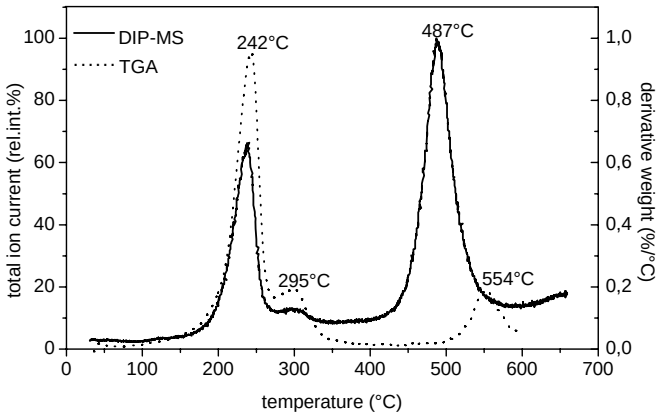

Figure V.7: *TGA thermogram (dotted line) and DIP-MS thermogram (solid line) of the xanthate precursor polymer (**6**).*

Two signals were observed, one can be assigned to an elimination step (184-330°C), the other one to a degradation step (420-565°C). There is no difference in elimination temperature observed in TGA (nitrogen atmosphere) and DIP-MS (vacuum), e.g. maximum at 242°C. This implies that at this temperature, the elimination products that are liberated will evaporate immediately, even in a nitrogen atmosphere under normal pressure. These TGA

and DIP-MS data for the xanthate precursor polymers differ from those obtained for sulphinyl precursor polymers because the elimination reaction itself and the evaporation of the elimination products are kinetically separated in the latter [15] (Figure II.2, II.3). The elimination temperature observed with these techniques is higher than that obtained from the *in-situ* UV-Vis and *in-situ* FT-IR results. This difference is attributed to the difference in heating rate. The fragments analysed by MS correspond to the ones of the expected elimination products (Table V.2).

Table V.2: *Mass fragments of the elimination products.*

DIP-EI (**6**) (max.at 242°C)		DIP-EI (**7**) (max. at 124°C)		DIP-EI (**7**) (max.at 234°C)	
m/z	fragment	*m/z*	fragment	*m/z*	fragment
105	$CH_3CH_2CS_2^+$	290	$C_8H_{17}SSC_8H_{17}^+$	322	$C_8H_{17}S(O)_2SC_8H_{17}^+$
91	CS_2O^+	194	$SS(O)C_8H_{17}^+$	178	$HO_2SC_8H_{17}^+$
76	CS_2^+	161	$S(O)\ C_8H_{17}^+$	145	$SC_8H_{17}^+$
60	COS^+	145	$SC_8H_{17}^+$		
45	$CH_3CH_2O^+$				
44	CS^+				

V.C.2 Thermal conversion of the sulphinyl precursor polymer 7

The study of the thermal elimination and stability of precursor polymer **7** shows quite different results because here a sulphinyl group is eliminated to yield the double bond. In general much lower temperatures are needed to convert a sulphinyl precursor polymer to the conjugated structure compared to the xanthate precursor polymer [16]. As mentioned earlier, GPC showed that precursor polymer **7** is an oligomer and the elimination and stability behaviour of oligomers may be somewhat different from that of the corresponding polymers [17]. Indeed, in oligomer **7** a relatively large percentage of the sulphinyl groups acts as end groups, this allows to study the thermal stability behaviour of such sulphinyl end groups compared to the sulphinyl groups in the internal part of the oligomer backbone.

A first technique that was used to study the elimination and stability of oligomer **7** was DIP-MS. Three signals are observed in the thermogram, which are shown in Figure V.8. The first signal (76-167°C) can be assigned to the elimination of the sulphinyl groups in the oligomer main chain that form the double bonds. The fragments analysed by DIP-MS correspond to the expected thiosulphonate and disulphide elimination products (Table V.2). The second signal (174-276°C), based on the fragments detected, is probably caused by the thermolysis of the sulphinyl groups at the end of the oligomer chain. Although similar fragments are observed, these two processes must chemically proceed via totally different mechanisms. Furthermore, out of the data, a kinetic separation between them is possible. The third signal (400-550°C) in the thermogram accounts for the decomposition of the conjugated system.

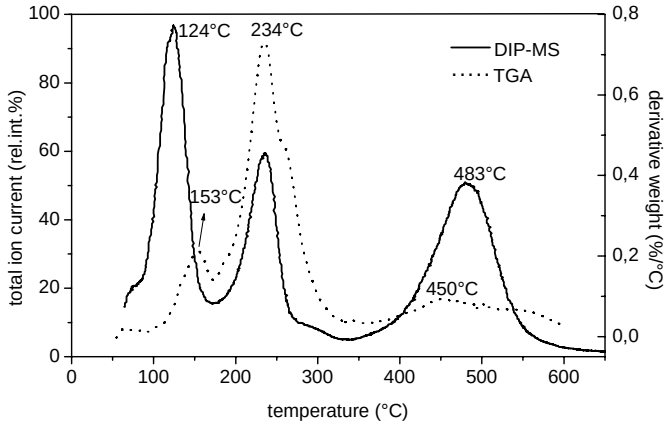

Figure V.8: *TGA thermogram (dotted line) and DIP-MS thermogram (solid line) of the sulphinyl oligomer (7).*

In TGA also three signals are present, also depicted in Figure V.8. A first one with a maximum at 153°C is caused by the evaporation of the elimination products. This signal appears at a higher temperature compared to the corresponding signal in DIP-MS (124°C) because of the difference in atmosphere used in both techniques (vacuum in DIP-MS and argon flow at normal pressure in TGA). A second signal in TGA with a maximum at 234°C is assigned to the thermolysis of the sulphinyl end groups, based on the data in DIP-MS. This implies that the products that are liberated at this temperature will evaporate immediately. The third signal at higher temperatures corresponds to the degradation of the conjugated polymer.

The thermal stability of oligomer **7** was also studied with *in-situ* FT-IR spectroscopy. A non-isothermal experiment was carried out at 2°C/min from ambient temperature up to 275°C under a continuous flow of nitrogen. In Figure V.9, the IR spectra at 4 different temperatures (60, 100, 175 and 250°C) are shown. At 60°C, the main absorptions arise from the sulphinyl stretching (1043 cm^{-1}) and from stretchings in the aliphatic region (2750-3000 cm^{-1}). When higher temperatures are reached, both these absorptions decrease strongly and a new absorption at 963 cm^{-1} appears, which can be assigned to the *trans* vinylene double bond. In this case, as in high molecular weight sulphinyl precursor polymers, no *cis* double bonds could be observed [15]. At 175°C, the sulphinyl absorption has disappeared completely and a new absorption peak appears at 1696 cm^{-1}, which may correspond to the formation of aromatic aldehydes [18].

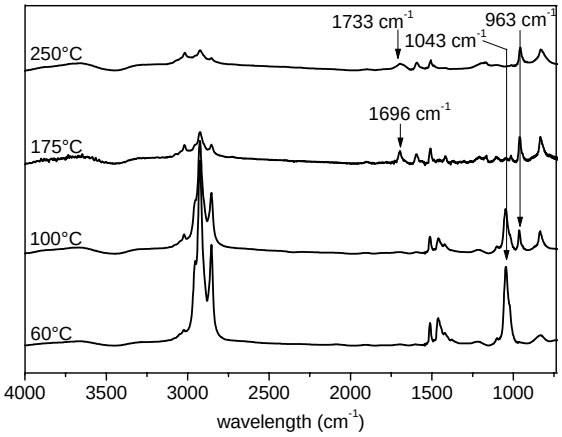

Figure V.9: *FT-IR spectra of the sulphinyl oligomer (**7**) at 60, 100, 175 and 250°C.*

When the absorbance of these absorption peaks are plotted versus increasing temperature, the trends in elimination behaviour of oligomer **7** become clear, as is demonstrated in Figure V.10.

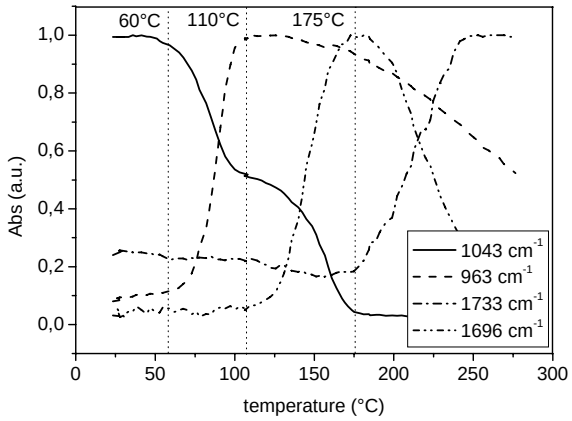

Figure V.10: *The absorbance at 1043, 963, 1733 and 1696 cm^{-1} versus temperature.*

The absorbance of the sulphinyl absorption (1043 cm^{-1}) decreases in two distinct steps. The first decrease takes place in a temperature domain between 60 and 100°C and is caused by the elimination of the sulphinyl groups in the oligomer main chain as it coincides with the increase in the absorbance of the *trans* vinylene double bond at 963 cm^{-1}, between 70 and 110°C. The second step in the decrease of the IR absorbance of the sulphinyl absorption occurs between 130 and 175°C. This second decline does not give rise to additional double bonds and thus has to originate from the thermolysis of the sulphinyl end groups. Note that the main chain sulphinyl groups and the sulphinyl end groups have similar intensities, which again suggests that both sulphinyl groups are present for approximately an equal amount. As mentioned earlier, this was also confirmed by ^{13}C-NMR spectroscopy. Furthermore, between 130 and 175°C the absorbance for the carbonyl stretching (1696 cm^{-1}) increases. This observation may indicate that an unidentified number of sulphinyl end groups is converted to carbonyl functionalities. At higher temperatures (175°C) the absorbance at 1696 cm^{-1} again decreases and a new absorption band at 1733 cm^{-1} appears, which partially overlaps the absorption at 1696 cm^{-1} and probably corresponds to higher oxidised products. These 2 steps, which happen during the thermal treatment of oligomer **7** are also demonstrated in Figure V.11.

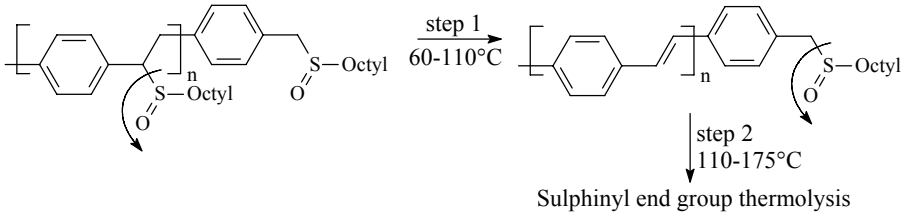

Figure V.11: *Elimination and thermolysis of the different sulphinyl groups in sulphinyl precursor oligomer* ***7****.*

Before commenting on the origin and the mechanism of formation of these carbonyl functionalities, we will discuss the results of the same experiment performed with *in-situ* UV-Vis spectroscopy, to further investigate the elimination behaviour. A non-isothermal heating program of 2°C/min up to 270°C under a continuous flow of nitrogen was used. Before heating, an absorption band at 324 nm is present from the precursor oligomer. After heating up to 270°C, a conjugated oligomer with a λ_{max} at 351 nm is obtained. When the absorption at this maximum wavelength is plotted versus temperature, two steps can be visualised in the elimination process, shown in Figure V.12. Between 60 and 110°C, the sulphinyl groups in the oligomer main chain are eliminated and a conjugated oligomer with an absorption maximum at 339 nm is formed. Starting from 175°C, a second small increase in the absorbance can be observed and eventually the absorption maximum of 351 nm is reached.

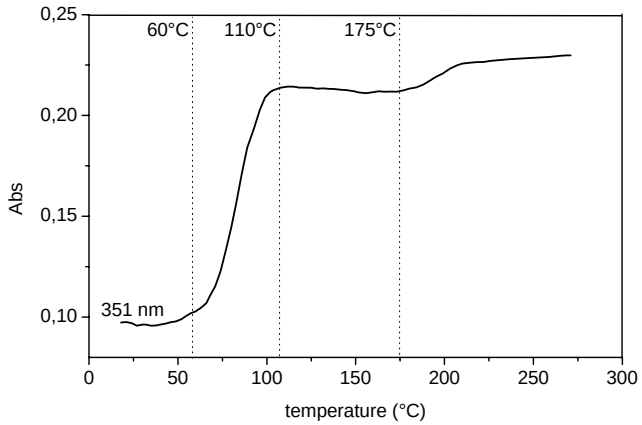

Figure V.12: *The absorbance at 351 nm versus temperature.*

Remember that it was clear from the previous FT-IR experiment that both the sulphinyl main chain as well as the sulphinyl end groups had been eliminated completely at 175°C. The second increase of the "effective conjugation length" observed in UV-Vis can therefore only be explained by a new subsequent process that follows the thermolysis of the sulphinyl end groups. Explaining the phenomena observed during the thermolysis of the sulphinyl end groups, was possible by combining literature data on thermal and/or photochemical conversion of sulphinyl functionalities in general [19,20,21] and what is known on the dimerisation and disproportionation behaviour of sulphenic acids [15]. Mislow *et al*. suggested the benzylic C-S bond to be notable weak in benzyl sulphinyl compounds [19,22]. At elevated temperatures this may result in homolytic cleavage and formation of a radical pair. The same cleavage was also observed in photochemical experiments on benzyl sulphinyl compounds [21]. These papers also report the presence of benzaldehyde upon thermolysis or photolysis of benzyl sulphinyl compounds. This explains the formation of aldehyde functionalities as observed in the FT-IR experiment in the temperature range domain between 110 to 175°C.

In order to clarify the second small increase in "effective conjugation length" observed in UV-Vis above 175°C, an additional experiment was set up in which we mimicked the thermal behaviour of the sulphinyl end groups, demonstrated in Figure V.13. To do so, a model compound **9** was heated at 200°C for 15 hours and the resulting reaction mixture was analysed by GC-MS. A complex reaction mixture resulted and products **15** to **23** were identified. Once the weak C-S bond is broken, the radicals formed (**10**, **11a-c**) can recombine to yield several reaction products. Product **15** clearly arises from radical coupling of two benzyl radicals. Combination of two sulphinyl radicals (**11b** and **11c**) results in the formation of the unstable product **12** which further disproportionates to form radicals **13** and **14**. Understanding the formation of benzaldehyde was possible by combining radicals **10** and **11c** to form the sulphenic ester **17**. Thermal decomposition of **17** can yield benzaldehyde **18** and thiol **19**. The other products in the reaction mixture arise from alternative recombination of the respective radicals. The observed stilbene (**16**) is presumed to be formed by oxidation of dibenzyl **15**. Probably radical **11c** acts as an oxidising agent in this reaction yielding a sulphenic acid and consequently also **22** and **23**. Extrapolation of this result toward the thermal behaviour of the oligomer **7** would lead to coupling of two oligomer chains followed by

oxidation and thus an extension of the "effective conjugated system" which can account for the observed red shift in UV-Vis spectroscopy at temperatures above 175°C, shown in Figure V.12.

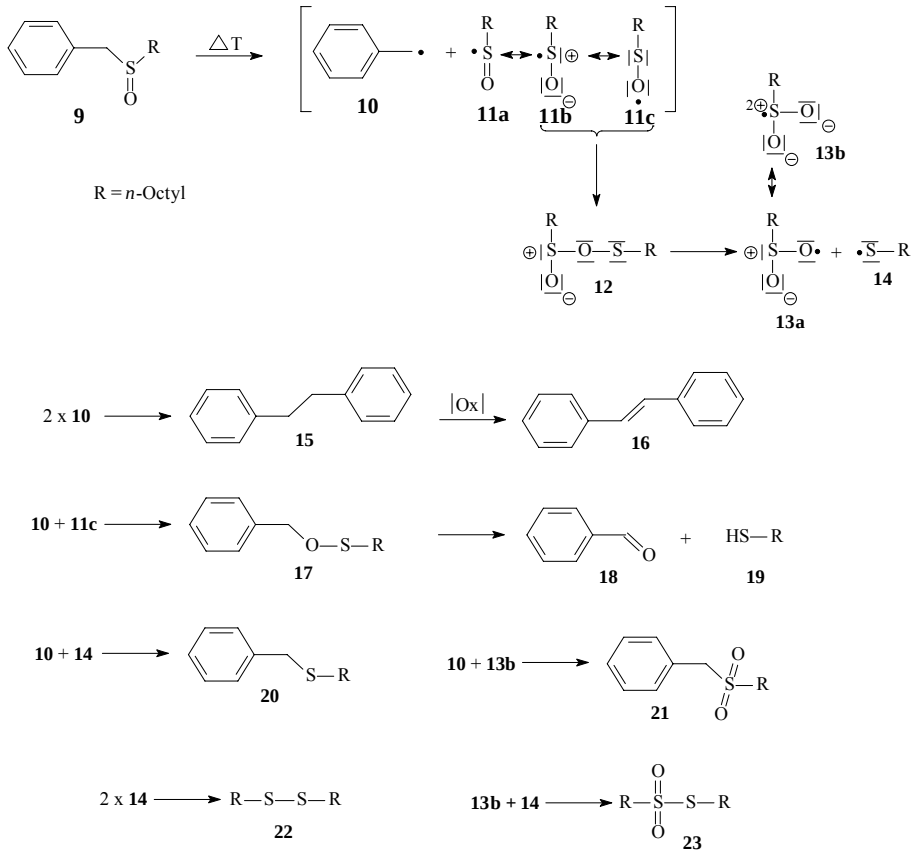

Figure V.13: *Schematic overview of the formation of products 15 to 23 upon homolytic cleavage of the C-S bond in compound 9.*

In order to demonstrate the kinetic separation in the elimination processes of the different sulphinyl groups present in oligomer **7**, an experiment was set up which should allow for the sulphinyl groups, that give rise to double bonds, to be eliminated selectively whereas the sulphinyl end groups are left unchanged. *In-situ* FT-IR spectroscopy was used to monitor the elimination process. In this experiment the sample was heated at 2°C/min up to 100°C, kept at this temperature for 3 hours and then heated further up to 300°C at 2°C/min. In Figure V.14, this temperature program is shown next to the absorbance

profiles for the *trans* double bond (956 cm^{-1}) and the sulphinyl groups (1043 cm^{-1}). At 100°C, all sulphinyl groups which give rise to double bonds have been eliminated and the absorbance of the *trans* vinylene double bond has reached its maximal absorption. During the isothermal stay at 100°C neither of these absorptions change. In the third part of the heating program (100 up to 300°C), the sulphinyl absorbance further declines. This second decrease in sulphinyl absorbance progressed without formation of additional double bonds and thus has to originate from the elimination of the sulphinyl end groups. At 175°C, both the main chain sulphinyl groups and the sulphinyl end groups have been eliminated completely from the oligomer.

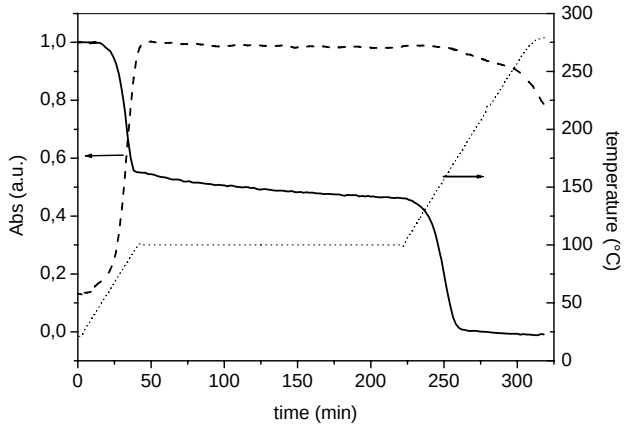

Figure V.14: *The absorbance at 963 cm^{-1} (dashed line) and 1043 cm^{-1} (solid line) as a function of time and temperature (dotted line).*

The selective elimination was further investigated on a sample of precursor oligomer **7** which was converted to the conjugated oligomer **8** by heating a thick precursor film for 3 hours at 100°C under vacuum. The resulting conjugated oligomer **8** still proved to be soluble in common organic solvents. The UV-Vis spectrum (in toluene) of this conjugated oligomer shows several maxima at different wavelengths (Figure V.15, solid line). These maxima probably arise from a distribution in conjugated chain lengths. The first maximum in the UV spectrum of the oligomer at 327 nm corresponds to that of *trans*-stilbene (328 nm). The other maxima at 341, 363 and 390 nm probably correspond to the larger conjugated systems were n is 2, 3 and 4 respectively.

These wavelengths are in the line of expectation when compared with the wavelengths of PPV oligomers synthesised previously [23]. When the sample was heated further till 270°C the sulphinyl end groups were removed and the conjugated oligomers became insoluble. A spectrum of the oligomer **8** in film after heating till 270°C is also shown in Figure V.15 (dash dotted line).

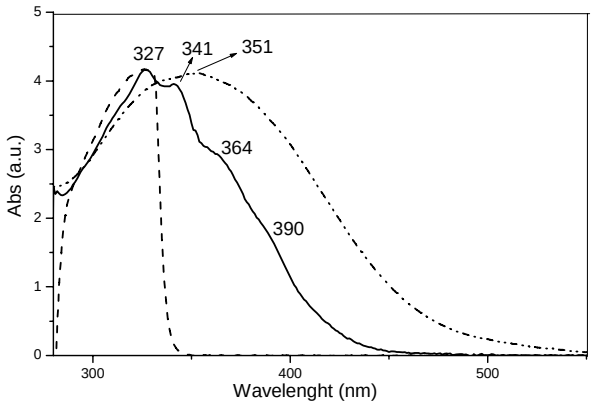

Figure V.15: *UV spectrum in toluene of the conjugated oligomer **8** (solid line) and trans-stilbene (dashed line) and the oligomer **8** in film after heat treatment till 270°C (dash dotted line).*

The selective elimination was also confirmed by ^{13}C-NMR spectroscopy. In the ^{13}C spectrum of the precursor oligomer **7** chemical shifts of several carbon atoms of the main chain sulphinyl groups slightly differ from those of the sulphinyl end groups. In Figure V.16, an enlarged part of the ^{13}C spectrum for both the precursor and the conjugated oligomer are shown. On the precursor stage, different signals can be observed which can be assigned from C1 to C5 [24]. In the conjugated structure only the two signals for the sulphinyl end groups C1 and C2 remain. All sulphinyl groups in the main chain have been eliminated and this results in the formation of a new ^{13}C signal at 127 ppm which is attributed to the carbon atoms of the double bond.

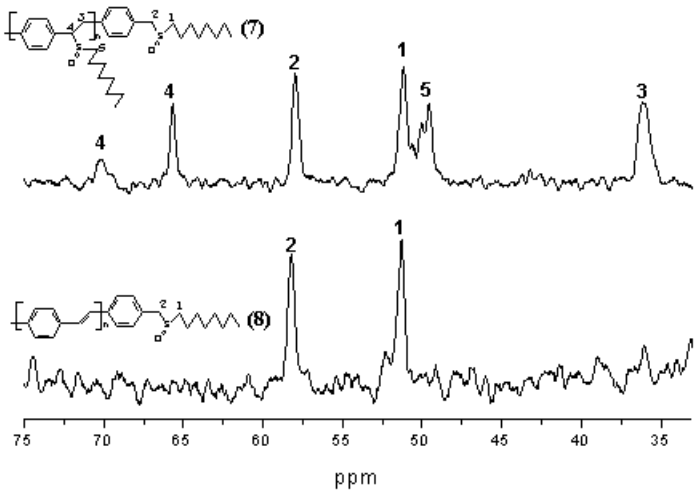

Figure V.16: *Enlarged part of the ^{13}C-NMR spectrum of the sulphinyl precursor oligomer **7** (upper) and the conjugated oligomer **8** (lower).*

V.D Conclusions

From these measurements it is concluded that elimination of the xanthate precursor polymer **6** towards a PPV polymer when performed beneath 195°C will lead to a mixed *cis-trans* configuration. To obtain an all *trans* PPV structure the conversion should be done at a temperature around 250°C. At both these temperatures all elimination products will immediately evaporate and degradation does not yet occur (Figure V.17).

The experiments concerning the elimination behaviour of precursor oligomer **7** clearly demonstrate that it is kinetically possible to separate the elimination of the main chain sulphinyl groups and thermolysis of the sulphinyl end groups in the oligomer chain. At lower temperatures the sulphinyl groups from the main chain are eliminated and the double bonds are formed. At higher temperatures thermolysis of the sulphinyl end groups occurs. Furthermore, above 175°C, we found indications that these sulphinyl end groups were partially converted to carbonyl functionalities or that two oligomer chains may couple, which after oxidation, leads to an extension of "effective conjugation length".

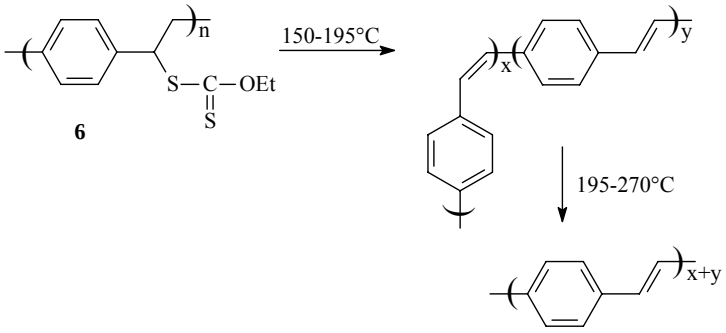

Figure V.17: *Schematical overview of the elimination reaction and cis-trans isomerisation of PPV prepared via the xanthate precursor route.*

V.E Experimental part

V.E.1 General remarks and instrumentation

All chemicals were purchased from Aldrich or Acros and used without further purification unless otherwise stated. Tetrahydrofuran (THF) was distilled over sodium/benzophenone.

^{1}H-NMR spectra were obtained in $CDCl_3$ at 300MHz on a Varian Inova Spectrometer using a 5 mm probe. Chemical shifts (δ) in ppm were determined relative to the residual $CHCl_3$ absorption (7.24 ppm). The ^{13}C-NMR experiments were recorded at 75 MHz on the same spectrometer using a 5 mm broadband probe. Chemical shifts were defined relative to the ^{13}C resonance shift of $CHCl_3$ (77.0 ppm). Molecular weights and molecular weight distributions were determined relative to polystyrene standards (Polymer Labs) with a narrow polydispersity by Size Exclusion Chromatography (SEC). Separation to hydrodynamic volume was obtained using a Spectra series P100 (Spectra Physics) equipped with a pre-column (5 μm, 50 mm*7.5 mm, guard, Polymer Labs) and two mixed-B columns (10 μm, 2x300 mm*7.5 mm, Polymer Labs) and a Refractive Index (RI) detector (Shodex) at 40°C. SEC samples are filtered through a 0.45 μm filter. HPLC grade THF (p.a.) is used as the eluent at a constant flow rate of 1.0 ml/min. Toluene is used as flow rate marker. The molecular weight of the sulphinyl precursor oligomers **7** was also measured on

a low-molecular weight column (5 μm, 300 mm*7.5 mm, 100Å, Polymer Labs). The results obtained from these measurements are nearly identical to those obtained on the high molecular weight column.

TGA measurements are performed on a TA instrument 951 thermogravimetric analyser with a continuous argon flow of 80 ml/min and a heating rate of 10°C/min. Samples of precursor polymer (10 mg) are inserted in the solid state.

Direct Insert Probe Mass Spectrometry analysis is carried out on a Finnigan TSQ 70, electron impact mode, mass range of 35-500. Electron energy is 70 eV. A $CHCl_3$ solution of precursor polymer is applied on the heating element of the direct insert probe. A similar heating rate of 10°C/min was used to ensure a good comparison with TGA data.

The *in-situ* elimination reactions were performed in a Harrick High Temperature cell (purchased from Safir), which is positioned in the beam of a Perkin Elmer spectrum one FT-IR spectrometer (nominal resolution 4 cm^{-1}, summation of 16 scans). The temperature of the sample is controlled by a Watlow (serial number 999, dual channel) temperature controller. The precursor polymer was spincoated from a $CHCl_3$ solution (6 mg/ml) on a KBr pellet at 500 rpm. The spincoated KBr pellet (diameter 25 mm, thickness 1 mm) is in direct contact with the heating element. All experiments were performed at 2°C/min under a continuous flow of nitrogen. "Timebase software" supplied by Perkin Elmer is used to investigate regions of interest.

The *in-situ* UV-Vis measurements were performed on a Cary 500 UV-Vis-NIR spectrophotometer, specially adapted to contain the Harrick High Temperature cell (scan rate 600 nm/min, continuous run from 200 to 600 nm). Precursor polymer (**6** or **7**) was spincoated from a $CHCl_3$ solution (6 mg/ml) on a quartz glass (diameter 25 mm, thickness 3mm) at 1000 rpm. The quartz glass was heated in a specially adapted Harrick High Temperature cell. The cell was positioned in the beam of the UV-Vis-NIR-spectrophotometer and spectra were taken continuously. The heating rate was 2°C/min up to 300°C. All measurements were performed under a continuous flow of nitrogen. "Scanning Kinetics software" supplied by Varian is used to investigate regions of interest.

V.E.2 Materials

V.E.2.a Synthesis of the monomers (2'-5)

Synthesis of 1,4-bis(tetrahydrothiopheniomethyl)xylene dichloride (1) and 1-(chloromethyl)-4-[(*n*-octylsulphinyl)methyl]benzene (2') These products were synthesised according to a procedure described elsewhere [11].

Synthesis of 1,4-bis[ethoxy(thiocarbonyl)thiomethyl]benzene (3) This monomer was prepared by stirring a solution of 1,4-bis(chloromethyl)benzene (2.5 g, 0.0143 mol) and *O*-ethoxyxanthic acid potassium salt (5 g, 0.03125 mol) in methanol (50 ml) for 2 hours at room temperature. The reaction mixture was poured into water and the aqueous solution was extracted with chloroform and dried over magnesium sulphate. The filtrate was concentrated in vacuum and recrystallised from chloroform/hexane (10/90) and yielded product **3** as white needles. (4.7 g, yield: 95%). ^{1}H-NMR ($CDCl_3$,300 MHz): δ 7.27 (4H, s), 4.63 (4H, q, J =7.2 Hz), 4.32 (4H, s), 1.40 (6H, t, J =7.2 Hz) ppm; ^{13}C-NMR ($CDCl_3$, 75 MHz): δ 135.36, 129.53, 70.35, 40.22, 14.01 ppm; UV-VIS (λ_{max}, CH_2Cl_2): 356 nm; m.p.: 57.2-58°C; FT-IR (KBr): 2980 (ν_{C-H} aliph.), 1510-1397 (ν_{C-H} CH_3,CH_2), 1251 (*p*-phenylene C-H out of plane bend), 1217-1107-1048 ($\nu_{SC(S)OCH2CH3}$), 688 (ν_{C-S}) cm^{-1}.

Synthesis of [1-ethoxy(thiocarbonyl)thiomethyl-4-(chloromethyl)]benzene (4) NatBuO (1.83 g,19 mmol) and *O*-ethoxyxanthic acid potassium salt (2.96 g, 19 mmol) were stirred in methanol (40 ml) for 30 minutes at room temperature. The clear solution was added in one portion to a stirred solution of 1,4-bis(tetrahydrothio pheniomethyl)xylene dichloride (**1**) (10 g, 19 mmol) in methanol (100ml). After one hour the reaction mixture was neutralised with aqueous HCl (1 M) and concentrated in vacuum. The crude product was diluted with chloroform (200 ml) and the precipitate was filtered off. The filtrate was concentrated and *n*-octane (75 ml) was added. The *n*-octane was concentrated in vacuum to remove tetrahydrothiophene. This sequence was repeated three times. The reaction mixture was purified using column chromatography (SiO_2, eluent: $CHCl_3$/hexane 50/50). (yield: 75%). ^{1}H-NMR ($CDCl_3$, 300 MHz): δ 7.32 (2H, s), 7.27 (2H, s), 4.60-4.67 (2H, q, *J* = 7.2 Hz), 4.55 (2H, s), 4.34 (2H, s), 1.38-1.42 (3H, t, *J* =7.2 Hz) ppm; ^{13}C-NMR ($CDCl_3$, 75MHz): δ 137.87 (1C),

135.37 (1C), 129.53 (2C), 129.16 (2C), 70.39 (1C), 45.91 (1C), 40.18 (1C), 14.00 (1C) ppm; UV-VIS (λ_{max}, CH_2Cl_2): 353 nm; m.p.: 114.7-116°C; FT-IR (KBr): 2980 (ν_{C-H} aliph.), 1510-1397 (ν_{C-H} CH_3,CH_2), 1251 (*p*-phenylene C-H out of plane bend), 1217-1107-1048 ($\nu_{SC(S)OCH2CH3}$) ,688 (ν_{C-S}) cm^{-1}.

Synthesis of 1-((*n*-octylsulphinyl)methyl)-4-(ethoxy(thiocarbonyl)thio methyl)benzene (5) *O*-ethoxyxanthic acid potassium salt (1.5 eq) was added portion wise to a solution of 1-(chloromethyl)-4-[(*n*-octylsulphinyl) methyl] benzene (prepared as reported earlier) [13] (2 g, 6.6 mmol) in methanol (50 ml). The mixture was stirred for 12 hours at room temperature. The reaction mixture was poured into water and extracted three times with chloroform. The organic layer was dried over magnesium sulphate and concentrated in vacuum to yield the pure product (**4**). (2.42 g, yield: 95%). ^{1}H-NMR ($CDCl_3$, 300 MHz): δ 7.32 (2H, d, *J* = 8.4 Hz), 7.20 (2H, d, *J* = 8.4 Hz), 4.61 (2H, q, *J* = 7.2 Hz), 4.32 (2H, s), 3.90 (2H, dd, *J* = 13.2 Hz), 2.52 (2H, t, *J* = 7.8 Hz), 1.70 (2H, m), 1.38 (3H, t, *J* = 7.2 Hz), 1.22 (10H, s(br)), 0.83 (3H, t, *J* = 6.9 Hz) ppm; ^{13}C-NMR ($CDCl_3$, 75MHz): δ 136.28 (1C), 130.46 (1C), 129.85 (2C), 129.51 (2C), 70.42 (1C), 58.02 (1C), 51.26 (1C), 40.16 (1C), 31.92 (1C), 29.37 (1C), 29.21 (1C), 29.04 (1C), 22.82 (1C), 22.68 (1C), 14.30 (1C), 14.01 (1C) ppm; UV-VIS (λ_{max}, CH_2Cl_2): 355 nm; m.p.: 81.4-82.8°C; FT-IR (KBr): 2957-2918-2849 (ν_{C-H} aliph.), 1511-1486-1419 (ν_{C-H} CH_3,CH_2), 1211-1117-1071 ($\nu_{SC(S)OCH2CH3}$), 1056-1025 (ν_{S-O}), 849 (1,4-subst.arom.) cm^{-1}.

V.E.2.b Synthesis of the precursor polymer (6 and 7)

All polymerisations were carried out under the same conditions in dry tetrahydrophuran (THF, dried over sodium with benzophenon) at different temperatures (Table V.1). Solutions of monomer (1 mmol in 6.5 ml THF) and base (potassium-*tert*-butoxide; 1.05 mmol in 3.5 ml THF) were prepared and degassed for 1 hour by a continuous flow of nitrogen. The base solution was added in one portion to the stirred monomer solution. During the reaction the temperature was kept constant and the passing of nitrogen was continued. After 1 hour the reaction mixture was poured into well stirred ice water whereupon the polymer precipitated. The water layer was extracted with chloroform to ensure that all polymer and residual fraction was collected, and the combined organic fractions were concentrated in vacuum. The polymer was precipitated in cold diethylether/hexane (1/1; 100 ml; 0°C), collected by filtration and dried in

vacuum. GPC was performed in THF versus polystyrene standards. Polymerisation results are summarised in Table V.1. The rest fractions only contain monomer residues.

Precursor polymer 6: ^{1}H-NMR ($CDCl_3$, 300 MHz): δ 6.90-6.99 (4H), 4.79 (1H), 4.51 (2H), 3.27 (1H), 3.05 (1H), 1.29 (3H) ppm;^{13}C-NMR ($CDCl_3$, 75 MHz): δ 213.97 (1C), 137.68-137.35 (2C), 129.27 (2C), 127.88 (2C), 69.78 (1C), 55.28 (1C), 41.97 (1C), 13.67 (1C) ppm; FT-IR (KBr): 2980, 1510, 1397, 1251, 1217, 1107, 1048, 688 cm^{-1}.

Precursor oligomer 7: ^{1}H-NMR ($CDCl_3$, 300 MHz): δ 6.80-7.50 (4H), 3.25-3.99 (2H), 2.39-2.78 (1H), 1.95-2.23 (2H), 1.45-1.75 (2H), 1.11-1.42 (10H), 0.75-0.9 (3H) ppm; ^{13}C-NMR ($CDCl_3$, 75 MHz): δ 137.87, 130.10, 129.66, 129.30, 128.88, 128.58, 126.48, 70.02, 65.32, 57.67, 50.89, 49.65, 49.27, 36.02, 31.51, 28.97, 28.80, 28.69, 22.84, 22.40, 13.92 ppm; FT-IR (KBr): 2957, 2918, 2849, 1511, 1486, 1419, 1056, 1025 cm^{-1}.

Conjugated oligomer 8: This compound was made from the precursor oligomer **7** by heating a film of **7** (30 mg in 2 ml $CHCl_3$ and allow the chloroform to evaporate) at 100°C for 3 hours under vacuum. ^{13}C-NMR ($CDCl_3$, 75 MHz): δ 137.45, 130.42, 129.08, 127.01, 57.99, 50.92, 31.76, 29.21, 29.04, 28.87, 22.65, 22.46, 14.14 ppm; FT-IR (KBr): 3025, 1511, 956, 858, 834 cm^{-1}; UV-Vis spectra of the conjugated oligomer **8** were taken in toluene at room temperature (λ_{max} at 327, 341, 364 and 390 nm). For comparison, the spectrum of *trans*-stilbene (purchased from Aldrich and used as received) was also taken in the same conditions (λ_{max}= 328 nm).

V.F References

[1] J.H. Burroughes, D.D.C. Bradley, A.R. Brown, R.N. Marks, R.H. Friend, A.B. Holmes, *Nature,* 347 **(1990)** 539.

[2] R.A. Wessling, *J. Polym. Sci., Polym. Symp*., 72 **(1985)** 55.

[3] H.G. Gilch, W.L. Wheelwright, *J. Polym. Sci. Part A: Polym. Chem*., 4 **(1966)** 1337.

[4] F. Louwet, D. Vanderzande, J. Gelan, J. Mullens, *Macromolecules,* 28 **(1995)** 1330.

[5] S. Son, A. Dodabalapur, A.J. Lovinger, M.E. Galvin, *Science*, 269 **(1995)** 376.

[6] S.-C. Lo, L.-O. Palsson, M. Kilitziraki, P.L. Burn, I.D.W. Samuel, *J. Mat. Chem*., 11 **(2001)** 2228.

[7] D. Vanderzande, A. Issaris, M. Van Der Borght, A. van Breemen, M. de Kok, J. Gelan, *Macromol. Symp*., 125 **(1997)** 189.

[8] S. Gillissen, M. Jonforsen, E. Kesters, T. Johansson, M. Theander, M.R. Andersson, O. Inganäs, L. Lutsen, D. Vanderzande, *Macromolecules,* 34 **(2001)** 7294.

[9] S.-C. Lo, A. Sheridan, I.D.W. Samuel, P.L. Burn, *J. Mat. Chem*., 9 **(1999)** 2165.

[10] S.-C. Lo, A. Sheridan, I.D.W. Samuel, P.L. Burn, *J. Mat. Chem.,* 10 **(2000)** 275.

[11] A. van Breemen, D. Vanderzande, P. Adriaensens, J. Gelan, *J. Org. Chem*., 64 **(1999)** 3106.

[12] D. Van Den Berghe *Internal communication.*

[13] G.A. Keil, Y. Liszewski, Y. Peng, B. Hsieh, *Polymer Preprints,* 41 **(2000)** 826.

[14] G.A. Keil, Y. Liszewski, J. Wilking, B. Hsieh, *Polymer Preprints,* 42 **(2001**) 306.

[15] M.M. de Kok, A.J.M.M. van Breemen, R.A.A. Carleer, P.J. Adriaenssens, D.J. Vanderzande, *Acta Polym.,* 50 **(1999)** 28.

[16] E. Kesters, L. Lutsen, D. Vanderzande, J. Gelan, *Synthetic Metals,* 119 **(2001)** 311.

[17] E. Kesters, L. Lutsen, D. Vanderzande, J. Gelan, T.P. Nguyen, P. Molinié, *Thin Solid Films*, 120 **(2002)** 403.

[18] N.B. Colthup, L.H. Daly, S.E. Wiberley, *Introduction to Infrared and Raman Spectroscopy*, 3 rd. ed., Academic, San Diego, **(1990)** p. 289.

[19] E.G. Miller, D.R. Rayner, H.T. Thomas, K. Mislow, *J. Amer. Chem. Soc.,* 90 **(1968)** 4861.

[20] D.G. Barnard-Smith, J.F. Ford, *Chem. Commun.*, **(1965)** 120.

[21] Y. Guo, W.S. Jenks, *J. Org. Chem.,* 60 **(1995**) 5480.

[22] K. Mislow, M. Axelrod, D.R. Rayner, H. Gotthardt, L. Coyne, G.S. Hammond, *J. Amer. Chem. Soc.,* 87 **(1965)** 4958.

[23] K. Müllen, G. Wagner, Wiley-VCH, *Electronic Materials: The Oligomer Approach,* Weinheim Germany, **(1998)** p.58.

[24] A.J.J.M. van Breemen, M.M. de Kok, P.J. Adriaenssens, D.J. Vanderzande, J. Gelan, *Macromolec. Chem. Phys.,* 2 **(2001)** 202.

Summary

In this work, the possibilities of *in-situ* analytical techniques (TGA, DIP-MS, FT-IR spectroscopy, UV-Vis spectroscopy and MTDSC) are exploited to study the elimination process of different precursor polymers towards conjugated materials. The stability of the conjugated polymers is also investigated with these *in-situ* techniques.

In Chapter I the background of conjugated polymers was described and an overview was given of known precursor routes to PPV, including their elimination behaviour.

In Chapter II the elimination and degradation reaction of *n*-alkyl-sulphinyl PPV (precursor) polymers with *in-situ* spectroscopic techniques is presented. The method to follow the elimination reaction with *in-situ* FT-IR and UV-Vis spectroscopy is explained in this chapter. From *in-situ* FT-IR and UV-Vis experiments, we can conclude that the elimination reaction starts around 65°C in nitrogen flow (heating rate: 2°C/min). In case of larger aliphatic chains on the eliminable group, a kinetic separation occurs between the elimination reaction and the evaporation of the elimination products. The PPV polymer remains stable up to 350°C. Above that temperature, degradation occurs, implying that the "effective" conjugation length irreversibly decreases. PPV can also be formed out of the thermal conversion of sulphonyl PPV precursor polymers. However, the PPV that is prepared from an *n*-alkyl-sulphonyl PPV

precursor polymer has optical properties which are quite different from the PPV derived from the phenyl-sulphonyl PPV precursor polymer. The *n*-alkyl derivative, yields a PPV with large amounts of structural defects which give rise to a restricted "effective" conjugation length. The phenyl derivative however, yields PPV which is almost identical to PPV obtained from sulphinyl precursors. In Chapter II also the modification of sulphinyl groups was presented. Oxidation leads to sulphonyl functionalities, which show a different thermal behaviour in comparison with sulphinyl functionalities. Because the modified groups are thermally more stable than sulphinyl groups, these groups can be eliminated selectively. The synthesis of poly (thienylene vinylene) (PTV) polymers with varying extents of conjugation was achieved by selective elimination of the sulphinyl groups from a PTV precursor copolymer that contains a random distribution of sulphinyl and sulphonyl groups. These sulphonyl groups function as sp^3-defects in the conjugated material. This method provides a new tool for tuning the material properties.

In Chapter III the elimination and degradation behaviour of the OC_1C_{10}-PPV polymer was studied with TGA, DIP-MS, *in-situ* FT-IR and UV-Vis spectroscopy. The OC_1C_{10}-PPV polymer, soluble before and after elimination, can be synthesised via the Gilch and sulphinyl route. We have demonstrated that the *in-situ* FT-IR experiments are reproducible. We also have observed that the thickness of the polymer film does not have an influence on the elimination reaction itself, whereas the evaporation of the elimination products is dependent on the thickness of the polymer film. Non-isothermal heating experiments at different heating rates, yield a valuation for the activation energy of the conversion reaction. The elimination reaction of the *n*-alkyl-sulphinyl OC_1C_{10}-PPV precursor polymers starts around 70°C in nitrogen flow (heating rate: 2°C/min). At 110°C (after elimination) an absorption maximum at 490 nm is obtained for the conjugated OC_1C_{10}-PPV polymer. The corresponding effective conjugation length decreases again, by degradation of the conjugated system at 230°C. After elimination, a certain amount of elimination products, which are set free during the elimination reaction, remain in the polymer matrix, while in pure PPV (without alkoxy chains), the elimination products are ejected more extremely from the polymer matrix. When the elimination reaction is performed in vacuum conditions (10^{-2} mmHg), the elimination reaction shifts to a lower temperature (53-95°C). In these vacuum conditions also the elimination products diffuse and evaporate better

out of the polymer matrix. The smaller the alkyl chain, the lower the boiling point of the elimination products, the more easy for the elimination products to evaporate or to diffuse out of the polymer matrix.

In the first part of Chapter IV the kinetics of the conversion reaction of *n*-octyl-sulphinyl OC_1C_{10}-PPV polymer was described. From isothermal elimination reactions studied with *in-situ* FT-IR and UV-Vis spectroscopy, an activation energy (E_A) of 100 kJ/mol and 92 kJ/mol was obtained respectively. This experimental E_A value is in good agreement with the E_A value theoretical calculated for the conversion reaction to *trans*-stilbene (104.6 kJ/mol). In a second part of Chapter IV, MTDSC is used to study the elimination process of the *n*-alkyl-sulphinyl OC_1C_{10}-PPV precursor polymers and TGA is used to study the diffusion and evaporation of the elimination products. From a combination of isothermal and non-isothermal MTDSC experiments in solid state, we could say that the elimination process is a combination of consecutive reaction steps. The different reactions of the elimination process are very difficult to separate. Unfortunately, in MTDSC no criterion is obtained which is directly related to the elimination reaction. The disproportionation reaction occurs in a temperature range between 85 and 135°C. After 150°C, side reactions occur through interactions of the elimination products with the conjugated polymer, that causes network formation. Since network formation could occur, it is better to do the elimination reaction at relative low temperatures (< 120°C) and in solution. Reaction heats are normally visible in the NR-heat flow signal. Studying the elimination process in isothermal conditions, no clear heat effect is visible in the NR-heat flow. Therefore, the change in heat capacity is used to follow the different reactions of the elimination process. The change in heat capacity is mainly due to the formation of water, but also to the formation of elimination products. Till now, no real kinetic parameters are obtained from these measurements. In the near future, it is the intention to do some modelling on these isothermal experiments in solid state to get some idea of the kinetics of the conversion reaction. We also have studied the elimination process in solution (toluene / chlorobenzene) with MTDSC. In (non)-isothermal MTDSC measurements, an indication for phase-separation is obtained. The non-isothermal MTDSC measurements show that phase-separation between polymer-solvent systems could be measured as a small baseline shift in the heat capacity signal. Performing such MTDSC heating-cooling experiments over a large concentration range allows in

principle the construction of the phase diagram. From isothermal TGA experiments, the diffusion of the elimination products out of the polymer matrix is studied. A smaller alkyl group, a higher isothermal temperature and a thinner polymer film promote the diffusion of the elimination products.

In Chapter V the polymerisation behaviour of xanthate containing monomers towards PPV precursor polymers was investigated. After the synthesis of these precursor polymers also the elimination behaviour was studied with TGA, DIP-MS, *in-situ* FT-IR and UV-Vis spectroscopy. The elimination of a xanthate precursor polymer towards a conjugated PPV polymer when performed beneath 195°C will lead to a mixed *cis-trans* configuration. To obtain an all-*trans* PPV structure the conversion should be done at a temperature around 250°C. At both these temperatures all elimination products will immediately evaporate and degradation does not yet occur. The experiments concerning the elimination behaviour of the *n*-octyl-sulphinyl precursor oligomer clearly demonstrate that it is kinetically possible to separate the elimination of the main chain sulphinyl groups and thermolysis of the sulphinyl end groups in the oligomer chain. At lower temperatures the sulphinyl groups from the main chain are eliminated and the double bonds are formed. At higher temperatures thermolysis of the sulphinyl end groups occurs. Furthermore, above 175°C, we found indications that these sulphinyl end groups were partially converted to carbonyl functionalities or that two oligomer chains may couple, which after oxidation, leads to an extension of “effective conjugation length”.

Samenvatting

In dit doctoraatswerk worden de mogelijkheden van *in-situ* analytische technieken (TGA, DIP-MS, FT-IR spectroscopie, UV-Vis spectroscopie en MTDSC) aangewend om de eliminatie reactie van verschillende precursor polymeren naar geconjugeerde materialen te bestuderen. Deze *in-situ* technieken worden eveneens gebruikt om de stabiliteit van de geconjugeerde polymeren te onderzoeken.

In hoofdstuk I wordt de achtergrond van geconjugeerde polymeren beschreven en wordt een overzicht gegeven van de verschillende precursor routes voor de synthese van PPV, inclusief het mechanisme van de eliminatie reactie voor de verschillende precursor polymeren naar PPV.

In hoofdtuk II worden de *in-situ* FT-IR en UV-Vis spectroscopie technieken uitgebreid uitgelegd. De eliminatie en degradatie reactie van *n*-alkyl-sulfinyl PPV (precursor) polymeren worden bestudeerd met deze *in-situ* spectroscopische technieken. De eliminatie reactie start rond 65°C in stikstof atmosfeer (opwarmsnelheid: 2°C/min). In het geval van een *n*-alkyl-sulfinyl elimineerbare groep met een lange alifatische groep (*n*-octyl) stellen we een kinetische scheiding vast tussen de eliminatie reactie enerzijds en de verdamping van de eliminatie producten anderzijds. Het geconjugeerde PPV polymeer blijft stabiel tot een temperatuur van ~ 350°C. Vanaf 350°C zal de degradatie reactie optreden van het geconjugeerde polymeer, hetgeen gepaard

gaat met een irreversibele afname in de effectieve conjugatie lengte. Het is ook mogelijk om PPV te bekomen uitgaande van de thermische conversie van sulfonyl ($S(O)_2$) PPV precursor polymeren. Nochtans, het PPV dat verkregen wordt vanuit een *n*-alkyl-sulfonyl PPV precursor polymeer bevat optische eigenschappen die sterk verschillen van het PPV dat verkregen wordt na conversie van het fenyl-sulfonyl PPV precursor polymeer. Het *n*-alkyl-derivaat levert een PPV op met grote hoeveelheden structurele defecten die aanleiding geven tot een beperkte effectieve conjugatie lengte. Het fenyl-derivaat daarentegen levert een PPV op dat bijna identiek is aan het PPV dat verkregen wordt vertrekkende van *n*-alkyl-sulfinyl PPV precursoren. In hoofdstuk II wordt ook de modificatie van sulfinyl groepen beschreven. Oxidatie van sulfinyl groepen zal aanleiding geven tot sulfonyl functionaliteiten, dewelke een verschillend thermisch gedrag vertonen in vergelijking met de sulfinyl functionaliteiten. Omdat deze gemodificeerde groepen bij een hogere temperatuur elimineren dan de oorspronkelijke sulfinyl groepen kunnen deze laatste groepen selectief geëlimineerd worden. De synthese van poly(thiënyleen vinyleen) (PTV) polymeren met een variërende hoeveelheid van conjugatie is dus tot stand gekomen door een selectieve eliminatie van de sulfinyl groepen van een PTV precursor copolymeer die een random verdeling van sulfinyl en sulfonyl groepen bevat. Deze sulfonyl groepen, die niet geëlimineerd worden, zullen fungeren als sp^3-defecten in het geconjugeerde materiaal. Met behulp van deze methode is het mogelijk om de materiaaleigenschappen van een polymeer te regelen.

In hoofdtuk III wordt het eliminatie- en degradatiegedrag van het OC_1C_{10}-PPV polymeer bestudeerd met TGA, DIP-MS, *in-situ* FT-IR en UV-Vis spectroscopie. Het OC_1C_{10}-PPV polymeer, zowel oplosbaar voor als na conversie, kan gesynthetiseerd worden via de Gilch en de sulfinyl route. Wij hebben vastgesteld dat de dikte van de polymeer film geen invloed heeft op de eliminatie reactie zelf, terwijl het verdampen van de eliminatie producten wel afhankelijk is van de dikte van de polymeer film. Uitgaande van niet-isotherme opwarmingsexperimenten aan verschillende opwarmsnelheden was het mogelijk om een idee te verkrijgen omtrent de activeringsenergie (E_A) van de conversie reactie. De eliminatie reactie van het *n*-alkyl-sulfinyl OC_1C_{10}-PPV precursor polymeer begint rond 70°C in stikstof atmosfeer (opwarmsnelheid: 2°C/min). Op 110°C (na eliminatie) wordt een absorptie maximum van 490 nm verkregen voor het geconjugeerde OC_1C_{10}-PPV polymeer. De overeenkomstige effectieve

conjugatie lengte zal vanaf 230°C terug afnemen. Deze afname wordt veroorzaakt door de degradatie van het geconjugeerd systeem. Na eliminatie zal er een zekere hoeveelheid van eliminatie producten achterblijven in de polymeer matrix. In het geval van PPV (zonder alkoxyketens op de fenylring) zullen de eliminatie producten extremer uit de matrix diffunderen. Wanneer de eliminatie reacties uitgevoerd worden in vacuum omstandigheden (10^{-2} mmHg) in plaats van stikstof atmosfeer, zal het temperatuursgebied, in dewelke de eliminatie reactie optreedt, verschuiven naar een lagere temperatuur (53-95°C). In vacuum condities zullen ook de eliminatie producten gemakkelijker uit de polymeer matrix verdampen of diffunderen. Eliminatie reacties kunnen het best uitgevoerd worden met precursor polymeren met een zo kort mogelijke alkyl keten op de sulfinyl elimineerbare groep, want zoveel te korter de alkyl keten, zoveel te lager het kookpunt van de overeenkomstige eliminatie producten, zoveel te gemakkelijker het voor de eliminatie producten is om uit de polymeer matrix te verdampen.

In een eerste gedeelte van hoofdstuk IV wordt de kinetica van de conversie reactie van het *n*-octyl-sulfinyl OC_1C_{10}-PPV precursor polymeer beschreven. Uitgaande van isotherme eliminatie reacties, bestudeerd met *in-situ* FT-IR en UV-Vis spectroscopie, wordt experimenteel een E_A bekomen van respectievelijk 100 kJ/mol en 92 kJ/mol. Deze experimentele E_A waarden zijn in goede overeenkomst met de waarde van de E_A die theoretische berekend is voor de conversie reactie naar *trans*-stilbeen (104.6 kJ/mol). In een tweede gedeelte van hoofdtuk IV wordt MTDSC gebruikt om het eliminatie proces van *n*-alkyl-sulfinyl OC_1C_{10}-PPV precursor polymeren te bestuderen en TGA wordt gebruikt om de diffusie en verdamping van de eliminatie producten te bestuderen. Uitgaande van een combinatie van isotherme en niet-isotherme MTDSC experimenten in vaste toestand kunnen we besluiten dat het eliminatie proces een combinatie is van opeenvolgende reactie stappen die kinetisch zeer moeilijk van elkaar te onderscheiden zijn. Spijtig genoeg is er in MTDSC geen enkel criterium waargenomen dat rechtstreeks in verband staat met de eliminatie reactie zelf. De disproportioneringsreactie grijpt plaats in een temperatuurs-gebied tussen 85 en 135°C. Vanaf 150°C kunnen nevenreacties optreden tengevolge van interacties van de eliminatie producten met het geconjugeerde polymeer. Dit geeft aanleiding tot netwerkvorming. Omdat netwerkvorming kan optreden is het beter om de eliminatie reacties uit te voeren bij relatief lage temperaturen (< 120°C) en in oplossing. Normaal gezien zijn reactiewarmten

zichtbaar in de NR-heat flow. Tijdens het bestuderen van het eliminatie proces in isotherme omstandigheden is er geen duidelijk warmteeffect waargenomen in de NR-heat flow. Om deze reden gaan we de verandering in warmtecapaciteit volgen om de verschillende reacties van het eliminatie proces te bestuderen. De toename in warmtecapaciteit is vooral te wijten aan de vorming van water tijdens de eliminatie reactie, maar ook aan het vrijkomen van de eliminatie producten. Tot op heden zijn er nog geen kinetische parameters verkregen uit deze isotherme MTDSC metingen in vaste toestand. In de nabije toekomst is het de bedoeling om deze isotherme MTDSC metingen te modelleren, om een idee te verkrijgen omtrent de kinetiek van de conversie reactie bestudeerd met MTDSC. Met MTDSC hebben we eveneens het eliminatie proces bestudeerd in oplossing (tolueen / chloorbenzeen). Uitgaande van de (niet)-isotherme MDSC metingen in oplossing hebben we een indicatie voor fasescheiding vastgesteld. Niet-isotherme MTDSC metingen tonen aan dat de fasescheiding in polymeer-solvent systemen kunnen vastgesteld worden als een kleine basislijn verschuiving in het warmtecapaciteitssignaal. Wanneer we zulke MTDSC opwarmings-afkoelings experimenten uitvoeren over een grote concentratie range is het in principe mogelijk om een fasediagram op te stellen. Fasescheiding in isotherme omstandigheden is ook aangetoond met *in-situ* UV-Vis spectroscopie (lichtverstrooiing). De diffusie van de eliminatie producten uit de polymeer matrix is bestudeerd aan de hand van isotherme TGA experimenten. De diffusie van de eliminatie producten uit de polymeer matrix zal gemakkelijker verlopen met een kleinere alkyl groep, een hogere isotherme temperatuur en een dunnere polymeer film.

In hoofdstuk V wordt het polymerisatie gedrag van xanthaat bevattende monomeren naar PPV precursor polymeren bestudeerd. Naast de synthese van deze precursoren wordt ook het eliminatie gedrag van deze precursoren bestudeerd. Wanneer de eliminatie reactie van een xanthaat PPV precursor polymeer naar een geconjugeerd PPV polymeer uitgevoerd wordt bij een temperatuur lager dan 195°C zal deze aanleiding geven tot een mengsel van *cis-trans* configuraties. Om een volledig *trans* PPV polymeer te bekomen zal de eliminatie reactie moeten uitgevoerd worden bij een temperatuur rond 250°C. Bij deze temperaturen zullen de eliminatie producten onmiddellijk verdampen en degradatie zal nog niet optreden. De experimenten betreffende het eliminatie gedrag van het *n*-octyl-sulfinyl PPV precursor oligomeer demonstreren duidelijk dat het kinetisch mogelijk is om de eliminatie van de sulfinyl groepen

van de hoofdketen te scheiden van de thermolyse van de sulfinyl eindgroepen in de oligomeerketen. Bij lagere temperaturen worden de sulfinyl groepen van de hoofdketen geëlimineerd en worden de dubbele bindingen gevormd. Bij hogere temperaturen zal de thermolyse van de sulfinyl eindgroepen plaatsgrijpen. Bij temperaturen hoger dan 175°C zijn er indicaties dat deze sulfinyl eindgroepen omgezet worden tot carbonyl functionaliteiten. Het is ook mogelijk dat twee oligomeerketens koppelen die dan na een oxidatie aanleiding geven tot een uitbreiding van de effectieve conjugatielengte.

List of abbreviations

PA	Polyacetylene
PEDOT	Poly(ethylenedioxythiophene)
PPP	Poly(*para*-phenylene)
VB	Valence Band
CB	Conduction Band
HOMO	Highest Occupied Molecular Orbital
LUMO	Lowest Unoccupied Molecular Orbital
E_g	Bandgap
PLED	Polymer Light Emitting Diode
PPV	Poly(*para*- phenylene vinylene)
EL	Electroluminescence
PL	Photoluminescence
ITO	Indium Tin Oxide
PET	Poly(ethylene terephtalate)
T_g	Glass transition temperature
THT	Tetrahydrothiophene
EDX	Energy-Dispersive X-ray analysis
DBS	Dodecylbenzenesulphonate
GPC	Gel Permeation Chromatography
THF	Tetrahydrophuran
DM(E)OPPV	Poly(2,5-dimethoxy-1,4-phenylene vinylene)
PTV	Poly(2,5-thienylene vinylene)

OC_1C_{10}-PPV	Poly[2-(3',7'-dimethyloctyloxy)-5-methoxy-*para*phenylene vinylene
DIP-MS	Direct Insert Probe Mass Spectrometry
TGA	ThermoGravimetric Analysis
FT-IR	Fourier Transform InfraRed spectroscopy
UV-Vis	Ultraviolet Visible spectroscopy
MTDSC	Modulated Temperature Differential Scanning Calorimetry
EI	Electron Impact
HHT-cell	Harrick High Temperature cell
m-CPBA	*Meta*-chloroperbenzoic acid
DHO-PPV	Poly(*para*-2,5-dihexyloxy phenylene vinylene)
NBS	*N*-bromosuccinimide
NCS	*N*-chlorosuccinimide
MEH-PPV	Poly[2-methoxy-5-((2'-ethylhexyl)oxy)-1,4-phenylene vinylene]
TLC	Thin Layer Chromatography
PVK	Poly(*N*-vinylcarbazole)
Rpm	Rotation per minute
NR	Non reversing heat flow
C_p^*	Complex heat capacity
RCS	Refrigerated Cooling System
PMMA	Poly(methylmetacrylate)
PE	Perkin Elmer
HPS	High Pressure Steel
LNCA	Liquid Nitrogen Cooling Accessory
CCA	Controlled Cooling Accessory
UCST	Upper Critical Solution Temperature
PD	Polydispersity
M_w	Molecular weight